UNIVERSITÀ DEGLI STUDI DI TRIESTE

Università Ca'Foscari Venezia

UNIVERSITÀ DEGLI STUDI DI TRIESTE
e
UNIVERSITÀ CA' FOSCARI DI VENEZIA

XXXIV CICLO DEL DOTTORATO DI RICERCA IN

CHIMICA

Development of analytical methods for therapeutic drug monitoring of first- and second-line therapies for hepatocellular carcinoma

Settore scientifico-disciplinare: CHIM/06

DOTTORANDA
Martina Zanchetta

COORDINATORE
PROF. ENZO ALESSIO

SUPERVISORE DI TESI
PROF. FEDERICO BERTI
GIUSEPPE TOFFOLI, M.D.

CO-SUPERVISORE DI TESI
BIANCA POSOCCO, Ph.D.

ANNO ACCADEMICO 2020/2021

Questo lavoro di tesi è stato svolto presso la Scuola di Dottorato
in Chimica interateneo Università degli Studi di Trieste-
Università Ca' Foscari di Venezia, diretta dal Prof. Enzo Alessio
in collaborazione con la Struttura Operativa Complessa
di Farmacologia Sperimentale e Clinica del
Centro di Riferimento Oncologico di Aviano
(Istituto di ricerca e cura a carattere scientifico),
diretta dal Dott. Giuseppe Toffoli.

A colei che non vuole essere

chiamata Vecchia volpe

Table of Contents

List of Figures

List of Tables

List of Equation

List of Abbreviations

% REC: percentage recovery

A_a: peak area of the i^{th} analyte

ACN: acetonitrile

AEs: adverse effects

AIFA: Agenzia Italiana del Farmaco

A_{IS}: peak area of the IS

AmAc: ammonium acetate

AS: autosampler

ATE: atezolizumab

ATP: adenosine triphosphate

AUC: area under the curve

BC/pla: red blood cells-to-plasma partitioning

BCLC: Barcelona Clinic Liver Cancer

BCRP: breast cancer resistance protein

BEVA: bevacizumab

C.E.U.R.: Comitato etico unico regionale

C.R.O.: Centro di Riferimento Oncologico – National Cancer Institute

CABO: cabozantinib

CAD: CAD gas

C_b: concentration in the plasma fraction deriving from spiked whole blood samples

C_{DBS}: the analyte concentration in the DBS samples;

C_{DBS}: the determined DBS concentration;

CE: Collision Energy

CF: conversion factor

CH_3COOH: acetic acid

CI: confidence interval

CLSI: Clinical and Laboratory Standard Institute

C_{max}: peak plasma concentration

C_{min}: minimum concentration

C_{pla}: the determined plasma concentration;

CRC: colorectal cancer

C_{srpla}: concentration in spiked reference plasma

CUR: curtain gas

CV: coefficient of variation

CXP: Collision Cell Exit Potential

CYP3A4: cytochrome P450 3A4

DAUNO: daunorubicin

DBS: Dried Blood Spot

DC: direct-current

des-oxREGO: N-desmethyl-REGO-N-oxide

DMSO: Dimethyl Sulfoxide

DP: Declustering Potential

DTC: differentiated thyroid carcinoma

EBF: European Bioanalysis Forum

ECOG: Eastern Cooperative Oncology Group

EC_{pla}: estimated plasma concentration

EGFR: epidermal growth factor receptor

EMA: European Medicines Agency

EP: Entrance Potential

ESI: electrospray ionization

FDA: Food and Drug Administration

FGFR: fibroblast growth factor receptor

FIA: Flow Injection Analysis

F_p: plasma fraction

GC: gas chromatography

GIST: gastrointestinal stromal tumor

GS1: gas 1

GS2: gas 2

H: height

HBV: hepatitis B virus

HCC: hepatocellular carcinoma

HCOOH: formic acid

Hct: hematocrit

HCV: hepatitis C virus

HFSR: hand-foot skin reaction

HIV: human immunodeficiency virus

HPLC: high-performance liquid chromatography

HR: hazard ratio

IATDMCT: International Association for Therapeutic Drug Monitoring and Clinical Toxicology

ICH: International Council for Harmonization

IDA: idarubicin

IDOL: idarubicinol

iPrOH: isopropanol

IS: internal standard

ISR: incurred samples reanalysis

ISV: ionSpray Voltage

K: partition coefficient

k': capacity factor

$K_{BC/pla}$: red blood cells-to-plasma partitioning coefficient

L: length

LC: liquid chromatography

LCCC: Lin's concordance correlation coefficient

LC-MS/MS: liquid chromatography coupled with tandem mass spectrometry

LENVA: lenvatinib

LENVA-D_4: lenvatinib D_4

LLE: Liquid-Liquid Extraction

LLOQ: lower limit of quantification

m: slope

MCA: multiple count acquisition

MeOH: methanol

MF: matrix factor

MilliQ H_2O: "Type 1" ultrapure water

MP: mobile phase

MRM: Multiple reaction monitoring

MS/MS: tandem mass spectrometry

MS: mass spectrometry

MS2: product ion mode

N: number of analyzed sample pairs.

NAFLD: non-alcoholic fatty liver disease

NP: normal phase

nRTK: non-receptor tyrosine kinase

OR: odds ratio

ORR: objective response rate

OS: Overall Survival

oxREGO: REGO-N-oxide

oxSORA: SORA-N-oxide

PDGFR: platelet-derived growth factor receptor

PFS: Progression Free Survival

P-gp: P-glycoprotein

PK: pharmacokinetic

PP: protein precipitation

PTFE: Polytetrafluoroethylene

q: intercept

Q1MI: Q1 multiple ions

Q1MS: Q1 full scan

Q2: second quadrupole

Q3: third quadrupole

QC: Quality Control

QCH: Quality Control High

QCL: Quality Control Low

QCM: Quality Control Medium

r: Pearson's correlation coefficient

RAMU: ramucirumab

RCC: renal cell carcinoma

REGO: regorafenib

REGO-D_3: regorafenib-D_3

RF: radiofrequency

RF: radiofrequency

RP: reverse phase

R_s: resolution

RTK: tyrosine kinase receptor

S/N: signal-to-noise ratio

SD: Standard Deviation

SIL: Stable Isotope Labelled

SIM: Selected Ion Monitoring

SLE: Solid Phase Extraction

SORA: sorafenib

SORA-L4: sorafenib-$^{13}C_1$-D_3

SP: Stationary Phase

sQ1: first quadrupole

SRM: Single Reaction Monitoring

SST: System Suitability Test

t_0: dead volume;

$t_{1/2}$: elimination half-life

TACE: transarterial chemoembolization

TDM: therapeutic drug monitoring

TEM: temperature

THF: tetrahydrofuran

TIC: total ion current

TK: tyrosine kinase

TKI: tyrosine kinase inhibitor

t_r: analyte retention time;

TTP: Time To Progression

UGT1A9: UDP-glucuronosyltransferase 1A9

VEGFR: vascular endothelial growth factor receptor

ULOQ: upper limit of quantification

w_b: peak with at the base-line

WS: Working Solution

$X_{i:}$ determined concentration value of the i^{th} analyte

XIC: extracted ion current

$X_{n:}$ nominal concentration

α: selectivity

ABSTRACT

Hepatocellular carcinoma (HCC) is a widespread malignant neoplasm, which accounts for >80% of liver cancers. HCC is classified as one of the most chemo-resistant cancer types and it is characterized by dismal survival outcomes. Response and toxicity to oral therapies used in advanced HCC differ among patients treated at the same dose. The differences in treatment outcome may be due to high inter-patient variability in plasma concentrations that depends on several factors, such as individual pharmacokinetics, pharmacogenetic background, concomitant assumptions of other drugs, etc.

A useful strategy to potentially improve treatment outcome is represented by Therapeutic Drug Monitoring (TDM), a practice that aims to personalize and improve drug dosage through the measurement and interpretation of its concentration (*e.g.,* C_{min} at the steady state) in patients' biological fluids. Despite its undeniable advantages, TDM is scarcely applied in oncology due to different reasons. On one side, to quantify a drug in biological fluids, the availability of robust, sensitive, and reproducible analytical method is needed. On the other side, plasma sample collection for drugs quantification represents a barrier for TDM implementation. The use of more patient-friendly sample collection procedures, such as Dried Blood Spots (DBS) may improve TDM applicability.

This PhD project considers four different oral anticancer drugs used to treat advanced HCC patients: sorafenib (SORA), regorafenib (REGO), lenvatinib (LENVA), and idarubicin (IDA), whose safety and efficacy as a third-line therapy option is currently under investigation.

SORA, REGO and LENVA are involved in a cross-validation study (internal protocol code: CRO-2018-83) ongoing at *Centro di Riferimento Oncologico (C.R.O.) di Aviano*, whose primary aim is the cross-validation between the plasma-based LC-MS/MS method and the DBS-based LC-MS/MS assay to demonstrate that DBS can be used alternatively to plasma sample to quantify these drugs. Instead, the quantification of IDA and its active metabolite (idarubicinol - IDOL) in human plasma was required as a secondary aim of phase II clinical study (internal protocol code: CRO-2017-42) ongoing at the *C.R.O. di Aviano*.

For all these drugs, exposure-response and -toxicity data are still limited or lacking, thus highlighting the necessity of deepening this type of investigation.

To assess drug plasma concentration in biological matrices, reliable analytical methods are needed. In the literature, different analytical methods have already been published, but they were not suitable for our purposes, either because they covered a not adequate analytical range or they were not cost-effective.

Thus, the aim of this PhD project was the development and validation, according to international guidelines, of suitable LC-MS/MS methods for the quantification of SORA, REGO, LENVA and IDA in human plasma. In addition, LC-MS/MS methods for the quantification of SORA, REGO and LENVA in DBS were also developed, validated and cross-validated comparing the obtained results with those obtained with plasma methods used as reference.

The LC-MS/MS methods reported in this PhD thesis used a Prominence UFLC XR or Nexera XR LC 20 system (Shimadzu), which was coupled with a triple quadrupole mass spectrometer (API 4000 QTrap; Sciex) equipped with an electrospray ionization (ESI) source.

In particular, two LC-MS/MS methods were developed and validated according to EMA and FDA guidelines to simultaneously quantify SORA, REGO, and 3 active metabolites (SORA-N-oxide, REGO-N-oxide, and N-desmethyl-REGO-N oxide), both in human plasma and DBS. These methods have the same analytical range (50-8000 ng/mL) for SORA and REGO and (30-4000 ng/mL) for the metabolites, the same chromatographic column (Synergi™ Fusion-RP column - 4 µm, 50 x 2.0 mm, 80 Å), the same gradient elution with 10 mM ammonium acetate aqueous solution (mobile phase A – MP A) and a methanol/isopropanol, 90:10 (v/v) mixture (MP B), both containing 0.1% formic acid (v/v) with a short run time (7 min). The plasma-based analytical method required a low amount of patient plasma (5 µL), which was processed by simple and rapid protein precipitation. This method showed great results in terms of linearity ($R \geq 0.998$), intra- and inter-day precision and accuracy (≤ 7.2% and 89.4-109%, respectively), analytes recovery from the matrix (≥ 85.5%), sensitivity, selectivity, dilution integrity, analytes stability under various conditions and absence of matrix effect. The DBS-based method is characterized by a volumetric sampling of 5 µL on Whatman 31 ET CHR filter paper and the whole spot was extracted to avoid the hematocrit (Hct) and spot volume effects. The parameters assessed during the validation process were recovery (≥ 51.7%), the absence of matrix effect, process efficiency (near 80% for SORA and REGO, near 50%, 70%, and 30% for oxSORA, oxREGO, and des-oxREGO, respectively), Hct effect (CV ≤ 9% and accuracy within 89.9-114%), linearity ($R \geq 0.998$), intra- and inter-day precision (CV ≤ 10%) and accuracy (92.1 - 108%), selectivity and sensitivity, dilution integrity, reproducibility with ISR and stability. After the validations, these methods were applied to quantify 66 plasma samples and 63 DBS samples obtained from 16 patients, treated with SORA (49) or REGO (14) and enrolled in CRO-2018-83 cross-validation study.

This analysis allowed us to obtain preliminary data regarding the concentrations of the drugs in patients and the correlation between plasma and DBS paired samples. Several DBS-to-plasma conversion methods were applied and the best predictive performances were obtained using $K_{BC/pla}$-based equation for SORA and CF-based equation for REGO. The application of proper statistical analyses for the cross-validation study showed the absence of a strong correlation, especially for REGO due to the paucity of samples.

Two additional LC-MS/MS methods were developed for the quantification of LENVA both in human plasma and DBS. These methods were validated according to EMA, FDA, and DBS references guidelines. The plasma-based method has a wide analytical range (0.5-2000 ng/mL) and it was applied to quantify 24 plasma samples obtained from 6 patients treated with LENVA and enrolled in CRO-2018-83 cross-validation study. The corresponding DBS-based method has a slightly reduced analytical range (5-2000 ng/mL) and it was applied for the analysis of 4 DBS patients' samples. These methods used the same MPs (A: milliQ-water and B: methanol:isopropanol 90:10 (v/v), each acidified with 0.1% formic acid (v/v) and the analyte's elution was

performed on Synergi™ Fusion-RP (4 µm, 30 x 2.0 mm, 80 Å) column with a short run time (4 min). The LC-MS/MS for the plasma quantification required 100 µL of the patient's plasma sample that was processed with protein precipitation. The developed method obtained great results in terms of linearity (R ≥ 0.997), intra- and inter-day precision and accuracy (CV ≤ 11.3% and Acc% within 93.6-109%), analyte recovery from the matrix (≥ 95.6%), sensitivity, selectivity, dilutional integrity, reproducibility with ISR, absence of matrix effect and stability under various conditions. The DBS-based method required a volumetric sampling of 10 µL and the extraction of the whole spot to avoid Hct and spot effects. The validation was performed on both Whatman 31 ET CHR and Whatman 903 filter papers according to international DBS validation (IATDMCT) guidelines, assessing the recovery (≥ 77% for both filter papers), the absence of matrix effect, process efficiency (near 72% for Whatman 31 ET CHR and near 77% for Whatman 903), Hct effect (CV ≤ 6.2% and accuracy within 103-112% and CV ≤ 5.5% and accuracy within 96-105% for Whatman 31 ET CHR and Whatman 903, respectively), linearity (R ≥ 0.998 for Whatman 31 ET CHR and R ≥ 0.999 for Whatman 903), intra- and inter-day precision (CV ≤ 7% and 8.8% for Whatman 31 ET CHR and Whatman 903, respectively) and accuracy (92.8 - 108% and 95.9 – 104% for Whatman 903), selectivity and sensitivity, reproducibility with ISR and stability.

No correlation studies have been performed yet due to the paucity of patients' samples collected till now. Preliminary evaluation showed that DBS concentrations were on average 70% compared to plasma levels.

For the quantification of IDA, a plasma-based LC-MS/MS method was developed with a calibration range of 0.10-200 ng/mL. A proper analytes separation was obtained with a Luna Omega Polar C18 column (3 µm, 50 x 2.1 mm, 100 Å) by using a multi-step chromatographic method based on a gradient elution with milli-Q water (MP A) and acetonitrile (MP B), each acidified with 0.1% acetic acid (v/v) and with a short run time (7 min). The sample preparation was based on protein precipitation and an evaporation step to concentrate the analytes. In addition, the method demonstrated preliminary linearity of the calibration curve, but, sadly, the evaporator breakage prevented the validation conclusion within the deadline of the thesis work.

In conclusion, this PhD project led to the development of LC-MS/MS analytical methods for:

- the quantification of SORA, REGO, and their active metabolites both in plasma and DBS matrices. These methods were also successfully validated and applied to quantify patients' samples. Correlation study between plasma and DBS concentrations suggested to enlarge patients number and to re-evaluate Hct and spot-volume effect to enhance the DBS-to-plasma conversion performance;
- the quantification of LENVA both in plasma and DBS samples. These methods were also fully validated and applied to quantify samples from patients affected by HCC and treated with LENVA. No correlation test has been performed yet;
- the quantification of IDA and IDOL in plasma samples from patients with HCC.

In this way, there is the hope to implement the application of TDM for these anticancer drugs in clinical practice.

The application of these analytical methods to the ongoing studies at the *C.R.O. di Aviano* should allow to collect useful data to deepen the knowledge about the possibility of establishing a correlation between drug exposure levels and patients' outcome or toxicity development.

1.INTRODUCTION

1.1. Hepatocellular carcinoma

Cancer is one of the leading causes of death worldwide (9.96 million deaths in 2020), with an incidence and mortality that are rapidly growing globally [1]. The causes to explain this phenomenon are both growth and aging of the population, together with changes in distribution and prevalence of the main cancer risk factors, several of which are associated with socio-economic development [2].

Liver cancer is the fifth most common cancer for males (632,320 new cases in 2020 worldwide, incidence 6.3% of all cancer cases) and the ninth for females (273,357 new cases in 2020 worldwide, incidence 2.6%) [3].

Hepatocellular carcinoma (HCC) accounts for > 80% of primary liver cancers worldwide [4] and it is the fourth most common cause of cancer-related death worldwide and its incidence is increasing over time [5]. The HCC incidence increases gradually with advancing age, achieving a peak at 70 years [6,7]; it has a strong male preponderance, with a male to female *ratio* of 2-2.5:1 [3,8]. Approximately 85% of HCC cases occur in low or middle-resource countries as sub-Saharan Africa and Eastern Asia (more than 50% of the cases occurring in China) [8]; furthermore, the incidence in Europe is lower except for Southern Europe, as France, Germany, Italy, and Spain [9].

HCC etiology is known in 90% of the cases since its outbreak is generally a result of evolving liver diseases [5]. The principal risk factor is liver cirrhosis because it progresses to HCC in 80-90% of the cases with a median onset time of approximately 10 years from cirrhosis development [10]. Moreover, HCC can be caused both directly and indirectly (*i.e.,* inducing cirrhosis), by different risk factors:

- chronic viral hepatitis: it is caused by hepatitis B virus (HBV) and hepatitis C virus (HCV), whose viral proteins can amend host pathways involved in hepatocytes proliferation, angiogenesis, apoptosis, and DNA repair [9,11]. HBV and HCV account for 80% of cases of virus-associated HCC globally [6], whose onset may be due to the presence or absence of liver cirrhosis; HBV accounts for 50-80% of the cases, while HCV for 10-25% [12,13]. Furthermore, co-infection with HBV and HCV increases the risk for HCC progression [14], while human immunodeficiency virus (HIV) co-infection can accelerate the progression of chronic viral hepatitis and escalate the risk of liver cirrhosis and HCC [15];
- non-alcoholic fatty liver disease (NAFLD): patients with NAFLD associated with metabolic syndrome such as obesity, diabetes, dyslipidemia have a higher HCC incidence [16–19];
- chronic alcohol abuse: irresponsible alcohol consumption causes alcoholic liver cirrhosis associated with an increased risk of HCC development [20];
- dietary exposure to aflatoxin B1: aflatoxins are strong hepatocarcinogenic mycotoxins that contaminate many kinds of cereals and oilseeds as a result of inappropriate post-harvest processing. Aflatoxin B1 is the most aflatoxin form involved in liver carcinogenesis, which can damage DNA,

generating a mutation (*e.g.,* TP53 tumor suppressor gene) that was recognized in up to 30-60% of patients affected by HCC [6,21];

- genetic hemochromatosis: up to 45% of patients affected by this pathology develop HCC [22].

Global variations in HCC incidence and mortality are caused by differences in environmental and infectious risk factors exposure and healthcare resource availability: chronic HBV and aflatoxin B1 exposure are the main risk factors in sub-Saharan Africa and Asia; HCV and excessive alcohol intake are peculiar in USA and Europe; while NAFLD is becoming important in developed countries [23].

Primary prevention is maybe the only realistic approach for decreasing the problem of HCC: it consists of the promotion of healthy lifestyle as an important preventive factor, including decrease alcohol and hypercaloric food consumption and universal vaccination against HBV infection, recommended especially in countries where HBV is endemic; viral hepatitis screening programs and antiviral treatments, which may prevent liver disease progression and thus HCC development [24]. Data suggest a lower HCC incidence after the five years of therapy against HBV [25], as well as interferon-based therapies against HCV, showed more than 70% reduction of HCC incidence [26].

Secondary prevention, *i.e.,* surveillance programs in patients with high-risk features, can increase the detection of HCC at an early stage when the patient is still eligible to receive potentially curative treatments which may improve the dismal outcomes of this pathology [24].

HCC diagnosis and staging depend on computed axial tomography (CT) and magnetic resonance imaging (MRI) [8]. Ultrasound, although not recommended as first-line imaging technique, is used as second-line when both CT and MRI are inconclusive or contraindicated for the diagnosis [27]. Nevertheless, ultrasound represents the most widely used imaging test for HCC surveillance thanks to the absence of risks, non-invasiveness, moderate costs, and its ability to detect a great number of HCC tumors before they are clinically presented [8,28]. Semi-annual ultrasound-based surveillance is recommended, resulting to be essential since tumor biomarkers for an accurate early HCC detection are still lacking [8].

Moreover, the pathohistological diagnosis is the gold standard tool in defining HCC and its differential diagnosis, since the classification of liver cancer is based on morphological parameters. Liver biopsy-based diagnosis of HCC allows evaluating focal liver lesions in cirrhosis, to distinguish HCC from benign and premalignant lesions and also from other primary/secondary liver malignancies. Furthermore, immuno-histological analysis for markers linked to malignant transformations can be helpful to support diagnosis [8].

During the hepatocarcinogenesis process, hepatocytes accumulate an average of 40-60 somatic alterations over time in protein-coding regions of the genome [29]. The most representative molecular alterations in human HCC include: inactivation of p53 (40-50% of cases) [30], overexpression of MDM2 (45%) [31], increased gankyrin expression (nearly 100%) [32], which inhibits p53-checkpoint function [33] and also Rb-checkpoint function [34], repression of p16 (>80%) [35], loss of IGF2R (> 60%) [36]. All the aforementioned

molecular alterations, involved in cell cycle regulation, lead to the loss of cell cycle checkpoints and apoptosis resistance, contributing to hepatocarcinogenesis.

The aberrant activation of oncogenic signaling pathways is a heterogeneous process involved in HCC development and it includes the overexpression of various vascular factors, growth factors, and oncogene receptors that increase the activation of downstream multi-kinases involved in cell growth, angiogenesis, proliferation, and metastasis [37]. Some of the main proteins overexpressed in HCC are vascular endothelial growth factor receptor (VEGFR) family, platelet-derived growth factor receptor (PDGFR) family, fibroblast growth factor receptor (FGFR), angiopoietins Ang-1 and Ang-2, and proteins of mitogen-activated protein kinases (MAPK) pathway that, once been activated, act trough Ras protein that delivers signals to the nucleus via downstream components of the pathway (*e.g.,* ERK1, RAF, MEK) [37,38].

Furthermore, during tumor development HCC cells produce immune modulators as cytokines, chemokines, and metabolites that establish a surrounding immunosuppressive environment that further sustains hepatocarcinogenesis [37].

All these vascular and growth factors and receptors work in a complementary and coordinated way to regulate tumor growth and angiogenesis, representing an optimal target to therapy against HCC.

1.2. Hepatocellular carcinoma treatments

Prognosis establishment and selection of adequate treatment based on the cancer classification are critical steps in the management of HCC. At the moment, Barcelona Clinic Liver Cancer (BCLC) staging system is the widest recognized clinical algorithm used for HCC patient stratification and treatment allocation [8]. The main clinical prognostic factors in patients with HCC are related to:

- tumor status: defined by number and size of nodules, presence of vascular invasion, extrahepatic spread;
- liver function: defined by Child-Pugh's classification;
- general tumor-related health status: defined by the Eastern Cooperative Oncology Group (ECOG-PS), which are coupled with treatment-dependent variables obtained from cohort studies and randomized trials [23,39–42].

As a result of this algorithm which links tumor stage with treatment strategy in a dynamic manner, patients affected by HCC are subdivided into five categories, as schematized in Figure 1.

At early HCC stages (BCLC stage 0-A), treatment strategies as liver resection, ablation or transplantation are potentially curative. At intermediate HCC stages (BCLC stage B) the gold standard therapies are palliative locoregional ones, such as transarterial chemoembolization (TACE) [43]. In patients with BCLC stage B(intermediate stage), it is recommended to stop TACE if the patient develops toxicity, absence of response, disease progression after one or two courses of TACE, or progression with vascular or extrahepatic spread

(thus progression to BCLC stage C) [23]. However, as early symptoms of this pathology are often inconspicuous, most of patients are diagnosed at HCC advanced stage (BCLC stage C) when only systemic therapy is possible.

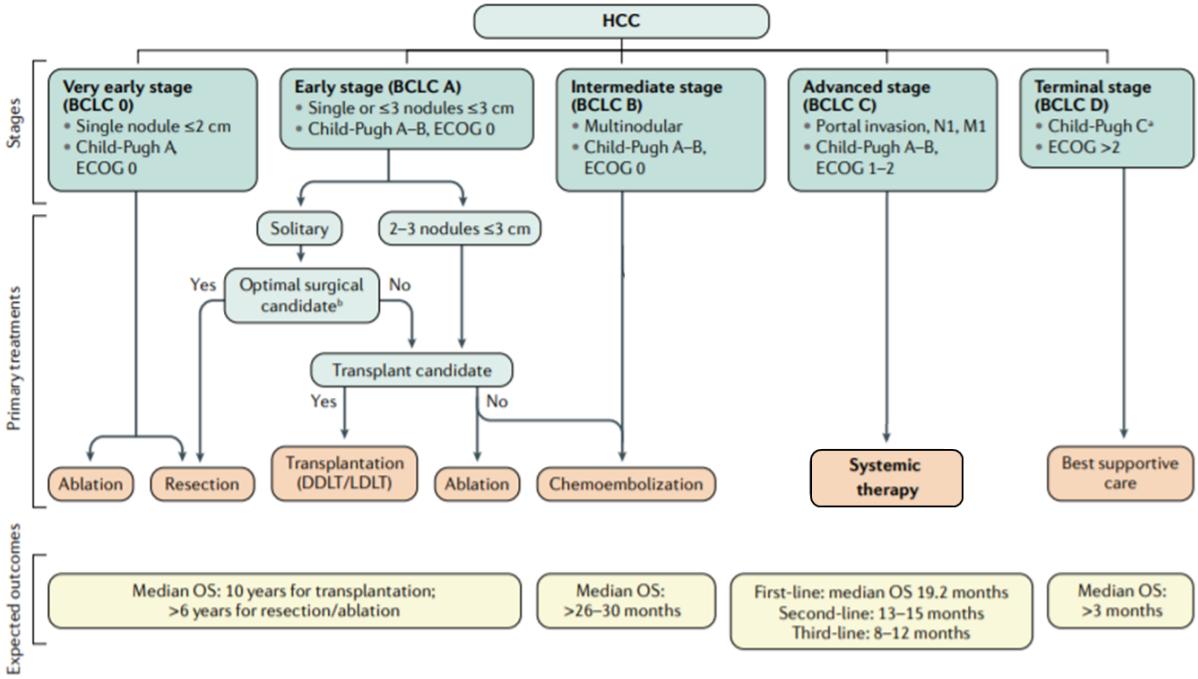

Figure 1. Barcelona Clinic Liver Cancer (BCLC) staging and treatment strategy. Adaptation of [43].

1.2.1. Systemic therapies for advanced hepatocellular carcinoma

Nowadays, the discovering of a promising systemic therapy is of great concern because this stage is sadly characterized by poor survival outcomes (about 1 year), and HCC is classified as one of the most chemo-resistant cancer types [8,29,39]. In the last decades, remarkable improvements have occurred in the treatment of advanced HCC since no pharmacological treatment for patients affected by this pathology was approved until 2007.

The systemic therapies approved by European Medicines Agency (EMA) for advanced HCC treatments is composted by 4 tyrosine kinase inhibitors (TKIs; sorafenib - SORA, lenvatinib - LENVA, regorafenib – REGO, and cabozantinib – CABO) and 3 monoclonal antibodies (ramucirumab – RAMU, atezolizumab in combination with bevacizumab – ATE + BEVA).

The systemic therapy approved by *Agenzia Italiana del Farmaco* (AIFA) and refunded by the Italian national health care system (*Sistema sanitario nazionale* – SSN) are only the 4 tyrosine kinase, summarized in Figure 2.

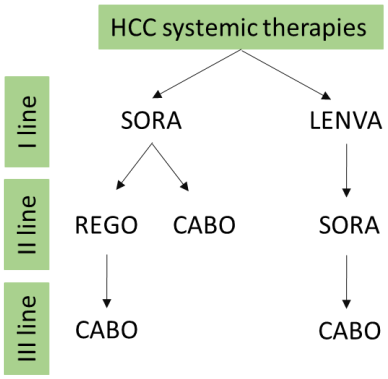

Figure 2. Schematic representation of approved systemic therapies for advanced HCC. CABO: cabozantinib; LENVA: lenvatinib; REGO: regorafenib; SORA: sorafenib.

The systemic therapy approved by AIFA is defined as molecular targeted therapy because it specifically acts against target molecules which are only or more expressed in cancer cells than in normal ones, and against up-regulated transduction pathways that trigger tumor formation through cells proliferation, cells survival, antiapoptotic effects and angiogenesis [11,44,45]. Generally, with this kind of approach, targets are represented by intracellular proteins or by receptors on the tumor cell surface [46].

The aberrant activation of these oncogenic pathways is due to the overexpression of a group of kinases dysregulated in HCC, namely tyrosine kinases (TKs), which are phosphorylating enzymes that catalyze the transfer of phosphate group from adenosine triphosphate (ATP) onto tyrosine residues of key proteins in signal transduction [47]. TK category includes membrane-bound tyrosine kinase receptors expressed on hepatoma cells and endothelial cells membrane as VEGFR, PDGFR, epidermal growth factor receptor (EGFR), FGFR, mast/stem cell growth factor receptor (c-KIT), and hepatocyte growth factor receptor (c-MET); but also non-receptor tyrosine kinases Ras/Raf/MEK/ERK and PI3K/Akt/mTOR/HIF pathways, which affect proliferation, growth, and survival of HCC cells by regulating gene expression [39,48].

Therefore, TKs resulted as valid targets for cancer treatment, leading to the development of several tyrosine kinase inhibitors (TKIs) that are currently used in advanced HCC treatment [48] and represent an optimal example of targeted therapy. TKIs are divided into three major groups:

- type 1: they act directly competing with ATP for ATP-binding site at the catalytic domain of various oncogenic TKs and thus decreasing phosphorylation of target molecules that trigger tumorigenesis [11]. Unfortunately, these molecules are not so specific and can target different TKs concurrently due to the high conservative ATP-binding sites in TK domains. Approximately all the current TKIs belong to this group.
- type 2 and type 3: they act binding to the TKs inducing conformational changes on the TK domain reducing its kinase activity [49]. These types are namely non-ATP competitors.

1.2.1.1. First-line therapy

The first-line therapy for HCC is characterized by two oral anticancer drugs: SORA or LENVA.

1.2.1.1.1. Sorafenib

Sorafenib tosylate, 4-(4-{3-[4-Chloro-3-(trifluoromethyl)phenyl]ureido}phenoxy)N2-methylpyridine-2-carboxamide 4-methylbenzenesulfonate, is the active ingredient of the oral anticancer drug Nexavar® (Bayer) and its chemical structure is reported in Figure 3.

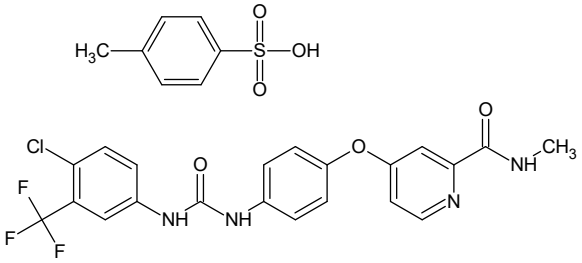

Figure 3. Chemical structure of sorafenib tosylate.

SORA is a multitargeted TKI with antiangiogenic, apoptotic, and antiproliferative activity [50]. It acts on tumor angiogenesis due to inhibition of VEGFR-1, VEGFR-2, VEGFR-3, PDGFR-β, and c-KIT signaling and Ras/Raf pathway [51–53]. In particular, SORA inhibits the kinase activity of both c-Raf and B-RAF (both wild type and mutant), so inhibiting downstream intracellular phosphorylation of kinases like MEK and ERK: this mechanism may force a sustained decrease of proliferative signal that triggers tumor growth and progression [48,51].

The approved therapeutic indications of SORA (standard dose: 400 mg twice daily) are unresectable HCC, advanced renal cell carcinoma (RCC), and locally recurrent or metastatic, progressive differentiated thyroid carcinoma (DTC) refractory to radioactive iodine. In particular, Food and Drug Administration (FDA) and EMA approved SORA as the first-line treatment for advanced and unresectable HCC in 2007 based on the positive results from the multicenter, randomized, phase III, controlled trial *versus* placebo (SHARP) conducted in the USA and Europe [11,39,48]. Enrolled patients were randomly assigned in a 1:1 *ratio* to receive continuous oral treatment with either 400 mg twice daily of SORA or corresponding placebo [54].

In fact, this trial demonstrated a delayed radiological progression (5.5 *versus* 2.8 months as compared to placebo; hazard ratio (HR) 0.58; 95% confidence interval (CI) 0.45-0.74; $p<0.001$) together with survival benefits, with a median overall survival (OS) about 2.5 months compared to placebo (10.7 months in SORA group *versus* 7.9 months in placebo group; HR 0.69; 95% CI 0.55-0.87; $p<0.001$) [11,54,55]. Moreover, these results were confirmed in the Asia-Pacific phase III SORA *versus* placebo trial conducted on the Asian population (6.5 *versus* 4.2 months compared to placebo; HR 0.68; 95% CI 0.50-0.93; $p=0.014$) [55]. Therefore,

the approved standard therapy with SORA in the HCC setting consists of 800 mg/die, precisely 400 mg (2 x 200 mg tablets) orally taken twice daily [44,56].

After oral administration of SORA tablets, the mean relative bioavailability was 38-49% when compared to an oral solution, with an absolute bioavailability lower than 50%. Since SORA intake with a high-fat meal reduced bioavailability by 29% compared to that in the fastens state, it is recommended to be administered without food. The peak plasma concentration (C_{max}) is achieved within approximately 3 h from administration, while the steady-state concentrations are reached after 7 days; furthermore, 99.5% of SORA circulates bound to human plasma proteins, with an 8.8-fold higher affinity for albumin to α1-acid glycoprotein [56,57].

Like nearly all drugs, SORA is metabolized primarily in the liver, undergoing oxidative metabolism, mediated by cytochrome P450 3A4 (CYP3A4), as well as glucuronidation mediated by UDP-glucuronosyltransferase 1A9 (UGT1A9). As an unchanged drug, SORA accounts for almost 70-85% of the circulating analytes in plasma at the steady-state. Eight metabolites of SORA have been identified, of which five have been detected in plasma. The main circulating metabolite of SORA in plasma, the pyridine N-oxide (oxSORA, reported in Figure 4), shows in vitro potency similar to that of SORA. This metabolite comprises about 9-16% of circulating analytes at the steady-state [56,58].

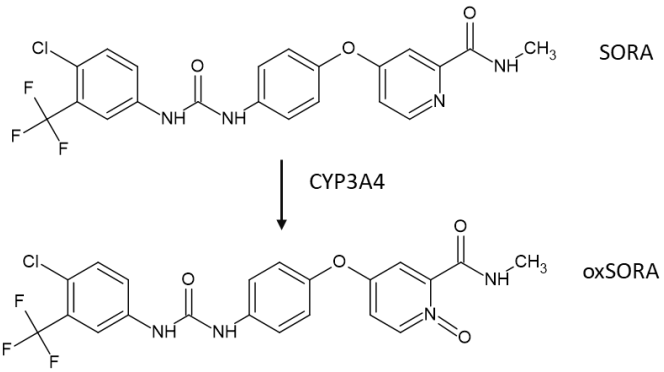

Figure 4. oxSORA formation through the N-oxidation reaction of SORA mediated by CYP3A4.

The mean plasma elimination half-life ($t_{1/2}$) of SORA is 25-48 h and its elimination occurs primarily through the fecal route, with 77% of the dose excreted in feces and 19% in urine [56].

Being SORA a substrate of CYP3A4, strong CYP3A4 inducers (*e.g.,* carbamazepine, dexamethasone, phenobarbital, phenytoin, rifampin, St. John's wort) decrease the systemic exposure to SORA, so their concomitant use should be avoided. Other factors such as hepatic and renal impairment, age, race, gender, and body weight do not significantly affect this drug pharmacokinetic (PK) [56].

SORA assumption is commonly safe, well-tolerated, and allows the patients to lead a normal life [8], but adverse reactions could occur. In particular, SORA is most commonly associated with manageable dermatological and gastrointestinal adverse effects (AEs) like hand-foot skin reaction (HFSR), rash/desquamation, alopecia, pruritus, fatigue, hypertension, nausea, and diarrhea [59]. Sometimes higher

toxicity can occur and the most common severe (grade 3) AEs include diarrhea and HFSR, which typically lead to dose reduction or treatment discontinuation in 10-15% of patients [8,48,60]. Nonetheless, SORA intolerance is not the only cause of therapeutic failure. Indeed, regardless of its broad pharmacodynamic activity, SORA is unable to stop the disease progression due to also the development of primary and acquired resistance to SORA. The acquisition of resistance to SORA is a complex phenomenon that is not completely understood: possible mechanisms are represented by hepatocyte epithelial-mesenchymal transition and changes in the tumor microenvironment, as well as the activation of escape mechanisms from the MAPK pathway [54,61,62].

Treatment with the above-mentioned recommended dose should continue until disease progression or until unacceptable toxicity occurs. If dose reduction or treatment discontinuation lead to disease progression, it will be necessary to proceed to the second-line treatment for HCC, which consists of the administration of another TKI: REGO or CABO if SORA was interrupted due to toxicity.

1.2.1.1.2. Lenvatinib

Lenvatinib mesylate 4-[3-chloro-4-(N'-cyclopropylureido)phenoxy]-7-methoxyquinoline-6-carboxamide methanesulfonate, is the active ingredient of the oral anticancer drug Lenvima® (Eisai Inc.) and its chemical structure is reported in Figure 5.

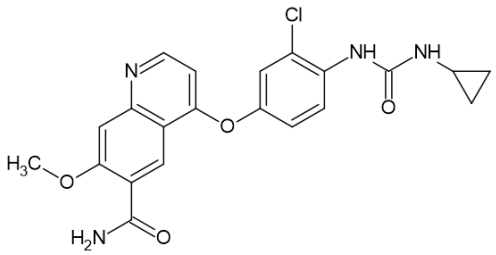

Figure 5. Lenvatinib mesylate chemical structure.

LENVA is an oral multikinase inhibitor that targets VEGFR 1–3, FGFR 1–4, PDGFR-α, RET, and KIT, strongly suppressing tumor angiogenesis and inhibiting FGFR signal transduction pathways involved in cells proliferation [63,64].

The EMA approved therapeutic indications of LENVA are progressing DTC no longer treated with radioactive iodine (standard dose: 24 mg/day), RCC (standard dose: 18 mg in combination with 5 mg everolimus orally once daily), and advanced or unresectable HCC in the patient who has received no prior systemic therapy [65,66]. Based on the results of randomized, multicentric, open-label, phase III non-inferiority to SORA trial (REFLECT) [67], first FDA and then EMA approved LENVA as another first-line targeted molecular therapy for advanced and unresectable HCC in 2018 [48]. Enrolled patients affected by unresectable HCC were randomly assigned in a 1:1 *ratio* to receive oral treatment either 12 mg for baseline body weight ≥ 60 kg or 8 mg for

baseline body weight < 60 kg once daily of LENVA or 400 mg twice daily of SORA until unacceptable toxicity or radiological disease progression occur [67].

In particular, REFLECT trial demonstrated LENVA no-inferiority to, although not superior to, SORA for OS (HR 0.92; 95% CI 0.79–1.06) with a median OS of 13.6 months *versus* 12.3 months, respectively [8,48]. Moreover, LENVA determined a significant increase in progression free survival (PFS; 7.3 months *versus* 3.6 months; HR 0.65; 95% CI 0.56-0.77; p<0.0001), in time to progression (TTP; 7.4 *versus* 3.7 months; HR 0.61; 95% CI 0.51-0.72; p<0.0001) and a higher objective response rate (ORR; 18.8 *versus* 6.5%; odds ratio (OR) 3.34; 95% CI 2.117-5.14; p<0.0001) rather than SORA [48,67].

Recently, a cost-utility analysis reported that LENVA had greater effectiveness at a lower cost than SORA, indicating that LENVA may be a cost-saving measure in patients with unresectable HCC, in which $23,719 could be saved per patient [68]. In particular, the daily cost of SORA for 400 mg twice daily is $195.60, and $5,476.62 for a 28-day cycle [69], while the daily cost of LENVA for 12 mg/die is $97.68 and $2,735.04 for a 28-day cycle [70]. However, it is important to consider that LENVA may fail to be cost-effective at a willingness-to-pay of $50,000, and would most certainly not be cost-saving if a significantly cheaper generic SORA becomes available. In fact, the expected patent expiry date is December 2020 for FDA and July 2021 for EMA [71].

LENVA C_{max} is typically reached from 1 to 4 h after drug intake, so it is rapidly absorbed, undergoing a 2 h delay when it is intake with a high-fat meal. At the moment, there are no recommendations to take LENVA with or without food and in particular with a high-fat meal, since an irrelevant change of its bioavailability was noted (*i.e.,* 5% decrease in C_{max}) [72]. LENVA $t_{1/2}$ is about 28 h and the steady-state concentration is reached within 6 days.

Moreover, 97.9-98.6% of circulating LENVA is bound to human plasma, predominantly with albumin (93.2%) and relatively less with α1-acid glycoprotein (6.1%) and γ-globulin (0.7%) [65].

Like most drugs, LENVA is extremely metabolized in the liver through dealkylation mediated by CYP3A4 which is the predominant (> 80%) isoform involved in the P450-mediated metabolism of LENVA. Moreover, also non-P450-mediated pathways contributed to a significant portion of the overall LENVA metabolism, such as oxidation and N-oxidation by aldehyde oxidase, hydrolysis, O-dearylation (chlorobenzyl moiety), a combination of these pathways, followed by further bio-transformations (*e.g.,* glucuronic acid or glutathione/cysteine conjugation and biodegradation/dimerization with intermolecular rearrangement) [65,72–74].

Approximately 50 metabolites were found in plasma, feces, and urine: the main ones are products of decyclopropylation (M1), demethylation (M2), N-oxidation (M3), and O-dearylation (M5), as reported in Figure 6 [74]. Nonetheless, the C_{max} of metabolites was at least 700-fold lower than LENVA C_{max}, therefore almost only the unchanged drug is responsible for the pharmacological/clinical effects and toxicity [74].

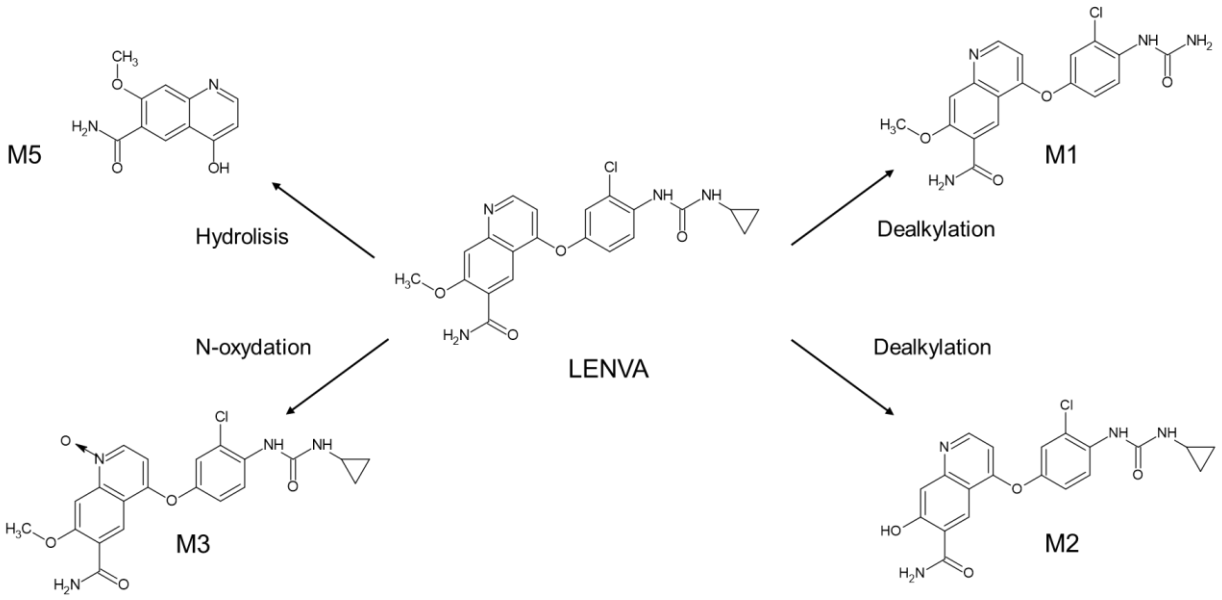

Figure 6. LENVA and its main metabolism pathways.

The extensive LENVA metabolism is confirmed by the fact that only 2.5% of the administered dose is found unchanged in urine and feces [65,74]. Twenty-five% of metabolites are circulating and eliminated via urine and nearly 64% are excreted via the biliary way in feces [65].

Regarding drug-drug interactions, although LENVA is a substrate of CYP3A4, ABC transporters as breast cancer resistance protein (BCRP) and P-glycoprotein (P-gp), no dose adjustment of LENVA is recommended when co-administered with CYP3A4, P-gp, and BCRP inhibitors (*e.g.,* ketoconazole), P-gp inhibitors (*e.g.,* rifampicin in single-dose) or CYP3A4 and P-gp inducers (*e.g.,* rifampicin in multiple doses) due to clinically relevant modification in LENVA exposure absence [75,76].

LENVA PK is modified in a clinically irrelevant way by age, gender, race, renal, and mild or moderate hepatic impairment. The drug adjustment is required only in case of severe hepatic impairment due to a 2-fold higher of both unbound and total area under the curve (AUC) [65].

On the other hand, LENVA PK is influenced by body weight due to a lower drug exposure appearing in patients with high body weight than a lower one. In fact, LENVA dose regimen is adjusted according to patient body weight to minimize the incidence of AEs, early dose reduction, or therapy interruption and at the same time provide the drug efficacy with an estimated similar exposure among patients [77]. Consequently, LENVA standard dosage for the treatment of HCC is 12 mg (3 x 4 mg capsules) orally taken once daily for patients with a baseline body weight major or equal to 60 kg and 8 mg (2 x 4 mg capsules) once daily for patients with a baseline body weight minor than 60 kg [54].

As reported in REFLECT trial, the overall incidence of grade ≥ 3 treatment-emergent AEs was higher with LENVA than with SORA (57% *versus* 49%) [29,67]. The most frequently reported AEs (occurring in ≥ 30% of patients) are hypertension (44.0%), diarrhea (38.1%), decreased appetite (34.9%), fatigue (30.6%) and decreased weight (30.4%) [65]. Moreover, fatal AEs occurred in 2% of patients treated with LENVA *versus* 1%

of patients with SORA and involved hepatic failure and encephalopathy, myocardial infarction, cerebral infarction, and respiratory failure [29,67]. In REFLECT trial, treatment-emergent AEs lead to LENVA dose reduction (37%) or treatment interruption (40%), while in the SORA arm the dose reduction was 37% and treatment interruption was 32% [67].

First-line treatment with LENVA proceeds until the patient is no longer clinically benefiting from therapy or until unacceptable toxicity occurs; in this case, it will be necessary to proceed with a second-line therapy with SORA.

1.2.1.2. Second-line therapy

SORA, REGO, or CABO are possible alternative second-line therapy for the treatment of advanced HCC after the failure of the first-line therapy.

1.2.1.2.1. Regorafenib

REGO, 4-[4-({[4-chloro-3-(trifluoromethyl) phenyl] carbamoyl} amino)-3-fluorophenoxy]-N-methylpyridine-2-carboxamide, is the active ingredient of Stivarga ® (Bayer) and its chemical structure is reported in Figure 7.

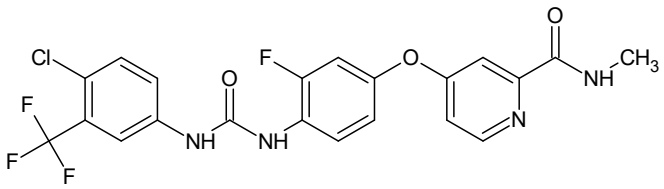

Figure 7. Structural formula of regorafenib.

REGO is a small multitargeted TKIs with both anti-proliferative and antiangiogenic proprieties. Moreover, REGO is characterized by higher potency and broader inhibitory activity rather than SORA, although similar structure [29,48]. Indeed, REGO inhibits targets of tumor angiogenesis (*e.g.,* VEGFR-1, VEGFR-2, VEGFR-3, and TIE2), oncogenesis (*e.g.,* KIT, RAF-1, B-RAF both wild-type and mutant, BRAF V600E), metastasis (*e.g.,* VEGFR-3, PDFGR, FGFR), and tumor immunity (*e.g.,* CSF1R) [78,79].

The approved therapeutic dosage of REGO is 160 mg (4 x 40 mg tablets) for 3 weeks on and 1 week off for the treatment of metastatic colorectal cancer (CRC) previously treated or who are considered not suitable for other available therapies; locally advanced, unresectable or metastatic gastrointestinal stromal tumor (GIST), after the failure of imatinib and sunitinib; and HCC previously treated with SORA as first-line [80,81].

In 2017, FDA and EMA approved REGO as second-line treatment for HCC after SORA failure based on a randomized, double-blind, placebo-controlled, phase III trial (RESORCE) [80,81]. Enrolled patients were

randomly assigned in a 2:1 *ratio* to receive 160 mg/die REGO orally or a corresponding placebo once daily for the first 21 days of each 28 days cycle. This trial reported an improvement in OS: 10.6 months *versus* 7.8 months in the REGO and the placebo arms, respectively (HR 0.63; 95% CI 0.50-0.79; p<0.0001) [76,82].

In particular, REGO assumption should be at the same time each day after a low-fat meal to help the drug absorption [80,81].

Regarding REGO PK, C_{max} is reached approximately after 4 h with a similar bioavailability of tablets compared to an oral solution that is 69% to 83%, respectively.

REGO is metabolized predominantly in the liver by oxidative metabolism mediated by CYP3A4 and by glucuronidation through UGT1A9. Two major and six minor metabolites of REGO have been identified in plasma. The main circulating metabolites of REGO in human plasma are REGO-N-oxide (oxREGO, also called M2) and N-desmethyl-REGO-N-oxide (des-oxREGO, also called M5), which are pharmacologically active and have similar concentrations as REGO at the steady-state, which is reached after 5 days and reported in Figure 8. oxREGO is further metabolized by oxidative metabolism through CYP3A4 and by glucuronidation mediated by UGT1A9 [80,81].

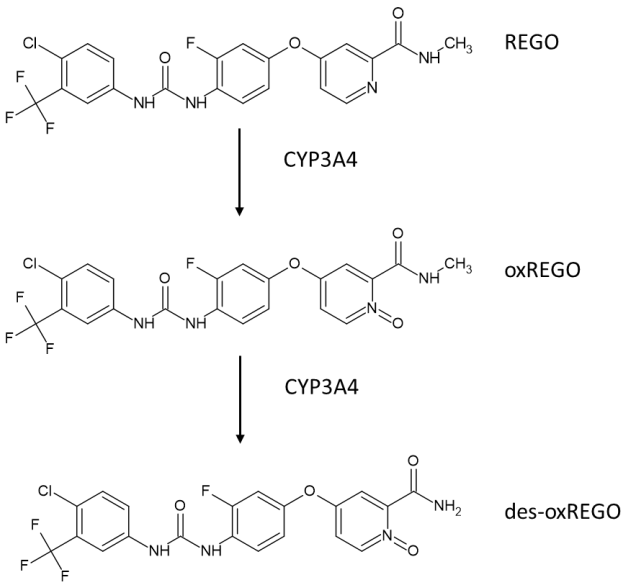

Figure 8. oxREGO and des-oxREGO formation through the N-oxidation and N-desmethylation reactions performed by CYP3A4 on REGO and oxREGO, respectively.

REGO, oxREGO, and des-oxREGO are highly binding to the plasma protein (99.5%, 99.8% and 99.95%, respectively). The mean plasma $t_{1/2}$ is 28, 25, and 51 h for REGO, oxREGO, and des-oxREGO, respectively, while approximately 71% of the dose is excreted in feces (47% as REGO and 24% as metabolites), and nearly 19% in urine as glucuronides [78,81].

Also REGO, as SORA, is a substrate of CYP3A4, thus co-administration with strong CYP3A4 inhibitors (*e.g.;* ketoconazole, itraconazole, voriconazole, and grapefruit juice) should be avoided since they reduce REGO metabolism and thus increase REGO plasma concentration, while active metabolites concentrations are

lower. Contrarily, co-administration with strong CYP3A4 inducers should lead to a reduction of REGO plasma concentration and increase for des-oxREGO plasma level, while no variation for oxREGO plasma concentration [78]. Furthermore, REGO is also a substrate for other proteins as P-gp and BCRP, nonetheless, clinical data about the interaction with inhibitors or inducers of these proteins are not known until now [81]. The most common AEs are very similar to the ones triggered by SORA assumption: HFSR, diarrhea, fatigue, and hypertension [8,29,82]. However, REGO is characterized by a slightly better drug tolerance profile in patients affected by HCC [82].

The treatment with REGO should continue until disease progression or unacceptable toxicity occur, the physician may evaluate other treatments as CABO in third-line therapy.

1.2.1.2.2. Cabozantinib

CABO, 1-N-[4-(6,7-dimethoxyquinolin-4-yl)oxyphenyl]-1-N'-(4-fluorophenyl)cyclopropane-1,1-dicarboxamide is the active ingredient of the oral anticancer drug Cabometyx® (Ipsen Pharma) and its chemical structure is reported in Figure 9.

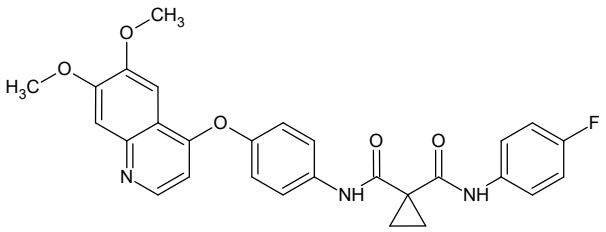

Figure 9. Cabozantinib structural formula.

CABO is a multitargeted TKI, which inhibits VEGFR 1-3, MET and AXL implicated in tumor progression and development of resistance to the standard initial treatment with SORA.

The approved therapeutic indication of CABO are advanced RCC alone or in combination with nivolumab and advanced HCC previously treated with SORA and the standard dose are 60 mg/die as monotherapy or 40 mg/die in combination [83,84]. In 2018, FDA and EMA approved CABO as second-line therapy in HCC setting based on the results of a phase III randomized, double-blind *versus* placebo trial (CELESTIAL). Enrolled patients were randomly assigned in a 2:1 *ratio* to receive 60 mg/die of CABO or a matching placebo [85]. This trial identified significantly longer OS with CABO compared to placebo, mean OS was 10.2 months *versus* 8.0 months, respectively (HR 0.76; 95% CI 0.63-0.92; p=0.005) and a significantly favorable PFS of 5.2 months with CABO *versus* 1.9 months for placebo (HR 0.44; 95% CI 0.36-0.5; p<0.001) and ORR were 4% and less than 1%, respectively (p=0.009) [85].

The most common grade ≥ 3 AEs in the CABO group were HFSR, hypertension, increased aspartate aminotransferase level, fatigue and diarrhea; their overall incidence was 68% compared to patients in the placebo group (36%) [85,86].

1.2.1.3. Third-line therapy

As mentioned before, HCC is highly resistant to conventional pharmacological treatments [87] and for this reason, nowadays several alternative therapies are investigated after the failure of the first- and second-line therapies, since, besides CABO, none of them is still approved as a standard third-line of treatment. One of the drugs under investigation as third-line therapy in HCC setting is idarubicin (IDA). This drug is administered to HCC patients after failure or intolerance to SORA and REGO, following a metronomic schedule in the context of phase II clinical trial ongoing at the National Cancer Institute of Aviano (*Centro di Riferimento Oncologico (C.R.O.) di Aviano* - PN, Italy).

1.2.1.3.1. Idarubicin

IDA hydrochloride [5,12-naphthacenedione,9-acetil-7-[(3-ammino-2,3,6-trideossi-cc-L-iyxo-hexopyranosyl) ossi]-7, 8, 9, 10-tetraidro-6, 9, 1 1-trihydroxyhydrochloride, (7S-cis)] is the active ingredient of the oral anticancer drug Zavedos® (Pfizer). IDA is a daunorubicin (DAUNO) derivative, composed of dyhydroxy-anthraquinone group bound to an aminoglycoside (daunosamine), and it is characterized by a hydrogen atom, which substitutes a methoxyl group in the D ring of the aglycone moiety, as reported in Figure 10.

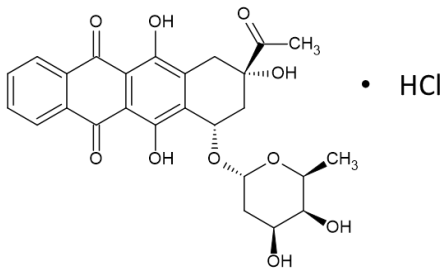

Figure 10. Idarubicin hydrochloride structural formula.

IDA belongs to the anthracyclines therapeutic class, thus its mechanism of action is multiple [88–90] and widely differs from the TKI, previously reported. In particular, at the level of the nucleus, IDA intercalates DNA mediated by the insertion of its anthracycline planar portion between the double helix, while the glycosidic structure stabilizes the interaction through weak bonds with the phosphate residues of the DNA [89,90]. Following this interaction, a ternary complex is formed between the IDA, Topoisomerase II (*i.e.,* the enzyme that triggers DNA strand breakage and reattachment), and DNA, which is followed by the stabilization of the "cut" situation, the blocking of DNA synthesis (preferably in phase S) and cell death for apoptosis [90–92]. The drug's most likely cytotoxic mechanism appears to be attributable to the formation of free radicals. At the microsomal level, the quinone groups can be reduced to semi-quinone radicals which, by reacting with molecules, give rise to the superoxide radical and/or the hydroxyl radical. By attacking DNA, radicals can oxidize their bases. Furthermore, these can mediate the peroxidation of membrane lipids, causing alterations

in cell permeability. This latter mechanism, if exercised at the cardiomyocyte level, is responsible for the characteristic cardiotoxicity of anthracyclines. Cancer cell death occurs by apoptosis, mediated by p53 DNA damage sensor and activated caspases and Fas-receptor ligand system [93,94].

The approved therapeutic indication of IDA in capsule as monotherapy or in association are advanced breast cancer after failure of first-line chemotherapy treatment, or in that of patients no longer responsive to hormone therapy and acute non-lymphoblastic leukemia both in first-line and in patients previously treated and not eligible for other intravenous therapy [95–97].

Based on pre-clinical and clinical trial evidence, IDA can be a possible candidate for the treatment of advanced HCC after the failure of the first- and second-line therapy offering a possibility to the chemotherapy paucity. In fact, in *vitro,* IDA appeared to be the most cytotoxic drug on three different HCC cell lines (HepG2, SBU-398, and SNU-449) [98]. In particular, SNU-449 is characterized by a high chemo-resistance to numerous chemotherapeutic agents. Moreover, the high lipophilicity of IDA can explain the wider cytotoxic activity compared to other anthracyclines due to higher hepatic cells penetration and so a greater accumulation in tumor cells and the possibility to overcome the multidrug resistance involved in chemoresistance [99–101].

The PK profile of oral IDA had been assessed in phase I, phase II, and PK studies in a heterogeneous population of patients affected by cancer [102]. IDA is rapidly absorbed after oral administration, the plasma C_{max} is reached after 1-4 h and $t_{1/2}$ in 13.7 h [103,104]. IDA suffers an extensive first-pass metabolism by aldo-keto reductase to produce demthoxy-13-dihydrodaunorubicinidarubicinol (IDOL) both in the liver and in extravascular tissue [105]. IDOL plasma C_{max} is achieved after 3-8 h and $t_{1/2}$ in 46 h [102], while in *vitro* its activity is nearly half of that of IDA [106,107] and its plasmatic level is approximately 2-12 times higher than IDA one [103]. After oral regime, 97% of IDA and 94% of IDOL circulate bound to plasma proteins [108].

The optimization of IDA administration modality has generated great interest due to its peculiar PK and pharmacological characteristic. Indeed, IDA is the only anthracycline in which both intravenous and oral administration is possible.

Moreover, an effective novel schedule was being assessed to IDA administration through metronomic therapy which consisted of hyper-fractionated doses over a long period. The oral route improved the formation of IDOL to intravenous one and therefore the collaboration of IDA and IDOL in determining cytotoxic effects; furthermore, the long plasmatic $t_{1/2}$ (13.7 h for IDA and 46 h for IDOL) of both compounds, reduces their plasmatic concentration fluctuations, exposing a higher number of tumor cells to steadier drug concentrations during the most chemo-sensitive phase of the cell cycle (*i.e.,* S-phase in IDA case) [104,105,109]. In this manner, the metronomic schedule can increase the efficacy of the IDA therapy and is also more suitable for patient compliance.

A phase I dose-finding trial conducted at *C.R.O. di Aviano* has evaluated metronomic IDA schedule in elderly patients affected by metastatic breast cancer. The treatment resulted well tolerated and feasible and the identified recommended dose for an additional phase II trial ranged between 5 and 7.5 mg/die [104].

Moreover, a phase II multicentric trial demonstrated the efficacy and safety of metronomic therapy with 5 mg/die of IDA (Zavedos ® 5 mg capsules) in elderly patients with visceral metastatic breast cancer [110]. This trial correlated also IDA and IDOL minimum plasma concentration (C_{min}) at the steady-state to patients' clinical outcomes. The C_{min} is the least variable point in the dosing interval, namely, the plasma concentration just before the patient takes the next daily dose of the drug [111].

The C_{min} were quantified on days 7, 14, and 21 of each 28 days cycle immediately before the daily dose intake. The obtained results for IDA and IDOL are reported in Table 1.

Table 1. Determined C_{min} of IDA and IDOL in the phase II trial.

Timing (day)	Mean C_{min} ± SD (ng/mL)	
	IDA	IDOL
7	0.34 ± 0.19	4.09 ± 1.81
14	0.37 ± 0.19	4.45 ± 2.02
21	0.32 ± 0.14	4.26 ± 1.90

The results underlying that IDA and IDOL concentrations remain constant during the entire chemotherapy cycle, once the steady-state is reached. Moreover, this phase II trial found out no correlation between IDA and IDOL plasma concentrations and tumor progression; nevertheless, their higher values (*i.e.,* 0.60 ± 0.20 ng/mL and 6.69 ± 2.09 ng/mL for IDA and IDOL, respectively) were associated with grade 3 or 4 of hematological toxicity [110].

An additional mechanism of action of anthracyclines, which may enhance therapy effectiveness is the triggering of an immunostimulatory response, called immunogenic cell death (ICD) [112]. ICD induces immunogenic apoptosis and autophagic cell death through a damage-associated molecular pattern (DAMPs) hallmarks with immunostimulatory properties, consequently reducing the peculiar immunosuppressive tumor environment [113–115].

On the basis of the pre-clinical and clinical evidences abovementioned, a phase II clinical study "*Studio di Fase II che valuta l'efficacia e la sicurezza del trattamento metronomico orale con Idarubicina in pazienti affetti da Epatocarcinoma allo stadio intermedio-avanzato dopo fallimento o intolleranza a Sorafenib e Regorafenib*" was designed and is currently ongoing at *C.R.O. di Aviano* and at *Azienda Sanitaria Universitaria Integrata of Udine* (UD, Italy). The protocol of this clinical trial (EUDRACT Number 2017-003653-42) had been revised and approved by the local ethics committee (*Comitato Etico Unico Regionale* - C.E.U.R.) and AIFA. Patients enrolled in the clinical study take 5 mg capsules of IDA with a metronomic schedule: drug assumption occurs on alternate days, at about the same time, during a 28-days therapy cycle.

To the best of our knowledge, this is the first trial, which evaluates the treatment of patients affected by advanced HCC with IDA metronomic schedule. Its primary aim is the evaluation of IDA efficacy in terms of OS at 6 months; while secondary-explorative aims include PFS, TTP, safety, tolerability evaluations, and translational PK, pharmacogenetics, immunology investigations.

1.2.1.4. Other therapies

Recently, monoclonal antibodies (immunotherapy) have been investigated in order to obtain a beneficial option for patients who have contraindications to or cannot tolerate first-line therapy with TKIs. In particular, FDA in May 2019 and EMA in June 2019 approved RAMU (VEGFR-2 antagonist) as second-line therapy in patients previously treated with SORA and with an alpha-fetoprotein (AFP) of ≥ 400 ng/mL at the baseline[116,117]. This approval is based on the results of phase III randomized, double-blind, placebo-controlled trial (REACH-2): median OS 8.5 months with RAMU *versus* 7.3 months with placebo (HR 0.710; 95% CI 0.531–0.949; p=0·0199) and PFS 2.8 months *versus* 1.6 months (HR 0.452; 95% CI 0.339-0.603; p<0·0001) were significantly improved in the RAMU arm compared with the placebo arm [118]. Enrolled patients were automatically randomly assigned in a 2:1 *ratio* to receive either RAMU (8 mg/kg) or matching placebo given intravenous every 2 weeks. At the moment, AIFA has not yet defined the reimbursement by the *SSN*, therefore it is not used in clinical practice.

FDA in May 2020 and EMA in September 2020 approved ATE (anti-programmed death-ligand 1- PD-L1) in combination with BEVA (anti-vascular endothelial growth factor molecule) as first-line therapy for advanced HCC for high selected and fit patients based on the results of an open-label randomized phase III (IMbrave150) [119]. Enrolled patients were randomly assigned in a 2:1 *ratio* to receive either ATE (1200 mg) plus BEVA (15 mg/kg) given intravenously every 3 weeks or SORA (400 mg twice daily) until unacceptable toxic effects occurred or there was a loss of clinical benefit. This trial confirmed the superiority of ATE + BEVA to SORA prolonging both the OS at 12 months that was 67.2% (95% CI 61.3 to 73.1) with ATE + BEVA and 54.6% (95% CI 45.2 - 64.0) with SORA and PFS which was 6.8 months with ATE + BEVA *versus* 4.3 months with SORA (HR 0.59; 95% CI 0.47-0.76; p<0.01). In 2022, AIFA will establish the reimbursement within the *SSN* for ATE + BEVA that could deeply change the HCC treatments scenario.

In April 2019, a promising ongoing trial that can change the treatment of HCC in an adjuvant setting is started. This is a phase III, randomized, double-blind, placebo-controlled multicenter trial of durvalumab monotherapy or in combination with BEVA as adjuvant therapy in patients affected by HCC who are at high risk of recurrence after curative hepatic resection or ablation (EMERALD-2) [120]. This is a very promising trial because at the moment there are no adjuvant therapies for the treatment of HCC.

Nivolumab received accelerated approval by FDA in 2017 for second-line therapy [121], while it has not yet received EMA approval and it is currently ongoing a phase III trial which compares nivolumab with SORA in front-line therapy [122]. Another trial comparing pembrolizumab *versus* placebo in second-line therapy is currently ongoing [123]. Finally, several studies are evaluating different TKIs and/or antibodies as well as a combination of them [124–126].

Various substances were tested for either non-inferiority or superiority for the above-mentioned drugs, but most of them failed. In fact, standard systemic chemotherapy with doxorubicin or FOLFOX (folinic acid + 5-

fluorouracil + oxaliplatin) regimens did not show survival benefits, since HCC is among the most chemo-resistant cancer type; furthermore, also different TKIs did not achieve their primary endpoints such as sunitinib, erlotinib, linfanib and brivanib [8].

When HCC progresses to its end-stage, palliative and best supportive care remain the only solutions to optimize quality of life, through the management of pain, nutrition, and psychological support [8,12].

1.3. Therapeutic drug monitoring

Therapeutic Drug Monitoring (TDM) is a branch of clinical chemistry and clinical pharmacology, which represents a potential strategy to improve and personalize the drug dosage in patients through the measurement of its concentration in biological fluids, *e.g.*, plasma, serum, whole blood, or urine [127]. Since the beginning of the 60s, TDM has been applied in the clinical practice to verify if the drug levels are within the therapeutic window or if there is the need to adjust the dose to reach the effective drug plasma concentration, thus maximizing the therapeutic effect and minimizing the occurrence of toxicity, as reported in Figure 11 [128]. Moreover, the utility of TDM consists of the monitoring of therapy adherence, the discovery of drug-drug interaction, and the identification of over- or under-dosed patients who can experience severe toxicity or worse outcome, respectively.

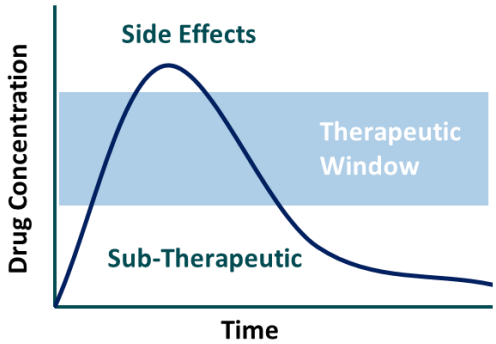

Figure 11. Schematic representation of a therapeutic window. Severe toxicity might occur if the drug concentration exceeds the upper limit, while the treatment efficacy might be compromised if the drug concentration falls below the lower limit.

Nonetheless, there are distinguishing factors necessary to properly perform the TDM practices, such as the appropriate administration of the drug, the adequate collection and processing of the biological samples, an accurate and precise analytical method of the quantification of the drug with or without its metabolites, and the appropriate interpretation of the results [129].

Therefore, TDM is a multidisciplinary approach involving different professional figures such as physician (who requires the TDM), nurse (who performs the biological fluid sampling), pharmacist (who prepares the pharmaceutical intravenous form and dispenses the medicine), pharmaceutical chemist/technician (who processes and analyzes the sample) and PK scientist (who contextualizes the concentration data and draws up the report).

Each of them has a specific role in the process and has to be conscious of the difficulties and limitations of the TDM, making an effort to optimize each task of his/her competence: the failure of only one among the steps is sufficient to compromise the whole process [129,130]. For example, a crucial parameter for a good TDM practice is the correct timing of the samples since if the actual sampling time is different from that established, and this is not noted, the resulting PK parameters are not reliable and this could compromise the clinical decision of the physician regarding the optimal dosage that fits for the patient [130]. The correct interpretation of the drug and/or metabolite concentration value could be extremely helpful for the physician to adjust the drug dosage according to the patient's clinical outcome, and other biochemical and/or clinical parameters [131].

Currently, this approach is widely applied in pharmacological treatments of many pathologies, as to dose antibiotics, antiepileptics, cardiovascular and anti-inflammatory agents, antidepressants, 6-mercaptopurine in pediatric acute lymphoblastic leukemia and Hodgkin's diseases, immunosuppressants, etc.

To be eligible for TDM approach, theoretically, a drug should fulfil several criteria as:

- to show limited intra-individual and a considerable inter-individual PK variability;
- the existence of a defined relationship between drug concentration and pharmacological effects;
- to have a narrow therapeutic window, namely a small difference among the minimum effective concentration (MEC) and the minimum toxic concentration (MTC);
- the absence of easily measurable biomarkers investigable to evaluate the drug efficacy;
- the availability of an accurate, robust, defined, and validated method for drug quantification in biological fluids [131,132].

Regarding the metronomic therapy which has been investigated as a substitute for conventional schedule [133], a useful approach to maintain drug concentrations within the targeted therapeutic window is to monitor the C_{min}. To perform it, the timing of the sample collection is crucial because the drug concentration varies during the dosing interval. Indeed, the samples to determine the C_{min} have to be taken at the steady-state, that is reached in 4-5 $t_{1/2}$ after starting the therapy [134]. Moreover, the correct sampling time should be determined also based on the drug adsorption and distribution. For example, digoxin monitoring should be performed after 6 h from the dose intake because before this time the drug is still undergoing distribution and plasma concentration would be erroneously high [135].

1.3.1. Therapeutic drug monitoring in oncology

During the last 10-30 years, cancer treatment have shifted from the use of cytotoxic drugs and nonspecific chemotherapy to chronic oral medicines with targeted molecular therapies [127].

These new targeted therapies represent a revolution of the oncologic patients' management because these drugs are orally administered and, in generally, for a long periods of time, transforming some previously

deadly disease into chronically manageable conditions [46]. Moreover, oral administration of these anticancer drugs is related to a better quality of life since patients take therapy at home and not at the hospital. However, there are also some disadvantages compared to intravenous administration: the generation of complex steps in the PK as gastrointestinal adsorption and first-pass metabolism by the liver [136], poor tolerability with resultant therapeutic failure [137], and the possibility of non-adherence to the therapy [138]. With oral targeted therapies, as well as with traditional chemotherapy, a wide inter-patient variability in treatment outcome is observed. Such variability in drug response among patients depends on several factors, including individual PK, pharmacogenetic background, environmental factors, and diet [139]. All these parameters define the drug plasma concentration profile over time, while the pharmacological effect is determined by the amount of drug which arrives at the site of interaction with target (*e.g.*, enzymes and receptors) [140]. Frequently, fixed dosage schedules develop different circulating concentrations of the active drugs among all the patients (up to 26-fold for targeted therapies) [126,141], causing undesirable toxicity in case of drug over-exposure or selection of resistant cellular clones in case of sub-therapeutic exposure [133].

However, while for drugs as digoxin, phenytoin, and aminoglycosides TDM is largely applied, in the case of anticancer drugs their quantification in plasma (or whole blood) is an uncommon practice to personalize the drug dosage, despite the high risk of therapeutic failure and toxicity. Methotrexate, a chemotherapy and immunosuppressant agent, is one of the most famous exception of TDM application in oncology field. In fact, its concentration is commonly measured in human serum by pharmacology and clinical toxicology laboratories, since the obtained data are useful to decide if the administration of folic acid as counter poison is a good choice in the case of too prolonged permanence of the drug in blood during a high-dose regimen [142].

Clinical suitability of TDM for anticancer drugs is actually limited by various factors, as:

- limited knowledge of PK and pharmacodynamic aspects, which are the most evident limiting factor to define a clear relationship among the therapeutic effect and the obtained concentration value. If the dose-response relationship is missing, a therapeutic window, which is the essential element for TDM, cannot be establish [143] and thus TDM approach turns into a random approach;
- wide heterogeneity of cancers; in fact, identical tumors do not exist: they show different sensitivity and resistance towards anticancer drugs. For this reason, every case has to be analyzed independently [144];
- more than one drugs is often used for the cancer treatment, thus making even more challenging to target the toxic and therapeutic effect at the pharmacodynamic level [145]. Drug–drug interactions are a major concern when treating patients with oral targeted therapies [146], making dosage adjustment strongly recommended in some circumstances;

- the presence of active metabolites, whose concentrations could be influenced by changes in the enzymes responsible for metabolism. This has to be taken into account when evaluating the drug's effects [147];
- the blood sampling timing in order to obtaining significant results. In fact, the sample has to be collected after distribution equilibrium to ensure that plasma concentrations better reflect those in tissue [144,148];
- the multidisciplinary approach, where the entire personnel has to be conscious of the difficulties and limitations of the TDM: a criticality that occurs only in one among the steps, is enough to compromise the whole process;
- availability of quantification method for the analytes of interest, which have to be simple, rapid, precise, accurate, sensitive, specific, not affected by matrix effects, and economically sustainable [149].

Regardless of the above-described limitations, the high promising utility of TDM in the oncological field (if correctly practiced) is noticeable because anticancer drugs normally satisfy several criteria to TDM applicability (see section 1.3), like a marked PK inter-individual variability and a low therapeutic window [46,145,150,150].

Moreover, anticancer treatment has to reach maximum efficacy to be useful but also it ideally should avoid cytotoxic adverse reactions, which are common for most of these drugs. Side effects could be very dangerous for patient's life, but also under-treatments can be, since it could contribute in compromising the probability of successful outcome. Several studies reported the benefits of a high-intensity treatment [143], indicating that curing patients with high dosages, which lead to drug concentrations very close to the upper limit of the therapeutic window, may represent a successful strategy. Consequently, if a concentration threshold for unacceptable toxic effects is established for each anticancer drug, TDM would be exploited to treat the patients with a high-intensity treatment, while minimizing the risks by keeping his/her drug concentrations below the toxicity threshold. Another resulting advantage of TDM approach could be the reduction of the PK inter-individual variability, the possibility of correctly adjusting the dosage in patients with renal and/or hepatic impairment, the improvement on patient compliance, due to the lower incidence of toxicity [144,150], and the accessibility of suitable data to better identify the drug-drug interactions [129]. Nevertheless, the modification of drugs dosage to personalize the therapeutic intervention is not a common practice, even though the high risk of toxicity and therapeutic failure.

TDM recommendation for SORA, REGO, and LENVA is now only exploratory due to the limited exposure-response and exposure-toxicity relationship studies [151].

Nonetheless, for SORA it was reported that patients who experienced grade 3 AEs had a higher C_{min} than those who did not [152]. SORA steady-state concentrations were reported to be higher in patients with grade ≥ 2 HSFR and hypertension than in those not having these AEs [153]. In a study based on 91 Japanese patients

treated with SORA (21 affected by RCC and 70 by HCC) revealed optimal SORA concentration cut-off of 5780 ng/mL and 4780 ng/mL to predict the development of grade ≥ 2 HSFR and hypertension, respectively [153]. Furthermore, in a small cohort of 25 HCC patients, the AUC ratio between SORA and oxSORA resulted as potential predictor of toxicity in order to provide safe and long-term therapy for each HCC patient treated with SORA [154].

Thus, until more studies become available, the most appropriate target for SORA TDM is C_{min} > 3750 ng/mL based on the mean C_{min} population, as reported by Verheijen et al. [155].

Regarding REGO, an exposure-response relationship for efficacy has been reported in a post-marketing study: VEGFR and VEGFR2 serum levels declined compared to baseline with a greater effect observed for daily doses of ≥ 60 mg [156]. The exposure-toxicity relationship was performed only in GIST patients noticing an exposure-dependent increase for rash, total bilirubin, and median indirect bilirubin, for parental and total (including oxREGO and des-oxREGO) REGO exposure. The potential TDM threshold could be a C_{min} > 1400 ng/mL for REGO based on the mean C_{min} population [151].

Currently, also for LENVA, exposure-response and -toxicity tests are still limited. The few available data mainly regard patients with DTC, in which higher drug exposure was found in patients with higher severe toxicity. Moreover, a longer PFS seemed to be correlated with the reduction in tumor size but not with LENVA exposure [157,158]. On the contrary, an exposure-toxicity relationship was found between LENVA concentration levels and treatment alterations, hypertension, proteinuria, nausea, vomiting, increasing of bilirubin and hepatic enzymes, *e.g.,* ALT and AST [77,157,159]. Taking into account all these limitations, the proposed TDM thresholds are C_{min} > 51.5 ng/mL [155], C_{min} > 43.4 ng/mL for patients treated with 8 mg/die of LENVA [151] and C_{min} > 95.6 ng/mL for patients treated with 24 mg/die of LENVA [151].

It is clear for all these drugs that more studies are necessary before applying TDM in clinical practice.

As concerns IDA, the only preliminary exposure-toxicity data available for its administration with the oral metronomic schedule are reported in the abovementioned trial in patients affected by metastatic breast cancer conducted at *C.R.O. di Aviano* [110]. For this reason, no specific PK targets have been identified for TDM applications yet. Nevertheless, the found relationship was between the higher IDA and IDOL C_{min} and grade 3 and 4 hematologic toxicity, while no associations were found between C_{min} and response to the therapy [110]. The obtained IDA and IDOL clinical plasma concentrations (standardized for dose/m^2) range at the steady-state were between 0.11 ± 0.04 ng*m^2/mL*mg (C_{min}) to 0.18 ± 0.07 ng*m^2/mL*mg (C_{max}) and between 1.02±0.39 ng*m^2/mL*mg (C_{min}) and 1.14 ± 0.39 ng*m^2/mL*mg (C_{max}), respectively.

To improve the knowledge about exposure-response or -toxicity relationships it is necessary to determine the concentration in patients' plasma samples. Two different studies, that include also the determination of the C_{min} in plasma samples, are currently ongoing at *C.R.O. di Aviano*:

- an analytical cross-validation study entitled: "Cross-validation study of innovative LC-MS/MS methods on Dried Blood Spot (DBS) with the Gold Standard LC-MS/MS assays on plasma samples for

the therapeutic drug monitoring of several oral anticancer drugs" (internal protocol code: CRO-2018-83). This protocol involved the following drugs: SORA, REGO, LENVA, palbociclib, ribociclib and abemaciclib. The last three drugs are used for the treatment of advanced and metastatic breast cancer. The aim of the study is to define the feasibility to quantify these drugs both in plasma and in Dried Blood Spot (DBS) mediated by a cross-validation between the two analytical methods (for details, see section 3.1);

- A phase II clinical study named "*Studio di Fase II che valuta l'efficacia e la sicurezza del trattamento metronomico orale con Idarubicina in pazienti affetti da Epatocarcinoma allo stadio intermedio-avanzato dopo fallimento o intolleranza a Sorafenib e Regorafenib*" (internal procotocol code: CRO-2017-42), reported in section 3.2;

Although for these studies, the C_{min} evaluations are only secondary aims, they may be useful to deepen the knowledge about different plasma levels: in fact, these studies will also give the possibility to collect preliminary data regarding the intra- and inter-patients variability of C_{min} values for the analyzed drugs. Indeed, the obtained data will be useful to evaluate more rationally the correlation between C_{min} values and patients' toxicity development or outcome.

Given these premises, it is obvious the necessity to have a robust, simple, rapid, reliable, sensitive, precise, and accurate analytical method to quantify drugs in patient samples both in plasma and in DBS, using adequate calibration ranges, which cover the expected clinical ones.

1.3.2. TDM performed using Dried Blood spot

As mentioned before, one of the main hurdles for routine use of TDM in clinical practice is sample collection. The typical matrix for TDM application is plasma or serum coming from a blood sampling, which requires a nurse for the blood drawn and moving the patient to the hospital [160]. Moreover, this sample type needs blood centrifugation and accurate sample storage before the analysis, which requires the cold chain.

A possibility to perform TDM with a patient-friendly and cost-effective routine diagnostic tool could be the DBS [161]. Indeed, DBS represents an innovative and less invasive sampling procedure in which a blood drop from a finger-prick is deposited on a suitable filter paper (*e.g.,* the same sampling that diabetic patient perform to determine his/her glycemia level) and let dry at room temperature before the storage. Once the sample is dried, it can be packed and sent to the laboratory for analysis, as reported in Figure 12.

In 1963 Robert Guthrie and Ada Susi introduced the DBS collection technique to perform the newborn screening for the determination of the phenylalanine to detect the phenylketonuria [162]. Even though this assay is now performed in that way, the term "Guthrie card" continues to be used to colloquially describe the DBS sampling technique. In 1976, the first application of MS to quantify fatty acid by direct chemical ionization from DBS matrix was reported [163].

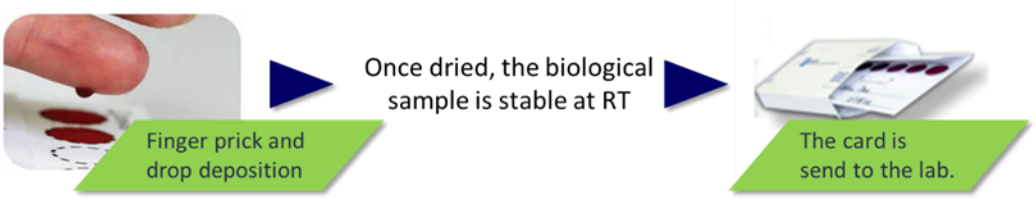

Figure 12. Graphical representation of how the DBS sampling technique works.

Up to now, the DBS technique has several applications in clinical practice, basic research, and population-based research. The most widely and common clinical use of DBS sampling collection is for newborn screening programs, which are primarily focused on the detection of metabolic disorders [164]. Other clinical applications in the published literature have been concerned with HIV surveillance, clinical chemistry, and TDM [165]. Basic research applications for DBS include drug discovery and development, biomarker development and validation, doping, systems biology, forensic science, and toxicology [166,167]. DBS is also applied for immunoassays in the analysis of SARS-CoV-2 antibodies [168–171].

The possible advantages of the DBS sampling technique for the TDM approach are the following:

- minimally invasive, less painful, and easy samplings: patients can perform the finger prick at home and no phlebotomist is necessary;
- only a small blood volume is required. In this way, blood samplings from neonates, children, the patients who suffer from phlebitis, are no longer a limitation [172]. Moreover, DBS facilitates the blood collection through tail vein promoting an animal-friendly preclinical drug development and contributes to the animals' protection for scientific reasons [173,174];
- convenient storage and transport: the shipment can be performed at room temperature by mail without taking special precaution and reducing the biohazard risk of hepatitis, HIV, or other blood-borne viruses origin for laboratory personnel when preparing blood unknown samples [175,176];
- most analytes are more stable in the DBS matrix than in frozen samples [177,178].

On the other hand, the DBS sampling technique has also some disadvantages:

- only small volumes are available and therefore a sensitive analysis technique is required to perform the analyte quantification. Often no replicates are possible since only one spot from the patient is accessible;
- the time of the blood sampling is patient self-reported and no check on the origin of the blood is performed;
- the sampling is not always successful, despite adequate training of the patient. Self-sampling could be associated with contaminations and samples with unacceptable quality [179];
- capillary concentration can be different from venous one since the blood deposited on the DBS card is composed of interstitial fluid, plasma, and blood cells [172];

- the clinical validation is obligatory because it is necessity to convert the DBS concentration into the corresponding plasma concentration because for most analyte the threshold is defined in the plasma matrix [180,181];
- an extensive validation procedure is required. The assay performance can be influenced by recovery, hematocrit (Hct) effect, spot volume, and spot homogeneity. Any change in filter paper type and/or manufacturer requires partial validation [181–183].

Liquid chromatography coupled with tandem mass spectrometry (LC-MS/MS) methods for the quantification of anticancer drugs in the DBS matrix reported in the literature are continuously increasing, but at the moment no methods are described for SORA, REGO, and LENVA.

1.4. LC-MS/MS for TDM application

In the last 40 years, analytical techniques used in cancer pharmacology to quantify drug concentration and to study drug metabolism have undergone significant improvements. The analytical techniques and the quantification methods are essential to perform TDM determining the drug concentration in biological fluids. In the beginning, the determination of drug concentration in biological fluids was obtained by liquid chromatography (LC)-UV/vis methods, followed by fluorescence techniques which are more sensitive and reliable. The real turning point in the bio-analysis field was represented by the development of bench-top mass spectrometry instrument, which allows simpler workflows and faster analytical times [184].

The history of mass spectrometry (MS) began more than 100 years ago with the work of the Nobel prize Sir Joseph John Thomson between 1897 and 1913 about the separation into two isotopic components from a stream of ionized neon gas by applying an electric and a magnetic field to it [185]. Successively, MS endured several and rapid technological development and became a largely applied analytical technique in chemical and physical sciences. Until the 1980s, when John Fenn perfectioned the electrospray ionization (ESI) allowing the soft ionization of large biomolecules [186,187], the MS application in biological specimens was limited only to low molecular weight compounds (until 200 Da) [188]. Another important improvement in MS applications for bio-analysis was during the mid and late 1990s with the shift from gas chromatography (GC) to LC as a MS front-end technology, which permitted much simpler workflows and significantly faster analytical times. Indeed, GC requires a certain level of analyte volatility, thus time-consuming and elaborate extraction and derivatization procedures had to be used because most biologically active molecules are involatile, thermolabile, and polar [189]. On the other hand, LC is able to separate components in a complex matrix with a high precision and reproducibility, while MS, particularly in tandem mass spectrometry (MS/MS), provides both qualitative and quantitative information about the several analytes in the biological matrix [190].

Nowadays, LC-MS/MS is the most widespread analytical technique used to determinate drug concentration in biological samples (*e.g.,* whole blood, plasma, serum, urine, and feces) [191].

1.4.1. Principles of liquid chromatography

In analytical chemistry, chromatography is the technique applied to purify and separate the different components contained in a mixture, exploiting their different affinity for the stationary phase (SP) - generally a solid - and a mobile phase (MP; composed by an aqueous-organic mixture) flowing over it, which could be gaseous or liquid according to the technique used (GC or LC, respectively). The separation of the analytes is based on their different distribution between the two aforementioned phases that depends on their physical-chemical properties (mass, polarity, charge, functional groups, etc.). During the elution, the analytes are involved in a dynamic transfer process between the two phases, passing through an infinite series of equilibrium states in each "infinitesimal" layer of the column. This phenomenon is described by the ratio between the analyte concentration in the SP (C_s) and in the MP (C_m), called the partition coefficient (K), which changes according to the compound's different affinity for one or the other phase. K is calculated with the Equation 1.

$$K = \frac{C_s}{C_m}$$

Equation 1. Equation for partition coefficient.

The lower the K value for a definite compound, the higher its affinity for the MP will be; in addition, being the SP equal, K values change based on the compound to be eluted and the composition of the MP. Consequently, the separation will be obtained thanks to the different migration of the compounds present in the mixture.

Based on the separation principle, which depends on peculiar analyte properties and the specific MP and SP used, different types of chromatography can be determined:

- partition chromatography: the separation of the compounds is based on the K relative to a biphasic (aqueous/organic) system. If the MP is more polar than the SP it will be called reverse phase (RP), whereas in the opposite case it is named normal phase (NP);
- adsorption chromatography: the separation of the compounds occurs according to the adsorption coefficient of the SP;
- affinity chromatography: separation of the compounds is based on reversible, biochemical, and very specific reactions;
- ion-exchange chromatography: SP contains active charged (negative or positive ion exchange resin) groups, able to exchange their counter ions with the ions in MP or in the sample due to a competitive mechanism;

- size exclusion chromatography: the separation of the compounds occurs according to molecular size. It is also called gel filtration/permeation chromatography.

The methods described in this PhD thesis are based on RP chromatography, which is usually indicated for the separation of lipophilic molecules (*e.g.,* most drugs) since the predominant retention mechanism is due to hydrophobic interactions with SP. Indeed, SP is normally a matrix (silica, polymer, or silica-polymer hybrid) derivatized with apolar chains of different lengths (*e.g.,* phenyl, octilsilyl, octadecilsilyl, etc.). During the chromatographic run, the analytes are retained on the SP and, as the MP continues to flow through the column, there will be the detachment of the different analytes retained by the SP based on their affinity for the MP.

At the end of the analysis, a chromatogram is obtained displaying the signal provided by the detector (Y-axis) as a function of time of analysis (X-axis) and peaks corresponding to the analytes eluting from the column which cause an increment of the detector response (Figure 13).

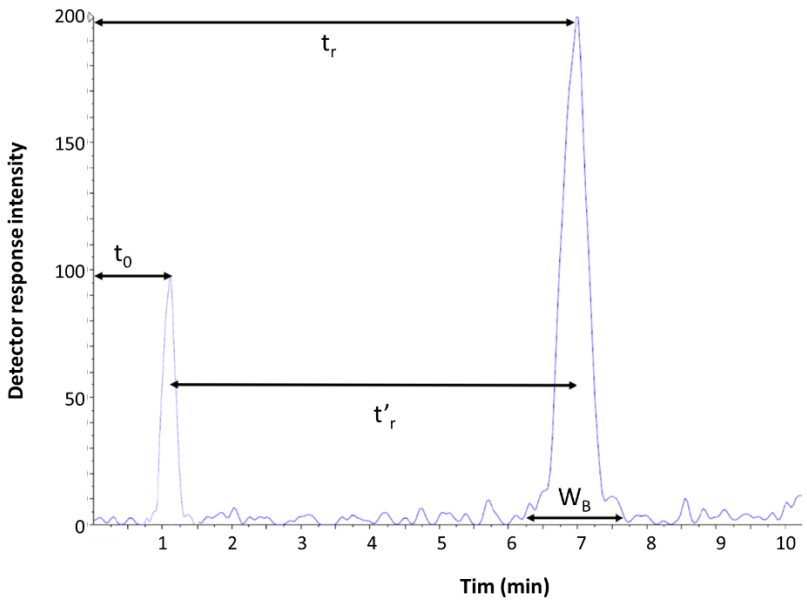

Figure 13. Representation of a generic chromatogram. t_0: dead volume; t_r: analyte retention time; t'_r: adjusted retention time.

A good chromatographic separation is characterized by symmetrical, narrow, and base-line separated peaks. The most important issue in chromatography is to achieve optimum resolution (R_s) in the minimum time ($R_s \geq 1.5$ to obtain the separation at the baseline).

The fundamental equation in chromatography is reported below:

$$R_s = \frac{\sqrt{N}}{4} x \left(\frac{\alpha - 1}{\alpha}\right) x \left(\frac{K'}{1 + K'}\right)$$

Efficiency Selectivity Capacity

Equation 2. Fundamental equation in chromatography.

This equation defined the R_s, which describes the capacity of the system to separate two consecutive chromatographic peaks and it is affected by three important parameters:

- efficiency, which is a determination of the dispersion of the analyte band as it travels through the column, reflecting the column performance. This parameter depends on the number of theoretical plates (N), *i.e.,* the ideal segment in which the column is divided. In particular, each plate identifies a single equilibrium stage of analytes distribution between SP and MP. As N increases, the quality of separation increases thanks to a greater number of exchanges between the SP and MP. In order to improve chromatographic efficiency, longer columns can be used, thus increasing total runtime. Moreover, N can be increased by using a column with smaller-sized particles to decrease plate height (H), preserving the same column length (L). The Equation 3 relates these three parameters:

$$H = \frac{L}{N}$$

Equation 3. Equation to determine the efficiency.

Moreover, efficiency can be determined also using the t_r and the peak width at the baseline (w_b) following the Equation 4.

$$N = 5.54 \ x \left(\frac{t_r}{w_b}\right)^2$$

Equation 4. Alternative equation to determine the chromatographic efficiency.

- selectivity (α), which implies the chromatographic system's ability to distinguish among two species (A and B) and it is obtained using the optimal MP and SP combination for the analyte of interest. α is determined by the ratio between the capacity factor of analyte A (k'_A) and the capacity factor of analyte B (k'_B), as reported in the Equation 5. The two compounds are separated only if α is major than 1.

$$\alpha = \frac{k'_A}{k'_B}$$

Equation 5. Equation to determine the selectivity.

- capacity factor (k') is the measure of the analyte's retention into the chromatographic column and it is calculated with the Equation 6:

$$k' = \frac{t_r - t_0}{t_0}$$

Equation 6. Equation to determine the capacity factor.

Where t_r is referred to the analyte elution time, while t_0 is the dead time, *i.e.*, the elution time of the non-retained compound. The lower is the k' value, the less the compound is retained by the SP, due to its lower affinity, and the earlier it elutes from the column and *vice-versa.*

R_s can be calculated by also using the Equation 7.

$$R = 2\,x\,\frac{t_{rB} - t_{rA}}{w_{bB} - w_{bA}}$$

Equation 7. Alternative equation to determine the resolution.

The analytical methods developed in this PhD thesis use a High-Performance LC (HPLC) apparatus coupled with a mass spectrometer, which allows to reach the best selectivity and sensitivity for quantitative analysis of compounds in complex matrices as plasma and DBS samples. The HPLC instrument offers several advantages compared to the classical LC apparatus, such as small sample volumes required, constant elution rate, guaranty of an excellent accuracy and precision of the results and it is automatable.

The HPLC SP is composed of solid adsorbent microparticles whose small particle size, generally between 3-10 µm, allows to increase SP-MP exchange surface. In addition, small particles are homogeneously packed inside the column. For this reason, HPLC differs from traditional LC because the operating pressures are significantly higher (5000 psi), while LC typically relies on gravity force to let MP flow through the column. MPs are characterized by high purity grade and low viscosity, and they are also immiscible with the SP and compatible with the detector.

1.4.2. Principles of (tandem) mass spectrometry

MS is an instrument able to detect charged analytes measuring the ratio between their molecular mass and charge (*m/z*), with an accuracy that may achieve 0.01%. Each spectrometer is constituted by four elements, sampler inlet, ion source, mass analyzer and detector. The ion source allows to ionize the neutral compound trough electron capture or ejection, deprotonation, protonation, or adduct formation to obtain charged molecules, which can be detected by the mass analyzer, as reported in Figure 14.

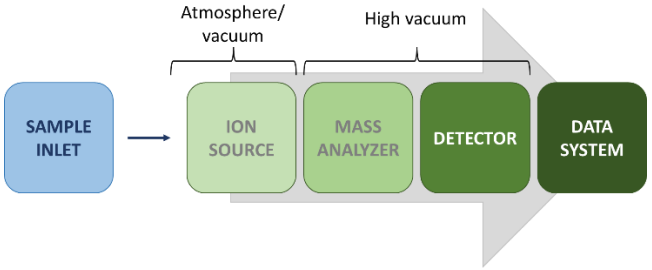

Figure 14. General representation of mass spectrometer components.

The spectrometer detect only the charged molecules, so the ionization process is crucial. The ionization techniques used in MS are classified based on their strength:

- "hard" technique: apply high energy causing extensive molecule fragmentations, *e.g.,* electron ionization (EI);
- "soft" techniques: apply low energy and produce only ions of the molecular species, *e.g.,* chemical ionization (CI), atmospheric pressure chemical ionization (APCI), electrospray ionization (ESI), fast atom bombardment (FAB). The matrix-assisted laser desorption ionization (MALDI) type also belongs to these "soft" techniques and it is exploited for the production of intact gas-phase ions from a broad range of large, thermally labile, and non-volatile compounds like synthetic polymers, oligonucleotides, and proteins.

ESI and MALDI are nowadays the most widespread ionization techniques for biomolecular mass spectrometry, offering excellent mass range and sensitivity. In particular, ESI is the most common ionization technique applied for the analysis of samples obtained from RP separation on the LC system.

Since the LC-MS/MS methods developed in this PhD thesis have used an ESI source, a detailed description of its operating mode is reported afterward and a schematic representation is shown in Figure 15. Moreover, some of the characteristics and conditions below described are specific of the SCIEX API 4000 Qtrap spectrometer, the instrument adopted for the methods development object of this PhD thesis project.

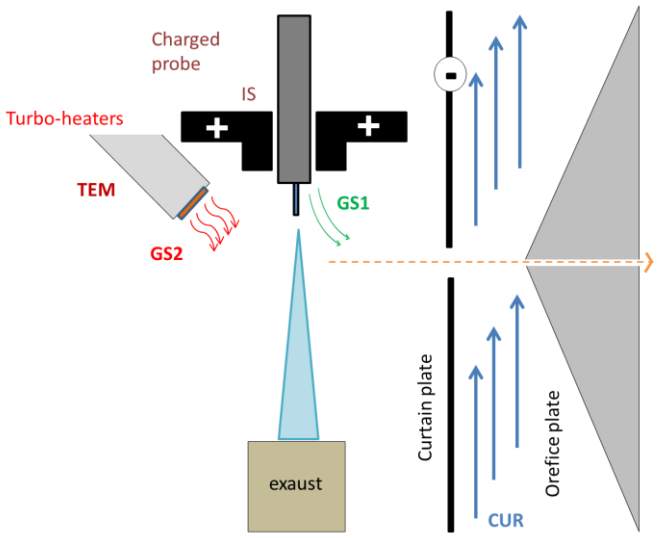

Figure 15. Schematic representation of an ESI source operating in negative mode. Red and green arrows represent nebulizer and heater gasses, respectively. The charged probe represents the anode (-), while the curtain plate is the cathode (+). Once the sample undergoes nebulization, analytes protonated molecules (orange dotted arrow) are accelerated to the mass analyzer. Curtain gas (blue arrows), which flows between the curtain plate and orifice place, prevents solvent and analytes neutral molecules from entering the mass analyzer. All the solvents and analyte particles that do not enter the instrument are conveyed towards the waste collector (exhaust).

ESI source produces gaseous ionized molecules directly from a liquid solution. In order to be analyzed, the compound is previously dissolved in a volatile MP added with a small amount (0.1-0.5%, v/v) of weak bases or acid that facilitate the ionization process, and then it is let to enter into a probe, which is a stainless-steel

capillary. Between its counter-electrode and the probe, a voltage (from +2 to +5 kV in positive ion mode or from -2 to -5 kV in negative ion mode) is applied, that allows the formation of a nebulized solution cone, also called Taylor's cone, made of charged species within the solution, just outside the capillary. Its formation is attributable to the presence of charged species within the solution, exposed to the electrostatic field existing among the counter-electrode and the capillary. After that, the droplets' formation is observed from the cone apex, and charged droplets further migrate through the atmosphere to the counter electrode [192]. The charged droplets formation at the apex of the cone is strongly influenced by ionic analytes and inorganic salts concentration, solvent physical-chemical characteristics, and the applied voltage.

At atmospheric pressure, each droplet undergoes solvent evaporation conserving their total charge value: the energy required for this step is provided by both two auxiliary heated gas flows (the heater gas (GS2) coming from the sides and the nebulizer gas (GS1), which flows longitudinally along the capillary perimeter) and by the environment thermal energy obtained using a heated capillary.

The droplets thus decrease their radius, still maintaining their total charge value; as their size decreases, surface charge density rises until the droplet radius reaches the stability limits of Rayleigh, meaning that the electrostatic repulsion equals the surface tension [193]. Subsequently, charged droplets reach instability and decompose through the "Coulombic explosion" process, thus producing microscopic droplets that release de-solvated ions at the end of the process [194].

The produced ions are then transferred from the source to the mass analyzer under high vacuum conditions (10^{-5} Torr), in order to avoid impact with atmospheric gas molecules that could affect their ionization yield. The entrance of the mass analyzer presents two conical, center-pierced, steel plates (*e.g.,* orifice plate and curtain plate), separated by a very tiny interstice, where a curtain gas, usually nitrogen, flows under pressure to prevent the entrance of neutral contaminants.

ESI leads to the formation of singly charged small molecules but it is also well-known for producing multiply charged species of larger molecules. This is an important phenomenon because a mass spectrometer measures the *m/z* ratio and therefore multiple charging makes the observation of large molecules possible even using an instrument with a relatively small mass range. Many solvents can be used in ESI: they are selected according to their volatility and ability to donate a proton and to the analytes' solubility. Usually, solvents such as methanol (MeOH), acetonitrile (ACN) or are used, but other solvents, as isopropanol (iPrOH) or dimethyl sulfoxide (DMSO), could be employed to increase the analytes' solubility. In some cases, the use of 0.1% of acid (formic -HCOOH or acetic – CH_3COOH) is also suitable to facilitate ionization. Buffer like Na^+, K^+, or phosphate present a problem in ESI by lowering the volatility of the droplets and the vapor pressure, resulting in a reduced signal through a droplet surface tension increase. Therefore, volatile buffers such as ammonium acetate (AmAc) can be used more effectively.

With the advent of ionization sources that can vaporize and ionize biomolecules, it has become necessary to improve mass analyzer performances compared to accuracy, resolution, and speed.

Several types of mass analyzers exist, each of them following different working principles to separate ions according to their *m/z* ratio; some separate ions by time, while others separate ions in space.

For example, time-of-flight (TOF) analyzer separates ions according to the time that each ion takes to pass through a free-field space, called flying tube; the quadrupole analyzer exploits the stability of the trajectories in presence of an oscillating electric field to separate ions according to their *m/z* ratios; the ion trap analyzer uses a radiofrequency (RF) quadrupolar field in two or three dimensions to trap ions with different masses together and expel them according to their masses to obtain a spectrum. Whereas, the analyzer based on magnetic sectors selects the ions according to their momentum, given a circular trajectory and a specific value of the magnetic field. Finally, some mass spectrometers combine several types of analyzers.

Among these types of analyzers, a triple quadrupole can generally be found coupled to an ESI-type source to perform tandem MS analysis for quantitative purposes.

A quadrupole is composed of four parallel metal rods and each opposite rod pair is connected electrically. A two components (RF and direct-current – DC) voltage is applied between adjacent rods. The focusing of ions with a wide *m/z* range occurs when only RF component is applied; when DC voltage is added to RF, only ions with a selected specific *m/z* value are allowed to pass through the quadrupole while ions with a higher or lower *m/z* value will be lost by colliding against the rods due to unstable trajectories [195] as reported in Figure 16. To acquire a mass spectrum, it is necessary to increase both the RF and DC voltages, while maintaining their ratio constant, in a way that a certain mass range could be scanned to transmit ions of increasing *m/z.*

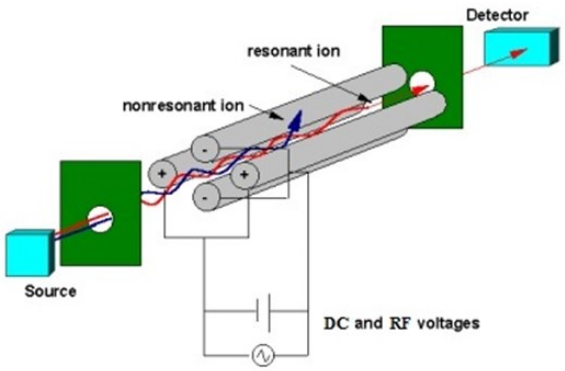

Figure 16. Graphic representation of a quadrupole analyzer and its operating principle. Resonant ions are able to pass through the quadrupole and be recorded by the detector; non-resonant ions collide against the rods.

A triple quadrupole analyzer consists of a system of three quadrupoles in series. In tandem mass spectrometry (MS/MS or MS^2), the first (Q1) and the third (Q3) quadrupole work as a filter that discriminates ions with a specific *m/z* value; the second quadrupole (Q2) works as a collision cell where a controlled fragmentation (also called collision-induced dissociation or CID) of the analyte takes place, with appropriate collision energy. At last, Q1 is preceded by Q0, a smaller quadrupole equipped only with RF and characterized

by an ions-focusing function. Depending on the analysis goal, Q1 and Q3 can be used in different modalities to acquire the data.

Through MS/MS is hence possible to obtain information both on the mass of the analyte of interest (precursor or parent ion) and of its fragments (product or daughter ions) obtained in Q2.

Normally, analyte *m/z* value gives information about its identity; in the case of low-resolution MS, analyte identity is obtained also by analyzing its fragmentation pattern. In fact, the fragmentation pattern of each compound is a sort of proper fingerprint.

For quantitative analysis, the most common scanning mode is selected reaction monitoring (SRM), and its application to more than one fragment is called multiple reaction monitoring (MRM). MRM mechanism is the following: Q1 acts as a first filter and selects analyte precursor ion which enters in Q2, where the inert gas (argon or nitrogen) triggers its fragmentation; product ions exit from Q2 and reach Q3 which acts as a second filter, focusing ions with a specific *m/z* value to the detector, as reported in Figure 17.

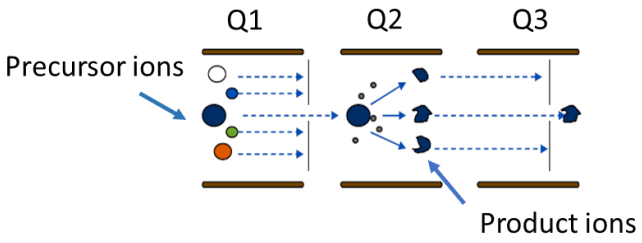

Figure 17. Schematic representation of the ion pathways during the SRM mode.

In this way, the obtained spectrum represents the fragmentation products of the selected ion. SRM mode allows to reach a high specificity and to achieve a high signal-to-noise ratio (S/N), allowing a great analysis sensitivity. These increased sensitivity and specificity given by SRM mode, have led to two important advantages: 1) the possibility of detecting drugs and metabolites at very low concentration values and, subsequently, the possibility of using very small sample volumes; 2) the opportunity of detecting the analytes of interest in the presence of a complex biological matrix such as tissues or whole blood.

The coupling of LC with MS/MS allowed to make this technique the most widespread and precise method for quantitative analyses, often used as a Gold Standard for comparison with other techniques.

Examples of the most prevalent uses of MS/MS in clinical diagnosis are the screening of newborns for congenital metabolic diseases such as aminoacidopathies, organic acidurias, and fatty acid oxidation disorders [187,196]. Other applications regard multi-analyte TDM especially for the administration of cocktail therapies involving immunosuppressants [197], anti-virals [198], oncology drugs [199], etc. The most obvious factor responsible for the limited throughput of LC-MS/MS is the time required for sample introduction into the LC and the subsequent time necessary for chromatography. Once a chromatographic system has been fully optimized to minimize the time needed to remove interferences and to separate analytes from solvent fronts, there is no space for further improvement in throughput.

1.5. Validation of a LC-MS/MS method

A LC-MS/MS method used for the quantitative determination of analytes in a biological matrix (*e.g.,* plasma, whole blood, urine, saliva, or DBS) needs to be validated according to the EMA (2011)[200] and/or FDA (2018) [201] guidelines, in order to give reliable and reproducible data. In fact, the main goal of method validation is to demonstrate the consistency of a determined method developed for the quantification of an analyte concentration in a specific biological matrix, like blood, serum, plasma, urine, or saliva.

Already in 1990, there was the necessity to define and spread among the pharmaceutical community the guidelines for the analytical method validation from the first American Association of Pharmaceutical Scientists (AAPS)/FDA bioanalytical workshop [202].

The validation principles, derived from teamwork between regulatory institutions and researchers in the bioanalytical field, were introduced into the health regulations in Canada in 1992, and, afterward, the FDA published the first edition of its Guidance on Bioanalytical Method Validation in May 2001 [202]. This guidance describes the required workflow for the validation of analytical procedures such as LC, LC-MS, GC, GC-MS, ligand binding assays (LBA), microbiological procedures, and immunological assays. Meanwhile the publication of the first FDA guidelines, the dialog significantly raised through scientific conferences not only in the USA but worldwide too: in 2011, the EMA presented the Guidance on Bioanalytical Method Validation in Europe [200]; in 2013, the FDA released a revised draft of the Guidance for Industry Bioanalytical Method Validation and then, finally a definitive version of the FDA guidelines was released in May 2018 [201].

It is useful to follow both the guidelines since the most validation parameters recommended are the same with the identical acceptance criteria, with the exception of recovery and matrix effect: FDA gives validation recommendations on recovery assessment and no indications on matrix effect evaluation, while EMA reports recommendations on matrix effect investigation but no indication on recovery assessment. Indeed, the International Council for Harmonization (ICH) proposes ICH M10 on bioanalytical method validation guidelines [203] to unify the due validation guidelines in order to improve the consistency and quality of the bioanalytical data in support of the development and market approval of both chemical and biological drugs. This version is now only in draft.

The validation of an analytical method is essential to successfully conduct clinical (many phase I and phase II trials) and non-clinical pharmacological studies which frequently have the aim to determine the concentration values of the analytes of interest for pharmacokinetic analysis; consequently, the quality and reliability of the collected data is essential for the study results [201,204]. For this reason, the validation method procedure has to be detailed and available reporting the instrumental conditions, the materials and the reagents to be used, and the preparation of standards and samples; moreover, several preliminary tests must be carried out to set up the bioanalytical method sufficient to solve all the critical aspects. The guidelines establish a detailed scheme of procedures that the operator has to follow in order to obtain

reliable data. The fundamental parameters for the validation of the LC-MS/MS method are linearity of the calibration curve, recovery of the analyte from the matrix, precision, accuracy, selectivity, sensitivity, matrix effect, dilutional integrity, stability under several laboratory conditions of the analytes both in the biological matrix and in stock and working solutions.

There are three different types and levels of method validation:

- full validation: all the validation parameters are determined because the method is new or already existing in literature but not yet validated, or the analysis of other metabolite(s) is added to an already validated method;
- partial validation: is performed if little modifications are introduced to an already validated method (*e.g.,* change of range, modification of sample processing, modification of storage condition, change of anticoagulant, etc.);
- cross-validation: comparison between validation parameters of two or more bioanalytical methods used in the same study or between data obtained from different laboratories using the same method is performed.

Regarding the DBS matrix, there are no specific guidelines established by regulatory organizations. In 2019, the International Association of Therapeutic Drug Monitoring and Clinical Toxicology (IATDMCT) proposed DBS specific guidelines for quantitative analysis of small molecules drugs and their metabolites using the chromatographic technique for TDM application based on several white papers on DBS matrix analysis [182,183,205], EMA [200], FDA [201] and Clinical and Laboratory Standard Institute (CLSI) guidelines [206]. The recommended parameters to be evaluated are selectivity, linearity, accuracy and precision, dilution integrity, carry over, recovery, matrix effect, and process efficiency, stability under different storage conditions, volume effect, Hct effect, and volcano effect.

2. AIMS OF THE PROJECT

Hepatocellular carcinoma (HCC) is the fourth most common cause of cancer-related death and it is characterized by a dismal patients outcome being highly resistant to conventional pharmacological treatments. For these reasons, nowadays, a great challenge is represented by the attempt to improve the efficacy of clinically approved therapies, together with the search for new drugs or the repositioning of existing therapeutic agents with different administration schedules, which may represent an important option to the paucity of chemotherapy choices. On this ground, this PhD project considers 4 orally administered drugs used in the treatment of HCC: sorafenib (SORA), regorafenib (REGO), lenvatinib (LENVA), which are approved first- and second-line therapies for this pathology, and idarubicin (IDA), a possible third-line treatment currently evaluated in an ongoing phase II clinical trial at *C.R.O. di Aviano*. SORA, REGO, and LENVA brought unequivocal advantages to HCC therapy, but their use is still associated with some limitations. In fact, they are still administered at standard fixed doses, but they usually display high inter-patient variability in plasma exposure, which may affect their toxicity or efficacy. As regards IDA, its oral administration is still experimental, being exposure-toxicity data of IDA and IDOL available only from one study, highlighting the necessity of deepening this type of investigation to increase knowledge on exposure-response and toxicity relationships of this drug.

Therapeutic Drug Monitoring (TDM) is the clinical practice of measuring a specific drug at defined intervals of time to maintain plasma concentrations within a targeted therapeutic window, to minimize toxicity and maximize efficacy. In this context, TDM could be a possible tool to deepen the knowledge of circulating drugs levels achieved by patients and finally to improve their clinical outcome.

Despite the undeniable advantages that TDM may bring to therapy optimization, its application in oncology field is still sporadic and generally scarce. Two of the main barriers for routine implementation of TDM in clinical practice are represented on the one side by the availability of robust, sensitive, and reproducible analytical methods to quantify drugs in biological fluids and on the other side by sample collection. The typical matrices for TDM analyses are plasma or serum, which require specialized personnel for the blood drawn, patient's attendance to the hospital, technical instrumentations for sample preparation and refrigerated sample transportation and storage. DBS is an innovative and less invasive sampling procedure that can represent a possibility to perform TDM in a patient-friendly and cost-effective way.

Given these premises, this PhD project was focused on:

- the development and validation according to international guidelines of LC-MS/MS methods for the quantification of the SORA, REGO, and their active metabolites in human plasma;
- the development and validation according to international guidelines of LC-MS/MS methods for the quantification of the SORA, REGO, and their active metabolites in DBS;
- the development and validation according to international guidelines of LC-MS/MS methods for the quantification of the LENVA in human plasma;

- the development and validation according to international guidelines of LC-MS/MS methods for the quantification of LENVA in DBS;
- to perform a cross-validation between the methods developed in plasma matrix (considered as reference methods) and those developed in DBS;
- the development and validation according to international guidelines of LC-MS/MS methods for the quantification of the IDA and its active metabolite in human plasma;

The drug quantification methods set up within this PhD project were developed in the context of two different studies ongoing at the *C.R.O. di Aviano*:

- "Cross-validation study of innovative LC-MS/MS methods on Dried Blood Spot (DBS) with the Gold Standard LC-MS/MS assays on plasma samples for the therapeutic drug monitoring of several oral anticancer drugs" (internal protocol code: CRO-2018-83): which assesses the reliability of innovative analytical methods based on DBS technique for the quantification of several oral anticancer drugs including SORA, REGO and LENVA. The reliability will be defined by analyzing patients' samples with the new DBS methods and comparing these results with those obtained with the Gold standard LC-MS/MS methods developed for the quantification of the same drugs in plasma.
- "*Studio di Fase II che valuta l'efficacia e la sicurezza del trattamento metronomico orale con Idarubicina in pazienti affetti da Epatocarcinoma allo stadio intermedio-avanzato dopo fallimento o intolleranza a Sorafenib e Regorafenib*" (internal protocol code: CRO-2017-42): evaluates the possibility to use IDA with an oral metronomic schedule as third-line therapy for the treatment of advanced HCC in patients previously treated with SORA and/or REGO. The quantification method developed with this PhD project will be used to collect preliminary data related to the possible correlation between IDA and IDOL (active metabolite) C_{min} and clinical outcome or hematological toxicities (grade > 2);

More in detail, particular attention was paid to the following aspects:

- the optimization of both spectrometric and chromatographic conditions for the rapid and specific detection of the analytes in a complex biological matrix (*e.g.,* human plasma and DBS samples);
- the optimization of the sample handling to obtain a simple and fast processing method, minimizing the needed sample volumes;
- the validation according to European Medicines Agency (EMA) and Food and Drug Administration (FDA) guidelines for the plasma-based method and also to European Bioanalysis Forum (EBF) recommendation and International Association of Therapeutic Drug Monitoring and Clinical Toxicology (IATDMCT) for the DBS-based method;
- the quantification of patients' samples collected thanks to the two after-mentioned clinical studies.

3. MATERIALS AND METHODS

The analytical LC-MS/MS methods both in plasma and DBS matrices proposed in this thesis were developed to support two different clinical trials ongoing at *C.R.O. di Aviano* (*Centro di Riferimento Oncologico* – National cancer institute of Aviano - PN, Italy). These trials are described in the two following sections.

3.1. The analytical cross-validation study (internal protocol code: CRO-2018-83)

The proposed LC-MS/MS methods for the quantification of 1 - SORA, REGO, and their active metabolites and 2 – LENVA, were developed in the context of an analytical cross-validation study entitled "*Cross-validation study of innovative LC-MS/MS methods on Dried Blood Spot (DBS) with the Gold Standard LC-MS/MS assays on plasma samples for the therapeutic drug monitoring of several oral anticancer drugs*" (internal protocol code: CRO-2018-83) ongoing at *C.R.O. di Aviano*. The study aims at assessing the reliability of innovative analytical methods based on DBS for the quantification of several anticancer drugs, including SORA, REGO, and LENVA, by comparing such assay with the Gold Standard LC-MS/MS methods in plasma.

For this reason, we developed and validated both the plasma-based LC-MS/MS quantification method (considered as "reference") and the DBS-based analytical method (considered as "comparator"). According to the principal guidelines for the validation of analytical methods (EMA and FDA [200,201]), to establish the reliability of the comparator's measurements, a cross validation study should be conducted on subject samples to be analyzed by both the reference and the comparator methods. Thus, to proceed with analytical validation of the new quantification methods based on DBS, it is necessary to have patients' samples in order to compare the resulting quantifications with those obtained with the reference assay (LC-MS/MS method in human plasma).

This analytical cross-validation study was approved on 5th March 2019 by the local ethics committee (*Comitato Etico Unico Regionale*- C.E.U.R.) and is conducted according to the Declaration of Helsinki principles [207]. Patients were informed by their oncologist about the analytical cross-validation study during their visits and were recruited only after the signature of written informed consent.

The enrolment of patients treated with SORA or REGO started in the March 2019, while for those treated with LENVA were enrolled starting from October 2020.

3.1.1. Patient's characteristics

Patients entered the study according to the following eligibility criteria:

- to be treated with SORA, REGO or LENVA according to the routine clinical practice at any dose and any treatment cycle, but patients should be at the steady state;
- age ≥ 18 years;
- life expectancy > 3 months;

- provide a signed written informed consent.

The exclusion criteria were:

- unreliable and/or non-collaborative patients;
- refusal of informed consent.

3.1.2. Treatment and sampling

Blood samples were collected at the steady state and possibly at a specific time in order to have the drug's concentration at the C_{min} level, *i.e.,* immediately before the next pill(s) intake. For this analytical cross-validation study, blood sampling was preferred at a specific time in order to collect preliminary data regarding intra (consecutive sampling from the same patients) and inter-patients C_{min} variability.

In particular, the steady-state, and thus the correct C_{min} value, is reached approximately after 5 drug half-lives: indications about when blood sampling should be performed were decided according to each drug pharmacokinetic properties. Furthermore, also the timing of pill(s) intake is crucial for an accurate estimation of the C_{min} in patient's sample. For this reason, the date of therapy starting, time of last pill intake and possible comedication were recorded.

Blood samples were collected approximately at each patients' clinical visit (*i.e.,* every month) and in the following list indication about sampling time for each drug are reported:

- SORA: at least 7 days after treatment initiation, since mean plasma elimination half-life ($t_{1/2}$) is 25-48 hours [58]. Moreover, the time that had to pass from the tablets intake and the blood collection was different based on the prescribed dosage: for doses of 400, 600 and 800 mg/die (where the tablets intake was twice daily) the sampling had to be performed 12 h after the last dose to be at C_{min}, whereas for 200 mg/die dose (where the tablet intake was once daily) the C_{min} was reached after 24 h. For this reason, patients have to assume SORA tablets every day at precise times, and the last administration has to be 12 or 24 h before the estimated time for blood collection.
- REGO: from day 5 to 21 of every therapy cycle, because the mean plasma $t_{1/2}$ is 25 hours [81] and the REGO schedule in HCC is 21 days on and 7 days off treatment to complete a 28 days cycle. Furthermore, REGO has a single administration regime and so the blood sampling was performed preferably 24 h after the last administration to determine the C_{min} value, independently from the prescribed dose.
- LENVA: at least 6 days after the treatment initiation, because the mean plasma $t_{1/2}$ is 28 h [65]. Moreover, as reported for REGO, the last administration should be 24 h before the estimated time for the blood collection to evaluate the C_{min}.

For each patient, three blood samples were collected:

- 2.7 mL K_2-EDTA Monovette tubes (Sarstedt, Nuembrecht, Germany) for collection of venous blood. Plasma was obtained immediately by centrifugation of the blood samples at 2600 g for 10 min at 4°C. The obtained plasma was split into three independent aliquots and stored at -80 °C until analysis.
- a 1 mL of fresh venous blood without anticoagulant taken within 5 min from the blood sampling. This blood was used to deposit blood drops (5 µL for SORA/REGO and 10 µL for LENVA) in 2 pieces of suitable filter paper (for more details see section 3.5.3.4.1) to be used as DBS controls. One sheet was stored in a plastic enclosed envelopment at -80°C, while the other was stored in a paper enclosed envelopment in dryer with silica at room temperature until the analysis.
- At least two blood drops from a fingertip puncture (finger-prick) deposited on Whatman 31 ETCHR filter paper. The prick was performed by a sterile lancet Accu-Check Safe-T-Pro Plus (Roche, Monza (MI), Italy) following the procedure described in section 3.5.3.4.2.

All types of DBS samples were let dry for 3 h at room temperature before storage.

Each sample was labeled with a code, avoiding the use of any identifying data. Moreover, all patients' samples and data were processed in accordance with European regulation n. 679/2016 (GDPR "*Protezione delle persone fisiche con riguardo al trattamento dei dati personali*") and the Italian law (D.lgs. 196/2003 "*Codice in materia ai protezione dei dati personali*" and D.lgs. 101/2018).

3.2. The phase II clinical study (internal protocol code: CRO-2017-42)

This phase II clinical study entitled "*Studio di Fase II che valuta l'efficacia e la sicurezza del trattamento metronomico orale con Idarubicina in pazienti affetti da Epatocarcinoma allo stadio intermedio-avanzato dopo fallimento o intolleranza a Sorafenib e Regorafenib*", was designed and is currently ongoing at C*.R.O. of Aviano* and at *Azienda Sanitaria Universitaria Integrata of Udine* (UD, Italy). This clinical trial (EUDRACT Number 2017-003653-42) had been revised and approved by local ethics committee (C.E.U.R.) and AIFA on 20th November 2018 and conducted according to the Declaration of Helsinki principles [207]. The aim of this clinical trial was to evaluate the treatment of patients affected by advanced HCC with IDA metronomic schedule in term of OS at 6 months. Among the secondary aims, there is the evaluation of:

- progression free survival (PFS) and time to progression (TTP);
- the safety and tolerability profile of the drug;
- the impact on the quality of life of metronomic treatment with IDA;
- the possible correlation between C_{min} levels of IDA and IDOL and hematological toxicity (G> 2) and the possible correlation between C_{min} and response.

The enrollment of the patients started in June 2019.

3.2.1. Patient's characteristics

Patients enter the study according to the principal following eligibility criteria:

- to be affected by intermediate HCC state (BCLC-B) not eligible or not responsive to TACE and developing intolerance or progression to SORA and/or REGO, or in which such treatments is contraindicated;
- to be affected by advanced HCC state (BCLC-C) and developing intolerance or progression to SORA and/or REGO, or in which such treatments is contraindicated;
- age ≥ 18 years;
- adequate medullar, hepatic, and renal function;
- provide a signed written informed consent.

The most important exclusion criteria are:

- unreliable and/or non-collaborative patients;
- life expectancy < 2 months;
- presence of clinically significant cardiovascular and/or cerebrovascular disease and/or clinically significant acute or chronic respiratory failure;
- uncontrolled systemic infections and/or HIV infection;
- women who are pregnant or breastfeeding;
- potentially fertile and sexually active women and men who refuse or are unable to use contraceptive methods.
- refusal of informed consent.

3.2.2. Treatment and sampling

The proposed oral metronomic schedule consists in 5 mg/die every other day for each 28 days cycle. The patient took the capsules approximately at the same time. The patient underwent an instrumental revaluation every two cycles and during those days the therapy was temporarily suspended and was resumed if there were evidence of response or disease stability.

Timing blood sampling was chosen according to drug PK properties, to accurately estimate drug C_{min}. The achievement of steady state occurred approximately after 5 half-lives and considering IDA and IDOL mean plasma elimination half-life of 14 and 48 hours [96], respectively, the blood samplings were performed from day 10 onwards. Moreover, an important aspect was patient education to take IDA capsules respecting the schedule of the clinical study, to further increase the accuracy of C_{min} quantification.

For each patient enrolled in the study, one 4.9 mL K_2-EDTA Monovette tubes (Sarstedt, Nuembrecht, Germany) of peripheral blood was periodically collected at day 1 of all even cycles, not considering odd cycles because of therapy suspension. Whole blood was centrifuged at 2600 g for 10 min at 4 °C and the obtained plasma was split into three aliquots and stored at -80°C until the analysis.

3.3. Instrumentation

Analytical standard powders were accurately weighted with a Mettler Toledo DeltaRange XPE205 analytical balance (Columbus, Ohio, USA).

Working solutions and whole blood samples were handled with a Microman set composed by M1000, M250, M100, M25 and M10 pipettes, while plasma samples with Pipetman P100 and P5, all purchased from Gilson (Villiers-le-Bel, France).

Plasma was obtained from whole blood using a 5810R centrifuge (Eppendorf, Hamburg, Germany), while a 5427R benchtop centrifuge (Eppendorf, Hamburg, Germany) was adopted for the centrifugation to complete the protein precipitation procedure.

For the experiments involving DBS technique the water bath Clifton (Nickel-Electro Ltd., Weston-Super-Mare, UK) was used to homogenize the drug added in whole blood samples at 37 °C.

ACD/ChemSketch (ACD/ChemSketch (Freeware) 2020.1.2, software by ACD/Labs) program was used to design chemical structure and to verify the fragmentation of each analyzed compound.

For the analysis of SORA, REGO and their active metabolites both in plasma and in DBS, the analytical methods have been developed and validated using a Prominence UFLC XR system composed by a SIL-20AC XR auto-sampler, two LC-20AD UFLC XR pumping modules, two FCV-11AL solenoid valve units, a DGU-20A3 degasser, a CBM-20A system controller and a CTO-20AC column oven (Shimadzu, Tokyo, Japan). This HPLC system was coupled with an API 4000Qtrap (SCIEX, Massachusetts, USA), a mass spectrometer characterized by a Turbo IonSpray source and a triple quadrupole analyzer. To quantify the analytes, data were processed using Analyst 1.6.3 and the chromatographic peaks were integrated with MultiQuant 2.1 (software package SCIEX). During the analysis, samples with SORA, REGO and their active metabolites were kept in autosampler polypropylene vials with Polytetrafluoroethylene (PTFE) caps purchased by Agilent Technologies (Santa Clara, California, USA), while samples with LENVA in borosilicate glass vials with a pro-slit PTFE caps acquired by Waters (Milford; Massachusetts, USA).

The analytical method for LENVA quantification both in plasma and DBS samples were developed and validated on a Nexera XR LC 20 system with two pump modules LC-20 AD XR, a SIL-20AC XR auto-sampler, two FCV-11AL solenoid valve units, a DGU-20A3R degasser, a CBM-20A system controller and a CTO-20AC column oven (Shimadzu, Tokyo, Japan). This LC system was coupled with an API 4000Qtrap (SCIEX, Massachusetts, USA), a mass spectrometer characterized by a Turbo IonSpray source and a triple quadrupole

analyzer. In this case, the analytes quantification was performed using Analyst 1.6.3 and the chromatographic peaks were integrated with Quantitation wizard (software package SCIEX). During the analysis, samples were kept in autosampler borosilicate glass vials with a pre-slit PTFE cap purchased from Waters (Milford; Massachusetts, USA). Statistical analyses were performed with Stata 14.2 (StataCorp, Texas USA).

3.4. Standard and chemicals

HPLC grade Dimethyl Sulfoxide (DMSO) was supplied by Alfa Aesar (Haverhill, Massachusetts, USA); LC-MS grade methanol (MeOH) was purchased from Carlo Erba Reagents (Cornaredo, Milano, Italy); Tetrahydrofuran (THF), isopropanol (iPrOH), acetonitrile (ACN), and analytical grade ammonium acetate (AmAc), formic acid (HCCOH) and acetic acid (CH_3COOH) were supplied by Merck-Sigma (Milano, Italy), while "Type 1" ultrapure water (MilliQ H_2O) was produced at our laboratory by a Milli-Q® IQ 7000 system (Merck Millipore, Billerica, MA, USA). The transfusion unit of *C.R.O. di Aviano* provided human whole blood/K_2EDTA from healthy volunteers, used to prepare daily standard calibration curves and quality control (QC) samples in DBS and to obtain control plasma.

The DBS analysis were performed using Whatman 31 ET CHR for SORA, REGO and their active metabolites method, while Whatman 31 ET CHR and Whatman 903 were used for LENVA quantification. Both filter papers were supplied by GE-Whatman (Little Chalfont, UK).

The analytical standard of SORA (batch: CS-WS-AAA-3464-01, purity: 99.36%), oxSORA (batch: CRC-0325-008, purity: 98.58%), REGO (batch: CS-WS-AAA-0890-02, purity: 99.52%), oxREGO (batch: CRC-0195, purity: 96.93%), des-oxREGO (batch: CRC-0298-142-P, purity: 97.55%), IDA (batch CS-WS-AAA-1142-01, purity 99.82%), the stable isotopically labeled internal standards, SORA-$^{13}C_1$-D_3 (SORA-L4; batch: CS-SF-484,purity: 99.30%), REGO-D_3 (batch: CRC-0196-Final-LS-II, purity: 99.61%) and LENVA-D_4 (batch: CS-SI-AAA-0949-01, chemical and isotopic purity: 99.18% and 99.48%, respectively) were purchased from Clearsynth LabsLtd. (Mumbai, India), while LENVA (batch: 6-JTN-66-1; purity: 98%) and IDOL mixture of diastereoisomers (batch 17-MMH-5-120-3, purity 97.82%) were supplied by Toronto Research and Chemical Inc. (North York, Ontario, Canada), instead DUANO (batch: SVI-ALS-17-058, purity 98.6%) was obtained from Alsachim (Illkirch Graffenstaden, France).

3.5. LC-MS/MS method development

During the development of the methods reported in this dissertation, the following instrumental conditions were optimized:

- the mass-spectrometric conditions (see section 3.5.1.), to unequivocally identify the analytes of interest, and to obtain the best signal-to-noise ratio (S/N) for them;

- the chromatographic conditions (see section 3.5.2.), to separate the analytes as much as possible, and to get the best selectivity to avoid the matrix effect due to other interferents present in plasma or DBS (*e.g.,* salts, phospholipids);
- the sample preparation workflow (see section3.5.3.) to obtain a reliable and easy sample extraction method, and, at the same time, a calibration curve in a proper concentration range that covers the expected clinical levels.

3.5.1. Mass spectrometric conditions optimization

To achieve the greatest sensitivity and the best S/N for the analytes of interest, two types of mass spectrometry parameters have to be tuned: the compound-dependent parameters that have to be optimized individually for each compound based on its ionization efficiency and fragmentation pattern (see section 3.5.1.1.), and the source-dependent parameters that are dependent on the flow rate and the mobile phase composition (see section 3.5.1.2.).

3.5.1.1. Compound dependent parameters optimization

The compound dependent parameters that need to be optimized are:

- Declustering Potential (DP): parameter which controls the potential difference between Q0 and the orifice plate. It is used to minimize the cluster formation due to the aggregation between ions and solvent droplets.
- Entrance Potential (EP): parameter which controls the potential that focuses and guides the ions through the high-pressure Q0 region.
- Collision Energy (CE): parameter which represents the amount of energy that the precursor ion receives once accelerated into Q2, where it collides with the gas molecules and other fragments.
- Collision cell Exit Potential (CXP): parameter which controls the potential that focuses and accelerates ions exiting Q2. It is the potential difference between Q2 and ST3 (a lens that separates Q2 and Q3).

To optimize these parameters a methanolic solution containing separately each analyte of interest (for the concentration, see sections 3.5.1.1.1. for SORA, REGO and their active metabolites, 3.5.1.1.2. for LENVA and 3.5.1.1.3. for IDA and IDOL) was direct infused in the mass spectrometer with a flow rate of 20 µL/min. The mass spectrometer was configured in manual tuning mode with the default values of all source dependent parameters.

The first step was to identify the presence of the analyte and to check if the analyte was more sensitive in positive or negative ion mode (*i.e.*, if the ion current is higher for its protonated molecule $[M-H]^+$ or deprotonate molecule $[M-H]^-$, also called pseudo-molecular or precursor or parent ion).

The spectrometer was set in Q1 full scan (Q1MS) with positive or negative ion mode. In this configuration, the mass spectrometer worked as a single quadrupole since no energy was applied to Q2 that, together with Q3, operated in RF only and focused the positive or negative ions from Q1 to the detector without filtering them (Figure 18).

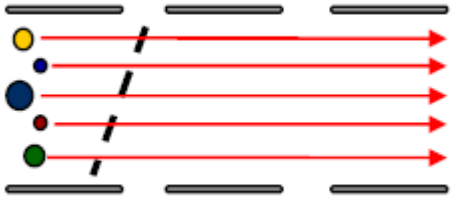

Figure 18. Schematic representation of the triple quadrupole analyzer in Q1MS configuration.

This scan was performed selecting an adequate range of *m/z* values to detect the pseudo-molecular ion of the analyte of interest, and eventually the presence of positive adducts (*e.g.,* $[M+Na]^+$, at + 23 amu respect the expected *m/z* value; $[M+K]^+$ at +39 amu) o negative adducts (*e.g.,* $[M+Cl]^-$, at -+ 35 amu respect the expected *m/z* value; $[M+HCOO]^-$ at + 45 amu; $[M+CH_3COO]^-$ at + 59 amu) in positive or negative ion mode, respectively.

Moreover, another important factor to obtain accurate readings was the dwell time (or scan time). In fact, to achieve an adequate number of duty cycles, the scan time was set using the following Equation 8:

$$Scan\ time = 10\ msec\ x\ \Delta_{amu}$$

Equation 8. Scan time calculation.

Where Δ_{amu} corresponds to the range of *m/z* values analyzed.

Once the total ion current (TIC) was stabilized, a spectrum was recorded activating the multiple count acquisition (MCA) mode, that totaled all the detected events hence increasing the S/N and allowing a more accurate reading of the *m/z* value of the pseudo-molecular ion.

After that, the optimization of DP and EP parameters was performed. The mass spectrometer was set in Q1 multiple ions (Q1MI) mode, which means Q1 worked in selected ion monitoring (SIM) mode by picking the pseudo-molecular *m/z* value formerly identified, while Q2 and Q3 worked in RF only, as shown in Figure 19.

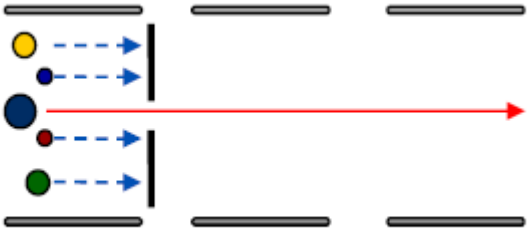

Figure 19. Schematic representation of the triple quadrupole analyzer in Q1MI configuration.

By ramping the DP (for the set values, see sections 3.5.1.1.1. for SORA, REGO and their active metabolites, 3.5.1.1.2. for LENVA and 3.5.1.1.3. for IDA and IDOL), the intensity trend of the extracted ion current (XIC) was monitored to select the most correct DP value for the pseudo-molecular ion. Normally, as the DP increases, the signal intensity has a tendency similar to a Gaussian curve, and the optimal DP value was found at the apex of its curve. This was important, as too high DP values may cause an in-source fragmentation, whereas too low values will produce a lower ion intensity current due to interference from clusters.

Following the DP value setting, the optimal EP value (for the set values, see sections 3.5.1.1.1. for SORA, REGO and their active metabolites, 3.5.1.1.2. for LENVA and 3.5.1.1.3. for IDA and IDOL), was established in the similar way, although it is often left at the default value without any impact on the analyte detection limit because EP has a minor effect in compound ionization efficiency.

To define the two remaining compound-dependent parameters, all the three quadrupoles were utilized in a MS/MS configuration.

Initially, an analysis of the fragmentation pattern was performed for each compound with the spectrometer set in product ion mode (MS2), meaning that pseudo-molecular ion is filtered in Q1 and fragmented in Q2, while Q3 performed a scan of all the fragments (also defined product ion), as shown in Figure 20.

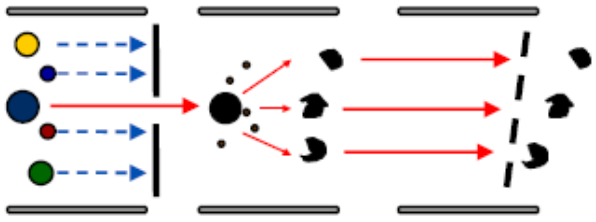

Figure 20. Schematic representation of the triple quadrupole analyzer in MS2 configuration.

Several spectra were recorded slowly ramping CE value (for the set values, see sections 3.5.1.1.1. for SORA, REGO and their active metabolites, 3.5.1.1.2. for LENVA and 3.5.1.1.3. for IDA and IDOL) activating the MCA

mode and adopting the optimized DP and EP values for the analyzed compound. In this way, a first evaluation of the most representative fragments was carried out, exploring a range between 100 and 550 *m/z*, because fragments lower than 100 *m/z* are not informative for all the compound analyzed in this PhD thesis.
The main 4 fragments for each compound (after the verification of the real possibility to be generated using ChemSkecth program) had been selected for the optimization of CE value. This parameter was optimized concurrently for each 4 fragments by setting the mass spectrometer in multiple reactions monitoring (MRM) mode. In this setting, Q1 filtered the specific selected precursor ion, that is fragmented in Q2, while Q3 worked as a second filter, selecting the precise 4 fragment set, as shown in Figure 21.

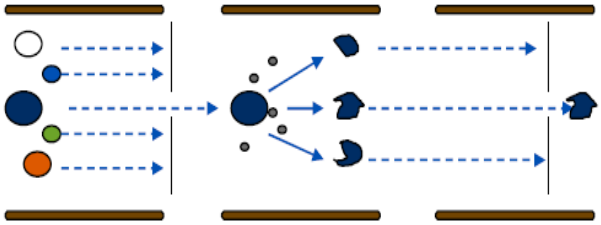

Figure 21. Schematic representation of the triple quadrupole analyzer in MRM configuration.

By ramping CE value over time (for the set values, see sections 3.5.1.1.1. for SORA, REGO and their active metabolites, 3.5.1.1.2. for LENVA and 3.5.1.1.3. for IDA and IDOL), a spectrum with XIC intensity for each fragment was recorded. The optimal CE value for each fragmentation was represented by the apex of XIC curve, which has a trend like a Gaussian curve. The fragment with the highest signal intensity was selected as the most suitable for the quantification (*i.e.,* the quantifier), while the second one or the second and third ones in intensity were used as qualifier, with the aim of increasing the analyte specificity.
In a similar way the CXP value was selected, setting the DP, EP and CE optimized values for each fragment. This optimization was always done in MRM mode (for the set values, see sections 3.5.1.1.1. for SORA, REGO and their active metabolites, 3.5.1.1.2. for LENVA and 3.5.1.1.3. for IDA and IDOL).
The precursor ions of each analyte and IS with the optimal value of DP and EP, could be filtered and fragmented with the optimal CE and CXP to obtain the desired product ions for the simultaneous quantification and confirmation of the compounds of interest.

3.5.1.1.1. Sorafenib, regorafenib and their active metabolites

The optimization of the compound dependent parameters for SORA, REGO, their active metabolites and two ISs was performed in negative ion mode following the procedures reported in section 3.5.1.1. The specific details of these procedures are the following:

- direct infusion into the mass spectrometer at a flow rate of 20 µL/min of a methanolic solution with a concentration of 200 ng/mL for each compound separately;
- DP ramp from -300 to 0 V with step of 1 V in Q1MI mode;
- EP ramp from -15 to -1 V with step of 1 V in Q1MI mode;
- CE ramp from -100 to – 5 V with step of 1 V in MS2 mode;
- CE ramp from -100 to - 5 V with step of 1 V and dwell time of 200 msec for each fragment in MRM mode;
- CXP ramp from -30 to -1 V with step of 1 V and dwell time of 200 msec for each fragment in MRM mode;

3.5.1.1.2. Lenvatinib

To optimize the compound dependent parameters for LENVA and its IS the procedure reported in section 3.5.1.1. was followed in positive ion mode. The specific details of these procedures are the following:

- direct infusion into the mass spectrometer at a flow rate of 20 µL/min of a methanolic solution with a concentration of 100 ng/mL for each compound separately;
- DP ramp from 0 to 250 V with step of 1 V in Q1MI mode;
- EP ramp from 2 to 15 V with step of 1 V in Q1MI mode;
- CE ramp from 5 to 130 V with step of 1 V in MS2 mode;
- CE ramp from 5 to 130 V with step of 1 V and dwell time of 200 msec for each fragment in MRM mode;
- CXP ramp from 0 to 55 V with step of 1 V and dwell time of 200 msec for each fragment in MRM mode;

3.5.1.1.3. Idarubicin and idarubicinol

To optimize the compound dependent parameters for IDA, IDOL and DAUNO the procedure reported in section 3.5.1.1. was followed in positive ion mode. The specific details of these procedures are the following:

- direct infusion into the mass spectrometer at a flow rate of 20 µL/min of a methanolic solution with a concentration of 100 ng/mL for each compound separately;
- DP ramp from 0 to 250 V with step of 1 V in Q1MI mode;
- EP ramp from 2 to 15 V with step of 1 V in Q1MI mode;
- CE ramp from 5 to 130 V with step of 1 V in MS2 mode;
- CE ramp from 5 to 130 V with step of 1 V and dwell time of 200 msec for each fragment in MRM mode;

- CXP ramp from 0 to 55 V with step of 1 V and dwell time of 200 msec for each fragment in MRM mode;

3.5.1.2. Source dependent parameters optimization

The source dependent parameters that need to be optimized are:

- Curtain gas (CUR): parameter which controls the pressure of the curtain gas that flows between the curtain plate and the orifice preventing the contamination of the ion optics by minimizing the entrance of solvent droplets;
- CAD gas (CAD): parameter which controls the pressure of collision gas in Q2 that in MS/MS experiments has the function of fragmenting the precursor ions;
- IonSpray Voltage (ISV): parameter which controls the voltage applied to the needle that ionizes the sample, thus influencing the spray stability;
- temperature (TEM): parameter which controls the temperature of the turbo gas;
- gas 1 (GS1): parameter which controls the pressure of the nebulizer gas that has the function of helping to generate small droplets of sample flow;
- gas 2 (GS2): parameter which controls the pressure of the turbo gas that has the function of helping the spray droplets evaporation avoiding solvent entrance into the analyzer.

The optimization of these source dependent parameters was performed for only one compound of each method developed in this PhD project. The chosen compound was the one with the lowest signal intensity and ionization efficacy. All the optimized values were applied for the other compounds, because these parameters are equal for all the compounds analyzed within the same analytical MS/MS method.
The Flow Injection Analysis (FIA) configuration was used to perform the optimizations of these parameters, as shown in Figure 22. In fact, FIA configuration mimics the real working conditions of the system: LC system was enabled, a union connector was used instead of the chromatographic column, a specific analyte solution was directly injected from the autosampler with a regular interval of time (0.5 min) into the mass spectrometer with a flow rate of MPs. The mass spectrometer was set in SRM scan mode for that analyte with its optimized compound dependent parameter, to obtain a constant XIC intensity signal. Subsequently, each source dependent parameter was manually varied after 3 sample injections with a stable XIC: the optimal value for each of them was the one that allowed to achieve the maximum signal intensity for the quantifier transition used.
In sections 3.5.1.2.1. for SORA, REGO and their active metabolites, 3.5.1.2.2 for LENVA and 3.5.1.2.3. for IDA and IDOL, the specific details were reported.

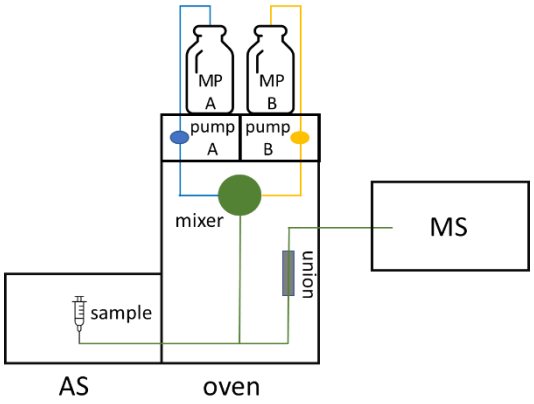

Figure 22. Schematic representation of the LC-MS/MS set up for the optimization of the mass spectrometer source-dependent parameters. AS: autosampler; MP: mobile phase; MS: mass spectrometer.

3.5.1.2.1. Sorafenib, regorafenib and their active metabolites

The optimization of source dependent parameters for SORA, REGO, their active metabolites and two ISs was performed following the procedures reported in section 3.5.1.2. The optimization was performed with a 200 ng/mL solution of oxREGO in methanol. Two µL of oxREGO solutions were injected from the autosampler at time interval of 0.50 min, into flowing MP coming from HPLC pumps. The composition of MP was 20% MP A (10 mM AmAc aqueous solution with 0.10% of HCOOH, v/v) and 80% MP B (MeOH:iPrOH (90:10, v/v) with 0.10% of HCOOH (v/v)).

Only for this analytical method the source dependent parameters obtained with oxREGO were confirmed also with a 200 ng/mL methanolic solution of des-oxREGO, because this analyte also was characterized by a lower signal intensity and ionization efficacy.

3.5.1.2.2. Lenvatinib

The optimization of source dependent parameters for LENVA and its IS was performed following the procedures reported in section 3.5.1.2. The optimization was performed with a 100 ng/mL methanolic solution of LENVA. Two µL LENVA solution were injected from the autosampler at time interval of 0.50 min, into flowing MP coming from HPLC pumps. The composition of MP was 10% MP A (H_2O with 0.10% of HCOOH, v/v) and 90% MP B (MeOH:iPrOH (90:10, v/v) with 0.10% of HCOOH (v/v)).

3.5.1.2.3. Idarubicin and idarubicinol

The procedures reported in section 3.5.1.2. were followed to optimize the source dependent parameters for IDA, IDOL and DAUNO. The optimization was performed with a 100 ng/mL methanolic solution of IDA,

because it was the analyte with a very Lower Limit of Quantification (LLOQ). Four µL of IDA solutions were injected from the autosampler at time interval of 0.50 min, into flowing MP coming from HPLC pumps. The composition of MP was 60% MP A (H_2O with 0.10% of HCOOH, v/v) and 40% MP B (ACN with 0.10% of HCOOH (v/v)).

3.5.2. Chromatographic conditions optimization

During the chromatographic method development, the following characteristics are considered:

- good separation between the analytes, *i.e.*, resolution;
- symmetric peaks with a minimum width and maximum height that is without fronting and/or tailing;
- reproducibility of consecutive analysis;
- minimum runtime;
- good control of the carryover. This phenomenon consists in a type of system contamination that causes analyte peak in subsequent runs, which do not really contain the analyte, *e.g.*, blank samples after a sample with a high analyte concentration.

The chromatographic method development started with the collection of information relating to the physicochemical properties of the analytes of interest. In fact, the SP type depends on the physicochemical properties of the analytes, the column length varies according to the number of compounds to be analyzed and the column particle size depends on the required resolutions. Moreover, the possible addition of a pre-column depending on the sample preparation type and the nature of the matrix was evaluated too.
Once the SP had been chosen, the afterward important steps were the MPs composition (MP A - aqueous solvent or “weak solvent” and MP B - organic solvent or “strong solvent”), the flow rate and the column temperature. MPs composition influenced both the flow rate and the column temperature because high viscous solvents could cause too high backpressure into the chromatographic system. In fact, MPs flow rate should be set to a proper value to obtain a reasonable runtime and simultaneously to avoid too high backpressure, while using high column temperature, it was possible to reduce MPs viscosity and favor analytes partition between the two phases (SP and MP), with the aim to obtain a better chromatographic resolution.
The assessed parameters were peak shape, signal stability and analytes retention time.
Following, the selection of the chromatographic method was done, which was the most time-consuming step. The first point was the selection of one of the following types of chromatographic method:

- totally isocratic method: the MPs composition is kept constant during the whole chromatographic run;

- multi-step method: the MP A/MP B ratio changes over time, which generally followed the step described below in RP chromatography and schematized in Figure 23:
    I. conditioning phase of the column: a low percentage of MP B, which helped the correct packing of the analytes at the column head, lessen analytes diffusion phenomena through the column. Indeed, the initial condition of the analytical run determines the environmental encountered by the sample after its injection into the column. For example, if the initial percentage of MP B was too high and the analytes did not pack at the head of the column, it could interfere with the interaction between the analytes and the functional groups on the column particles. This could cause wide and asymmetrical peaks and a considerable decrease in resolution (R_s) and/or undesired peak-spilt of the analyte, that was the same compound eluted in two phases, one of which with the solvent front.

    During the chromatographic method development, different percentages of MP B and different durations of this phase were tested (even the possibility to remove it to further reduce the runtime).

    II. Elution phase of the analytes: it could be in isocratic or gradient scheme. The pick between the two schemes was assessed investigating different slopes for the gradient regime and different amount of MP B for the isocratic one. Moreover, the duration of this phase has to be sufficient in order to avoid the analytes elution during the washing and reconditioning phases, which were the following.

    III. Washing phase: a high percentage of MP B allowed the elution of more lipophilic interferents in the matrix (*e.g.,* phospholipids, peptide residuals, etc.) still bound to the SP. This phase was important also to improve the column life and might have reduced the carryover problem.

    IV. Reconditioning phase: the eluent composition returned to the initial condition. The duration of this step depended on the MP flow rate and column volume. Conventionally, a column was considered reconditioned after the flowing of 10 MPs column volumes. During method development, the duration of this phase was optimized when the retention time was constant after several consecutive runs. Indeed, reconditioning failure can lead to alterations in retention times and therefore to reproducibility lack of repeated runs.

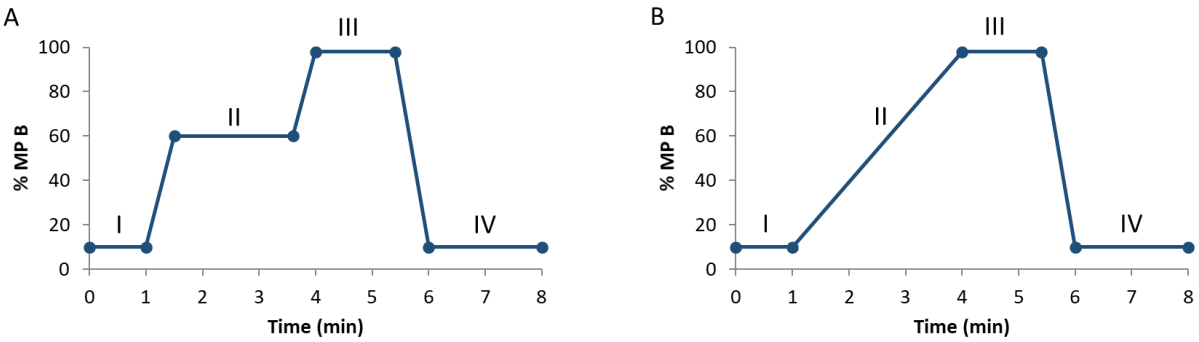

Figure 23. Schematic representation of a multi-step chromatographic method with (A) isocratic elution and (B) gradient elution. I-IV refer to the different phases of the multistep method described in the text.

3.5.2.1. Sorafenib, regorafenib and their active metabolites

The development and optimization of the chromatographic method for SORA, REGO and their active metabolites was performed with methanolic samples at two different concentration levels: LLOQ at 50 ng/mL of SORA and REGO and 30 ng/mL for all the metabolites and Upper Limit of Quantification (ULOQ) at 8000 ng/mL of SORA and REGO and 4000 ng/mL for all the metabolites. Moreover, different sample injection volumes of 1, 2, and 4 µL, compatible with column volume, were tested to introduce the sample into the LC-MS/MS system.

3.5.2.2. Lenvatinib

For this analytical method, the development and optimization were evaluated with methanolic samples containing LENVA and LENVA-D_4 at a concentration of 100 ng/mL, i.e., an intermediate concentration value within the analytical range used.

3.5.2.3. Idarubicin and idarubicinol

Three different concentrations (0.10 ng/mL (LLOQ), 0.20 ng/mL and 200 ng/mL (ULOQ) of IDA and IDOL) in MeOH were used to develop and optimize this chromatographic method. Furthermore, different injection volumes (4, 5 and 6 µL) were tested to improve IDA sensitivity.

3.5.3. Sample preparation for quantitative analysis

Sample preparation is one of the most time-consuming steps: its aim is to remove interferents from biological matrix, solubilize analytes of interest in a suitable solvent for their ionization and, if necessary, pre-concentrate them.

3.5.3.1. Calibration curve and quality controls preparation

To perform quantitative analysis, LC-MS/MS instruments had to be calibrated with a set of samples having known and increasing concentrations of the compound in order to determine a relationship between the detected signal and the analyte concentration. To do this, it was necessary to prepare these calibration samples, called calibrators, in the same matrix of those samples for which the quantification method was developed (*e.g.,* human plasma or DBS). Moreover, it was of fundamental importance, that calibrators underwent the identical treatment applied to unknown samples.

From the signal intensities of these calibrators, a calibration curve was built. If there was proportionality between analyte concentration and its signal intensity measured with LC-MS/MS instrument, the curve was considered linear over the concentration range defined by the calibrators. The calibration curve range should cover the analyte concentrations expected from the patients' samples: in this manner the developed method fits for its aim.

The calibration curve was fitted using the least squares regression method weighted by $1/x^2$: this was particularly meaningful for wide range calibration curves, characterized by an instrument response standard deviation that varied according to analyte concentration. The weighting factor attributed more importance to data points with a low variance compared to those with high variance, generating a calibration curve with uniformly distributed error.

The calibration curve had to be built with a minimum of 6 calibrators, including the LLOQ, according to EMA [200] and FDA [201] bioanalytical method validation guidelines.

To verify the performance of the bioanalytical method and hence the integrity and validity of the results, guaranteeing the quality of the quantification during the analysis, samples with a known analyte concentration prepared in the same matrix of the real samples, called QCs, were used. It is important to note that calibration curve and QCs working solutions were prepared from two different stock solutions to assure the QC function.

In each analytical run, three replicates of low (QCL), medium (QCM) and high (QCH) were analyzed and each replicate was uniformly distributed throughout the analytical run, to guarantee the analytical quality for the whole series of quantified samples.

Moreover, QC samples were used also to assess the analyte stability under several conditions (for more details see section 3.5.3.3. for plasma samples and 3.5.3.4. for DBS samples). The QCs should be bought or prepared in house, as in the case of the methods presented in this thesis.

According to EMA [200] and FDA [201] guidelines, QCs concentration values should diverge from the calibrators' ones, and they should be distributed within the range covered by the calibration curve with the following characteristics:

- QCL: low concentration, within three times the LLOQ;

- QCM: average concentration, that tumbles around 30-50% of the calibration curve range;
- QCH: high concentration, at least 75% of the ULOQ.

3.5.3.2. Internal standard

The LC-MS/MS developed methods presented in this thesis based the quantification of the analyte on the IS method. According to this method, during sample preparation, a known quantity of IS was added to each sample (*i.e.,* calibrators, QCs, and patients' samples). Then, analytes quantification was based on the ratio between the analyte and IS peaks areas (area ratio).

The IS had to have very similar physical-chemical proprieties to the analyte of interest. In this manner, all the errors introduced during sample processing or throughout the analysis had the same effect on both the analyte and IS, without influencing the performance of the developed analytical method. Indeed, the IS addition rendered the results of analysis independent from variations in extraction, recovery, volume injected, and ionization efficacy.

Usually, excellent candidate for LC-MS/MS analysis are stable isotope labelled (SIL) analogues of the analyte (*e.g.,* deuterium labelled, ^{13}C labelled or ^{15}N labelled compounds). SILs showed a closely identical chromatographical behavior to the compound of interest: they co-eluted but were perfectly detectable due to the different *m/z* value and were subjected to the same possible matrix effect, therefore minimizing its impact on the analyte quantification. Unfortunately, SILs are very expensive powders and sometimes they are synthesized to order causing very high production costs. For this reason and thanks to its structural analogy to IDA, DAUNO was chosen as IS for the quantification of IDA and IDOL. Indeed, DAUNO has only an additional methoxy group in position 4 of the aglycone D ring, so it has similar physical-chemical properties as IDA and IDOL.

The typical application of IS in liquid samples, such as plasma samples, may be performed in two ways: by its addition in small volumes directly to the samples which then were processed, or by preparing an IS solution in extraction solvent and using it to process samples. For solid matrices as DBS, the strategy used in this thesis was the addition of IS within the extraction solution, as described in the literature as the most appropriate technique [208]. Other possibilities reported in the literature are to spray the IS evenly onto the sample before the extraction [209] or precoat the filter paper with the IS [210].

The following ISs were selected for the quantification of the analytes of interest:

- SORA-L_4 for the quantification of SORA and oxSORA;
- REGO-D_3 for the quantification of REGO and its metabolites;
- LENVA-D_4 for the quantification of LENVA;
- DAUNO for the quantification of IDA and IDOL, as reported in Figure 24.

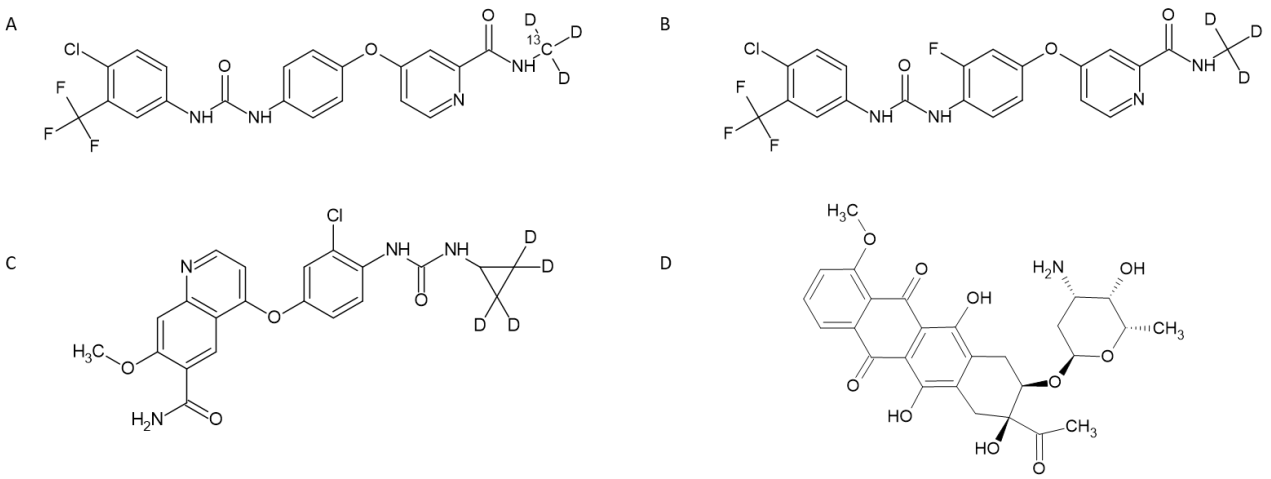

Figure 24. Chemical structure of (A) SORA-L4, (B) REGO-D_3, (C) LENVA-D_4 and (D) DAUNO.

3.5.3.3. Plasma sample extraction optimization

The biological matrices are highly complex and may contain some endogenous components, for instance lipids and proteins that could interfere with the detection and quantification of the analytes. Moreover, these compounds might cause several problems, such as damage and dirty of both the chromatographic column and mass spectrometer source, but they also could influence the matrix effect, due to ion enhancement and ion suppression events which cause variations on analyte ionization efficiency. Therefore, the main objective of sample preparation in biological matrices is to remove the largest number of interferences as possible and simultaneously to solubilize the analytes of interest in an appropriate solvent for their quantification.

The most used extraction techniques in the PKs area are 3:

- Solid Phase Extraction (SPE);
- Liquid-Liquid Extraction (LLE) with immiscible solvents;
- Protein Precipitation (PP) with organic solvents miscible with water [211];

The last technique is generally selected for analysis of drugs in human plasma, because it is the simplest and less time-consuming, although it is also the technique that cleans less the samples. PP consists in the addition to the sample a determined volume (at least 3 times greater than the plasma samples) of organic solvents miscible with water, usually ACN or MeOH [212]. Organic solvents inducing a displacement of water molecules from plasma proteins' surface, leading to the breakage of the weak interactions responsible for their tertiary structure, to the aggregation of proteins by electrostatic and dipole attractive forces, and thus to their precipitation. Furthermore, the larger the volume of organic solvent added, the more efficient the extraction and the cleaner the sample to be injected on the LC-MS/MS instruments will be. On the other hand, large volumes of organic solvents lead also to dilute samples that might cause analytical problems if the compound of interest shows low signal intensity. Thus, the volume of solvent used to perform the PP should be a compromise between these two opposite effects.

3.5.3.3.1. Sorafenib, regorafenib and their active metabolites

For this method different solvent were tested: MeOH, MeOH with 0.10% of HCOOH (v/v), CAN, and ACN with 0.10% of HCOOH (v/v). After the identification of the best solvent to use, different sample:solvent ratios (1:10, 1:20, 1:50, 1:100 and 1:200, v/v) were tested with the purpose of achieving a quantifiable peak (S/N > 5) from the LLOQ sample and a signal from ULOQ sample within the saturation limit of the detector, under equal extraction conditions.

3.5.3.3.2. Lenvatinib

During the development of LENVA quantification method, the protein precipitation was evaluated using MeOH and ACN both plus 0.10% of HCOOH (v/v). Two different sample:solvent ratios (1:6 and 1:20, v/v) were evaluated, in order to obtain a quantifiable peak (S/N >5) for the LLOQ and a signal within the saturation limit of the mass spectrometer detector for the ULOQ.

3.5.3.3.3. Idarubicin and idarubicinol

The protein precipitation in IDA and IDOL quantification method was assessed both in ACN and in MeOH and using different sample:solvent ratios (1:3, 1:4 and 1:5, v/v). To obtain a quantifiable peak (S/N >5) for the LLOQ at 0.10 ng/mL of IDA, it was necessary to concentrate the sample using the evaporator. Different solvents, including MilliQ H_2O, ACN, MeOH, iPrOH, MilliQ H_2O:ACN (50:50, v/v), MilliQ H_2O:MeOH (50:50, v/v), MilliQ H_2O:iPrOH (50:50, v/v), all acidified with 0.10% HCOOH (v/v) and several volumes (50, 100, 200 and 400 µL) were evaluated to redissolve the dry residue obtaining a limpid solution and a quantifiable LLOQ at 0.10 ng/mL.

3.5.3.4. Optimization of dried blood spot parameters

Several pre-analytical, analytical, and post-analytical parameters could influence the DBS analysis and have to be considered during both development and validation of the DBS based LC-MS/MS quantification method. The most important parameters are described in the following sections.

3.5.3.4.1. Type of paper

For DBS analysis, the cellulose-based papers are the most common used matrix. The paper types have different characteristics regarding their composition, particle retention, pore size, thickness and resistance to spreadability of blood. According to these characteristics, the paper type could influence the extraction,

recovery, matrix effect, analyte stability, chromatographic behavior, spot volume and Hct effect. There are two main types of paper card: chemically treated paper with denaturing agents or enzyme inhibitors and untreated one (most commonly used). Only for the second type, FDA approved two card types as class II medical device: Whatman 903 and Perkin Elmer 226 (previously Ahlstrom). These two DBS cards are continuously and extensively monitored for consistent performance between batches [213,214]. The Whatman 903 card is composed by cotton-based filter paper within a rigid cardboard frame for handling and labelling. This filter paper is characterized by 5 half-inch circles ink printed, where the patient deposits directly the finger blood drops. Each circle is able to hold 75-80 µL of whole blood. Whatman 903 is a quite expensive filter paper, being validated to perform DBS sampling. On the market there are several no validated filter paper, that consequently are cheaper. An example is Whatman 31 ET CHR, which is an untreated filter paper composed by pure cellulose. This type of paper was already used by Vu et al. for collecting DBS from patients treated with moxifloxacin, with good results compared to Whatman 903 [215]. Using a no validated filter paper keeps low sampling cost, allowing to develop a cost-effective and reliable quantification method to used routinely in TDM.

The LC-MS/MS quantification method in DBS matrix for SORA, REGO and their active metabolites was developed and validated on Whatman 31 ET CHR filter paper. Instead, LENVA DBS method was developed and validated in both Whatman 903 and Whatman 31 ET CHR papers, in order to verify the comparability of the results and confirm the possibility to use the no validated filter paper to reduce costs.

3.5.3.4.2. DBS collection procedure

DBS sample collection has to follow uniform procedures to minimize pre-analytical errors, such as contaminations, overlapping or messy spots. Contamination is the main concern for DBS sampling, since it can lead to inaccurate determination of drug concentration in the sample. It can result from the use of topic anesthetics creams, disinfectants, etc. In this regard, the European Bioanalytical Forum (EBF) proposed the concept of good blood-spotting practices [182]:

1. prior to the collection, any contact with the target site of the matrix card must be avoided;
2. wash hands with soap and warm water for at least 30 sec and completely dry hands. If the patient's hands are cold, massaging or warming the collection site from palm to fingertip before pricking can stimulate local blood flow, but not "milk" the finger to encourage blood flow;
3. clean the puncture site (middle or ring finger) with 70% isopropyl alcohol and let dry for at least 40 sec;
4. use a sterile, single-use lancet to prick the finger just off the center of the tip of the selected finger and wipe the first blood drop away with a sterile gauze pad to remove the tissue fluid from the sample;

5. allow a large blood drop to form and carefully position the suitable filter paper below the finger and allow the drop to fall. The patient's finger should never touch the DBS matrix. Furthermore, do not place blood on top of blood, since it can result in sample concentration. At least 2 blood drops should be collected;
6. clean the finger and, if needed, place a patch on the puncture site;
7. dry for at least 3 h in horizontal position, allowing contact with air on both sides of matrix in a no humid environment at room temperature on a clean and flat surface;
8. store/transport samples in plastic bags with desiccant, under room temperature, refrigerated or frozen, depending on analyte stability.

3.5.3.4.3. Drug extraction optimization

The extraction efficiency of the analytes from a complex matrix, containing hundreds of denaturated proteins, depends on several factors: the compound's chemical properties, solvents and timing of the extraction procedure, and the filter paper used. Generally, the extraction efficiency does not need to be near to 100%, but it necessarily has to be constant and reproducible over different analyte concentrations (from high to low concentrations with respect to the calibration curve).

Water-miscible solvents are the most commonly used to extract small molecule compounds from DBS samples [216]. MeOH, ACN or mixture of them, also with water, are the most frequent used. However, the higher the aqueous content, the higher the dissolution of blood cells and other endogenous components from DBS, causing a potential greater matrix effect. To compensate the matrix effect, ISs are added in the extraction solvent. Usually, the best solvent is the one in which the analytes are soluble, because the solvent needs to have the strength to extract the drug from the paper and bring it back in solution. For the methods reported in this PhD thesis, different solvents and volumes were tested to extract the analytes from DBS samples (for more details, see sections 3.5.3.4.3.1. for SORA, REGO and their active metabolites and 3.5.3.4.3.2. for LENVA).

After the solvent addition, the DBS sample is vortexed or shacked for an amount of time that is analyte dependent, usually from 5 min to 4 h to allow analytes extraction. Time longer than 1 h may improve the reproducibility, but they do not affect the analyte recovery [217]. The optimization of this parameter is important to develop a reproducible and no time-consuming method.

In summary, the drug extraction optimization is characterized by three parameters: solvent type, volume of solvent, and the extraction time. Each parameter was assessed analyzing each QCs concentration level in triplicate. The following sections describe the procedure used for SORA, REGO and their active metabolites and for LENVA.

3.5.3.4.3.1. Sorafenib, regorafenib and their active metabolites

The DBS extraction parameters were evaluated using each QC concentration level in triplicate, obtained from whole blood spiked with QC working solutions (WSs; 95 µL of whole blood + 5 µL of proper WS) and incubated for 1 h at 37°C. For each QC sample several 20 µL blood drops were deposited on Whatman 31 ET CHR. Once the blood was dried, each spot was punched in the center for getting a 3 mm disc, corresponding approximately to 3 µL of blood, with a pneumatically-activated device (Analytical S&S, USA). To determine the best parameter, each DBS sample was compared with the corresponding sample prepared in solvent (which theoretically represents an extraction of 100%).

Firstly, 225 µL of the following extraction solvents were added to a 3 mm disc in order to select the best performing one: MeOH + 0.10% of HCOOH (v/v), MeOH + 0.30% of HCOOH (v/v) or mixture of MeOH:MilliQ H_2O (90:10, v/v) with 0.10% of HCOOH (v/v). After that, different volumes of the selected solvent were tested: 180 µL, 225 µL and 450 µL. In the end, 4 different extraction times from 30 min to 4 h, were evaluated.

3.5.3.4.3.2. Lenvatinib

The DBS extraction parameters were evaluated using each QC concentration level in triplicated obtained from spike whole blood with QC WSs (190 µL of whole blood + 10 µL of proper WS) after 1 h of incubation at 37 °C. At the beginning, for each QC sample was deposited several 20 µL blood drops on Whatman 31 ET CHR. Once the spiked blood on the filter paper was dried, one spot was punched in the center for getting 3 mm disc, corresponding to almost 3 µL of blood, with a pneumatically-activated device (Analytical S&S, USA). In this phase, the solvents tested were MeOH, ACN, MeOH + 0.10% of HCOOH (v/v), ACN + 0.10% of HCOOH (v/v), MeOH:iPrOH (50:50, v/v) or mixture of MeOH: MilliQ H_2O (90:10, v/v) with 0.10% of HCOOH (v/v), while the volumes tested were 45, 60, 75 and 120 µL. After reviewing the sample preparation, several 10 µL of QC spiked whole blood were deposited on Whatman 31 ET CHR. Once the spiked blood on the filter paper was dried, whole spot was manually punched obtaining 8 mm disc and extracted with 300 µL of MeOH + 0.10% of HCOOH (v/v), MeOH or MeOH:MilliQ H_2O (90:10, v/v) with 0.10% of HCOOH (v/v). After that, different volumes (300, 400 and 500 µL) of the selected extraction solvent were tested. At the end, the 8 mm discs were extracted with the optimized volume and solvent for 4 different time point from 30 min to 4 h.

3.5.3.4.4. Incubation time

The incubation time is another important sample preparation parameter. This parameter needs to mimic the drug partitioning into the blood. The optimal incubation time was determined analyzing QC DBS samples in

triplicate for each concentration level deposited on suitable filter paper at specific interval of incubation time (from 30 min to 24 h) and compared with the corresponding sample prepared in solvent.

For SORA, REGO and their active metabolites DBS based method, 15 µL of proper WS were added to 285 µL of whole blood and the spiked blood were incubated at 37 °C up to 24 h. Then, 5 or 20-µL aliquots of spiked blood were spotted on Whatman 31 ET CHR paper at 30 min, 1 h, 2h, 4 h, 8 h, and 24 h and allowed to air dry for 3 h before the extraction with the parameters obtained for the procedure described in section 3.5.3.4.3.1.

Similarly for the LC-MS/MS quantification method of LENVA in DBS samples, 300 µL of QC spiked whole blood (285 µL of whole blood + 15 µL of proper QC WSs) were incubated from 30 min to 24 h at 37 °C. At the beginning, several 20 µL spiked blood drop were deposited on Whatman 31 ET CHR at a defined interval of time. Each sample was automatically punched in the center for getting a 3 mm disc and then extracted with 45 µL of IS WS mixing for 1 h. After the modification of the sample preparation, aliquots of 10 µL of spiked blood were deposited on both Whatman 903 and Whatman 31 ET CHR at 30 min, 1 h, 2 h, 4 h, 8 h and 24 h. In this case, the whole spot was punched and extracted.

3.6. LC-MS/MS method validation study in plasma

The analytical LC-MS/MS methods in human plasma described in this thesis were newly developed and optimized. The methods for SORA, REGO and their active metabolites and LENVA were subsequently completely validated according to the EMA [200] and FDA [201] bioanalytical method validation guidelines. During the validation procedures, the following parameters were assessed: recovery of the analyte of interest from the biological matrix, matrix effect, linearity of the calibration curve, intra- and inter-day precision and accuracy, limit of quantification, selectivity and sensibility, dilution integrity, reproducibility with the incurred sample reanalysis (ISR) and stability of the analyte in biological samples under different conditions and in solvents.

3.6.1. Recovery

The recovery of an analyte from a complex matrix assesses its extraction efficiency as required by FDA guidelines [201]. Percentage recovery (% REC) was evaluated for each analyte in human pooled plasma samples at three concentration values (QCL, QCM and QCH) prepared in quintuplicate without adding IS. The recovery was established by comparing the peak areas of plasma samples spiked with the analyte and the peak area of extracted blank plasma samples spiked with the analyte, which ideally represented a 100% of the recovery.

For each concentration level, analyte %REC was calculated with the following Equation 9:

$$\% \, REC = \frac{analyte \; peak \; area \; (in \; matrix)}{mean \; analyte \; peak \; area \; (in \; extracted \; matrix)} \times \; 100$$

Equation 9. Recovery (% REC) calculation.

The analyte recovery does not need to be equal to 100%; however, its value should be reproducible, precise, and consistent among different analysis and for all the different concentrations (QCL, QCM, QCH).

3.6.1.1. Sorafenib, regorafenib and their active metabolites

To assess the % REC the following two set of samples were prepared:

- quintuplicate of each QC concentration levels (5 x QCL, 5 x QCM and 5 x QCH) in pooled plasma: 5 µL of proper QC WS were added to 95 µL of pooled plasma, the mixture was vortexed for 10 sec. Then, 5 µL of spiked plasma were precipitated with 495 µL of MeOH with 0.10% of HCOOH (v/v). The sample was vortexed for 10 sec and centrifuged at 16200 g and 4 °C for 10 min. For the analysis, 200 µL of the resulting clean supernatant were transferred into an autosampler propylene vial;
- quintuplicate of each QC concentration levels (5 x QCL, 5 x QCM and 5 x QCH) in extracted pooled plasma: 19 µL of pooled plasma were precipitated with 1980 µL of MeOH + 0.10% of HCOOH (v/v) and then vortexed for 10 sec and centrifuged at 16200 g and 4 °C for 10 min. One µL of proper QC WS was added to the extracted plasma sample, the mixture was vortexed for 10 sec and centrifuged for 10 min at 16200 g and 4°C. For the analysis, 200 µL of the resulting clean supernatant were transferred into an autosampler propylene vial.

3.6.1.2. Lenvatinib

For the evaluation of % REC for LENVA the following two set of samples were prepared:

- quintuplicate of the 3 QC concentration levels in pooled plasma (5 x QCL, 5 x QCM and 5 x QCH): 5 µL of proper QC WS were added to 95 µL of pooled plasma, the mixture was vortexed for 10 sec. Then, the protein precipitation was performed by adding 500 µL of MeOH + 0.10% of HCOOH (v/v) to the spiked plasma, vortexed for 10 sec and centrifuged at 16200 g and 4 °C for 25 min. For the analysis, 200 µL of the resulting clean supernatant were transferred into an autosampler glass vial;
- quintuplicate of the 3 QC concentration levels in extracted pooled plasma (5 x QCL, 5 x QCM and 5 x QCH): 95 µL of pooled plasma were precipitated with 500 µL of MeOH + 0.10% of HCOOH (v/v), vortexed for 10 sec and centrifuged at 16200 g and 4 °C for 25 min to perform the protein

precipitation. Five µL of proper QC WS were added to the extracted plasma, the mixture was vortexed for 10 sec and centrifuged at 16200 g and 4 °C for 25 min. Then, 200 µL of the resulting clean supernatant were transferred into an autosampler glass vial for the LC-MS/MS analysis.

3.6.2. Matrix effect

Matrix effect is a phenomenon caused by presence of endogenous components in the biological matrix (*e.g.,* salts, amines, phospholipids, triglycerides, *etc.*), but also from substances coming from sample containers or such plasticizers or anticoagulants [218].

Endogenous compounds that co-elute with the analyte of interest could interfere with its desolvation and charging steps in the ESI source: this process can modify the analyte ionization process in a negative (ion suppression) or positive (ion enhancement) way [219]. Also, some substances contained in the MP might alter the analyte signal producing ion enhancement or suppression, but in this case, this is not considered as matrix effect, because it is not sample specific [219]. Both ion enhancement and ion suppression phenomena might compromise sensitivity, selectivity, precision, and accuracy of the developed method and, subsequently, the consistency of the produced analytical data. For this reason, the EMA guidelines underline the importance to assess this phenomenon in mass spectrometry with a quantitative evaluation.

The samples to assess this parameter were prepared according the article proposed by Matuszewski [220]. This evaluation of matrix effect was performed using 6 replicates of the QCs (6 x QCL and 6 x QCH) and IS using matrix from 6 different lots of human plasma from healthy donors (3 females and 3 males) and by comparing the peak area ratio of post extraction QCs (QC WS added to extracted plasma sample) or IS (plasma sample extracted with the IS) with those obtained from QCs or IS prepared in pure methanol (absence of matrix) obtaining the matrix factor (MF) for analyte or IS, as reported in Equation 10:

$$\%\ MF = \frac{analyte\ or\ IS\ peak\ area\ (in\ extracted\ matrix)}{mean\ analyte\ or\ IS\ peak\ area\ (in\ solvent)} \times\ 100$$

Equation 10. Matrix factor (MF) calculation.

Moreover, the IS normalized MF was calculated as the ratio between the MF of analyte and the MF of IS (Equation 11). The coefficient of variation (CV%) of IS normalized MF should not be greater than 15%.

$$IS\ norm\ MF = \frac{analyte\ ME}{mean\ IS\ ME}$$

Equation 11. Internal standard (IS) normalized matrix factor (MF) calculation.

Moreover, the possible influence of the matrix effect on the quantification of the LLOQ was also investigated during the validation process. In this case, plasma samples at LLOQ concentration using 6 lots of matrix from 6 different donors (3 females and 3 males) were prepared. The matrix effect can be considered negligible, if the accuracy is within 80-120% of the nominal concentration and with a precision as CV% ≤ 20% for at least 5 of the 6 samples. Furthermore, the S/N ratio for each LLOQ sample was evaluated.

The matrix effect was also assessed with a qualitative evaluation through post-column infusion [221].

In this experiment, a constant concentration of the analyte was introduced directly into the mass spectrometer source over an infusion pump for all the duration of the chromatographic run of a blank plasma sample. The extracted blank plasma sample eluted from the LC column and the constant analyte flow from the infusion pump were combined through a zero dead volume tee union and inserted into the mass spectrometer, as shown in Figure 25. The signal of the infused compound is monitored during the analysis by the MRM scan mode. Endogenous or exogenous components eluting from the column can cause a reduction or an increase of analyte signal; if both ion suppression and ion enhancement phenomena do not occur close to the retention time of the analyte, the matrix effect can be considered negligible.

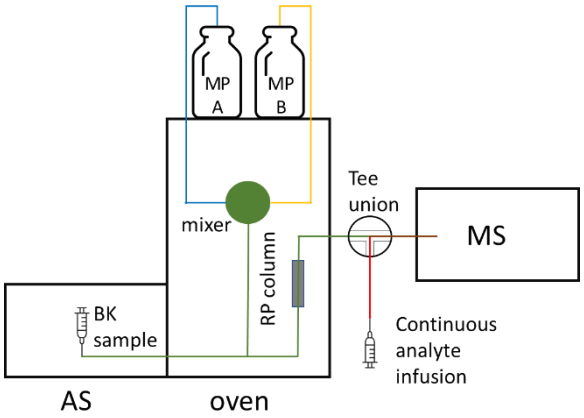

Figure 25. Schematic representation of LC-MS/MS system set up for the post column infusion. AS: autosampler; MP: mobile phase; RP: reverse phase; MS: mass spectrometer.

3.6.2.1. Sorafenib, regorafenib and their active metabolites

For the quantitative evaluation of the matrix effect for SORA, REGO and their active metabolites the following two sets of samples were prepared:

- QCL, QCH and blank with IS in extracted plasma from 6 single donor (6 x QCL, 6 x QCH and 6 x BK+IS): 95 µL of single donor plasma were precipitated with 1980 µL of MeOH + 0.10% of HCOOH (v/v) or 1980 µL of 20 ng/mL of SORA-L4 and REGO-D_3 in acidified MeOH, then vortexed for 10 sec and centrifuged at 16200 g and 4 °C for 10 min. One µL of proper QC WS or MeOH was added to the extracted plasma sample, the mixture was vortexed for 10 sec and centrifuged for 10 min at 16200

g and 4 °C. For the analysis, 200 µL of the resulting clean supernatant were transferred into an autosampler polypropylene vial;

- a triplicate of QCL, QCH and BK with IS in pure solvent (MeOH): 5 µL of proper QC WS or 5 µL of MeOH were added to 95 µL of MeOH, the mixture was vortexed for 10 sec. Then, 5 µL of spiked MeOH were diluted with 495 µL of MeOH + 0.10% of HCOOH (v/v) or 495 µL of 20 ng/mL SORA-L4 and REGO-D_3 in MeOH plus 0.10% of HCOOH (v/v) to simulate the protein precipitation and vortexed for 30 sec. For the analysis, 200 µL of the resulted clean solution were transferred into an autosampler polypropylene vial.

The LLOQ samples were prepared by spiking 95 µL of single donor plasma with 5 µL of LLOQ WS and vortexed for 10 sec. Five µL of spiked plasma were precipitated with 495 µL of 20 ng/mL SORA-L4 and REGO-D_3 and SORA acidified methanolic solution, vortexed for 10 sec and centrifuged at 16200 g and 4 °C for 10 min. Then, 200 µL of the resulting clean supernatant were transferred into an autosampler polypropylene vial for the analysis.

For the qualitative evaluation of matrix effect a 200 ng/mL methanolic solution of each analyte separately was infused into the ion source through an infusion pump with a flow rate of 20 µL/min during the LC-MS/MS analysis of a blank sample (2 µL as injection volume).

3.6.2.2. Lenvatinib

For the quantitative evaluation of the matrix effect for LENVA and it IS the following two sets of samples were prepared:

- QCL, QCH and blank with IS in extracted plasma from 6 single donor (6 x QCL, 6 x QCH and 6 x BK+IS): 95 µL of single donor plasma were precipitated with 500 µL of MeOH + 0.10% of HCOOH (v/v) or 500 µL of 50 ng/mL LENVA-D_4 acidified methanolic solution, vortexed for 10 sec and centrifuged at 16200 g and 4 °C for 25 min to perform the protein precipitation. Five µL of proper QC WS or MeOH were added to the extracted plasma, the mixture was vortexed for 10 sec and centrifuged at 16200 g and 4 °C for 25 min. Then, 200 µL of the resulting clean supernatant were transferred into an autosampler glass vial for the LC-MS/MS analysis;
- a triplicate of QCL, QCH and BK with IS in pure solvent (MeOH): 5 µL of proper QC WS or 5 µL of MeOH were added to 95 µL of MeOH, the mixture was vortexed for 10 sec. Then 500 µL of MeOH + 0.10% of HCOOH (v/v) or 500 µL of 50 ng/mL LENVA-D_4 in MeOH plus 0.10% of HCOOH (v/v) were added to the spiked MeOH to mimic the protein precipitation, vortexed for 30 sec. For the analysis, 200 µL of the resulted clean solution were transferred into an autosampler glass vial.

The LLOQ samples were prepared by spiking 95 µL of single donor plasma with 5 µL of LLOQ WS, vortexed for 10 sec. The samples were precipitated with 500 µL of 50 ng/mL LENVA-D_4 acidified methanolic solution,

vortexed for 10 sec and centrifuged at 16200 g and 4 °C for 25 min. Then, 200 µL of the resulting clean supernatant were transferred into an autosampler glass vial for the analysis.
For the qualitative analysis a 200 ng/mL solution of LENVA in MeOH was infused into the ion source through an infusion pump with a flow rate of 20 µL/min during the LC-MS/MS analysis of blank sample (4 µL as injection volume).

3.6.3. Linearity

The linearity of an analytical method represents its ability, within a given concentration range, to obtain results directly proportional to the concentration of the analyte present in the sample. The linearity was assessed by preparing 8 calibration curves, which were freshly processed during 8 different working days. For each calibrator, the area ratio was calculated and plotted against the nominal concentration of each analyte in the sample.
The intercept on y-axis (q) and the slope (m) of the linear Equation 12 were calculated by processing the values of y_i and x_i obtained from each calibrator.

$$y_i = mx_i + q$$

Equation 12. Equation of linear calibration curve.

Where:
x_i = determined concentration value of the i^{th} analyte;
$y_i = A_a/A_{IS}$;
A_a = peak area of the i^{th} analyte;
A_{IS} = peak area of the IS;

The calibration curves were obtained using a weighted quadratic regression model ($1/x^2$), while the fitting quality was assessed using Pearson's determination coefficient (r) and comparing the nominal concentrations with the back-calculated ones using the calibration curve. In each analytical and validation run, at least 75% of the calibrators, including the LLOQ and the ULOQ, had to be within 85–115% of the nominal concentration (80–120% at the LLOQ).
The calibration curves linearity over the 8 working days was evaluated calculating for each calibrator its arithmetic mean, its standard deviation (SD), its precision (as coefficient of variation - CV%, which had to be not greater than 15%) and accuracy, which had to be within 85-115%, respectively (with the usual exception of LLOQ, whose CV% had to be ≤20% and accuracy had to be between 80% and 120%).

The accuracy describes the closeness of the measured value to the nominal concentration of the analyte expressed as percentage of the back-calculated value of each calibrator. It is calculated with the following Equation 13:

$$Accuracy\% = \frac{X_i}{X_n}\ x\ 100$$

Equation 13. Accuracy (Acc%) calculation.

Where:

X_i: determined concentration value of the i^{th} analyte

X_n: nominal concentration value

Instead, the precision describes the closeness of repeated individual measures of analyte expressed as the CV% and it is calculated with Equation 14:

$$CV\% = \frac{SD}{\bar{X}}\ x\ 100$$

Equation 14. Precision (CV%) calculation.

Where:

$\bar{X}$: mean calculated concentration.

Moreover, the reproducibility of each calibration curves was evaluated by arithmetic mean, SD, and CV% of both slope and Pearson's determination coefficient.

3.6.4. Intra-day and inter-day precision and accuracy

Intra-day precision and accuracy were determined during a single working day by analyzing 6 replicates of the LLOQ and of each QC concentration, while inter-day precision and accuracy were assessed on 5 different working days, analyzing 3 replicates of the LLOQ and of each QC concentration using a calibration curve freshly prepared every day. The measured concentrations had to be within ±15% of the nominal value (accuracy% between 85% and 115%) with a CV% ≤ 15% for at least 67% of the QCs at each concentration level in each run (only one QC for each concentration level could be excluded). For the LLOQ samples, the measured concentration had to be within ±20% (accuracy% between 80% and 120%) and had to have a CV% ≤ 20%.

3.6.5. Limit of quantification and selectivity

Sensitivity is defined by the LLOQ, which is the lowest concentration that could be measured with a precision within 20%, accuracy between 80% and 120%, and a S/N ratio ≥ 5. The LLOQ of the analytical method was

verified by analyzing precision, accuracy, and S/N ratio obtained from 6 samples of pooled blank human plasma added with the least concentrated WS. To be accepted, this analysis should show, for each analyte, an acceptable precision (≤20%) and accuracy (80-120%) for at least 5 out of 6 replicates.
The selectivity identifies the ability of the analytical method to quantify the analyte of interest and the IS, differentiating them from interferents present in the matrix such as endogenous components, degradation products or other co-administered medications.
Selectivity was investigated by analyzing 6 blank human plasma samples obtained from 6 different donors (3 females and 3 males). These samples should be free of interference at the retention time of the analyte of interest (a response lower than 20% of the LLOQ for each analyte and lower than 5% for the IS).

3.6.6. Dilution integrity

Dilution integrity has to be demonstrated in order to be sure that a sample with a concentration above the ULOQ of the analytical method can be correctly quantified after its dilution. This evaluation was performed for two dilution factors, i.e., 1:10 and 1:100, using blank pooled plasma matrix as a diluting agent. Each dilution factor was tested in quintuplicate, and the measured concentration had to be within ±15% of the nominal value with a CV% ≤ 15%.

3.6.6.1. Sorafenib, regorafenib and their active metabolites

Dilution integrity was assessed on a plasma sample at 8000 ng/mL of SORA and REGO and 4000 ng/mL for their active metabolites.
Ten samples at the ULOQ concentration were prepared adding 5 µL of the proper WS to 95 µL of pooled plasma. After 10 sec of vortex-mixing, from five replicate a 5 µL-aliquot was realized and diluted 1:10 by adding 45 µL of pooled plasma, while 5 µL of the other five replicates were diluted 1:100 adding 495 µL of pooled plasma. Five µL of each sample were precipitated with 495 µL of 20 ng/mL SORA-L4 and REGO-D_3 in acidified MeOH, vortexed for 10 sec and centrifuged for 10 min at 16200 g and 4 °C. Then, 200 µL of clean supernatant were transferred into an autosampler polypropylene vial.

3.6.6.2. Lenvatinib

Dilution integrity was evaluated on a plasma sample at a LENVA concentration of 3000 ng/mL, using 1:10 and 1:100 dilution factors.
Each sample was prepared adding 5 µL of the 3000 ng/mL LENVA WS to 95 µL of pooled plasma. After 10 sec of vortex-mixing, from each replicate a 10 µL-aliquot was realized and diluted 1:10 by adding 90 µL of pooled

plasma. Subsequently, a 10 µL-aliquot from one of the 5 initial replicates of plasma sample (at the concentration of 3000 ng/mL) was diluted 1:10 with pooled plasma as previously described. From this sample, five 10 µL-aliquots were obtained and each of them was diluted 1:10 by adding 90 µL of pooled plasma to achieve a final dilution of 1:100. All samples were then processed adding 500 µL of 50 ng/mL LENVA-D_4 in acidified MeOH, vortexed for 10 sec and centrifuged for 25 min at 16200 g and 4 °C. Then, 200 µL of clean supernatant were transferred into an autosampler glass vial.

3.6.7. Stability

The stability of an analyte is function of the matrix in which it is dispersed, of the conditions of its storage and of the chemical properties of the analyte itself. Assessing the stability of the analyte in stock solutions, WS and in the matrix is essential to ensure the consistency of the results achieved from the LC-MS/MS analytical method. This evaluation includes all the situation which can be encountered during the whole analytical procedure. Thus post-processing stability, short- and long-term stability, freeze-thaw stability, WS and stock stability were evaluated.

Bench-top and long-term stability were assessed for each analyte using QCs prepared in triplicate at each concentration (QCL, QCM, QCH): bench-top stability in plasma was investigated after 4 h at room temperature; the post-processing stability of the extracted QCs was evaluated in autosampler set at 4 °C re-analyzing the samples about 24, 48, 72 and 96 h after the first injection; freeze (-80°C)/thaw stability was assessed by analyzing 3 freshly prepared aliquots of each QCs concentration, and then again after one, two and three freeze/thaw cycles. Long-term stability was investigated both in plasma, to assess patient samples stability after storage at -80 °C, and in solvent (MeOH or DMSO) to assess WSs or stock solutions stability after storage at -20 °C and -80 °C, respectively. Stability tests were considered verified if the samples tested with a fresh calibration curve did not exceed ±15% from the nominal concentrations at each QCs concentration for at least 2 of the 3 QCs per concentration level.

3.6.8. Incurred samples reanalysis

The incurred samples reanalysis (ISR) represents an additional measure of the assay reproducibility as reported in the 2013 FDA Bioanalytical validation guidance, that considered the AAPS/FDA seminar on the reanalysis of the assayed sample [222]. This evaluation is also present in the latest version of both EMA (2011) [200] and FDA (2018) [201] bioanalytical validation guidelines, underling the importance of the method reproducibility.

The ISR was verified by repeating the analysis of a subset of patients' samples in separate runs in different working days. The two analyses could be considered equivalent for each analyte of interest if the percentage

difference (% diff) between the first and the second concentration measured was within ±20% for at least 67% of the analyzed samples. The Equation 15 was used to calculate the % diff:

$$\%\ diff = \frac{repeat\ mesurament - original\ mesurament}{arithmetic\ mean\ of\ the\ two\ mesuraments}\ x\ 100$$

Equation 15. Percentage difference (%diff) calculation.

3.6.8.1. Sorafenib, regorafenib and their active metabolites

The ISR was evaluated using a set of 29 patients of which 21 plasma sample from patients affected by HCC and treated with SORA and 8 plasma samples of patients treated with REGO. All the plasma samples used for this analysis derived from the analytical cross-validation study (internal protocol code: CRO-2018-83).

3.6.8.2. Lenvatinib

The ISR was assessed in a set of 14 plasma samples from patients affected by HCC and treated with LENVA. All the plasma samples used for this analysis derived from the analytical cross-validation study (internal protocol code: CRO-2018-83).

3.7. LC-MS/MS method validation study in dried blood spot

The analytical LC-MS/MS methods in DBS reported in this thesis were newly developed and optimized. The method for SORA, REGO and their active metabolites were subsequently completely validated according to the EMA [200] and FDA [201] bioanalytical method validation guidelines and EBF recommendation on the validation of bioanalytical [182,183]. The validation of the LC-MS/MS method for the quantification of LENVA in DBS followed also the official IATDMCT guideline [181], that were not available at that time of the SORA and REGO method validation.

During the validation procedures, the following parameters were assessed: Hct effect, influence of spot volume, recovery of the analyte of interest from the biological matrix, the matrix effect, process efficiency, linearity of the calibration curve, intra- and inter-day precision and accuracy, limit of quantification, selectivity and sensibility, dilution integrity, reproducibility with the ISR and stability of the analyte in biological samples under different conditions.

3.7.1. Effect of hematocrit and spot volume

Hct effect and spot volume are two parameters of the DBS sampling, which are linked together. Hct is the ratio between the volume of the red blood cells to the total volume of blood. This parameter influences spot formation, homogeneity and size because the spread of the blood on the DBS cards depends on its viscosity, which raises with the increase of the Hct [223]. In fact, the viscosity of the blood affects the proportion between red blood cells and plasma in the sample and the amount of sample present in a matrix punch of fixed size, thus bringing to a modifications in the relative concentration of the drug on these blood compartments [224]. Moreover, the Hct influences drying time, recovery of the analyte and specially the robustness and reproducibility of the assays [182,225].

To evaluate the Hct and spot effect, samples with at least 2 different Hct from one K-EDTA healthy donor whole blood were artificially created by centrifuging it for 10 min at 2600 g and 4 °C and then adding or removing defined volume of plasma as preferred procedure reported in the literature [225]. During the validation, the created Hct values have to cover the entire Hct range expected from the study population. Triplicates of each QC concentration level were prepared for each created Hct value and for each sample 4 different spot volume were deposited on the suitable filter paper. These samples were quantified using a DBS calibration curve prepared at fixed Hct value and spot volume. The DBS samples with different Hct and spot volume have to have an accuracy between 85-115% of the nominal concentration and a precision (CV%) ≤ 15% to considered the Hct and spot effects as negligible.

3.7.1.1. Sorafenib, regorafenib and their active metabolites

According to the Hct range observed in the patients treated with SORA or REGO enrolled in our analytical cross-validation study (internal protocol code: CRO-2018-83), which was between 32.2% and 48.5%, the created Hct values chosen were 30% and 50%. The spot volumes tested were 5, 10, 20 and 40 µL deposited on Whatman 31 ET HCR.

At the beginning, each DBS sample was punched automatically in the center for getting a 3 mm disc and then extracted with 225 µL of IS WSs in acidified MeOH and 1 h for shacking. The Hct evaluation was also performed depositing 5 µL of QC DBS samples with different Hct on Whatman 31 ET CHR. In this latter case, the DBS sample was manually punched for getting a 6 mm disc and then extracted with 375 µL of IS WSs and mixed for 1 h before the analysis.

3.7.1.2. Lenvatinib

The Hct of the patients' treated with LENVA and enrolled in the analytical cross-validation study (internal protocol code: CRO-2018-83) was between 31.0% and 50.0%, so the Hct values chosen were 25%, 35%, 45% and 55% in the first experiment performed deposing 4 different spot volumes (5, 10, 20 and 40 µL). These samples were quantified on a calibration curve with 40.4% of Hct and 20 µL as spot volume. Each sample with each Hct and each different spot volume was punched in the center for getting a 3 mm disc. These discs were extracted with 45 µL of IS WS.

After changing the sample preparation, the Hct value tested were 25% and 55%, while the spotted volume was only 10 µL on both Whatman 903 and Whatman 31 ET CHR. In this case, all the spots were extracted with 300 µL of IS WS and shacked for 30 min before the analysist. These samples were quantified on a calibration curve with a Hct of 39.7 %.

3.7.2. Recovery

As reported in section 3.6.1., % REC was evaluated for each analyte in DBS samples at three concentration values (QCL, QCM and QCH) without adding IS. The recovery was established by comparing the peak areas of DBS samples spiked with the analyte and the peak area of extracted blank DBS samples spiked with the analyte, which ideally represented a 100% of the recovery.

For each concentration level, analyte %REC was calculated with Equation 9.

The analyte % REC does not need to be equal to 100%; however, its value should be reproducible, precise, and consistent among different analysis and for all the different concentrations (QCL, QCM, QCH).

3.7.2.1. Sorafenib, regorafenib and their active metabolites

To assess the %REC the following two set of samples were prepared:

- a single sample at each QC level (1x L, 1x M and 1x H) using a single donor of blood, and this was repeated for six different blood donors (3 males and 3 females) for a total of 6 samples at each QC concentration level (6 x QCL, 6 x QCM and 6 x QCH): 5 µL of proper QC WS were added to 95 µL of whole blood, the samples were gently mixed and incubated for 1 h at 37 °C. Then, 5 µL of spiked blood were deposited on Whatman 31 ETCHR and allowed to air dry for 3 h at room temperature. The whole spot was punched by manual device for getting a disc with 6 mm of diameter, which was extracted with 375 µL of MeOH with 0.10% of HCOOH (v/v). The sample was shacked for 1 h and 200 µL of the resulting clean supernatant were transferred into an autosampler polypropylene vial for the analysis;

- a single sample at each QC level in extracted blank DBS (1x L, 1x M and 1x H) using a single donor of blood, and this was repeated for six different blood donors (3 males and 3 females) for a total of 6 samples at each QC concentration level (6 x QCL, 6 x QCM and 6 x QCH): 5 µL of single donor blank blood were deposited on Whatman 31 ETCHR and allowed to air dry for 3 h at room temperature. The whole spot was punched by manual device for getting a disc with 6 mm of diameter, which was extracted with 375 µL of MeOH with 0.10% of HCOOH (v/v). The sample was shacked for 1 h, and then 95 µL of blank extracted DBS were spiked with 5 µL of proper QC WS. Then, 5 µL of spiked extracted DBS were diluted with 375 µL of MeOH + 0.10% of HCOOH (v/v) and vortexed for 30 sec. For the analysis, 200 µL of the resulting clean supernatant were transferred into an autosampler polypropylene vial.

3.7.2.2. Lenvatinib

For the evaluation of the % REC for LENVA the following two set of samples were prepared:

- a triplicate of the 3 QC concentration levels in 6 lots of single donor blood (3 males and 3 females), to obtain a total of 18 x QCL, 18 x QCM and 18 x QCH samples. In addition, with the blood deriving from one of these donors, two samples at different Hct (one lower and one higher than the donor's Hct) were artificially created as above described. These blood samples at 2 different Hct were used to create two more sets of triplicates at each QC concentration level. Ten µL of proper QC WS were added to 190 µL of single donor whole blood, the samples were gently mixed and incubated for 30 min at 37 °C. Then, 10 µL of spiked blood were deposited on Whatman 31 ETCHR and on Whatman 903 and allowed to air dry for 3 h at room temperature. The whole spot was punched by manual device for getting a disc with 8 mm of diameter, which was extracted with 300 µL of 50 ng/mL of LENVA-D_4 in MeOH with 0.10% of HCOOH (v/v). The sample was shacked for 30 min and 100 µL of the resulting clean supernatant were diluted with 50 µL of MB A. After the mixing, the solution was transferred into an autosampler glass vial for the analysis;
- A triplicate of the 3 QC concentration levels in 6 lots of single donor blood (3 males and 3 females) in extracted DBS, to obtain a total of 18 x QCL, 18 x QCM and 18 x QCH samples. In addition, with the blood deriving from one of these donors, two samples at different Hct (one lower and one higher than the donor's Hct) were artificially created as above described. These blood samples at 2 different Hct were used to create two more sets of triplicates at each QC concentration level. Ten µL of single donor whole blood were deposited on Whatman 31 ETCHR and on Whatman 903 and allowed to air dry for 3 h at room temperature. The whole spot was punched by manual device for getting a disc with 8 mm of diameter, which was extracted with 300 µL of 50 ng/mL of LENVA-D_4 in MeOH with 0.10% of HCOOH (v/v). Ninety-five µL of extracted matrix were spiked with 5 µL of proper QC WS and

mixed for 10 sec. Then, 5 µL of spiked extracted DBS were diluted with 145 µL of blank extracted DBS and mixed for 10 sec. An aliquot of 100 µL of the resulting clean supernatant was diluted with 50 µL of MB A. After mixing, the solution was transferred into an autosampler glass vial for the analysis.

3.7.3. Matrix effect

The assessment of matrix effect in DBS samples was performed in two different ways:

- at QCL and QCH concentrations (with IS) using matrix from 6 different lots of whole blood from healthy donors (3 females and 3 males) and by comparing the peak area of post extraction QCs (QC WS added to extracted DBS sample) with those obtained from QCs prepared in pure MeOH (absence of matrix). This allows to obtain the MF for analyte, as reported in Equation 10. The peak area comparison was also performed for IS, obtaining the MF of IS.

  The IS normalized MF was calculated as the ratio between the MF of analyte and the MF of IS Equation 11. The CV% of IS normalized MF should not be greater than 15%;
- on DBS samples at LLOQ concentration prepared from 6 lots of matrix from 6 different donors (3 females and 3 males). The matrix effect could be considered negligible if the accuracy was within 80-120% of the nominal concentration and the precision had as CV% ≤ 20% for at least 5 of the 6 samples. Furthermore, the S/N ratio for each LLOQ sample had to be > 5.

3.7.3.1. Sorafenib, regorafenib and their active metabolites

For the quantitative evaluation of the matrix effect for SORA, REGO and their active metabolites the needed set of samples were prepared as follows:

- QCL, QCH and blank with IS in extracted matrix from 6 single donor (3 males and 3 females): 5 µL of single donor blank blood were deposited on Whatman 31 ETCHR and allowed to air dry for 3 h at room temperature. The whole spot was punched by manual device for getting a disc with 6 mm of diameter, which was extracted with 375 µL of MeOH with 0.10% of HCOOH (v/v). The sample was shacked for 1 h, and then 95 µL of blank extracted DBS were spiked with 5 µL of proper QC WS. Then, 5 µL of spiked extracted DBS were diluted with 375 µL of MeOH + 0.10% of HCOOH (v/v) and then vortexed for 30 sec. For the analysis, 200 µL of the resulting clean supernatant were transferred into an autosampler polypropylene vial;
- triplicate of QCL, QCH and BK with IS in pure solvent (MeOH): 5 µL of proper QC WS or 5 µL of MeOH were added to 95 µL of MeOH, the mixture was vortexed for 10 sec. Then, 5 µL of spiked MeOH were diluted with 370 µL of MeOH + 0.10% of HCOOH (v/v) or 370 µL of 20 ng/mL SORA-L4 and REGO-D_3

in MeOH plus 0.10% of HCOOH (v/v), and vortexed for 30 sec. For the analysis, 200 µL of the resulted clean solution were transferred into an autosampler polypropylene vial.

The LLOQ samples were prepared by spiking 95 µL of single donor whole blood with 5 µL of LLOQ WS, the samples were gently mixed and incubated for 1 h at 37 °C. Then, 5 µL of spiked blood were deposited on Whatman 31 ETCHR and allowed to air dry for 3 h at room temperature. The whole spot was punched by manual device for getting a disc with 6 mm of diameter, which was extracted with 375 µL of 20 ng/mLSORA-L4 and REGO-D_3 and SORA acidified methanolic solution. The sample was shacked for 1 h and 200 µL of the resulting clean supernatant were transferred into an autosampler polypropylene vial for the analysis.

3.7.3.2. Lenvatinib

For the quantitative evaluation of the matrix effect for LENVA and its IS the needed set of samples were prepared as follows:

- Post-extraction QC: 10 µL of single donor whole blood were deposited on Whatman 31 ETCHR and on Whatman 903 and allowed to air dry for 3 h at room temperature. The whole spot was punched by manual device for getting a disc with a diameter of 8 mm, which was extracted with 300 µL of MeOH with 0.10% of HCOOH (v/v). Ninety-five µL of extracted matrix were spiked with 5 µL of proper QC WS and mixed for 10 sec. Then, 5 µL of spiked extracted DBS were diluted with 145 µL of blank extracted DBS and mixed for 10 sec. One-hundred µL of the resulting clean supernatant were diluted with 50 µL of MB A. After the mixing, the solution was transferred into an autosampler glass vial for the LC-MS/MS analysis.
- Samples in pure solvent (MeOH): 5 µL of proper QC WS or 5 µL of MeOH was added to 95 µL of MeOH, the mixture was vortexed for 10 sec. Then 5 µL of spiked MeOH were added to 145 µL of MeOH + 0.10% of HCOOH (v/v) or 145 µL of 50 ng/mL LENVA D_4 in MeOH plus 0.10% of HCOOH (v/v), vortexed for 30 s. For the analysis, 100 µL of the resulting clean supernatant were diluted with 50 µL of MB A, mixed and transferred into an autosampler glass vial for the LC-MS/MS analysis.

The LLOQ samples were prepared by spiking 190 µL of single donor whole blood with 10 µL of LLOQ WS, the samples were gently mixed and incubated for 30 min at 37 °C. Then, 10 µL of spiked blood were deposited on Whatman 31 ETCHR and on Whatman 903 and allowed to air dry for 3 h at room temperature. The whole spot was punched by manual device for getting a disc with 8 mm diameter, which was extracted with 300 µL of MeOH with 0.10% of HCOOH (v/v). The sample was shacked for 30 min and 100 µL of the resulting clean supernatant were diluted with 50 µL of MB A. After the mixing, the solution was transferred into an autosampler glass vial for the analysis.

3.7.4. Process efficiency

The process efficiency was assessed for each analyte at each QC concentration level (QCL, QCM and QCH) in 6 lots of single donor blood (3 males and 3 females), comparing the analyte area ratio of DBS samples spiked with the analyte with those obtained from QCs prepared in pure methanol (absence of matrix), which ideally represented a 100% of the process efficiency. For LENVA, in addition, with the blood deriving from one of the donors, two samples at different Hct (one lower and one higher than the donor's Hct) were artificially created as above described. These blood samples at 2 different Hct were used to create two more sets of triplicates at each QC concentration level. For each concentration level, analyte process efficiency was calculated with Equation 16.

$$Process\ efficiency = \frac{analyte\ area\ ratio\ (in\ matrix)}{mean\ analyte\ area\ ratio\ (in\ solvent)} \times\ 100$$

Equation 16. Process efficiency calculation.

3.7.4.1. Sorafenib, regorafenib and their active metabolites

For the calculation of the process efficiency for SORA, REGO and their active metabolites the following two set of samples were prepared:

- QC from 6 healthy donors' blood (6 x QCL, 6 x QCM and 6 x QCH): 5 µL of proper QC WS were added to 95 µL of whole blood, the samples were gently mixed and incubated for 1 h at 37 °C. Then, 5 µL of spiked blood were deposited on Whatman 31 ETCHR and allowed to air dry for 3 h at room temperature. The whole spot was punched by manual device for getting a disc with 6 mm of diameter, which was extracted with 375 µL of 20 ng/mL of SORA-L4 and REGO-D_3 in MeOH with 0.10% of HCOOH (v/v). The sample was shacked for 1 h and 200 µL of the resulting clean supernatant were transferred into an autosampler polypropylene vial for the analysis;
- triplicate of QCL, QCH and BK with IS in pure solvent (MeOH): 5 µL of proper QC WS or 5 µL of MeOH were added to 95 µL of MeOH, the mixture was vortexed for 10 sec. Then, 5 µL of spiked MeOH were diluted with 370 µL of 20 ng/mL SORA-L4 and REGO-D_3 in MeOH plus 0.10% of HCOOH (v/v), vortexed for 30 sec. For the analysis, 200 µL of the resulting clean solution were transferred into an autosampler polypropylene vial.

3.7.4.2. Lenvatinib

The assessment of process efficiency for LENVA was performed using the following two set of samples:

- QCs from 6 healthy donors' blood and from the 2 samples with artificially-created Hcts, were prepared in triplicate (24 x QCL, 24 x QCM, 24 x QCH): 10 µL of proper QC WS was added to 190 µL of single donor whole blood, the samples were gently mixed and incubated for 30 min at 37 °C. Then, 10 µL of spiked blood were deposited on Whatman 31 ETCHR and on Whatman 903 and allowed to air dry for 3 h at room temperature. The whole spot was punched by manual device for getting a disc with 8 mm of diameter, which was extracted with 300 µL of 50 ng/mL of LENVA-D_4 in MeOH with 0.10% of HCOOH (v/v). The sample was shacked for 30 min and 100 µL of the resulting clean supernatant were diluted with 50 µL of MB A. After the mixing, the solution was transferred into an autosampler glass vial for the analysis;
- a triplicate of QCL, QCH and BK with IS in pure solvent (MeOH): 5 µL of proper QC WS or 5 µL of MeOH were added to 95 µL of MeOH, the mixture was vortexed for 10 sec. Then 5 µL of spiked MeOH were added to 145 µL of 50 ng/mL LENVA D_4 in MeOH plus 0.10% of HCOOH (v/v), vortexed for 30 s. For the analysis, 100 µL of the resulting clean supernatant were diluted with 50 µL of MB A, mixed and transferred into an autosampler glass vial for the LC-MS/MS analysis.

3.7.5. Linearity

The linearity was assessed by preparing several calibration curves, which were freshly processed during several different working days. Also, for the DBS matrix the same evaluation reported in section 3.6.3. used for the plasma matrix were performed.

3.7.6. Intra-day and inter-day precision and accuracy

Intra-day and inter-day precision and accuracy assessments for the DBS matrix were performed as reported in section 3.6.4. for the plasma matrix.

3.7.7. Limit of quantification and selectivity

As reported in section 3.6.5., sensitivity is defined by analyzing precision, accuracy, and S/N ratio obtained from 6 LLOQ samples in DBS. To be accepted, LLOQ has to have an acceptable precision (≤20%) and accuracy (80-120%) for at least 5 out of 6 replicates for each analyte.
Selectivity was investigated by analyzing 6 blank DBS samples obtained from 6 different donors (3 females and 3 males). These samples should be free of interference at the retention time of the analyte of interest (a response lower than 20% of the LLOQ for each analyte and lower than 5% for the IS).

3.7.8. Dilution integrity

Also for the DBS matrix, the dilution integrity was investigated in a similar way and with the same acceptance criteria described in section 3.6.6. In this case, the dilution agent was blank DBS extracted matrix.

3.7.8.1. Sorafenib, regorafenib and their active metabolites

Dilution integrity was assessed on ten DBS samples at 8000 ng/mL of SORA and REGO and 4000 ng/mL for their active metabolites.

The samples were prepared adding 5 µL of the proper WS to 95 µL of whole blood. After gentile mixing and incubation for 1 h at 37 °C, 5 µL of spiked blood were deposited on Whatman 31 ETCHR and allowed to air dry for 3 h at room temperature. The whole spot was punched by manual device for getting a disc with 6 mm of diameter, which was extracted with 375 µL of 20 ng/mL SORA-L4 and REGO-D_3 in acidified MeOH. The sample was shacked for 1 h and 5 µL of extracted DBS were added with 45 µL of blank plus IS DBS extracts (1:10 dilution factor) or with 495 µL of blank plus IS DBS extracts (1:100 dilution factor). Samples were vortexed for 10 sec and analyzed.

3.7.8.2. Lenvatinib

In this case, the dilution integrity was not evaluated due to the very wide analytical range (5-2000 ng/mL) and on the basis of the LENVA concentration determined in plasma samples.

3.7.9. Stability

For the DBS matrix, the long-term stability of each was assessed at the storage conditions both in plastic envelopes at -80°C and in paper envelopes inside the dryer at room temperature at determine time intervals. The working and stock solutions used for DBS matrix were the same employed for plasma matrix, thus their stability was assessed only once as previously described (section 3.6.7).

For LENVA DBS matrix, also short term stability at elevated temperatures for until 4 days at 50 °C (to mimic the possible high temperature which can occur during sample transportation) and stability after 3 freeze (-80 °C)/thaw cycle according to IATDMCT guidelines [181] were evaluated. These tests were performed analyzing QCL and QCH samples kept in the conditions to be tested (i.e. at high temperature or freeze/thawed) in quintuplicate over a calibration curve freshly prepared and in extracted matrix in the autosampler by repeatedly analyzing the samples 24, 48, 72 and 94 h after the first injection. For the DBS

method for the quantification of SORA, REGO and their active metabolites, the stability tests were executed analyzing each QC concentration level in triplicates.
The acceptance criteria were the same as those described in section 3.6.7.

3.7.10. Incurred samples reanalysis

ISR as additional measure of assay reproducibility in DBS matrix was assessed as described in section 3.6.8. with the same acceptance criteria. All the DBS samples used for this analysis derived from the analytical cross-validation study (internal protocol code: CRO-2018-83).

3.7.10.1. Sorafenib, regorafenib and their active metabolites

For this analytical method a set of 15 patients' DBS samples (8 samples with SORA and 7 samples with REGO) were analyzed in two different analytical sessions.

3.7.10.2. Lenvatinib

The ISR was assessed in a set of 4 DBS samples from patients affected by HCC and treated with LENVA.

3.8. Clinical application of LC-MS/MS quantification method

The patients' samples were analyzed together with the calibrators and the QCs, to calibrate the instrument and to monitor and assure the analysis quality, respectively. The QC samples should be evenly divided over the run, in such way precision and accuracy is ensured during the entire run.
At the beginning of each analysis, a series of samples has to be checked to ensure that all the necessary conditions for starting a reliable quantification are met. These samples constitute the system suitability test (SST) and are the following:

- a blank sample, containing only the extracted matrix;
- a zero sample, that is a blank sample containing only the IS;
- a LLOQ sample in matrix.

Both the EMA and FDA guidelines [200,201] describe the criteria for considering the analysis acceptable:

- the SST should guarantee the LLOQ quantification and the absence of a quantifiable signal of each analyte into the blank sample;
- calibrators should have a CV% ≤15% and an accuracy within 85-115%, with the exception of the LLOQ (≤20% and within 80-120%, respectively); at least 75% of the calibrators, with a minimum of six, have to satisfy these criteria;

- the QCs should have a CV%≤15% and an accuracy within 85-115%; at least 67% of the QC samples and at least 50% at each concentration level should comply with these criteria. In our case, only one QC for each concentration level could be excluded.

3.8.1. Sorafenib, regorafenib and their active metabolites

The developed and validated LC-MS/MS method for the quantification of SORA, REGO and their active metabolites was used to determine the plasma and DBS concentration of these drugs in about 66 patients' samples.

In particular, for SORA, 52 patients' plasma samples and 49 paired venous DBS were analyzed. All the samples derived from patients affected by HCC. For REGO, 14 patients' paired plasma and DBS samples were analyzed. Five samples came from patients affected by HCC and treated with REGO, while the 6 samples belonged to patients treated with REGO but affected by CRC or GIST. REGO represents the third-line treatment for both these type of gastroenteric cancer.

3.8.2. Lenvatinib

Once the validation had been completed, the LC-MS/MS method was applied to quantify the LENVA concentration in 24 plasma samples collected from patients affected by advanced HCC and enrolled in the analytical cross-validation study (internal protocol code: CRO-2018-83, described in the section 3.1.) ongoing at the National Cancer Institute of Aviano.

LENVA concentration was also determined in 4 venous DBS patients' samples.

3.9. Cross-validation of the DBS method

The interpretation of drug concentration measurements in the context of TDM is usually based on reference ranges established in plasma or serum samples, because plasma/serum concentrations are used to define efficacy or toxicity concentration targets on which a clinical choice, such as dose adjustment, can be made. For this reason, values obtained by analyzing an alternative matrix, such as DBS, need to be translated into plasma concentrations to be compared with data obtained from exposure-efficacy/toxicity or phase 1 studies [134].

The development of a strategy for estimating plasma concentration from the analysis of the corresponding DBS samples is a critical element for the application of DBS in TDM. As recommended by several bridging studies and summarized in a review recently published by our group [180], different conversion strategies

were evaluated to obtain estimated plasma concentrations (EC_{pla}). DBS values were mathematically elaborated in different manners:

- using the plasma fraction (F_p), which is the ratio between blood and plasma drug concentrations. The F_p was calculated assuming that drug concentration in DBS sample (C_{DBS}) equals the concentration of the drugs in whole blood, applying the following Equation 17:

$$F_p = \frac{\sum \left(C_{pla}\, x\, \frac{\left(\frac{1 - Hct}{100}\right)}{C_{DBS}} \right)}{N}$$

Equation 17. Plasma fraction (F_p) calculation.

Where:

C_{pla} is the determined plasma concentration;

C_{DBS} is the analyte concentration in the DBS samples;

N is the number of analyzed sample pairs.

- applying a conversion factor (CF) calculated as the mean ratio between DBS and plasma paired values;
- building up a drug distribution model resulting from red blood cells-to-plasma (BC/pla) partitioning for each analyte. The specific BC/pla partitioning coefficients ($K_{BC/pla}$) were empirically calculated following the methodology proposed by Yu et al. [226]. The $K_{BC/pla}$ resulted by the application of the formula (Equation 18):

$$K_{BC/pla} = \frac{1}{Hct}\, x\, \left(\frac{C_{srpla}}{C_b} - 1 \right) + 1$$

Equation 18. Red blood cells-to-plasma partitioning coefficient ($K_{BC/pla}$) calculation.

Where:

C_{srpla} is the concentration in spiked reference plasma;

C_b is the concentration in the plasma fraction deriving from spiked whole blood samples.

The Hct value needed to calculate both F_p and $K_{BC/pla}$, was provided by the Hematology Department of our institution for blood donors and obtained from the medical record in the case of patients.

Once Hct, F_p, and $K_{BC/pla}$ were available, the subsequent formulas were applied to estimate the plasma concentrations of each analyte from DBS data:

- for DBS conversion by means of F_p

$$EC_{pla} = \frac{C_{DBS}}{1 - Hct} \; x \; F_p$$

Equation 19. Estimated plasma concentration (EC_{pla}) conversion by means plasma fraction (F_p).

- for DBS conversion with CF

$$EC_{pla} = C_{DBS} \; x \; CF$$

Equation 20. Estimated plasma concentration (EC_{pla}) calculation with conversion factor (CF).

- for DBS conversion using the $K_{BC/pla}$

$$EC_{pla} = \frac{C_{DBS}}{(1 - Hct) + \; K_{BC/pla} \; x \; Hct}$$

Equation 21. Estimated plasma concentration (EC_{pla}) conversion using red blood cells-to-plasma partitioning coefficient ($K_{BC/pla}$).

This calculation was found to be applied for DBS-plasma and blood-plasma conversions in other bridging studies regarding other drugs [227,228].

Moreover, EC_{pla} were compared to actual plasma values by means of:

- Passing-Bablok regression analysis: a set of study samples will be analyzed by both the plasma-based LC-MS/MS method (reference, that will produce a X_i value for the i-sample) and the DBS-based LC-MS/MS method (comparator, that will produce a Y_i value for the i-sample). Plotting the measurements obtained with the two analytical methods, we will obtain a graph, where the measurements obtained with the reference method are reported in the x-axis, while the results obtained with the comparator method are reported in the y-axis. The equation is:

$$Y_i = \beta X_i + \alpha$$

Equation 22. Passing-Bablok regression equation (α: intercept; β: slope).

  In case the two methods will be totally equivalent, we will obtain α = 0 and β = 1. Otherwise, α will give indication of presence of a constant (over the concentrations range) systematic error in the comparator method, while β will indicate the presence of a proportional (respect to the concentrations) systematic error .

- Bland-Altman plot*:* the same measurements obtained from the set of study samples used for Passing-Bablok analysis will be used to calculate the following values:

  1) Mean of the X_i and Y_i from each *i*-sample:

$$M_i = \frac{X_i + Y_i}{2}$$

Equation 23. Mean of the X_i and Y_i from each i-sample.

2) Difference between X_i and Y_i from each *i*-sample:

$$d_i = X_i - Y_i$$

Equation 24. Difference between X_i and Y_i from each i-sample.

Plotting these two values we will obtain the Bland-Altman graph, that can give several information, the most important are:

- the mean of the differences (called BIAS);
- the 95 % confidence interval (CI) of the differences (*e.g.,* ± 1.96 SD).

Therefore, it is necessary to evaluate if the variation of the differences within the confidence interval (CI) is clinically relevant. Moreover, the inclusion of the value d_i=0 within the CI interval is important to assess the agreement between the two methods.

- Lin's concordance correlation coefficient (LCCC): is a popular index for measuring the agreement or reproducibility of continuous measurements with natural scales. It evaluates the accuracy between two readings, by measuring the variation of the fitted linear relationship from the 45° line through the origin (the concordance line), and the precision, by measuring how far each observation deviates from the fitted line. As reported above, the LCCC can be expressed as the product of the Pearson correlation coefficient (ρ) and Cb:

$$LCCC = \rho C_b$$

Equation 25. Lins' concordance correlation coefficient calculation.

Where ρ measures how far each observation deviates from the best-fit line (*i.e.,* the line of perfect concordance), while C_b is the bias correction factor that measures how far the best-fit line deviates from the 45° line through the origin. CCC ranges from -1 to 1, with perfect agreement at 1. For the evaluation of the results, we will apply the following scheme:

Table 2. Lin's concordance correlation coefficient (LCCC) value and corresponding grade of agreement.

CCC value	**Grade of agreement**
<0.90	poor
0.90 to 0.95	moderate
0.95 to 0.99	substantial
> 0.99	almost perfect

Moreover, the two analytical methods were considered equivalent if the deviation of the first was in the range of ±20% compared to the second for at least 67% of the samples tested, as required by EMA and FDA guidelines [200,201]. Percentage differences were obtained with the Equation 15.

4. RESULTS AND DISCUSSION

4.1. LC-MS/MS method for the quantification of sorafenib, regorafenib and their active metabolites in human plasma

In the literature several LC–MS/MS methods for the quantification of SORA or REGO (with or without the active metabolites) [229–232] or for the simultaneous quantification of both drugs (always without the metabolites) [233] are reported. To the best of our knowledge, only one method has been published so far for the simultaneous determination of all 5 analytes in human plasma [234]. Nevertheless, this method presents some limitations regarding analytical ranges (50−5000 ng/mL for REGO and its metabolites and 80−5000 ng/mL for SORA and its metabolite): in particular they do not fit plasma concentrations found in patients, as reported by Blanchet et al. (SORA C_{min} of 4300 ± 2500 ng/mL) [152] and by Mross et al. (REGO C_{max} of 3904 ng/mL at the steady state with standard dose) [235]. On these bases, a new LC-MS/MS method for the quantification of SORA, REGO and their active metabolites was developed and validated according to EMA and FDA guidelines.

4.1.1. Mass spectrometric conditions optimization

4.1.1.1. Compound dependent parameters optimization

The optimization of compound dependent parameters for SORA, REGO, their active metabolites and two ISs was performed in negative ion mode because the sensibility was approximately 5-fold higher than in positive ion mode.

The monoisotopic masses of SORA, oxSORA, REGO, oxREGO and des-oxREGO are 464.82, 480.82, 482.82, 498.81 and 484.79 Da, respectively. During each Q1 full scan from 300 to 600 Da and working in negative ion mode with ESI source, the presence of the interest analyte was confirmed by the detection of the corresponding deprotonated molecule $[M-H]^-$ at 463.2, 479.0, 481.0, 497.1 and 483.0 *m/z*, respectively, as reported in Figure 26.

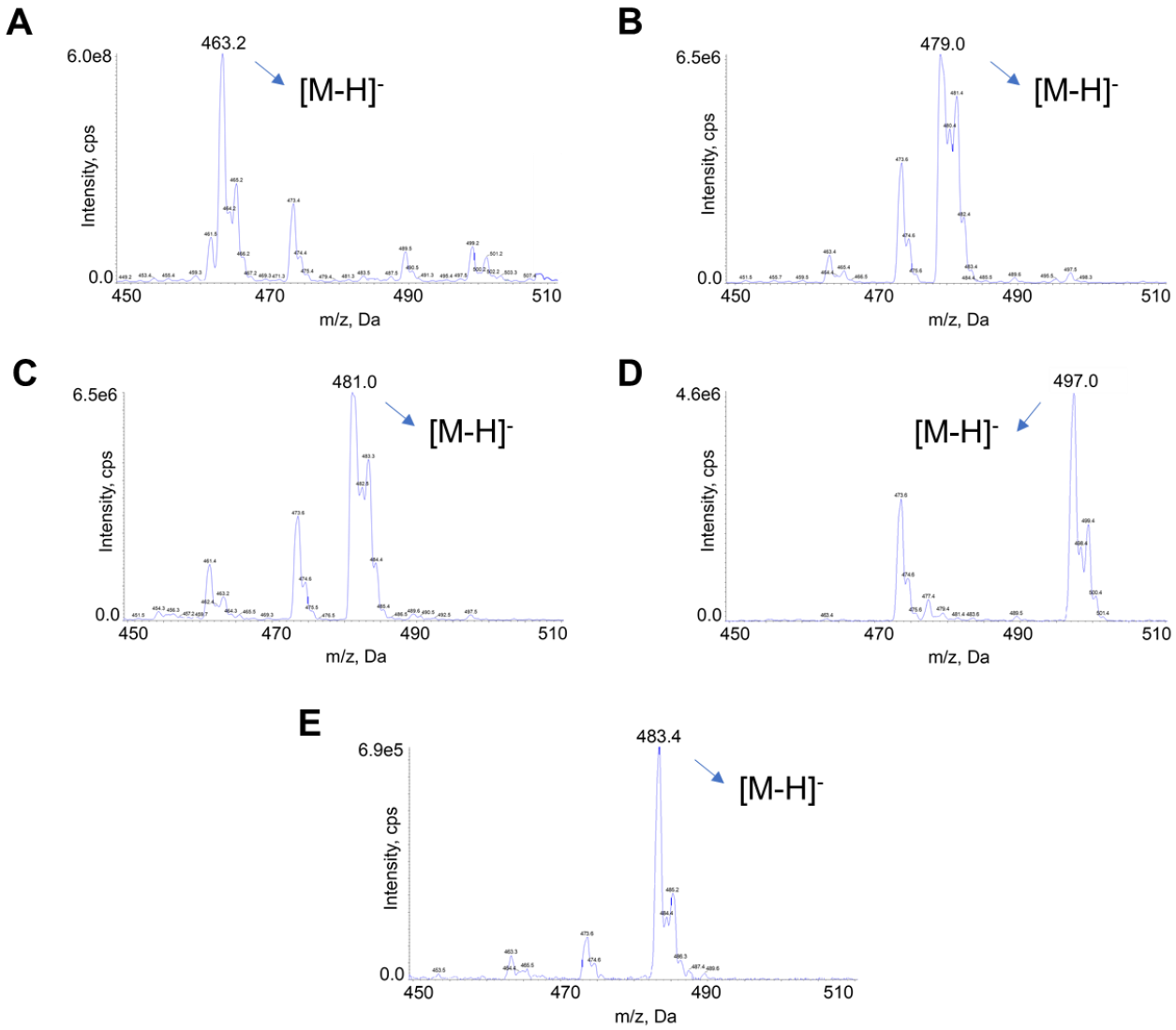

Figure 26. Spectra obtained in negative ion mode with a Q1 scan, which confirm the presence of (A) SORA, (B) oxSORA, (C) REGO, (D) oxREGO and (E) des-oxREGO.

After that, the DP was ramped from -300 to 0 V through Q1MI scan mode and monitoring the XIC of each deprotonated molecule. The optimal DP values, which correspond to the XIC highest intensity, were -130 V for SORA and oxSORA, -120 V for REGO and oxREGO and -110 V for des-oxREGO, as reported in Figure 27. These values represent the optimal values for a correct removal of clusters.

Analogously, the optimal EP value (ramp from -15 to -1 V) was defined to -9 V for each pseudo-molecular ion. In MS2 mode, the fragmentation pattern of each analyte precursor ion was evaluated by ramp the CE values from -100 to -5 V in the collision cells (second quadrupole – Q2). For each deprotonated molecule, two product ions were found and identified as reported in Figure 28.

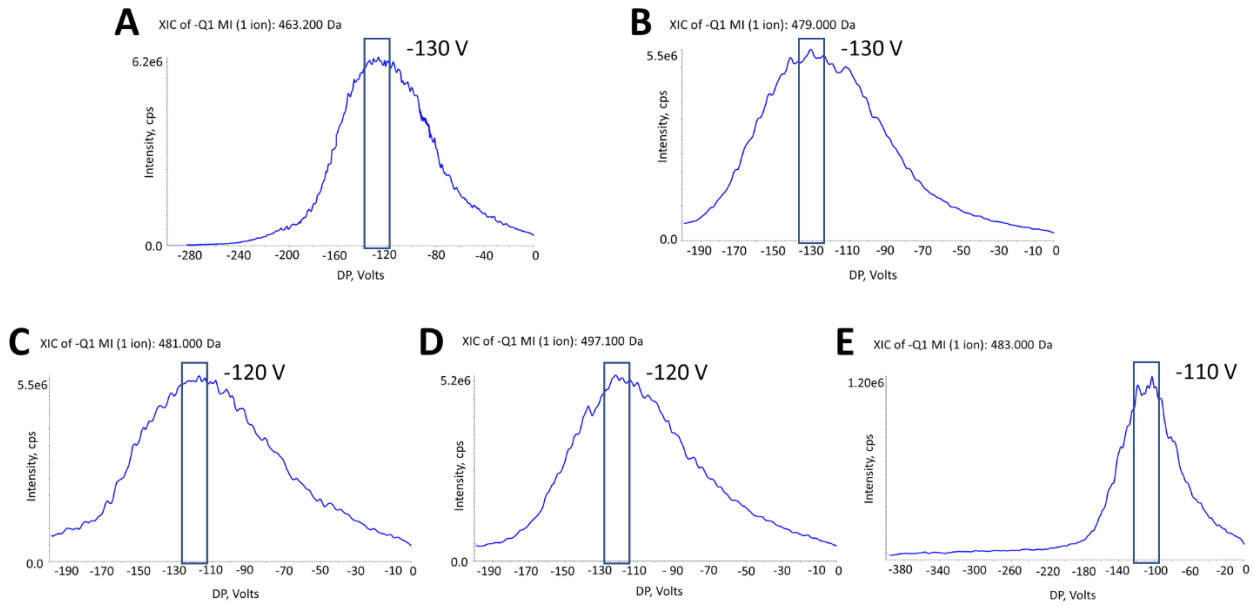

Figure 27. Spectra obtained ramping DP value in negative ion mode with Q1MI scan mode of (A) SORA, (B) oxSORA, (C) REGO, (D) oxREGO, and (E) des-oxREGO. The apex of the each XIC trend was chosen as the optimal DP value.

Consequently, through MRM scan by ramping CE value (from -100 V to -5 V), the signal intensity for each selected analyte fragment was monitored to assess the optimal CE value. The fragment ions, which had reached the highest XIC intensity, were selected as quantifier fragmentations (for example, see Figure 61). In particular, 463.2 > 194.0 *m/z* for SORA (CE = -23 V), 479.0 > 193.7 *m/z* for oxSORA (CE = -25 V), 481.0 > 193.7 *m/z* for REGO (CE = -25 V), 497.1 > 193.6 *m/z* for oxREGO (CE = -28 V) and 483.0 > 261.8 *m/z* for des-oxREGO (CE = -22 V). Furthermore, the daughter ions characterized by a lower signal intensity were exploited as qualifiers, for the analyte's identity confirmation: 463.2 > 242.0 *m/z* for SORA (CE = -26 V), 479.0 > 257.8 *m/z* for oxSORA (CE = -25 V), 481.0 > 259.8 *m/z* for REGO (CE = -25V), 497.1 > 275.7 *m/z* for oxREGO (CE = -22 V) and 483.0 > 193.8 *m/z* for des-oxREGO (CE = -25 V).

In a similar way, the optimal CXP value of -9 V was determined for all the fragments of each analyte. Furthermore, with the precursor ion scan mode it was possible to confirm the direct derivation of the two selected product ions from the precursor ion for each analyte.

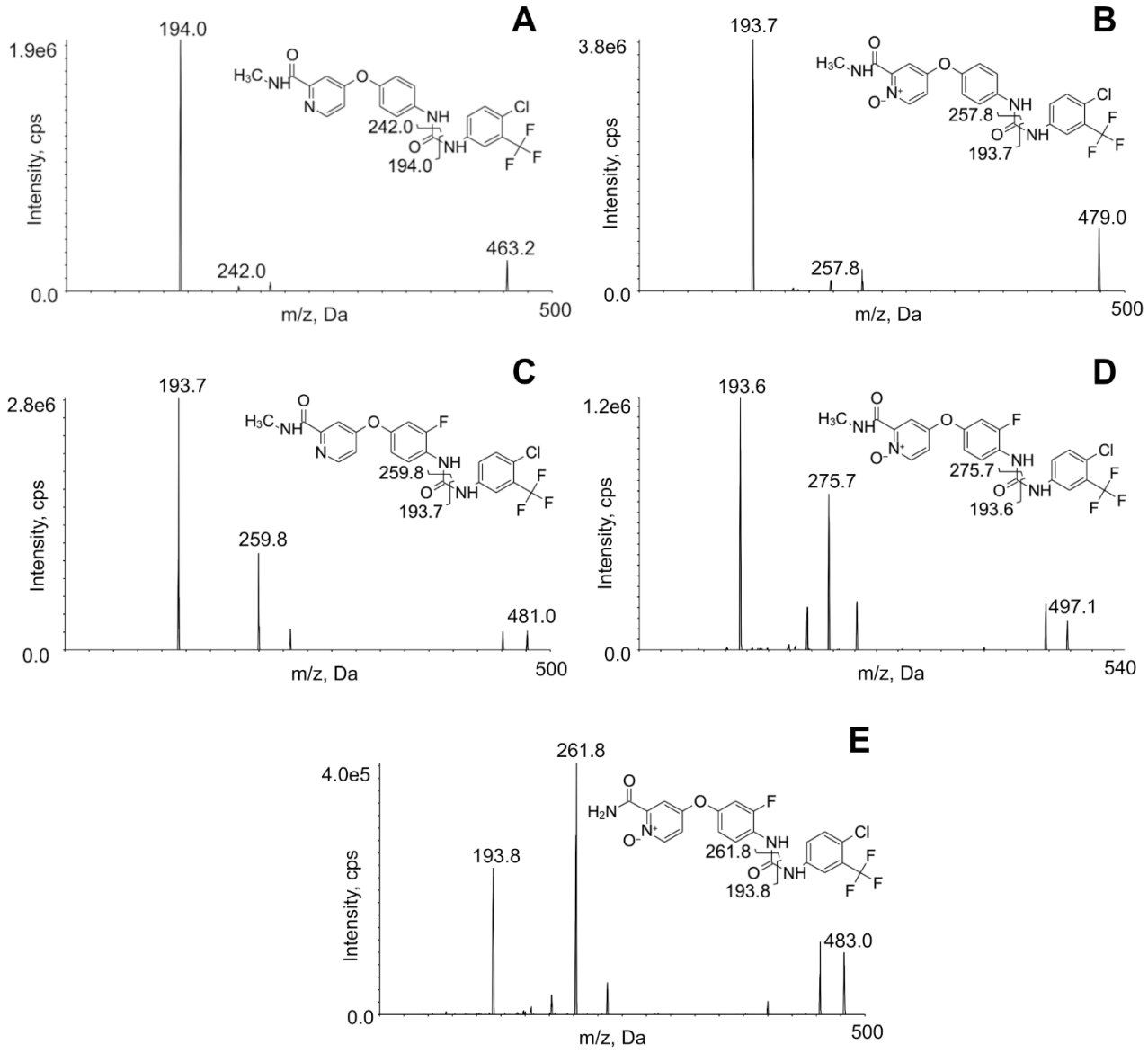

Figure 28. MS/MS mass spectra of each analyte. Chemical structures and identification of the fragment ions are reported for (A) SORA, (B) oxSORA, (C) REGO; (D) oxREGO, and (E) des-oxREGO; spectra were recorded with CE = 20 V for SORA and oxSORA, CE = 22 V for REGO and des-oxREGO, and CE = 24 V for oxREGO.

The compound-dependent parameters for the two ISs, SORA-L4 and REGO-D_3, were determined with the same experiments described for the other analytes. The results are summarized as follows: the presence of monoisotopic mass of SORA-L4 and REGO-D_3 was confirmed by the pseudo-molecular ion $[M-H]^-$ at 467.4 and 484.5 *m/z*, respectively. The optimal DP and EP values were -130 and -9 V for SORA-L4, respectively, and -100 and -9 V for REGO-D_3, respectively. The fragmentation patterns selected for the quantification corresponded to 467.4 > 194.1 *m/z* for SORA-L4 (CE = -25 V) and to 484.5 > 194.0 *m/z* for REGO-D_3 (CE = -23 V), meanwhile the qualifiers transitions corresponded to 467.4 > 246.0 *m/z* for SORA-L4 (CE = -26 V) and to

484.5 > 263.3 *m/z* for REGO-D_3 (CE = -25 V). The CXP value of -9 V was defined as optimal for the daughter ions of each analyte.

In Table 3 the compound dependent parameters optimized are summarized.

Table 3. Optimized compound dependent parameters of each analyte and IS.

Compound	Precursor ion			Product ion		
	Q1[a] (*m/z*)	DP[b] (V)	EP[c] (V)	Q3[d] (*m/z*)	CE[e] (V)	CXP[f] (V)
SORA	463.2	-130	-9	194.0	-23	-9
				242.0	-26	-9
oxSORA	479.0	-130	-9	193.7	-25	-9
				257.8	-25	-9
REGO	481.0	-120	-9	193.7	-25	-9
				259.8	-25	-9
oxREGO	497.1	-120	-9	193.6	-28	-9
				275.7	-22	-9
des-oxREGO	483.0	-110	-9	261.8	-25	-9
				193.8	-22	-9
SORA-L4	467.4	-130	-9	194.1	-25	-9
				246.0	-26	-9
REGO-D_3	484.5	-100	-9	194.0	-23	-9
				263.3	-25	-9

[a]first quadrupole mass; [b]declustering potential; [c]entrance potential; [d]third quadrupole mass; [e]collision energy; [f]cell exit potential.

4.1.1.2. Source dependent parameters optimization

The purpose of this experiment was to achieve the maximum signal intensity to reach the greatest sensitivity for oxREGO, which was the most critical analyte in terms of signal intensity. As reported in section 3.5.1.2, each source dependent parameter was manually varied after 3 consecutive samples with a stable XIC trend (for example, see Figure 62). For each sample 2 µL of 200 ng/mL oxREGO methanolic solution were injected. In particular, the principal variations applied to each source dependent parameter are summarized below:

- TEM: the optimal value was 550 °C. The tested values were 100 °C, 200 °C, 300 °C, 350 °C, 400 °C, 450 °C, 500 °C, 550 °C, 600 °C and 650 °C. The maximum signal intensity was observed at 650 °C, but 550 °C was selected as the optimal value because it represented the right balance between an adequate signal intensity and a lower stress for the turbo-heaters;
- ISV: the optimal value was -2000 V. The investigated values were -4500 V, -4000 V, -3500 V, -3000 V, -2500 V, -2000 V, -1500 V. Commonly, the higher is the voltage difference between the ionspray needle and the mass analyzer inlet, the greater is the ionization efficiency. In this case, the highest XIC intensity was between -2500 V and -1500 V and, thus the most appropriate value was -2000 V;

- CUR: the optimal value was 30 psi. The tested values were 5 psi, 10 psi, 15 psi, 20 psi, 25 psi, 30 psi, 35 psi, 40 psi, 45 psi and 50 psi. Generally, CUR should be at the highest possible value, to prevent contaminants or solvents from entering in the mass analyzer. The highest XIC intensity was reached between 25 and 35 psi, while a significant decrease in the XIC intensity was observed at lower or higher values;
- CAD: the optimal value was Medium, while with Low and High values were observed a decreasing of the XIC intensity;
- GS1 and GS2: the optimal values were 30 and 40 psi, respectively. These parameters were optimized together considering that commonly GS2 is higher than GS1 and the sum between these two parameters should not exceed the value of 100 psi that represents the nitrogen generator limit. The GS1-GS2 tested values were 30-30 psi, 30-40 psi, 30-50 psi, 30-60 psi, 40-40 psi, 40-50 psi, 40-60 psi, 60-30 psi, 50-30 psi, and 40-30 psi.

As mentioned in the section 3.5.1.2.1, the optimized source dependent parameters were confirmed also by monitoring the des-oxREGO quantifier fragmentation (483.0 > 261.8 *m/z*).
All the optimized source dependent parameters were summarized in Table 4.

Table 4. Optimized source dependent parameters for SORA, REGO and their active metabolites.

Polarity	Negative ion mode
CUR	30 psi
CAD	Medium
ISV	-2000 V
TEM	550 °C
GS1	30 psi
GS2	40 psi

4.1.2. Chromatographic conditions optimization

The chromatographic method development implies the determination of the best chromatographic conditions for the separation of these five analytes (SORA, REGO, and their active metabolites). Considering that the analyzer used for the detection in this analytical method was a triple quadrupole mass spectrometer, a high chromatographic R_s was not essential. In fact, the triple quadrupole mass analyzer is capable of precisely quantifying two co-eluting compounds, contrary to UV-Vis detector, which most of the time need base-line separated peaks [212]. Nonetheless, cross-talk phenomenon might occur and the quantification of two co-eluting compounds requires separation of the scan time between the two analytes, in order to decrease the number of data points describing each peak. On these bases, a minimum degree of separation between all the compounds was required. Moreover, the peak width and the duration of the total run time were considered as other important parameters during the development of this analytical method, in order

to maximize the overall sensitivity through narrow peaks and to obtain a method as less time consuming as possible.

Given SORA, REGO and their active metabolites physicochemical properties, the selected SP was C18. This SP grants to increase the very small difference in hydrophobicity of the selected analytes as they differ only in a fluorine atom, an oxygen atom, or a methyl group. Firstly, some tests were conducted on a SunFire® column (3.5 µm, 150 x 2.1 mm, 100 Å, Waters) hypothesizing that a better peaks R_s would have been obtained, due to its length. Experimentally, this effect was not confirmed and thus a shorter column was tested: a Synergi™ Fusion-RP column (4 µm, 50 x 2.0 mm, 80 Å, Phenomenex). This last column gave nearly the same peak R_s obtained with SunFire® column, but with a shorter run time. Furthermore, the length of 50 mm associated with 4 µm particle size allowed to considerably reduce the back-pressure during the MP flow and to use higher flow rate. The column was equipped with a Fusion-RP Security Guard™ pre-column, in order to prevent the contamination of the head column from the MP and the biological samples.

Both MeOH and ACN were tested as MP, and the first one was selected as organic solvent since the obtained peak shape was less indented and more symmetrical. Furthermore, the peak shape quality was improved adding 10% (v/v) of iPrOH in MeOH, thus modulating the eluting power of MeOH without increasing to much the system back-pressures. The viscosity of the MPs and thus the system back-pressure was reduced setting the oven column temperature at 50 °C. This led also to improve the R_s, due to an efficiency increase caused by the faster analytes interchange between the two phases (MP and SP).

In the end, the selected MPs were 10 mM AmAc buffer in MilliQ H_2O with 0.10% of HCOOH (v/v), as MP A to minimize the background noise, and MeOH:iPrOH (90:10, v/v) with 0.10% of HCOOH (v/v), as MP B.

Concerning the chromatographic method, the multistep gradient was selected, due to the relatively dirty sample to be analyzed and thus the need to regularly clean the column from the contaminants carried by the sample injection.

The most significant chromatographic tests are described below. The first method assessed was a slightly linear gradient from 1 to 90% of MP B in 9 min to evaluate the behavior of each analyte. Unfortunately, the analytes peaks were not completely separated at the baseline and partially co-eluted (Figure 29). However, from this method it was possible to extrapolate the percentage of MP B necessary for the elution of all the analytes, that ranged from 80 to 85% of MP B.

Consequently, a different method characterized by a shorter and steeper gradient with an isocratic phase was evaluated in order to reach an acceptable separation and simultaneously a less time-consuming chromatographic method.

The optimization of the conditioning phase was performed by testing different MP B percentage (10%, 20%, 30% and 40%) for 0.50 min followed by linear gradient up to 80% of MP B in 2 min and by an isocratic phase of 3 min. The analytes separation was like the one obtained with the linear gradient 1-90% of MP B in 9 min

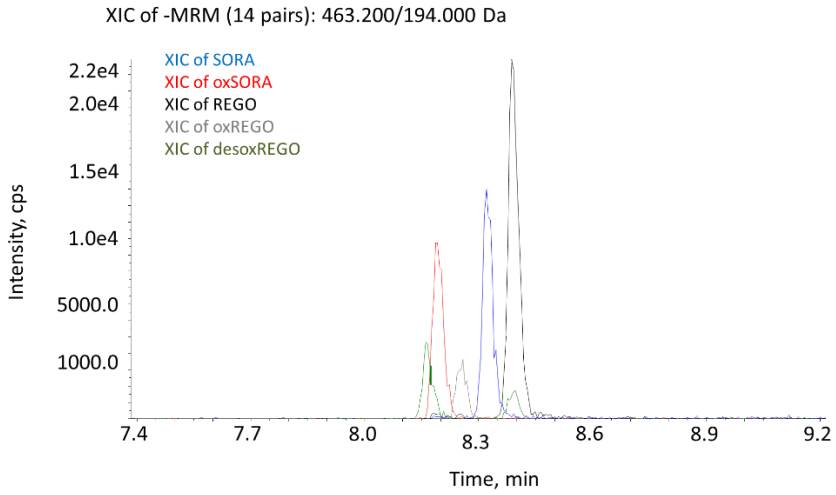

Figure 29. MRM chromatogram (from 7.4 to 9.2 min) of a plasma sample at the LLOQ concentration (50 ng/mL for SORA and REGO, and 30 ng/mL for oxSORA, oxREGO and des-oxREGO).

(Figure 29) for all the initial percentage of MP B tested. Moreover, the peaks obtained with the method starting with 40% of MP B were wider than the ones obtained in the other tests, demonstrating that the starting percentage of MP B was too high and the analytes were not properly packed at the column head. The peak width was 0.18 min for SORA and REGO and 0.16 min for all the metabolites using methods starting with 30, 20 and 10% of MP B without enhancements in peaks shape. The only difference was that the higher the starting percentage of MP B, the earlier the analytes were eluted, reducing the retention time of nearly 0.3 min at each 10% of MP B increase.

For these reasons, the 30% as initial percentage of MP B was chosen, but the analytes elution was still too delayed considering the desired short total run time.

The duration of the initial conditioning phase was also varied from 0 to 1.5 min at 30% of MP B followed by a linear gradient from 30 to 80% of MP B in 2 min. The selected duration time was 0.5 min because the peaks shape was more irregular with a conditioning step faster than 0.5 min, while with a conditioning step longer than 0.5 min the retention times were delayed.

Consecutively, the slope of the linear gradient (30-80% of MP B) was modified from 2 to 1 min to optimize the chromatographic method. The retention times of each analyte were anticipated of about 0.67 min ramping MP B from 30 to 80% in 1 min but no variations in term of degree of separation and peaks shape were observed. Thus, the more slanting linear gradient was selected in order to reduce the total run time.

Several total flow rates were tested to reduce the peaks width and to maintain the highest degree of peak separation. The tested flow rates were 0.30, 0.35 and 0.40 mL/min. Increasing the flow rate, the mean peaks width and the analytes retention times decreased. In particular, with 0.30 mL/min the mean peaks width was 0.15 min, and the retention time ranged between 3.22 and 3.53 min, while with a flow rate of 0.35 mL/min the mean peak width were 0.13 min and the retention time ranged from 2.96 to 3.18 min, whereas with a 0.40 mL/min the mean peak width was 0.11 min and the retention time ranged between 2.72 and 2.94 min.

The 0.35 mL/min was selected as optimal flow rate because it represents a good compromised between narrower peaks, the earlier elution, and a slight decreasing of the analytes separation degree. This decreasing in resolution was considered acceptable thanks to the precision of the triple quadrupole analyzer and, thus, a reduced total run time of the analysis was obtained.

After several variations of the linear gradient, the best one was characterized by 0.5 min at 30% of MP B as conditioning phase, in 1.25 min the percentage of MP B was increased up to 85% and maintained constant for 4.25 min to allow the analytes elution, with a flow rate of 0.3 mL/min. The slope of the gradient (30-85% of MP B) was not altered compared to the one previously described, but the mean peaks width slightly decreased (0.11 min) and peaks were less indented.

To make this latest method less time consuming, the isocratic phase was stopped after 3.35 min since the most retained analyte (the once with longer retention time) was eluted at 3.20 min.

At this point the cleaning phase was optimized to remove as efficaciously as possible the lipophilic interferents usually presents in plasma (*e.g.*, fatty acid, small peptides, and phospholipids) as well the possible analytes residues retained in the column. To perform an efficient column wash, in this phase the flow rate was increased at 0.55 mL/min, a value that was compatible both with the supported system back-pressure and the column characteristics. The duration of this phase was 1.75 min, that corresponded to the passage of 10 column volumes (column volume circa 97 µL), considered a sufficiently long time to guarantee a good cleaning of the system with advantage for the column life.

Anyway, different durations of the reconditioning phase were tested. In particular, with 1.7 min of this phase no shift in analytes retention time was noticed after several consecutive injections, while the analytes retention times were not constant with 1.2 min, and the method reproducibility was lost. This was in line with the necessity to use a reconditioning volume equal to 10 column volume, as reported above.

In summary, the analytes separation was obtained by applying the following gradient:

- 30% of MP B (conditioning phase) for 0.5 min with a flow rate of 0.35 mL/min;
- from 30% to 85% of MP B in 1.25 min and kept constant at 85% for 1.6 min (elution phase);
- from 85% to 95%of MP B in 0.1 min and kept constant for 1.7 min (washing phase);
- MP B initial condition was restored in 0.1 min and kept constant for 1.75 min (reconditioning phase).

During washing and reconditioning phases, the flow rate was increased from 0.35 to 0.55 mL/min to reduce the total run time (7 min).

This developed LC-MS/MS method was selective for these analytes and relative fast. In particular, the retention times were 3.12 min for SORA, 3.02 min for oxSORA, 3.20 min for REGO, 3.08 min for oxREGO and 2.99 min for des-oxREGO. In Figure 30 an example of chromatogram is reported and shows a partial co-elution between the three metabolites. The peaks were symmetrical and well-shaped, with a mean full width at half-height of 0.045 min. Furthermore, on average 20 points described each analytes peak, due to a dwell time of 25 msec for the quantifier fragmentation and of 9 msec for the qualifier ones. Several injection

volumes were tested and 2 µL for all samples was selected, consenting to obtain an instrumental response that was linear within the whole concentration range.

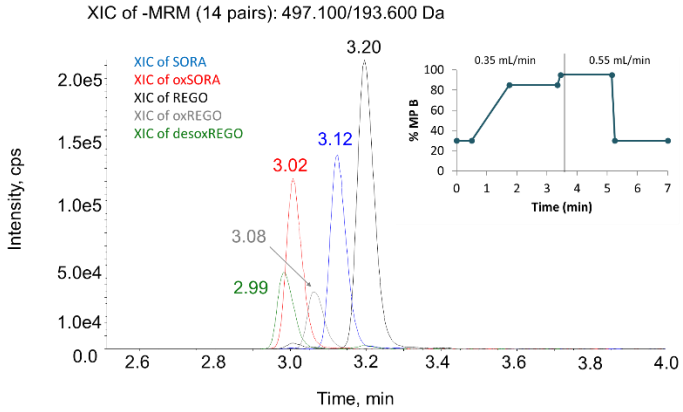

Figure 30. MRM chromatogram (from 2.6 to 4.0 min) of a plasma samples containing 50 ng/mL for SORA and REGO, and 30 ng/mL for oxSORA, oxREGO and des-oxREGO. Their retention times are shown. The developed chromatographic method is reported in the box on the right.

Due to the partial co-elution between the metabolites, it was necessary to verify the absence of signal interferences between them in order to consider this chromatographic method acceptable. On these bases, a sample containing only one analyte at a time was analyzed, as reported in Figure 31, and compared with a sample containing all the analytes together: the peak area of the each analyte alone was compared with the peak area of the same analyte injected with the other four analytes, and no significant differences were observed.

Notably, the partial co-elution of the three metabolites was an phenomenon that does not involve in patients' sample since patients can be treated with SORA or REGO alternatively, and never simultaneously.

The last evaluated phenomenon was the carryover that consists in the presence of a XIC analyte signal in a blank sample analyzed immediately after the injection of a high concentration samples (*e.g.*, ULOQ or QCH). Evaluation of carryover phenomenon is important because it might cause an overestimation of low concentration samples, especially relevant in quantitative analysis. Moreover, both EMA and FDA bioanalytical validation guidelines reported that, to consider the carryover as negligible, the peak area of the interested analyte in blank samples has to be minor than 20% of the peak area of the same analyte at the LLOQ concentration level and the IS peak area in the blank sample has to be minor than 5% of the peak area of the IS peak area in a sample containing. On this basis, to avoid carryover phenomenon several precautions were applied:

- efficient needle washing solutions composed by THF:MilliQ H_2O (80:20, v/v);
- strong column washing at 95% of MP B for 1.75 min;
- relative high percentage of MP B (30%) at the beginning of the chromatographic method;
- injection of the smallest sample volume possible to minimize the quantity of interferents and contaminants injected in the LC system.

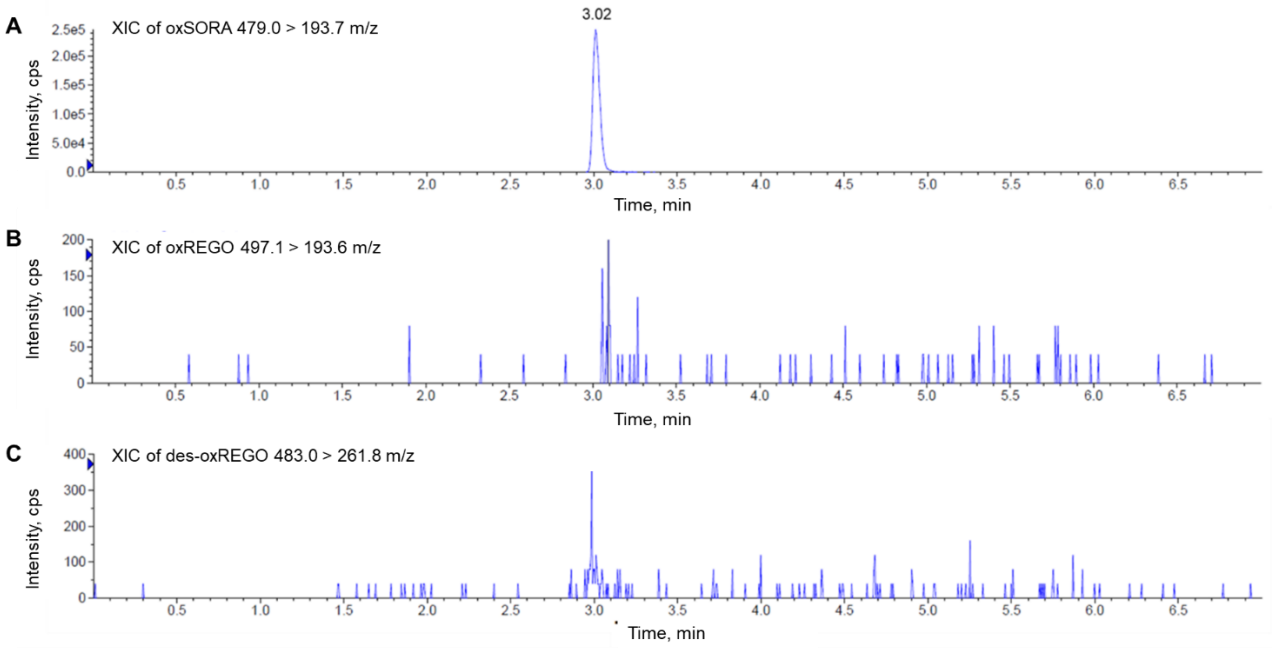

Figure 31. MRM chromatogram of a plasma samples with 750 ng/mL of oxSORA. The XIC trend of (A) oxSORA , (B) oxREGO and (C) des-oxREGO are reported.

Only for SORA a quantifiable peak (S/N > 5) was detected in the second blank sample injected after the ULOQ sample. Nonetheless, this peak area was always minor than 5% of its LLOQ.

For this reason, two blank samples were analyzed after the injection of a sample with high or unknown concentration. In this way, no additional cleaning runs were necessary, saving time and money due to the negligible carryover phenomenon.

4.1.3. Sample preparation for quantitative analysis

4.1.3.1. Plasma sample extraction optimization

PP was selected as sample extraction method due to its simplicity and rapidity. In particular, PP allows to minimize mistakes during sample preparation and to perform a rapid sample processing which is welcome in TDM practice. Moreover, the PP perfectly fit with SORA and REGO detection since about 99% of the circulating drugs is bound to plasma proteins [56,58,80,81].

MeOH plus 0.10% of HCOOH (v/v) was chosen as extraction solvent for PP because it allowed to obtain a higher extraction yield for each analyte compared to other tested solvents (MeOH, ACN and acidic ACN (0.10% of HCOOH, v/v)). Moreover, PP was performed by using ice-cold solutions containing both SORA-L4 and REGO-D_3 (ISs WS). The optimal *ratio* between plasma sample and the ISs WS volume was 1:100, *i.e.,* 5 µL of plasma sample were precipitated with 495 µL of ISs WS. This proportion allowed on one side to obtain an excellent S/N for each analyte at the LLOQ concentration and, on the other side, to avoid the detector saturation (detector limit nearly 3 x 10^6 cps) at the ULOQ level.

In fact, lower plasma:solvent *ratio* were tested (1:10, 1:20 and 1:50) but they were not acceptable because the signals obtained at the ULOQ level caused detector saturation, suggesting that samples were not enough diluted (even injecting 1 µL of sample volume into the column). Although the signal at LLOQ concentration was quantifiable and the detector was not saturated at the ULOQ concentration, the 1:200 *ratio* was discarded because it gave less benefits than the 1:100 dilution in terms of peaks shape and it used twice solvent volume, so it was more expensive.

Lastly, the autosampler temperature was set at 4 °C to minimize MeOH evaporation and to extend the analytes stability.

4.1.3.2. Calibration curve and quality controls preparation

For each analyte, two primary stock solutions (one for calibrators and one for QCs) were prepared in DMSO at the concentration of 1 mg/mL and stored at -80 °C.

To obtain the WS for the 7 points-calibration curve (from A to G), stock solutions of all 5 analytes were mixed together and diluted with MeOH to achieve the final concentrations of: 160, 80, 40, 15, 6, 2 and 1 µg/mL for SORA and REGO; 80, 40, 20, 10, 5, 2 and 0.6 µg/mL for oxSORA, oxREGO and des-oxREGO. Similarly, stock solutions for QCs (QCH, QCM and QCL) were mixed together and diluted with MeOH to obtain the final concentrations of 120, 30 and 1.2 µg/mL for SORA and REGO; 60, 15 and 1.2 µg/mL for metabolites. For all the WSs, 1-mL aliquots were stored at -20 °C to be used for the sample's preparation and the remaining WSs were kept in polypropylene tubes and stored at -80 °C.

ISs stock solutions were prepared in DMSO for SORA-L4 and REGO-D_3 at the concentration of 1 mg/mL. These two solutions were then mixed together and diluted with MeOH plus 0.10% of HCOOH (v/v) to reach the final concentration of 20 ng/mL for both SORA-L4 and REGO-D_3. This solution was directly used to precipitate plasma proteins during the sample processing. The stock and intermediate solutions were kept in polypropylene tubes and stored at -80 °C, while the WS were stored at -20 °C until use.

The seven calibrators and, at least, three replicates of each QC concentration level were freshly prepared every day during the validation study and for patients' samples quantification.

Calibration curve and QCs were freshly prepared through the following steps: to 95 µL of blank pooled human plasma 5 µL of proper WS were added (dilution 1:20) and vortexed for 10 sec, after that 5 µL-aliquot of this mix was added with 495 µL of cold IS WS (dilution 1:100) to induce PP, vortexed and then centrifuged for 10 min at 16200 g and 4 °C. Finally, 200 µL of supernatant were transferred to a polypropylene tube for LC-MS/MS analysis.

Thus, plasma samples presented the following concentrations for the calibration curve and QCs reported in Table 5.

Table 5. Final concentrations of calibrators and QCs in plasma samples for each analyte.

Sample	SORA and REGO conc. (ng/mL)	oxSORA, oxREGO and des-oxREGO conc. (ng/mL)
G	50.0	30.0
F	100	100
E	300	250
D	750	500
C	2000	1000
B	4000	2000
A	8000	4000
QCL	60.0	60.0
QCM	1500	750
QCH	6000	3000

Several 5 µL-aliquots of the three QCs have been stored at −80 °C to check the stability of the analytes and as controls for future assays.

4.1.4. LC-MS/MS method validation

During the validation procedures according to EMA and FDA guidelines, the following parameters were assessed: analytes recovery from the plasma matrix, the matrix effect, linearity of the calibration curve, intra- and inter-day precision and accuracy, limit of quantification, selectivity and sensibility, dilution integrity, ISR and stability of the analyte in plasma samples under different conditions and in solvents.

4.1.4.1. Recovery

As reported in section 3.6.1, the recovery was assessed in quintuplicate of each QC concentration level using the Equation 9.

For each analyte the recovery, expressed as percentage and reported inTable 6, resulted to be ≥ 85.5%. Moreover, it was reproducible and consistent over the tested concentrations. In particular, the recovery resulted to be within 85.5 - 95.3% (CV ≤ 3.9%) for SORA, 89.8 - 98.2% (CV ≤ 3.4%) for oxSORA, 87.8 - 95.8% (CV ≤ 4.0%) for REGO, 89.1 - 96.7% (CV ≤ 3.7%) for oxREGO and 88.4 - 98.2% (CV ≤ 4.1%) for des-oxREGO.

Table 6. Recovery of SORA, oxSORA, REGO, oxREGO and des-oxREGO from human plasma (conc.: concentration; N: number of replicates; SD: standard deviation).

Analyte	Nominal conc. (ng/mL)	Recovery (%) ± SD	CV (%)
SORA (N = 5)	60.0	93.9 ± 2.2	2.4
	1500	85.5 ± 3.3	3.9
	6000	95.3 ± 2.5	2.6
oxSORA (N = 5)	60.0	95.2 ± 3.2	3.4
	750	89.8 ± 1.4	1.6
	1500	98.2 ± 3.0	3.0
REGO (N = 5)	60.0	95.5 ± 1.2	1.3
	1500	87.8 ± 3.5	4.0
	6000	95.8 ± 2.2	2.3
oxREGO (N = 5)	60.0	94.9 ± 3.5	3.7
	750	89.1 ± 0.9	1.0
	1500	96.7 ± 0.9	1.0
des-oxREGO (N = 5)	60.0	94.3 ± 3.8	4.1
	750	88.4 ± 2.6	2.6
	1500	98.2 ± 4.0	4.1

4.1.4.2. Matrix effect

The absence of matrix effect was demonstrated using both quantitative (estimated matrix factor (% MF) calculation and analyzing LLOQ samples using single donor plasma) and qualitative tests (post-column infusion test).

First, the quantitative evaluation of the matrix effect was performed comparing the analytes peaks areas in presence of matrix (single donor human plasma) and in absence of matrix (MeOH), at QCL and QCH concentration levels. In particular, IS norm MF calculating with Equation 11 was found to be between 0.9 and 1.1 with a CV%≤6.8, as reported in Table 7. These results indicate that the method was not significantly affected by endogenous and exogenous components present in the matrix.

Table 7. Estimated matrix factor (MF) and IS normalized matrix factor (IS norm MF) of each analyte and ISs in deproteinized human plasma. (conc.: concentration; N: number of replicates; SD: standard deviation).

Analyte	Nominal conc. (ng/mL)	MF (%) ± SD	CV (%)	IS norm MF (%) ± SD	CV (%)
SORA (N = 6)	60.0	101 ± 6.3	6.3	1.0 ± 0.06	6.3
	6000	99.0 ± 3.3	3.3	0.9 ± 0.03	3.3
oxSORA (N = 6)	60.0	97.8 ± 6.6	6.8	0.9 ± 0.06	6.8
	1500	93.4 ± 5.0	5.3	0.9 ± 0.05	5.3
REGO (N = 6)	60.0	96.2 ± 4.7	4.9	0.9 ± 0.04	4.9
	6000	100 ± 3.8	3.8	0.9 ± 0.04	3.8
oxREGO (N = 6)	60.0	106 ± 5.6	5.3	1.0 ± 0.05	5.3
	1500	111 ± 3.6	3.3	1.1 ± 0.03	3.3
des-oxREGO	60.0	102 ± 6.3	6.1	1.0 ± 0.06	6.1

Analyte	Nominal conc. (ng/mL)	MF (%) ± SD	CV (%)	IS norm MF (%) ± SD	CV (%)
(N = 6)	1500	106 ± 3.1	2.9	1.0 ± 0.03	2.9
SORA-L4 (N = 6)	20.0	104 ± 4.5	4.3	-	-
REGO-D_3 (N = 6)	20.0	106 ± 4.0	3.8	-	-

Moreover, the absence of matrix effect has also been proved through the analysis of 6 LLOQ samples from different donors (3 males and 3 females), being the obtained accuracy and precision (as CV%), respectively: 97.6% and 5.0% for SORA, 98.3% and 4.3% for oxSORA, 89.3% and 3.8% for REGO, 98.9% and 5.0% for oxREGO and 88.8% and 5.0% for des-oxREGO.

Furthermore, applying to the post-column infusion evaluation, neither ion suppression nor enhancement of the extracted ions signals were observed at the retention time of the analytes, as reported in Figure 32.

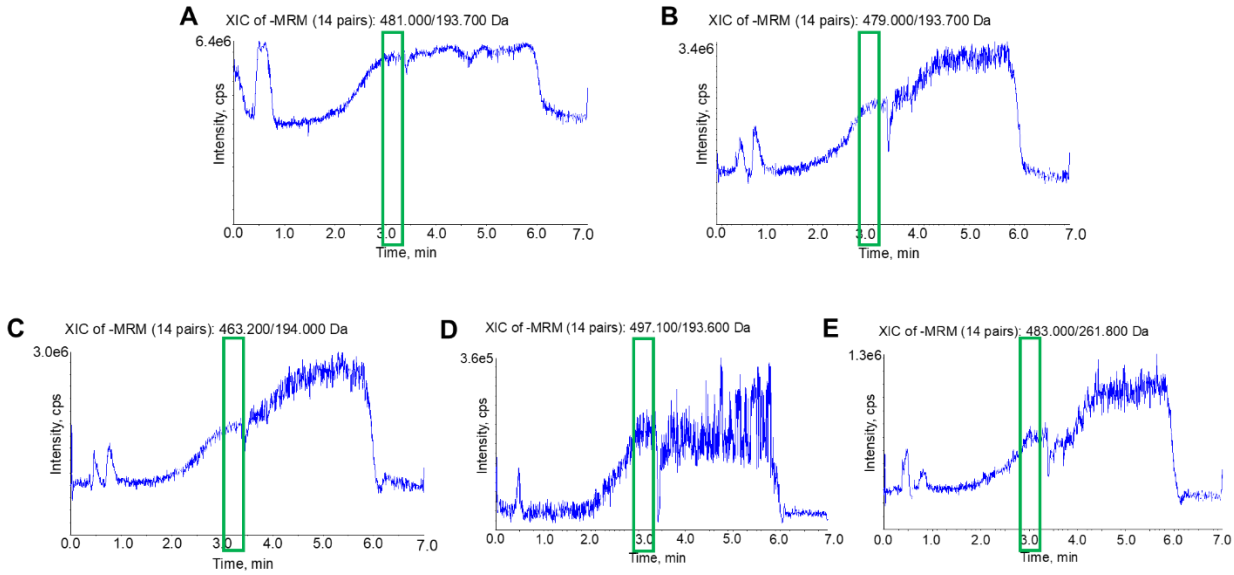

Figure 32. Evaluation of matrix effect through a post-column infusion evaluation: the XIC trend of each analyte shows both ion enhancement and ion suppression areas. These phenomena did not affect the analytes of interest, whose retention times were highlighted with the green rectangles. (A) SORA, (B) oxSORA, (C) REGO, (D) oxREGO, (E) des-oxREGO.

4.1.4.3. Linearity

Linearity of the proposed method was tested over the selected ranges (50-8000 ng/mL for SORA and REGO and 30-4000 ng/mL for respective metabolites).

The mean Pearson's correlation coefficient (r) values were 0.9993±0.0004 for SORA, 0.9988±0.0007 for oxSORA, 0.9981±0.0006 for REGO, 0.9993±0.0005 for oxREGO and 0.9988±0.0005 for des-oxREGO. In Figure 33 the calibration curves prepared during the validation procedure for each analyte are reported.

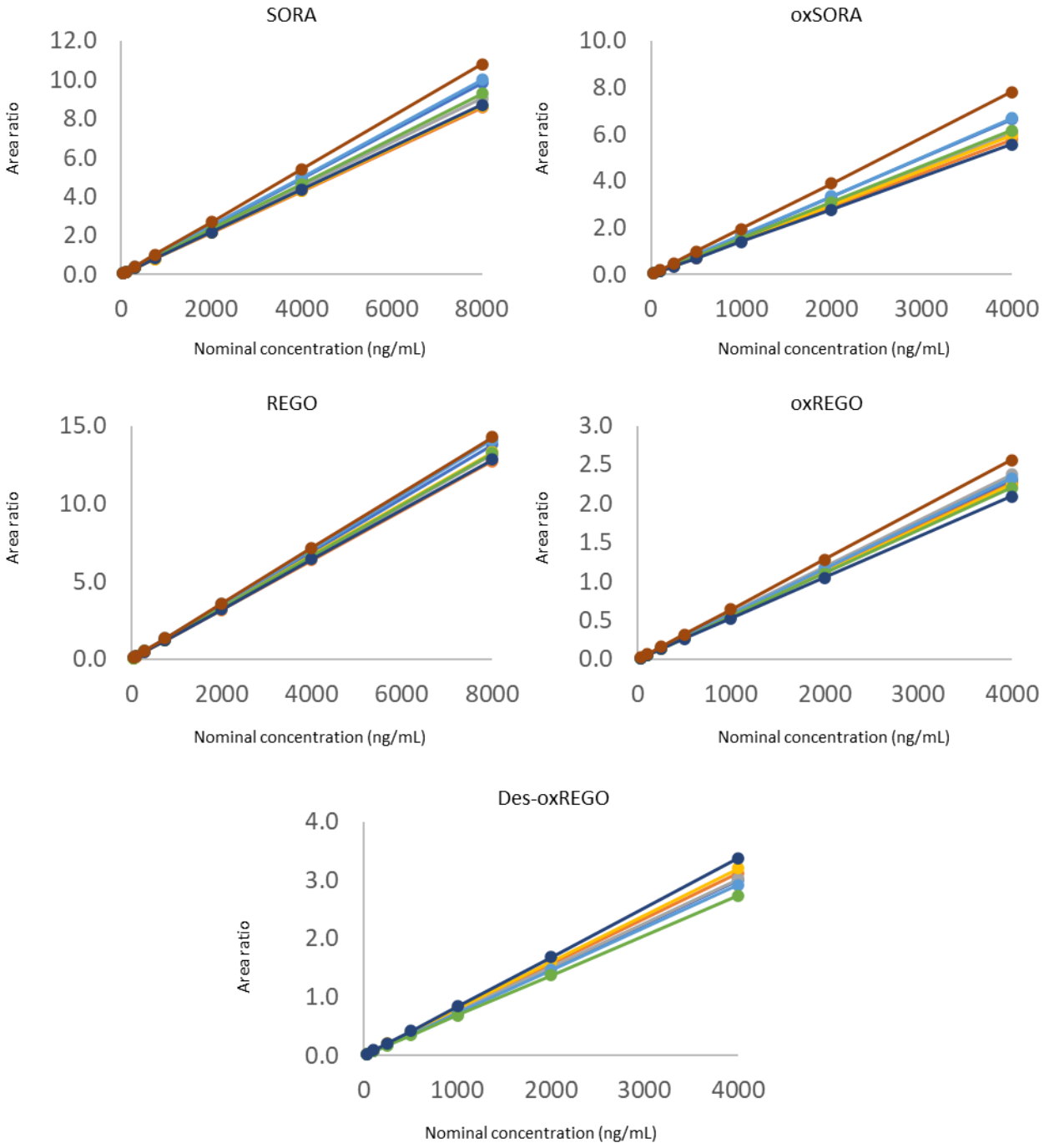

Figure 33. Calibration curves (N = 8) obtained for SORA, oxSORA, REGO, oxREGO and des-oxREGO in human plasma.

The accuracy obtained for SORA and oxSORA was between 94.7-107% and between 92.7-107% for REGO and its two active metabolites; finally, the CV was always ≤ 4.0% (Table 8).

Table 8. Accuracy (%) and precision (CV%) data of SORA, REGO and their active metabolites calibration curves in human plasma (conc.: concentration; N:number of replicates; SD: standard deviation).

Nominal conc. (ng/mL)	Mean ± SD	CV%	Accuracy%
SORA (N = 8)			
50.0	49.2 ± 0.4	0.8	98.4
100	104 ± 1.9	1.9	104
300	293 ± 8.4	2.9	97.7
750	751 ± 18	2.5	100
2000	2051 ± 27	1.3	103
4000	3982 ± 72	1.8	99.5
8000	7824 ± 236	3.0	97.8
oxSORA (N = 8)			
30.0	29.5 ± 0.2	0.6	98.5
100	107 ± 2.2	2.1	107
250	237 ± 8.3	3.5	94.7
500	502 ± 7.2	1.4	101
1000	1017 ± 16	1.6	102
2000	1986 ± 35	1.7	99.3
4000	3941 ± 151	3.8	98.5
REGO (N = 8)			
50.0	48.4 ± 0.5	1.1	96.8
100	107 ± 2.1	2.0	107
300	293 ± 7.2	2.5	97.6
750	768 ± 9.9	1.3	102
2000	2102 ± 40	1.9	105
4000	3945 ± 67	1.7	98.6
8000	7414 ± 118	1.6	92.7
oxREGO (N = 8)			
30.0	29.2 ± 0.3	1.1	99.4
100	103 ± 4.1	4.0	103
250	243 ± 6.8	2.8	97.3
500	495 ± 6.8	1.4	99.0
1000	1034 ± 18	1.8	103
2000	1997 ± 33	1.6	99.9
4000	3926 ± 102	2.6	98.1
des-oxREGO (N = 8)			
30.0	29.5 ± 0.4	1.2	98.6
100	106 ± 3.5	3.3	106
250	242 ± 8.8	3.6	96.9
500	508 ± 9.8	1.9	102
1000	1033 ± 19	1.8	103

Nominal conc. (ng/mL)	Mean ± SD	CV%	Accuracy%
2000	1970 ± 36	1.8	98.5
4000	3826 ± 139	3.6	95.6

4.1.4.4. Intra-day and inter-day precision and accuracy

As related to the intra-day precision and accuracy, measured in 6 samples at each QC concentration and at LLOQ level, the achieved values were CV ≤ 8.7% and between 89.4-104% for all analytes, respectively (Table 9).

Table 9. Intra-day precision (CV%) and accuracy (%) for SORA, REGO and their active metabolites in human plasma (conc: concentration; N: number of replicates; SD: standard deviation).

Intra-day (N = 6)				
Analyte	**Nominal conc. (ng/mL)**	**Mean ± SD**	**CV %**	**Accuracy %**
SORA	50.0	47.3 ± 3.1	6.5	94.7
	60.0	61.3 ± 2.6	4.5	102
	1500	1554 ± 43	2.8	104
	6000	6024 ± 127	2.1	100
oxSORA	30.0	29.0 ± 1.8	6.1	96.7
	60.0	57.6 ± 2.2	3.9	96.1
	750	739 ± 34	4.6	98.5
	3000	3018 ± 54	1.8	101
REGO	50.0	50.1 ± 3.6	7.2	100
	60.0	53.6 ± 1.2	2.4	89.4
	1500	1516 ± 62	4.1	101
	6000	5644 ± 110	1.9	94.1
oxREGO	30.0	29.3 ± 1.6	5.6	97.7
	60.0	58.1 ± 0.9	1.6	96.9
	750	698 ± 37	5.2	93.0
	3000	2827 ± 51	1.8	94.2
des-oxREGO	30.0	29.9 ± 2.6	8.7	99.6
	60.0	60.7 ± 3.5	5.8	101
	750	760 ± 28	3.7	101
	3000	3061 ± 83	2.7	102

Meanwhile, as compared to the inter-day tests conducted in 5 different working days at the same concentrations (LLOQ and QCs), the precision and accuracy values were CV ≤ 7.2% and between 92.0-109%, respectively (Table 10). The method resulted very precise and accurate, in both intra- and inter-day assessment.

Table 10. Inter-day precision (CV%) and accuracy (%) for SORA, oxSORA, REGO, oxREGO and des-oxREGO in human plasma (conc: concentration; N: number of replicates; SD: standard deviation).

Inter-day (N = 15)				
Analyte	**Nominal conc. (ng/mL)**	**Mean ± SD**	**CV %**	**Accuracy %**
SORA	50.0	50.4 ± 3.0	6.0	101
	60.0	61.8 ± 2.8	4.6	103
	1500	1553 ± 95	6.1	104
	6000	6091 ± 235	3.9	102
oxSORA	30.0	29.8 ± 0.7	2.2	99.2
	60.0	61.8 ± 4.1	6.8	103
	750	787 ± 57	7.2	105
	3000	3067 ± 166	5.4	102
REGO	50.0	53.5 ± 2.5	4.6	107
	60.0	58.8 ± 3.8	6.5	98.0
	1500	1578 ± 76	4.8	105
	6000	5710 ± 255	4.5	95.2
oxREGO	30.0	27.6 ± 1.9	6.8	92.0
	60.0	60.7 ± 4.0	6.7	101
	750	729 ± 35	4.9	97.2
	3000	2833 ± 131	4.6	94.4
des-oxREGO	30.0	30.2 ± 2.1	6.8	101
	60.0	65.3 ± 2.9	4.5	109
	750	809 ± 43	5.3	108
	3000	3021 ± 139	4.6	101

4.1.4.5. Limit of quantification and selectivity

As far as the sensitivity of the proposed method is concerned, the accuracy and precision obtained for the 6 LLOQ samples prepared in pooled blank plasma were, respectively: 114% and 0.9% for SORA, 112% and 2.8% for oxSORA, 105% and 3.0% for REGO, 111% and 3.4% for oxREGO, 105% and 2.7% for des-oxREGO. As shown in Figure 34 B, the S/N obtained by analyzing a LLOQ plasma sample was 122 for SORA, 460 for oxSORA, 62.0 for REGO, 185 for oxREGO and 54.8 for des-oxREGO.

Moreover, the method proved to be selective since no interferences were detected analyzing six blank plasma samples from different donors, especially at the analytes retention times, as reported in Figure 34 A.

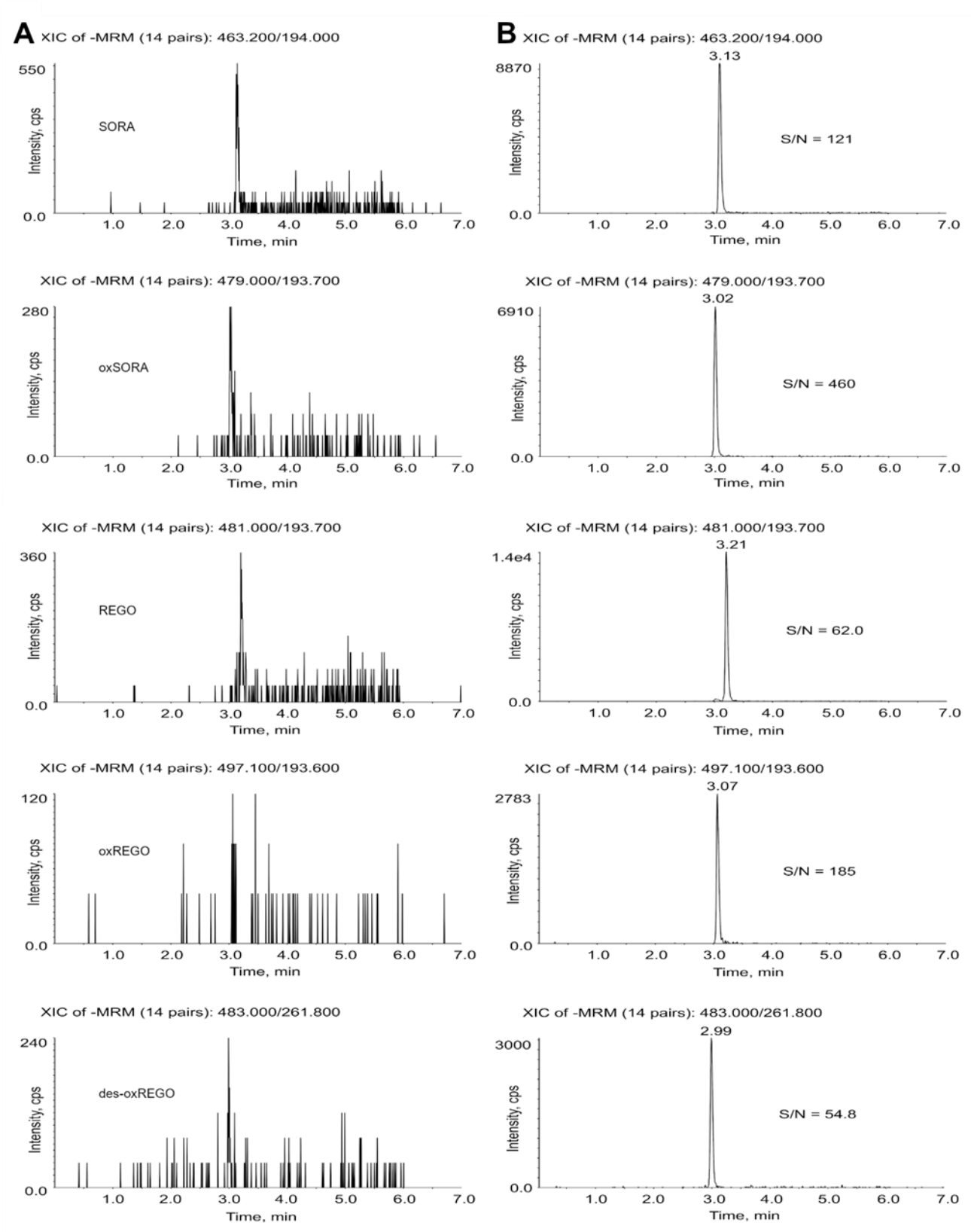

Figure 34. Examples of MRM chromatograms. (A): blank plasma sample from a single donor; (B): LLOQ (50 ng/mL for SORA and REGO and 30 ng/mL for all the metabolites) with signal to noise ratio (S/N) values calculated for each analyte.

4.1.4.6. Dilution integrity

The dilution integrity of plasma samples was assessed at two dilution factors: 1:10 and 1:100. Overall, the accuracy and precision were between 95.7-107% and ≤ 4.7%, respectively, for all analytes, as reported in Table 11. The method can be quantified a sample with a higher concentration than ULOQ level after appropriate dilution without affecting precision and accuracy of the analysis.

Table 11. Precision (CV%) and accuracy (%) data obtained with 1:10 and 1:100 dilution factors in plasma samples (conc.: concentration; N: number of replicates; SD: standard deviation).

Analyte	Nominal conc. (ng/mL)	Mean (ng/mL) ± SD	CV%	Accuracy%
SORA (N = 5)	80.0	76.9 ± 0.3	0.4	96.2
	800	831 ± 30	3.6	104
oxSORA (N = 5)	40.0	40.7 ± 0.8	1.9	102
	400	428 ± 20	4.7	107
REGO (N = 5)	80.0	78.9 ± 1.5	1.9	98.6
	800	832 ± 21	2.6	104
oxREGO (N = 5)	40.0	38.3 ± 0.6	1.5	95.7
	400	401 ± 14	3.6	100
des-oxREGO (N = 5)	40.0	39.8 ± 0.9	2.4	99.6
	400	412 ± 16	3.9	103

4.1.4.7. Stability

As reported in section 3.6.7, analytes stability was assessed by analyzing QC plasma samples at the three concentrations (QCL, QCM, QCH) under different conditions:

- after extraction, analytes were stable in autosampler at 4 °C for 76 h after the first injection being accuracy between 90.4-113% and a CV ≤ 7.6% for all analytes (Table 12);

Table 12. Post-processing stability of SORA, REGO and their active metabolites after 76 h in autosampler at 4 °C in human plasma (AS: autosampler; conc.: concentration; N: number of replicates; SD: standard deviation).

T = 76 h in AS (4 °C)				
Analyte	**Nominal conc. (ng/mL)**	**Mean (ng/mL) ± SD**	**CV%**	**Accuracy%**
SORA (N = 3)	60.0	54.2 ± 4.1	7.6	90.4
	1500	1494 ± 87	5.8	99.6
	6000	5616 ± 305	5.4	93.6
oxSORA	60.0	56.4 ± 3.0	5.3	94.0
	750	799 ± 44	5.5	107

T = 76 h in AS (4 °C)				
Analyte	**Nominal conc. (ng/mL)**	**Mean (ng/mL) ± SD**	**CV%**	**Accuracy%**
(N = 3)	3000	2926 ± 163	5.6	97.5
REGO (N = 3)	60.0	57.3 ± 1.0	1.8	95.6
	1500	1656 ± 26	1.6	110
	6000	5776 ± 149	2.6	96.3
oxREGO (N = 3)	60.0	55.6 ± 2.5	4.5	92.7
	750	750 ± 19	2.6	99.9
	3000	2822 ± 83	3.0	94.1
des-oxREGO (N = 3)	60.0	64.6 ± 2.3	3.6	108
	750	847 ± 20	2.3	113
	3000	2953 ± 47	1.6	98.4

- bench-top stability was verified after 4 h at room temperature (25 °C) with an accuracy between 94.3-113% and a CV ≤ 5.9% for all analytes (Table 13);

Table 13. Short-term stability of SORA, oxSORA, REGO, oxREGO and des-oxREGO after 4 h at room temperature in human plasma (conc.: concentration; N: number of replicates; SD: standard deviation).

T = 4 h at 25°C				
Analyte	**Nominal conc. (ng/mL)**	**Mean (ng/mL) ± SD**	**CV%**	**Accuracy%**
SORA (N = 3)	60.0	62.1 ± 3.6	5.9	103
	1500	1537 ± 13	0.8	102
	6000	6081 ± 41	0.7	101
oxSORA (N = 3)	60.0	65.6 ± 2.1	3.2	109
	750	794 ± 9.4	1.2	106
	3000	2999 ± 37	1.2	100
REGO (N = 3)	60.0	57.2 ± 1.3	2.2	95.4
	1500	1543 ± 20	1.3	103
	6000	5657 ± 108	1.9	94.3
oxREGO (N = 3)	60.0	61.1 ± 2.0	3.2	102
	750	743 ± 8.5	1.1	99.1
	3000	2869 ± 16	0.6	95.6
des-oxREGO (N = 3)	60.0	67.6 ± 0.8	1.1	113
	750	821 ± 27	3.3	109
	3000	3076 ± 35	1.1	103

- freeze (-80 °C)-thaw stability was verified after three cycles with an accuracy between 99.1-112% and a CV ≤ 5.6% for all analytes (Table 14);

Table 14. Stability of SORA, REGO and their active metabolites in human plasma samples after three freeze (-80°C)-thaw cycles (conc.: concentration; FTC: freeze-thaw cycle; N: number of replicates; SD: standard deviation).

T = 3° FTC				
Analyte	**Nominal conc. (ng/mL)**	**Mean (ng/mL) ± SD**	**CV%**	**Accuracy%**
SORA (N = 3)	60.0	60.7 ± 3.4	5.6	101
	1500	1621 ± 29	1.8	108
	6000	6314 ± 132	2.1	105
oxSORA (N = 3)	60.0	63.0 ± 0.7	1.1	105
	750	828 ± 35	4.2	110
	3000	3112 ± 50	1.6	104
REGO (N = 3)	60.0	59.5 ± 0.5	0.8	99.2
	1500	1681 ± 45	2.7	112
	6000	6151 ± 120	2.0	103
oxREGO (N = 3)	60.0	62.5 ± 2.5	4.1	104
	750	756 ± 20	2.6	101
	3000	2972 ± 69	2.3	99.1
des-oxREGO (N = 3)	60.0	66.7 ± 0.4	0.6	111
	750	841 ± 2.3	0.3	112
	3000	3212 ± 67	2.1	107

- long term stability was investigated in plasma after storage at -80 °C up to 146 days. An accuracy between 96.9-114% and a CV ≤ 4.2% was obtained in plasma for all the analytes (Table 15);

Table 15. Long-term stability of SORA, REGO and their active metabolites in human plasma samples stored at -80 °C for 146 days (conc.: concentration; N: number of replicates; SD: standard deviation).

T = 146 days (-80 °C)				
Analyte	**Nominal conc. (ng/mL)**	**Mean (ng/mL) ± SD**	**CV%**	**Accuracy%**
SORA (N = 3)	60.0	65.2 ± 1.2	1.8	109
	1500	1667 ± 23	1.4	111
	6000	6634 ± 281	4.2	111
oxSORA (N = 3)	60.0	61.3 ± 0.6	1.0	102
	750	772 ± 26	3.3	103
	3000	3138 ± 36	1.2	105
REGO (N = 3)	60.0	68.5 ± 0.3	0.5	114
	1500	1682 ± 25	1.5	112
	6000	6501 ± 170	2.6	108
oxREGO (N = 3)	60.0	59.0 ± 2.2	3.7	98
	750	755 ± 25	3.3	101
	3000	2906 ± 76	2.6	96.9
des-oxREGO (N = 3)	60	68.8 ± 0.5	0.7	114
	750	839.96 ± 3.0	0.4	112
	3000	3178.6 ± 72.5	2.3	106

- long term stability was investigated in MeOH after storage at -80 °C up to 77 days. An accuracy between 89.3-111.4% and a CV ≤ 9.8% was obtained in MeOH for all the analytes (Table 16);

Table 16. Long-term stability of SORA, REGO and their active metabolites in MeOH samples stored at -80 °C for 77 days (conc.: concentration; N: number of replicates; SD: standard deviation).

T = 77 days (-80 °C)				
Analyte	**Nominal conc. (ng/mL)**	**Mean (ng/mL) ± SD**	**CV%**	**Accuracy%**
SORA (N = 3)	60.0	64.2 ± 1.5	2.3	107
	1500	1569 ± 32	2.0	105
	6000	6244 ± 11	0.2	104
oxSORA (N = 3)	60.0	55.7 ± 2.5	4.5	92.8
	750	670 ± 14	2.1	89.3
	3000	2769 ± 1.2	0.0	92.3
REGO (N = 3)	60.0	64.8 ± 1.0	1.6	108
	1500	1672 ± 4.5	0.3	111
	6000	6151 ± 15	0.2	103
oxREGO (N = 3)	60.0	56.1 ± 3.9	7.0	93.5
	750	701 ± 12	1.6	93.5
	3000	2796 ± 3.0	0.1	93.2
des-oxREGO (N = 3)	60.0	57.9 ± 5.7	9.8	96.6
	750	731 ± 32	4.4	97.5
	3000	3009 ± 38	1.3	100

4.1.4.8. Incurred samples reanalysis

To further verify method reproducibility, a subset of 21 plasma samples from patients treated with SORA and 8 plasma samples from patients treated with REGO were analyzed twice, with independent runs in different working days. The percentage differences obtained between the first and the second analysis were always within ±20% thus confirming the good reproducibility of the proposed method (Figure 35). In particular, the calculated percentage differences ranged from -6.6 to +13.8% for SORA; from -9.4 to +15.8% for oxSORA; from -15.4 to +12.0% for REGO; from -13.6 to +6.5% for oxREGO and from -19.2 to 6.3% for des-oxREGO.

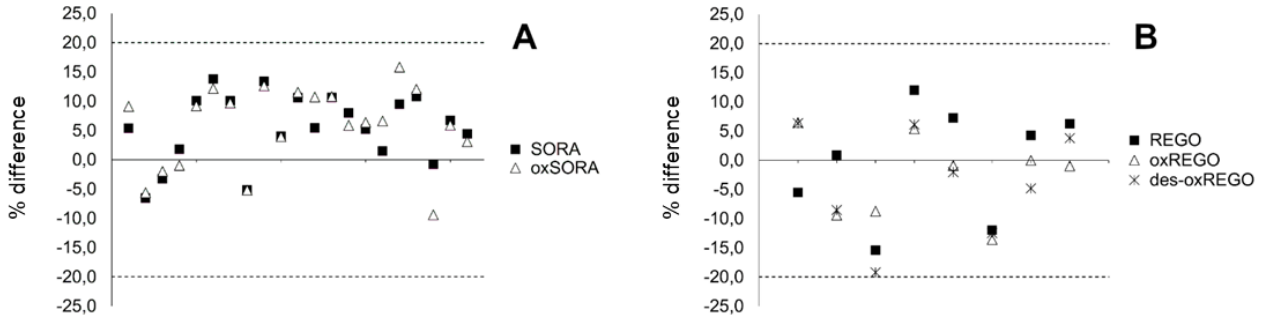

Figure 35. Percentage difference between the first and the second analysis for: (A) patients under treatment with SORA (N. 21 samples). (■) corresponds to SORA, (Δ) to oxSORA quantifications. (B) patients under treatment with REGO (N. 8 samples). (■) corresponds to REGO, (Δ) to oxREGO and (X) to des-oxREGO quantifications. The dotted lines represent the ±20% deviation limits.

4.1.5. Clinical application of LC-MS/MS quantification method

After validation, this LC-MS/MS method was applied for the quantification of SORA or REGO and their metabolites in plasma samples collected from patients treated with these drugs and enrolled in the above-mentioned clinical study (internal protocol code: CRO-2018-83) or received from an out-patient activity from March 2019 to April 2020.

Patients' plasma samples were analyzed with calibration curves and triplicates of each QC concentration levels freshly prepared as reported in section 4.1.3.2. The patients' samples were processed as follows: plasma was thawed at room temperature, vortexed for 10 sec and centrifuged for 10 min at 3000 g and 4 °C. Subsequently, 5 µL of plasma were treated with 495 µL of cold IS WS, vortexed, centrifuged (10 min at 16200 g and 4 °C) and 200 µL of the supernatant were transferred in polypropylene vial for the analysis.

In Figure 36, extracted plasma samples from patients treated with SORA (Figure 36 A) and REGO (Figure 36 B) are reported.

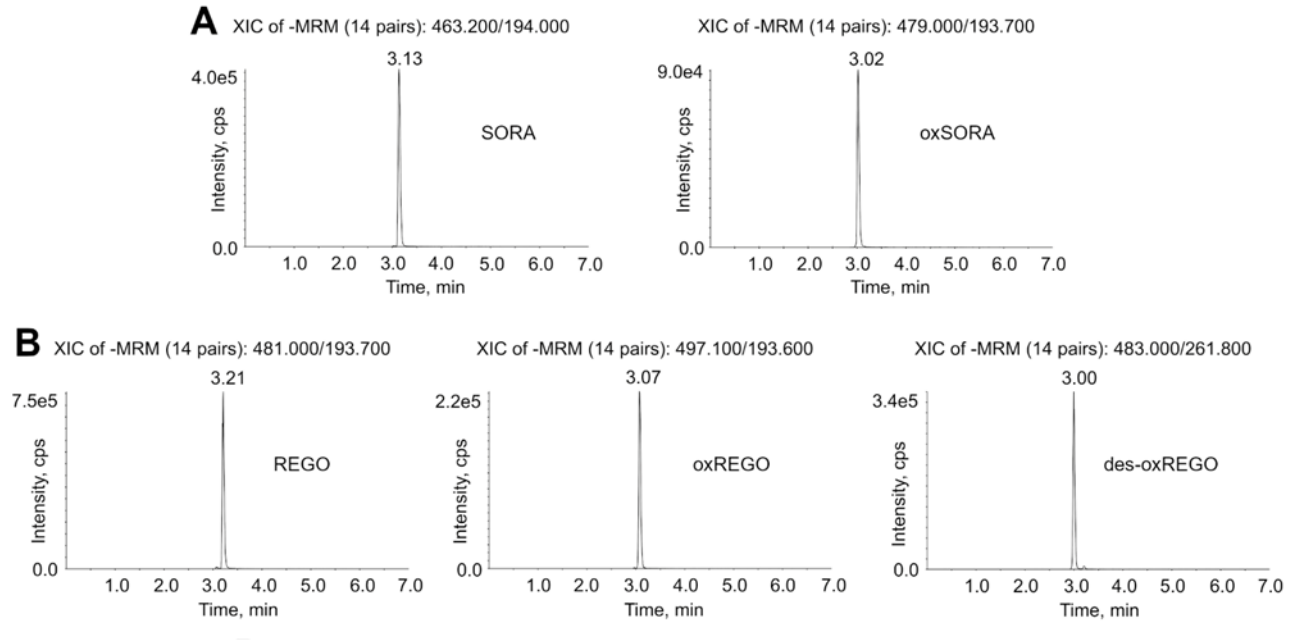

Figure 36. MRM chromatograms of patients' plasma samples. (A): patient treated with SORA (800 mg/day) showing the drug at the concentration of 2061 ng/mL and the metabolite oxSORA at a concentration of 346 ng/mL; (B): patient treated with REGO (160 mg/day) showing the drug at the concentration of 2026 ng/mL, and the metabolites at a concentration of 1871 ng/mL for oxREGO and 1961 ng/mL for des-oxREGO.

A total of 66 plasma samples were collected from 16 patients and then quantified. Demographic and clinical characteristics of the patient population are summarized in Table 17.

Table 17. Principal demographic and clinical characteristics of the enrolled patients (GIST: gastrointestinal stromal tumor; CRC: colorectal cancer; HCC: hepatocellular carcinoma; N: number of replicates).

Patient characteristics	**N**
Sex	13 males (81.3%)
	3 females (18.7%)
Mean age (range)	73 (63-80) years
Therapy	**SORA** 22 samples at 200 mg/day 15 samples at 400 mg/day 8 samples at 600 mg/day 7 samples at 800 mg/day
	REGO 7 samples at 80 mg/day 5 samples at 120 mg/day 2 samples at 160 mg/day
Pathology	**SORA:** 11 HCC patients
	REGO: 3 HCC patients 2 CRC patients 2 GIST patients

As reported in Table 17, most patients received different doses of SORA or REGO during therapy and 2 patients (# 5 and 7) switched from SORA to REGO treatment after therapy failure. Sequential blood samples (approximately every month from the enrollment) were collected from most of the patients: the total number of samples collected, and the respective dose, for each patient, is reported in Table 18.

Table 18. Number of collected samples (total samples#), pathology and treatment received (SORA or REGO) for each enrolled patient (CRC: colorectal cancer; GIST: gastrointestinal stromal tumor; HCC: hepatocellular carcinoma; Pt: patient).

Pt #	Total sample #	Pathology	SORA (mg/day)				REGO (mg/day)		
			200	400	600	800	80	120	160
1	4	HCC	4	-	-	-	-	-	-
2	4	HCC	-	1	1	2	-	-	-
3	5	HCC	-	1	1	3	-	-	-
4	19	HCC	15	4	-	-	-	-	-
5	10	HCC	-	3	4	-	3	-	-
6	1	HCC	-	1	-	-	-	-	-
7	5	HCC	-	-	2	1	1	-	1
8	1	HCC	-	1	-	-	-	-	-
9	5	HCC	3	1	-	1	-	-	-
10	2	HCC	-	2	-	-	-	-	-
11	1	HCC	-	1	-	-	-	-	-
12	3	HCC	-	-	-	-	-	2	1
13	3	CRC	-	-	-	-	3	-	-
14	1	CRC	-	-	-	-	-	1	-
15	1	GIST	-	-	-	-	-	1	-
16	1	GIST	-	-	-	-	-	1	-

The determined C_{min} values for SORA and oxSORA and REGO and its active metabolites are reported in Table 19 and Table 20, respectively. To protect the privacy, each patient was identified with a progressive number based on the enrolment date and each patient samples were named in a univocal way with an ID composed by the patient identification number followed by the sampling number. As an example, ID 1.1 indicates the plasma obtained from patient number 1 at the first blood sampling.

Table 19. C_{min} values for SORA and oxSORA determined from the quantification of 52 HCC patients' plasma samples (conc: concentration).

Patient sample	SORA dose (mg/day)	Timing (hh:mm)[a]	SORA conc. (ng/mL)	oxSORA conc. (ng/mL)
1.1	200	27:40	2727	458
1.2	200	26:00	4058	676
1.3	200	26:25	1941	238
1.4	200	26:30	1144	120
2.1	400	28:45	723	97.3

Patient sample	SORA dose (mg/day)	Timing (hh:mm)[a]	SORA conc. (ng/mL)	oxSORA conc. (ng/mL)
2.2	600	12:40	1466	299
2.3	800	14:15	2061	346
2.4	800	98:20	604	224
3.1	400	16:15	6762	692
3.2	800	17:50	8008	1198
3.3	800	12:30	9912	1899
3.4	800	06:05	2867	481
3.5	600	16:30	3384	572
4.1	200	18:30	4706	401
4.2	200	24:30	5239	422
4.3	200	18:05	2629	262
4.4	200	26:05	4498	423
4.5	400	15:15	5473	857
4.6	400	11:45	11805 *	1570 *
4.7	400	14:23	8050 *	1519 *
4.8	400	15:00	5488	681
4.9	200	26:00	6669	1158
4.10	200	26:45	5492	651
4.11	200	28:10	3917	481
4.12	200	27:27	3698	269
4.13	200	28:10	2828	213
4.14	200	27:40	1335	143
4.15	200	27:32	3399	265
4.16	200	27:30	1446	60.2
4.17	200	28:20	2967	276
4.18	200	28:25	2628	188
4.19	200	27:30	2543	166
5.1	400	13:30	1866	497
5.2	600	13:35	2001	685
5.3	600	13:01	2479	593
5.4	600	12:50	9902 *	2682 *
5.5	600	13:00	4266	1146
5.6	400	13:45	2021	411
5.7	400	14:30	4054	632
6.1	400	03:00	1451	247
7.1	800	07:40	5860	1399
7.2	600	20:30	4247	708
7.3	600	15:10	3374	668
8.1	400	14:26	4664	626
9.1	800	16:15	11510 *	5617 *
9.2	400	13:40	6630	2722
9.3	200	26:00	2765	470
9.4	200	27:30	1344	168
9.5	200	28:30	1029	185
10.1	400	14:47	3854	408

Patient sample	SORA dose (mg/day)	Timing (hh:mm)[a]	SORA conc. (ng/mL)	oxSORA conc. (ng/mL)
10.2	400	17:00	3135	511
11.1	400	06:10	5521	1095

[a]: time from the last pill intake expressed in hours; *: value obtained after dilution (dilution factor 1:10).

Table 20. C_{min} values for REGO, oxREGO and des-oxREGO determined from the quantification of 14 patients' plasma samples (conc: concentration).

Patient sample	REGO dose (mg/day)	Timing (hh:mm)[a]	REGO conc. (ng/mL)	oxREGO conc. (ng/mL)	des-oxREGO conc. (ng/mL)
5.8	80	25:55	1707	904	475
5.9	80	25:20	1058	535	424
5.10	80	26:20	902	418	253
7.4	80	28:45	2442	2098	1547
7.5	160	N/A	1984	1848	1937
12.1	160	49:15	827	418	296
12.2	120	14:30	2079	1412	521
12.3	120	26:00	931	977	1169
13.1	80	23:20	1130	280	139
13.2	80	27:10	1348	945	430
13.3	80	01:50	1871	842	396
14.1	120	24:20	1132	609	261
15.1	120	05:00	1779	1906	1862
16.1	120	03:00	3016	2054	1523

[a]: time from the last pill intake expressed in hours; N/A: not available.

The linear range of the calibration curve demonstrated to be suitable for clinical application since the quantified samples were within the LLOQ and ULOQ, with just few exceptions, adequately managed though sample dilution. The samplings collected from patients treated with SORA approximately at the C_{min} represented about the 76.9%. Among the samplings collected at C_{min}, overall only 17/40 samples are above the TDM threshold reported in the literature (3750 ng/mL).

Due to the paucity of the collected samples, no conclusive considerations can be drawn. However, a certain inter-patients variability in drug concentration can be hypothesized by comparing samples of patients treated at the same dosage and collected at comparable times. For example, considering the samples of patients treated with SORA at 200 mg/day and collected approximately at the C_{min} (24±3 h) drug concentration levels spans from 1144 to 6669 ng/mL. The same high variability was observed with samples from patients treated at 400, 600 or 800 mg/day collected approximately at the C_{min} (12±2h): the concentrations varied from a minimum of 1866 to a maximum of 11805 ng/mL (400 mg/day), from 1466 to 9902 ng/mL (600 mg/day) and from 2061 to 9912 ng/mL (800 mg/day).

The plasma samples of patient 2 obtained at increasing drug dosages show a certain proportionality between the dose and the concentrations observed, even if in all cases the plasma levels did not reach the desired threshold hypothesized for TDM application.

Patient 4 showed intolerable toxicity at the dose of 400 mg/die, which required a dose reduction of SORA to 200 mg/die. In fact, considering the concentration determined in samples 4.6 and 4.7 (collected approximately to the C_{min}), patient's drug levels far exceeded the proposed threshold and this could, at least partially, explain the observed toxicity. On the other hand, this patient had an incredibly long-lasting response despite the much lower dosage than the standard dose (200 mg/die *versus* 800 mg/die). In fact, he received a low dose of SORA (200 mg/die) for at least 19 months before tumor progression. It is noteworthy that the mean SORA duration therapy in the HCC setting is about 6 months [236]. Interestingly, his sampling demonstrated, in most cases, a C_{min} higher than or near to the proposed threshold (3750 ng/mL), despite the low dose received.

Regarding REGO, the samplings collected approximately to the C_{min} represent about 57.1% and generally, there is a wide inter-individual variability.

Among the samplings collected at the C_{min}, overall only 2/8 are above the proposed threshold reported in the literature (1400 ng/mL).

As demonstrated by the data from our small population, the majority of the patients did not tolerate the standard dose of either SORA or REGO, as most of them required dose reduction due to toxic effects. This is in line with data reported in the literature [153].

In Table 21 and Table 22 the mean plasma concentration (±SD) of each drug and metabolite is reported according to the dose level. Since the timing of blood sampling is important for a correct C_{min} evaluation, the mean time elapsed from the last pill intake to the blood sampling is also reported. This time was self-reported by the patient. Unfortunately, performing blood samples at the correct time for C_{min} evaluation (se section 3.1.) was not always possible in real life clinical routine and a reasonable variability in timing was observed. Despite this, a very high inter-variability was found between patients taking the same doses of SORA or REGO, in accordance with literature data [237]. Furthermore, the metabolites steady state concentrations were rather in line with literature data. In fact, oxSORA comprised approximately 10-20% of the total amount of the metabolite and the parent drug at steady state (reference value 9-16% [58] with an interesting increase of the percentage according to SORA dose (10% at 200 mg/day *versus* 20% at 800 mg/day). FDA reported that the two REGO metabolites reached steady-state concentrations that were equal to the parent drug [80] and, in our study, this was verified especially with ox-REGO (62-78% compared to REGO). Nonetheless, due to the paucity of patients, this data should be verified once the study enrollment will be completed.

Table 21. Mean SORA and oxSORA plasma concentrations obtained at each SORA dose level (SD: standard deviation).

Dose (mg/day) (samples#[a])	SORA (ng/mL) ± SD	oxSORA (ng/mL) ± SD	Timing (h)[b] ± SD
200 (22)	3191 ± 1596	367 ± 251	26 ± 3
400 (15)	3986 ± 2861	667 ± 641	17 ± 8
600 (8)	4002 ± 2245	863 ± 707	13 ± 4
800 (6)[c]	4732 ± 3159	1206 ± 1287	13 ± 5

[a]: number of collected samples for each dose level; [b]: time from the last pill intake expressed in hours; [c]: one sample was excluded from calculation because it was collected 98 h after the last pill intake (calculated concentrations of SORA and oxSORA were 603.9 and 224.4 ng/ml, respectively).

Table 22. Mean REGO, oxREGO and des-oxREGO plasma concentrations obtained at each REGO dose level (SD: standard deviation).

Dose (mg/day) (samples#[a])	REGO (ng/mL) ± SD	oxREGO (ng/mL) ± SD	des-oxREGO (ng/mL) ± SD	Timing (h)[b] ± SD
80 (7)	1494 ± 545	860 ± 603	523 ± 467	23 ± 9
120 (5)	1581 ± 899	1260 ± 634	967 ± 648	14 ± 10
160 (2)	1573 ± 831	1137 ± 694	939 ± 678	39 ± 14

[a]: number of collected samples for each dose level; [b]: time from the last pill intake expressed in hours.

4.2. LC-MS/MS method for the quantification of sorafenib, regorafenib and their active metabolites in dried blood spot

To the best of our knowledge, no LC-MS/MS method has been published so far for the simultaneous determination of all these 5 analytes in DBS matrix. For this reason, a new LC-MS/MS method for the quantification of SORA, REGO and their active metabolites in DBS was developed and validated according to EMA [200] and FDA [201] guidelines and EBF recommendation [182,183]. The interest toward the development of DBS-based analytical method was represented by the real possibility to make TDM more feasible in clinical practice exploiting this sample collection strategy.

The LC-MS/MS method for the quantification of DBS matrix was the same used for the quantification of plasma samples and described in section 4.1.1 for the mass spectrometer conditions and 4.1.2 for the chromatographic conditions. Briefly, the mass spectrometer worked in negative ion mode, MP A was 10 mM AmAc buffer in MilliQ H_2O with 0.10% of HCOOH (v/v) while MP B was MeOH:iPrOH (90:10, v/v) with 0.10% of HCOOH (v/v). The used column was a Synergi™ Fusion-RP column (4 µm, 50 x 2.0 mm, 80 Å) with Fusion-RP Security Guard™ pre-column; the injection volume was 2 µL; autosampler and column temperatures were set at 4 °C and 50 °C, respectively, and the total runtime was 7 min.

Moreover, also the analytical range was the same (50-8000 ng/mL) for SORA and REGO and (30-4000 ng/mL) for all the metabolites. Thus, WS for both analytes and ISs were the same used for the quantification of plasma samples (for more details, see section 4.1.3.2.).

4.2.1. Optimization of DBS parameters

4.2.1.1. Type of paper

For this analytical method Whatman 31 ET CHR was the only type of paper tested and used, in order to reduce the cost for each analyzed sample. In fact this filter paper costs 87% less than Whatman 903 (0.24 € *vs* 1.81 €), which is the certified paper for DBS application.

4.2.1.2. Drug extraction optimization

The optimization of the analytes' extraction is one of the fundamental step to consider during the development of a DBS-based quantification method. During this optimization, the initial incubation condition to obtain the spiked whole blood samples were 1 h at 37 °C. In a very preliminary test, analyzing QCL and QCH DBS samples in triplicate, MeOH was selected as extraction solvent, because the extraction yield with ACN was only 10% for all the analytes. Successively, the optimization of extraction solvent was performed as reported in section 3.5.3.4.3., testing MeOH + 0.10% of HCOOH (v/v), MeOH + 0.30% of HCOOH (v/v) and MeOH:MilliQ H_2O (90:10, v/v) with 0.10% of HCOOH (v/v) and the results are reported in Table 23. For this experiment, a 3 mm diameter disc was punched and the analytes were extracted with 225 µL of solvent under mechanic stirrer for 1 h.

Table 23. Optimization of extraction solvent of SORA, REGO and their active metabolites from DBS samples (SD: standard deviation).

SOLVENT (225 µL)	SAMPLE (N = 3)	% extraction yield (mean ± SD)				
		SORA	oxSORA	REGO	oxREGO	des-oxREGO
MeOH + 0.10% HCOOH (v/v)	QCL	69.1 ± 2.0	24.9 ± 1.2	81.8 ± 2.5	43.6 ± 1.8	45.8 ± 3.4
	QCM	68.5 ± 3.6	22.2 ± 1.9	72.3 ± 3.1	39.5 ± 2.7	42.3 ± 2.5
	QCH	68.6 ± 1.1	24.1 ± 2.0	74.0 ± 1.2	40.3 ± 0.7	43.5 ± 1.8
MeOH + 0.30% HCOOH (v/v)	QCL	61.2 ± 2.2	17.8 ± 0.4	74.1 ±4.2	38.4 ± 3.0	40.2 ± 4.1
	QCM	63.2 ± 1.8	15.9 ± 0.3	69.8 ± 3.2	31.7 ± 3.0	36.2 ± 2.7
	QCH	62.1 ± 3.6	16.7 ±0.7	67.6 ±3.4	33.3 ± 0.8	36.3 ± 2.5
90% acidified MeOH + 10%MilliQ H_2O (v/v)	QCL	73.1 ± 2.9	24.2± 2.0	83.1 ± 0.3	44.9 ± 1.9	50.6 ± 3.2
	QCM	69.3 ± 1.8	22.1± 0.8	71.8 ±1.7	37.5 ± 1.1	41.9 ± 0.6
	QCH	67.9 ± 1.6	23.5 ± 0.7	71.4 ±1.7	41.3 ± 1.7	43.6 ± 2.8

In particular, MeOH + 0.30% of HCOOH (v/v) was discarded due to the lower extraction yield and the more hemolysis than the other tested solvent that provided a brick red color to the extract.

The selected extraction solvent was MeOH + 0.10% of HCOOH (v/v) thanks to its higher extraction yield for almost all the analytes with lower SD and CV% respect than MeOH:MilliQ H_2O (90:10, v/v) with 0.10% of HCOOH (v/v). In fact, the mean extraction yield (± SD) and CV% obtained with the last two solvents were 68.7

± 0.3 with a CV of 0.5% *versus* 70.1 ± 2.7 with a CV of 2.7% for SORA, 23.7 ± 1.4 with a CV of 5.8% *versus* 23.3 ± 1.1 with a CV of 4.7% for oxSORA, 76.1 ± 5.1 with a CV of 6.7% *versus* 75.4 ± 6.6 with a CV of 8.8% for REGO, 41.1 ± 2.2 with a CV of 5.3% *versus* 41.2 ± 3.7 with a CV of 8.9% for oxREGO and 43.9 ± 1.8 with a CV of 4.1% *versus* 45.4 ± 4.6 with a CV of 10% for des-oxREGO.

Once the extraction solvent was determined, its volume was optimized. The tested volumes were 180 µL, 225 µL and 450 µL. The selected volume was 225 µL since QCH DBS samples extracted with 180 µL had to high signal intensity for SORA and REGO (peak height approximately of 2.0-3.0 x 10^6 cps) and ULOQ could cause detector saturation, while 450 µL diluted too much samples at low concentration and LLOQ sample might be at the limits of the quantification.

Eventually, the extraction time optimization was performed testing 30 min, 1 h, 2 h and 4 h of shacking. The extraction yield were similar between the time point, as reported in Table 24. The selected time was 1 h instead of 30 min due to the lower SD, while 2 and 4 h were discarded to reduce the duration of sample preparation workflow.

Table 24. Optimization of extraction time of SORA, REGO and their active metabolites from DBS samples (SD: standard deviation).

EXTRACTION TIME	SAMPLE (N = 3)	% extraction yield (mean ± SD)				
		SORA	oxSORA	REGO	oxREGO	des-oxREGO
30 min	QCL	72.9 ± 4.4	60.2 ± 2.0	67.7 ± 3.0	68.4 ± 4.4	55.8 ± 1.3
	QCM	78.0 ± 2.3	67.6 ± 1.9	75.1 ± 3.3	73.5 ± 3.9	65.8 ± 2.2
	QCH	77.2 ± 1.9	70.4 ± 1.9	77.1 ± 1.0	72.6 ± 2.5	68.6 ± 0.1
1 h	QCL	78.3 ± 5.0	64.3 ± 4.2	70.5 ± 6.3	69.6 ± 4.3	56.9 ± 2.4
	QCM	76.0 ± 4.1	63.6 ± 2.2	71.4 ± 3.4	70.0 ± 4.1	58.3 ± 2.7
	QCH	77.9 ± 3.0	71.0 ± 2.1	79.3 ± 1.8	73.6 ± 3.4	63.9 ± 3.2
2 h	QCL	79.6 ± 5.1	64.7 ± 1.5	74.5 ± 4.5	70.9 ± 2.7	56.8 ± 1.5
	QCM	75.6 ± 4.8	61.9 ± 3.3	71.2 ± 4.4	68.8 ± 3.3	55.3 ± 3.2
	QCH	78.3 ± 1.3	71.0 ± 0.8	80.4 ± 1.6	75.4 ± 1.1	65.3 ± 1.9
4 h	QCL	77.4 ± 2.1	64.5 ± 3.5	74.9 ± 3.5	69.2 ± 3.7	56.3 ± 3.9
	QCM	78.8 ± 4.7	65.2 ± 3.0	75.3 ± 5.0	71.7 ± 4.7	56.4 ± 6.0
	QCH	78.3 ± 1.9	68.9 ± 1.1	78.2 ± 1.0	73.9 ± 0.7	60.6 ± 1.3

4.2.1.3. Incubation time optimization

As reported in section 3.5.3.4.4., the incubation time was evaluated from 30 min to 24 h and the obtained results are reported in Table 25. The selected incubation time was 1 h in order to ensure the drug partitioning into the blood.

Overall, the optimized sample preparation workflow was characterized by 1 h of incubation, extraction with 225 µL of MeOH + 0.10% of HCOOH (v/v) and shacking for 1 h.

Table 25. Optimization of incubation time of SORA, REGO and their active metabolites from DBS samples (SD: standard deviation).

INCUBATION TIME	SAMPLE (N = 3)	% extraction yield (mean ± SD)				
		SORA	oxSORA	REGO	oxREGO	des-oxREGO
30 min	QCL	86.5 ± 4.8	68.8 ± 2.5	79.8 ± 5.1	80.0 ± 7.3	51.0 ± 2.2
	QCM	81.2 ± 0.6	66.0 ± 2.5	79.6 ± 1.5	76.8 ± 2.0	49.4 ± 3.0
	QCH	86.9 ± 0.2	70.9 ± 1.6	85.6 ± 1.3	79.5 ± 2.6	52.6 ± 1.0
1 h	QCL	92.6 ± 1.8	74.8 ± 2.2	85.3 ± 2.4	83.4 ± 6.3	54.0 ± 2.2
	QCM	86.7 ± 1.0	67.7 ± 2.2	81.7 ± 1.2	79.1 ± 1.4	50.6 ± 0.3
	QCH	76.6 ± 0.8	66.3 ± 3.0	80.7 ± 4.9	73.7 ± 3.3	48.5 ± 2.8
2 h	QCL	92.8 ± 0.5	68.8 ± 0.9	81.3 ± 1.3	79.9 ± 1.3	50.9 ± 2.3
	QCM	88.1 ± 4.9	67.8 ± 2.1	83.1 ± 3.7	80.7 ± 4.0	48.0 ± 1.6
	QCH	93.1 ± 3.9	75.3 ± 3.4	91.1 ± 3.4	85.2 ± 3.4	53.0 ± 2.0
4 h	QCL	97.5 ± 4.1	70.6 ± 4.8	85.8 ± 5.6	87.9 ± 4.6	51.8 ± 1.1
	QCM	86.2 ± 1.9	65.7 ± 1.7	80.5 ± 2.2	78.0 ± 1.2	45.3 ± 2.5
	QCH	88.6 ± 2.4	69.1 ± 1.8	85.5 ± 2.6	80.6 ± 3.1	47.0 ± 1.7
8 h	QCL	90.0 ± 0.6	65.3 ± 3.3	77.7 ± 2.2	78.3 ± 2.1	46.6 ± 2.3
	QCM	81.8 ± 3.0	60.9 ± 4.4	76.1 ± 5.7	75.3 ± 7.7	42.4 ± 3.5
	QCH	87.6 ± 3.9	64.0 ± 4.2	82.7 ± 3.7	76.6 ± 4.3	45.8 ± 3.3
24 h	QCL	92.9 ± 2.3	66.9 ± 3.1	81.5 ± 2.8	80.9 ± 2.9	47.8 ± 0.5
	QCM	78.5 ± 2.5	55.4 ± 1.9	70.1 ± 1.5	68.3 ± 2.2	38.1 ± 1.7
	QCH	93.3 ± 1.9	70.2 ± 3.4	89.2 ± 3.0	84.1 ± 3.3	48.8 ± 3.5

4.2.1.4. Calibration curve and quality controls preparation

The seven calibrators and, at least, three replicates of each QC concentration level were freshly prepared every day during the validation study and during patients' samples quantification.

A volume of 5 µL of each working solution (both for calibrators and QCs) was added to 95 µL of whole blood. The solutions were gently reversed a couple of times and then equilibrated for 1 h at 37 °C. Then, 5 or 20 µL aliquots of spiked whole blood were spotted on Whatman 31 ET CHR paper and allowed to air dry for 3 h at room temperature.

Once the spiked whole blood on the filter paper was dried, the 20 µL spots for calibration standards and QCs DBS were punched for getting 3 mm discs, corresponding to more or less 3 µL of blood, with a pneumatically-activated device (Analytical S&S, USA), meanwhile the 5 µL spots were punched with a manually device to take the entire spot, thus getting 6 mm discs.

Then, the discs were extracted adding 75 volumes of the ISs extracting solution, corresponding to 225 µL for the 3 mm discs and 375 µL for the 6 mm discs. After 1 h of gentle mixing, 200 µL of supernatant were transferred to a polypropylene autosampler vial for the analysis.

Thus, DBS samples presented the concentrations for the calibration curve and QCs reported in Table 5.

Several 5 µL-DBS samples of the three QCs have been stored in both plastic envelopes at -80 °C and in paper envelopes inside the dryer at room temperature to check the stability of the analytes and as controls for future assays.

4.2.2. LC-MS/MS method validation study

The validation process was conducted according to EMA and FDA guidelines and EBF recommendation[182,183,200,201].

4.2.2.1. Effect of hematocrit and spot volume

Firstly, effect of Hct were evaluated analyzing punch of 3 mm for 20 µL-volume spot in triplicated for each QC concentration levels.

Four different Hct values (30.0, 34.5, 48.0 and 60.0%) were prepared following the procedure reported in section 3.7.1 QCL, QCM, and QCH samples were prepared, as reported in section 4.2.1.4 in triplicate, for each of the five whole blood aliquots with different Hct values and quantified using a DBS calibration curve prepared at fixed Hct value (40.0%). The obtained results were reported in Table 26. The accuracy was between 77.4 and 138% for SORA, 73.9 and 128% for oxSORA, 71.9 and 139% for REGO, 70.4 and 139 for oxREGO and between 78.6 and 149% for des-oxREGO, at each QC level (L, M, and H). Precision was within 0.6 and 16% for all the analytes. This indicated a significant and not acceptable impact of Hct value to perform the analytes quantification because the accuracy increases as the Hct value increases.

Table 26. Hct effect on 3 mm punch for SORA, REGO and their active metabolites in DBS samples (conc.: concentration; Hct: hematocrit; N: number of replicates; SD: standard deviation).

Analyte	Nominal conc. (ng/mL)	Hct	Mean ± SD	Accuracy%	CV%
SORA (N = 3)	60.0	30.0%	52.7 ± 3.3	87.9	6.2
		34.5%	56.8 ± 3.9	94.7	6.9
		40.0%	70.8 ± 7.3	118	10
		48.0%	71.5 ± 0.8	119	1.1
		60.0%	82.6 ± 1.9	138	2.3
	1500	30.0%	1236 ± 21	82.4	1.7
		34.5%	1187 ± 44	79.1	3.7
		40.0%	1696 ± 51	113	3.0
		48.0%	1709 ± 30	114	1.8
		60.0%	2013 ± 104	134	5.2
	6000	30.0%	4781 ± 100	79.7	2.1
		34.5%	4645 ± 282	77.4	6.1
		40.0%	6265 ± 419	104	6.7
		48.0%	7540 ± 667	126	8.9
		60.0%	7201 ± 134	120	1.9
oxSORA (N = 3)	60.0	30.0%	53.7 ± 1.3	89.5	2.5
		34.5%	50.5 ± 3.6	84.2	7.2
		40.0%	67.4 ± 1.7	112	2.6
		48.0%	65.1 ± 2.9	108	4.4

Analyte	Nominal conc. (ng/mL)	Hct	Mean ± SD	Accuracy%	CV%
		60.0%	71.6 ± 5.9	119	8.3
	750.0	30.0%	619 ± 11	82.5	1.8
		34.5%	578 ± 29	77.0	5.1
		40.0%	800 ± 24	107	3.0
		48.0%	779 ± 8.1	104	1.0
		60.0%	961 ± 55	128	5.7
	300	30.0%	2337 ± 106	77.9	4.5
		34.5%	2217 ± 173	73.9	7.8
		40.0%	2822 ± 259	94.1	9.2
		48.0%	3745 ± 598	125	16
		60.0%	3553 ± 40	118	1.1
REGO (N = 3)	60.0	30.0%	52.8 ± 3.1	88.0	5.8
		34.5%	55.9 ± 4.1	93.1	7.3
		40.0%	69.3 ± 0.4	116	0.6
		48.0%	70.0 ± 0.4	117	0.6
		60.0%	83.5 ± 5.3	139	6.3
	1500	30.0%	1199 ± 28	79.9	2.4
		34.5%	1163 ± 53	77.6	4.6
		40.0%	1609 ± 72	107	4.5
		48.0%	1689 ± 21	113	1.2
		60.0%	1997 ± 126	133	6.3
	6000	30.0%	4583 ± 84	76.4	2.4
		34.5%	4315 ± 302	71.9	7.0
		40.0%	5536 ± 364	92.3	6.6
		48.0%	6803 ± 837	113	12
		60.0%	6794 ± 157	113	2.3
oxREGO (N = 3)	60.0	30.0%	51.9 ± 3.6	86.5	7.0
		34.5%	56.3 ± 3.6	93.9	6.3
		40.0%	63.8 ± 4.4	106	7.0
		48.0%	68.1 ± 3.7	114	5.5
		60.0%	83.5 ± 3.8	139	4.5
	750	30.0%	578 ±28	77.1	4.9
		34.5%	568 ± 15	75.7	2.6
		40.0%	778 ± 42	104	5.4
		48.0%	835 ± 43	111	5.1
		60.0%	960 ± 50	128	5.2
	3000	30.0%	2215 ± 113	73.8	5.1
		34.5%	2112 ± 174	70.4	8.3
		40.0%	2721 ± 271	90.7	9.9
		48.0%	3566 ± 456	119	13
		60.0%	3389 ± 84	113	2.5
des-oxREGO (N = 3)	60.0	30.0%	55.2 ± 2.2	91.9	3.9
		34.5%	53.9 ± 8.4	89.9	16
		40.0%	65.1 ± 1.2	109	1.9
		48.0%	69.5 ± 4.9	116	7.1
		60.0%	87.7 ± 2.7	146	5.6

Analyte	Nominal conc. (ng/mL)	Hct	Mean ± SD	Accuracy%	CV%
	750	30.0%	613 ± 15	81.8	2.5
		34.5%	602 ± 23	80.3	3.8
		40.0%	839 ± 11	112	1.3
		48.0%	822 ± 37	110	4.5
		60.0%	1117 ± 62	149	5.6
	3000	30.0%	2369 ± 31	79.0	1.3
		34.5%	2358 ± 231	78.6	9.8
		40.0%	2967 ± 138	98.9	4.7
		48.0%	3953 ± 526	132	13
		60.0%	4064 ± 156	136	3.8

*Not accepted value according to acceptance criteria

As concern to the spot size (or volume), whole blood QCs at three levels and in triplicate were prepared and deposited on the 31ET CHR using four different volumes: 5, 10, 20, 40 µL. The quantification of these QC samples was performed using a DBS calibration curve made by fixed 20 µL-volume spots. For all the samples 3 mm punch were extracted. Unfortunately, the accuracy was between 83.0 and 110% for SORA, 79.8 and 108% for oxSORA, 80.8 and 114% for REGO, 73.1 and 107% for oxREGO and between 81.0 and 120% for des-oxREGO (Table 27). The precision was within 0.6 and 13% for all the analytes. Also in this case, a significant impact of spot volume on SORA, REGO and their metabolites quantification in DBS was observed.

Table 27. Spot volume effect on 3 mm punch for SORA, REGO and their active metabolites in DBS samples (conc.: concentration; N: number of replicates; SD: standard deviation).

Analyte	Nominal conc. (ng/mL)	Spot volume (µL)	Mean ± SD	Accuracy%	CV%
SORA (N = 3)	60.0	5	49.8 ± 2.6	83.0	5.1
		20	59.9 ± 3.0	99.9	5.1
		40	65.1 ± 0.8	109	1.2
	1500	5	1371 ± 15	91.4	1.1
		20	1602 ± 21	107	1.3
		40	1645 ± 45	110	2.7
	6000	5	4999 ± 177	83.3	3.5
		20	5726 ± 108	95.4	1.9
		40	5819 ± 171	97.0	2.9
oxSORA (N = 3)	60.0	5	47.9 ± 3.6	79.8	7.5
		20	58.2 ± 1.9	97.1	3.2
		40	64.9 ± 2.0	108	3.1
	750	5	669 ± 18	89.3	2.7
		20	778 ± 21	104	2.7
		40	802 ± 20	107	2.5
	3000	5	2438 ± 53	81.3	2.2
		20	2750 ± 74	91.6	2.7
		40	2815 ± 70	93.8	2.5

Analyte	Nominal conc. (ng/mL)	Spot volume (µL)	Mean ± SD	Accuracy%	CV%
REGO (N = 3)	60.0	5	49.5 ± 3.7	82.5	7.5
		20	58.6 ± 2.2	97.6	3.8
		40	65.2 ± 0.9	109	1.3
	1500	5	1428 ± 81	95.2	5.7
		20	1658 ± 67	111	4.1
		40	1702 ± 48	114	2.8
	6000	5	4848 ± 114	80.8	2.4
		20	5625 ± 165	93.8	2.9
		40	5790 ± 200	96.5	3.5
oxREGO (N = 3)	60.0	5	48.7 ± 6.3	81.1	13
		20	57.7 ± 1.3	96.2	2.3
		40	63.9 ± 3.7	107	5.8
	750	5	649 ± 17	86.6	2.7
		20	735 ± 4.5	98.0	0.6
		40	776 ± 20	104	2.6
	3000	5	2192 ± 24	73.1	1.1
		20	2622 ± 112	87.4	4.3
		40	2693 ± 138	89.8	5.1
des-oxREGO (N = 3)	60.0	5	53.6 ± 4.8	89.4	8.9
		20	64.3 ± 3.8	107	6.0
		40	69.1 ± 2.9	115	4.2
	750	5	731 ± 41	97.5	5.6
		20	854 ± 29	114	3.4
		40	896 ± 12	120	1.4
	3000	5	2431 ± 76	81.0	3.1
		20	2830 ± 84	94.3	3.0
		40	2861 ± 93	95.4	3.2

*Not accepted value according to acceptance criteria

Acceptable impact of Hct within range from 30% to 50% was obtained extracting the whole spot. In particular, 5 µL of QC whole blood were deposited on Whatman 31 ET CHR and 6 mm punch was performed. In fact, at each Hct value tested, accuracy was between 104 and 113% for SORA, 93.8 and 105% for oxSORA, 98.1 and 110% for REGO, 95.7 and 114% for oxREGO and 89.9 and 108% for des-oxREGO, while precision was within 1.5 and 9.0% for all the compounds. Data are reported in Table 28. For this reason, the entire validation process was performed extracting the entire 5 µL DBS sample with 375 µL of 20 ng/mL of SORA-L4 and REGO-D_3 in MeOH + 0.10% of HCOOH (v/v).

Table 28. Hct effect on 6 mm punch for SORA, REGO and their active metabolites in DBS samples (conc.: concentration; Hct: hematocrit; N: number of replicates; SD: standard deviation).

Analyte	Nominal conc. (ng/mL)	Hct	Mean ± SD	Acc%	CV%
SORA (N = 3)	60.0	30%	65.0 ± 5.0	108	7.7
		39%	62.6 ± 1.1	107	5.9
		50%	67.8 ± 4.0	105	2.1
	1500	30%	1608 ± 95	104	1.7
		39%	1606 ± 30	107	1.8
		50%	1657 ± 80	105	1.7
	6000	30%	6286 ± 132	113	5.9
		39%	6274 ± 108	110	4.8
		50%	6355 ± 379	106	6.0
oxSORA (N = 3)	60.0	30%	62.5 ± 5.0	104	8.0
		39%	59.1 ± 1.2	104	9.0
		50%	65.0 ± 3.6	95.6	1.5
	750	30%	777 ± 70	98.5	2.1
		39%	747 ± 26	99.6	3.5
		50%	785 ± 53	93.8	3.9
	3000	30%	2868 ± 42	103	5.5
		39%	2814 ± 110	105	6.7
		50%	2873 ± 177	95.8	6.2
REGO (N = 3)	60.0	30%	65.0 ± 2.1	108	3.2
		39%	62.1 ± 3.0	106	8.0
		50%	65.8 ± 4.0	101	2.6
	1500	30%	1592 ± 128	103	4.8
		39%	1594 ± 38	106	2.4
		50%	1634 ± 44	98.1	4.5
	6000	30%	6033 ± 158	110	6.0
		39%	5886 ± 266	109	2.7
		50%	6043 ± 270	101	4.5
oxREGO (N = 3)	60.0	30%	68.5 ± 4.0	114	5.8
		39%	66.0 ± 2.9	104	7.0
		50%	68.4 ± 4.7	99.7	2.4
	750	30%	780 ± 55	110	4.4
		39%	788 ± 14	105	1.7
		50%	789 ± 27	95.7	3.3
	3000	30%	2990 ± 72	114	6.9
		39%	2871 ± 95	105	3.4
		50%	2904 ± 118	96.8	4.0
des-oxREGO (N = 3)	60.0	30%	64.8 ± 1.9	108	2.9
		39%	57.6 ± 4.4	104	7.1
		50%	64.2 ± 4.7	93.3	3.4
	750	30%	779 ± 55	95.9	7.6
		39%	790 ± 33	105	4.2
		50%	776 ± 23	89.9	3.1
	3000	30%	2798 ± 94	101	7.4

Analyte	Nominal conc. (ng/mL)	Hct	Mean ± SD	Acc%	CV%
		39%	2698 ± 83	103	2.9
		50%	2714 ± 157	90.5	5.8

4.2.2.2. Recovery

As reported in section 3.7.2.1., preparing a single sample at each QC level (1x L, 1x M and 1x H) using a single donor of blood, and this was repeated for six different blood donors (3 males and 3 females) for a total of 6 samples at each QC concentration level (6 x QCL, 6 x QCM and 6 x QCH). % REC was then calculated with the Equation 9.

According to the proposed method, analytes were extracted from DBS samples by simply adding to 6 mm-disc (corresponding to 5 µL of spotted blood) 375 µL of methanol added with 0.1% of HCOOH (v/v) and the ISs. The recovery resulted in the range 77.1-86.8% with a CV ≤6.4% for SORA, 61.8-67.7% with a CV ≤6.1% for oxSORA, 78.6-88.1% with a CV ≤6.5% for REGO, 70.8-77.9% with a CV ≤5.7% for oxREGO and 51.7-58.2% with a CV ≤9.3% for des-oxREGO, as shown in Table 29.

Table 29. Recovery of SORA, oxSORA, REGO, oxREGO and des-oxREGO from DBS matrix (conc.: concentration; N: number of replicates; SD: standard deviation).

Analyte	Nominal conc. (ng/mL)	Recovery (%) ± SD	CV (%)
SORA (N = 6)	60.0	77.1 ± 4.2	5.5
	1500	79.8 ± 5.1	6.4
	6000	86.8 ± 5.5	6.4
oxSORA (N = 6)	60.0	62.0 ± 3.8	6.1
	750	61.8 ± 3.1	5.0
	1500	67.7 ± 3.9	5.8
REGO (N = 6)	60.0	79.4 ± 4.3	5.4
	1500	78.6 ± 5.1	6.5
	6000	88.1 ± 4.9	5.6
oxREGO (N = 6)	60.0	70.8 ± 3.7	5.2
	750	73.8 ± 4.2	5.6
	1500	77.9 ± 4.4	5.7
des-oxREGO (N = 6)	60.0	52.0 ± 4.8	9.3
	750	51.7 ± 3.5	6.8
	1500	58.2 ± 4.2	7.2

4.2.2.3. Matrix effect

The method was not significantly affected by endogenous components of the matrix. The estimated MF was determined between 103-107% (CV% ≤ 6.2) for SORA, 72.5-73.5% (CV% ≤ 4.7) for oxSORA, 101% (CV% ≤ 3.8) for REGO, 78.6.-92.6% (CV% ≤ 7.8) for oxREGO and 61.0-78.9% (CV% ≤5.4) for des-oxREGO, as reported in

Table 30. The estimated MF was 96.8% (CV% = 7.7) and 100 (CV% = 2.6) for SORA-L4 and REGO-D_3, respectively. Furthermore, the IS normalized MF CV% was ≤6.3% for SORA, ≤4.7% for ox-SORA, ≤3.8% for REGO, ≤7.8% for oxREGO and ≤5.5% for des-oxREGO, as reported in Table 30.

Table 30. Estimated matrix factor (MF) and IS normalized matrix factor (IS norm MF) of each analyte and ISs in DBS matrix. (conc.: concentration; N: number of replicates; SD: standard deviation).

Analyte	Nominal conc. (ng/mL)	MF (%) ± SD	CV (%)	IS norm MF (%) ± SD	CV (%)
SORA (N = 6)	60.0	103 ± 6.4	6.2	1.05 ± 0.07	6.3
	6000	107 ± 2.8	2.6	1.09 ± 0.03	2.6
oxSORA (N = 6)	60.0	73.2 ± 2.2	3.0	0.75 ± 0.02	3.0
	1500	72.5 ± 3.4	4.7	0.74 ± 0.04	4.7
REGO (N = 6)	60.0	101 ± 3.9	3.8	0.99 ± 0.03	3.8
	6000	101 ± 3.3	3.3	0.99 ± 0.04	3.3
oxREGO (N = 6)	60.0	78.6 ± 6.1	7.8	0.77 ± 0.06	7.8
	1500	92.6 ± 3.6	3.8	0.91 ± 0.03	3.8
des-oxREGO (N = 6)	60.0	78.9 ± 4.2	5.4	0.79 ± 0.04	5.5
	1500	61.0 ± 1.9	3.2	0.60 ± 0.02	2.8
SORA-L4 (N = 6)	20.0	96.8 ± 7.5	7.7	-	-
REGO-D_3 (N = 6)	20.0	100 ± 2.6	2.6	-	-

Furthermore, the negligible matrix effect has also been proved through the analysis of 6 LLOQ samples from different donors (3 males and 3 females), being the found accuracy and precision (as CV%), respectively: 102% and 5.4% for SORA, 100% and 7.7% for oxSORA, 106% and 5.3% for REGO, 101% and 5.6% for oxREGO and 108% and 9.8% for des-oxREGO.

4.2.2.4. Process efficiency

The process efficiency was evaluated following the procedure reported in section 3.7.4.1. In particular, this parameter was relatively high for SORA, REGO and oxREGO (77.9-83.2%, 77.8-84.8% and 67.0-71.4%, respectively), as reported in Table 31. Lower process efficiency was observed for the other analytes: it was near 50% for oxSORA while it was between 26.5-30.1% for des-oxREGO.

Table 31. Process efficiency of SORA, oxSORA, REGO, oxREGO and des-oxREGO from DBS matrix (conc.: concentration; N: number of replicates; SD: standard deviation).

Analyte	Nominal conc. (ng/mL)	Process efficiency (%) ± SD	CV (%)
SORA (N = 6)	60.0	80.9 ± 4.4	5.5
	1500	77.9 ± 5.0	6.4
	6000	83.2 ± 5.3	6.4

Analyte	Nominal conc. (ng/mL)	Process efficiency (%) ± SD	CV (%)
oxSORA (N = 6)	60.0	46.7 ± 2.9	6.1
	750	43.4 ± 2.2	5.0
	1500	45.5 ± 2.6	5.8
REGO (N = 6)	60.0	79.2 ± 4.2	5.4
	1500	77.8 ± 5.1	6.5
	6000	84.8 ± 4.7	5.6
oxREGO (N = 6)	60.0	71.1 ± 3.7	5.2
	750	67.0 ± 3.8	5.6
	1500	71.4 ± 4.1	5.7
des-oxREGO (N = 6)	60.0	29.0 ± 2.7	9.3
	750	26.5 ± 1.8	6.8
	1500	30.1 ± 2.2	7.2

4.2.2.5. Linearity

The proposed method linearity was tested over the selected ranges (50-8000 ng/mL for SORA and REGO and 30-4000 ng/mL for respective metabolites.

The mean Pearson's correlation coefficient (r) values were 0.9986±0.0007 for SORA, 0.9999±0.0004 for oxSORA, 0.9982±0.0012 for REGO, 0.9988±0.0006 for oxREGO and 0.9981±0.0011 for des-oxREGO indicating a good linearity. In Figure 37 the calibration curves of each analyte prepared during each working day of the validation procedure are reported.

The accuracy obtained for SORA and oxSORA was between 97.8-104% and between 93.2-107% for REGO and its two active metabolites; finally, the CV was always ≤ 4.8% (Table 32).

Table 32. Accuracy (%) and precision (CV%) data of SORA, REGO and their active metabolites calibration curves in DBS samples (conc.: concentration; N: number of replicates; SD: standard deviation).

Nominal conc. (ng/mL)	Mean ± SD	CV%	Accuracy%
SORA (N = 9)			
50.0	49.0 ± 1.0	2.0	97.9
100	104 ± 4.1	3.9	104
300	302 ± 14	4.7	101
750	769 ± 21	2.7	103
2000	1984 ± 81	4.1	99.2
4000	3926 ± 142	3.6	98.2
8000	7821 ± 209	2.7	97.8
oxSORA (N = 9)			
30.0	29.7 ± 0.3	1.2	99.1
100	103 ± 3.1	3.0	103
250	249 ± 11	4.4	99.4

Nominal conc. (ng/mL)	Mean ± SD	CV%	Accuracy%
500	511 ± 15	2.9	102
1000	998 ± 37	3.7	99.8
2000	1975 ± 66	3.3	98.8
4000	3912 ± 202	5.2	97.8
REGO (N = 9)			
50.0	50.9 ± 1.3	2.3	102
100	94.5 ± 2.9	3.1	94.5
300	312 ± 7.0	2.3	104
750	801 ± 21	2.7	107
2000	2003 ± 32	1.6	100
4000	3962 ± 141	3.5	99.1
8000	7524 ± 265	3.5	94.1
oxREGO (N = 9)			
30.0	29.6 ± 0.4	1.2	98.8
100	103 ± 5.0	4.8	103
250	251 ± 11	4.2	100
500	507 ± 21	4.2	102
1000	985 ± 21	2.1	98.5
2000	2025 ± 70	3.5	101
4000	3847 ± 130	3.4	96.2
des-oxREGO (N = 9)			
30.0	29.4 ± 0.3	1.0	97.9
100	106 ± 3.3	3.1	106
250	255 ± 11	4.2	102
500	516 ± 17	3.4	103
1000	1001 ± 18	1.8	100
2000	1957 ± 78	4.0	97.8
4000	3729 ± 147	3.9	93.2

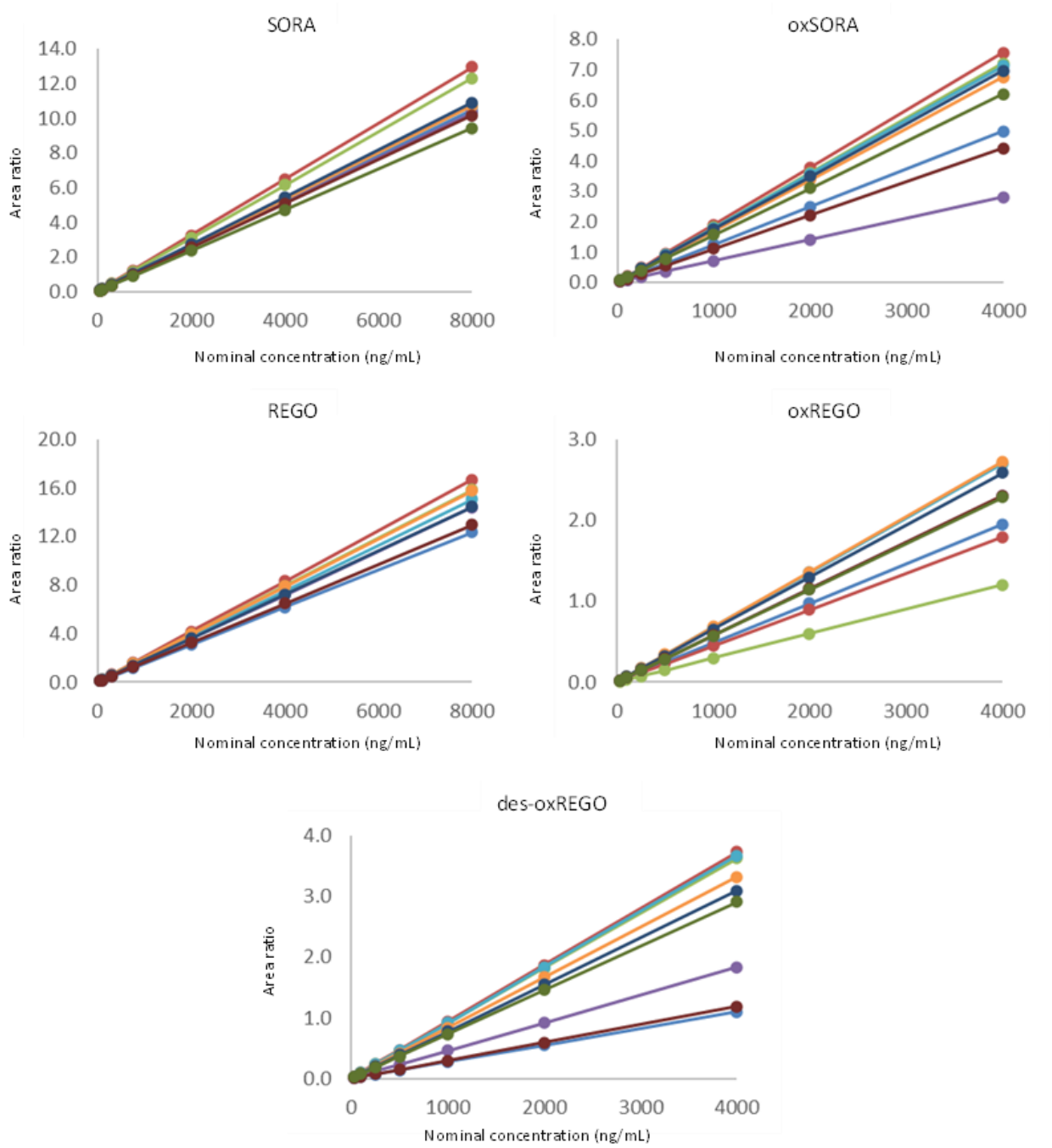

Figure 37. Calibration curves (N = 9) obtained for SORA, oxSORA, REGO, oxREGO and des-oxREGO in DBS matrix.

4.2.2.6. Intra-day and inter-day precision and accuracy

Precision and accuracy of this analytical method was determined as reported in section 3.7.6. In particular, intra-day precision (CV) and accuracy were, respectively, ≤ 10% and between 92.1-107% for all analytes (Table 33).

Table 33. Intra-day precision (CV%) and accuracy (%) for SORA, REGO and their active metabolites in DBS samples (conc: concentration; N: number of replicates; SD: standard deviation).

Intra-day (N = 6)				
Analyte	**Nominal conc. (ng/mL)**	**Mean ± SD**	**CV %**	**Accuracy %**
SORA	50.0	47.1 ± 3.3	6.9	94.2
	60.0	55.2 ± 2.7	4.8	92.1
	1500	1578 ± 44	2.8	105
	6000	5869 ± 225	3.8	97.8
oxSORA	30.0	29.5 ± 3.1	10	98.4
	60.0	58.2 ± 1.5	2.6	97.1
	750	794 ± 35	4.4	106
	3000	2955 ± 102	3.4	98.5
REGO	50.0	47.0 ± 1.7	3.6	94.0
	60.0	61.8 ± 3.5	5.7	103
	1500	1611 ± 61	3.8	107
	6000	5915 ± 160	2.7	98.6
oxREGO	30.0	30.0 ± 3.1	10	100
	60.0	61.4 ± 5.4	8.9	102
	750	777 ± 43	5.6	104
	3000	3043 ± 85	2.8	101
des-oxREGO	30.0	29.9 ± 1.8	5.9	99.7
	60.0	60.1 ± 6.0	9.9	100
	750	787 ± 40	5.1	105
	3000	2983 ± 286	9.6	99.4

Table 34. Inter-day precision (CV%) and accuracy (%) for SORA, oxSORA, REGO, oxREGO and des-oxREGO in DBS matrix (conc.: concentration; N: number of replicates; SD: standard deviation).

Inter-day (N = 15)				
Analyte	**Nominal conc. (ng/mL)**	**Mean ± SD**	**CV %**	**Accuracy %**
SORA	50.0	49.8 ± 4.1	8.2	99.6
	60.0	62.6 ± 3.7	6.0	104
	1500	1561 ± 75	4.8	104
	6000	6145 ± 349	5.7	102
oxSORA	30.0	29.2 ± 2.5	8.5	97.3
	60.0	61.3 ± 4.4	7.2	102
	750	766 ± 49	6.4	102
	3000	3016 ± 168	5.5	101
REGO	50.0	52.3 ± 3.0	5.8	105
	60.0	64.7 ± 2.9	4.5	108
	1500	1621 ± 59	3.7	108
	6000	6219 ± 227	3.7	104
oxREGO	30.0	29.8 ± 2.5	8.5	99.4
	60.0	62.8 ± 3.5	5.6	105
	750	789 ± 35	4.5	105
	3000	3100 ± 163	5.3	103
des-oxREGO	30.0	28.8 ± 2.5	8.8	96.1
	60.0	62.3 ± 3.4	5.3	104
	750	768 ± 46	6.0	102
	3000	2993 ± 192	6.4	99.8

4.2.2.7. Limit of quantification and selectivity

The LLOQ of the proposed method was fixed at 50 ng/mL for SORA and REGO and at 30 ng/mL for oxSORA, oxREGO and des-oxREGO. As shown in Figure 38 B, the S/N ratio resulted always higher than 24 for all the analytes. Accuracy and CV were, respectively, 94.2% and 6.9% for SORA, 98.4% and 10% for oxSORA, 94.0% and 3.6% for REGO, 100% and 10% for oxREGO and 99.7% and 5.9% for des-oxREGO.
From the analysis of six blank DBS samples no significant interferences were detected at the retention times of our compounds, meaning that the method provides a good selectivity. In Figure 38 A, an example of one of the six blank DBS samples analyzed is reported.

4.2.1.1. Dilution integrity

DBS samples with a higher concentration than the ULOQ (8000 ng/mL for SORA and REGO and 4000 ng/mL for the metabolites) can be quantified after appropriate dilution. Thus, during the validation the independence of the analysis from the dilution was assessed at two dilution factors (1:10 and 1:100). From the obtained data (reported in Table 35) it is possible to affirm that the dilution did not compromise the precision and accuracy of the analysis. In fact, taking together all the analytes for both the dilution factors CV was always ≤ 6.8% and accuracy ranged between 92.3 and 103%.

Table 35. Precision (CV%) and accuracy (%) data obtained with 1:10 and 1:100 dilution factors in DBS samples (conc.: concentration; N: number of replicates; SD: standard deviation).

Analyte	Nominal conc. (ng/mL)	Mean (ng/mL) ± SD	CV%	Accuracy%
SORA (N = 5)	80.0	79.8 ± 4.5	5.6	99.8
	800	820 ± 52	6.4	103
oxSORA (N = 5)	40.0	38.3 ± 2.1	5.4	95.8
	400	380 ± 26	6.8	95.1
REGO (N = 5)	80.0	81.9 ± 4.0	4.9	102
	800	806 ± 42	5.2	101
oxREGO (N = 5)	40.0	39.1 ± 2.4	6.1	97.7
	400	389 ± 20	5.1	97.3
des-oxREGO (N = 5)	40.0	37.5 ± 2.1	5.5	93.9
	400	369 ± 15	4.1	92.3

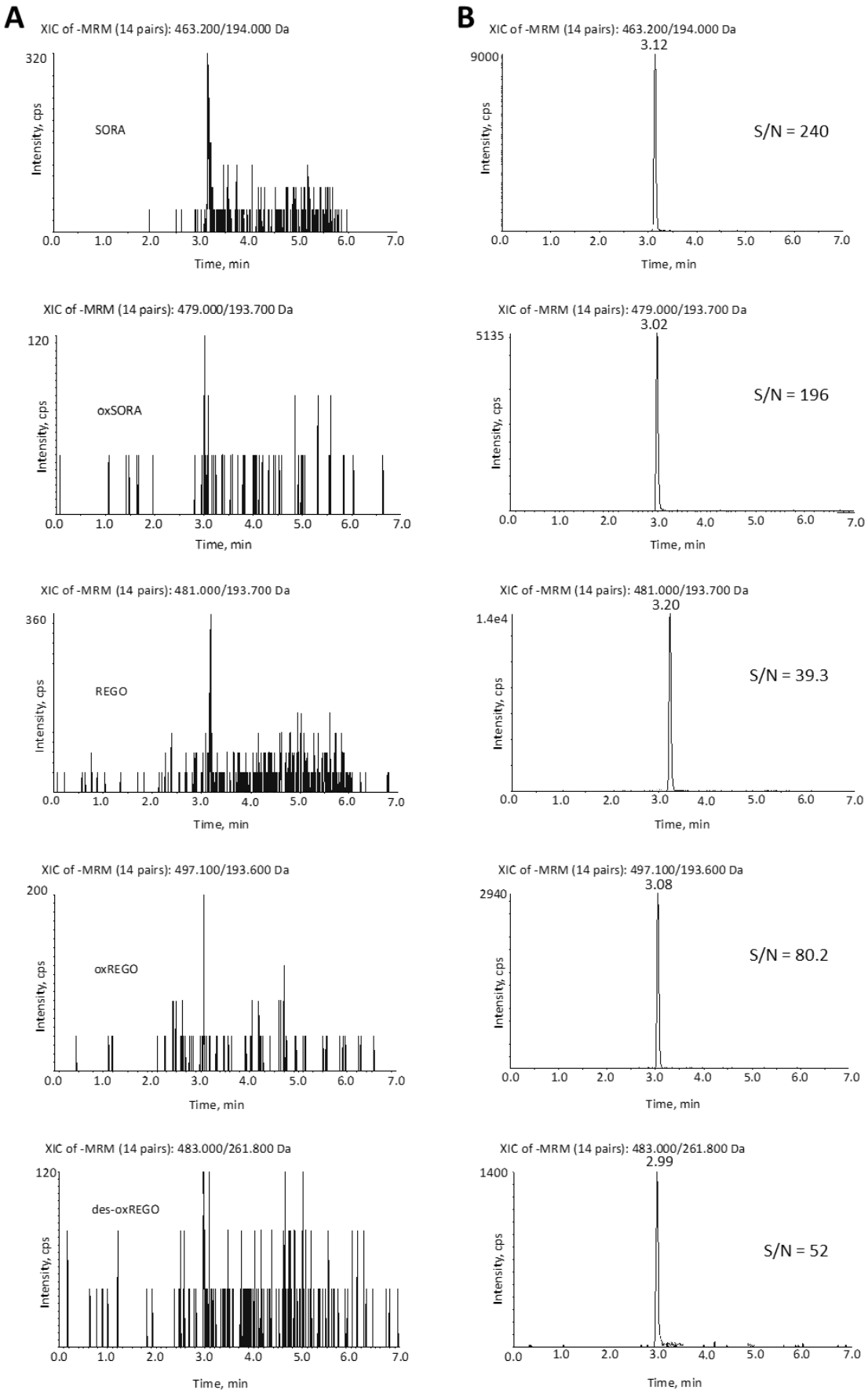

Figure 38. MRM chromatograms in DBS matrix. (A) blank sample from a single donor; (B) LLOQ (50 ng/mL for SORA and REGO and 30 ng/mL for all the metabolites) with signal to noise ratio (S/N) values calculated for each analyte.

4.2.1.2. Stability

Stability of SORA, REGO and their metabolites was assessed only in DBS extract in AS by analyzing QC samples prepared in triplicate. All the five analytes were stable in extracted DBS samples for 24 h at 4 °C with accuracy between 89.4 and 105% and a CV ≤6.6, as reported in Table 36.

Table 36. Post-processing stability of SORA, REGO and their active metabolites after 24 h in autosampler at 4 °C for DBS matrix (conc.: concentration; N: number of replicates; SD: standard deviation).

T = 24 h in AS (4 °C)				
Analyte	**Nominal conc. (ng/mL)**	**Mean (ng/mL) ± SD**	**CV%**	**Accuracy%**
SORA (N = 3)	60.0	60.5 ± 4.0	6.6	101
	1500	1472 ± 8.3	0.6	98.1
	6000	5976 ± 92	1.5	99.6
oxSORA (N = 3)	60.0	58.2 ± 1.0	1.7	97.0
	750	759 ± 41	5.4	101
	3000	2874 ± 51	1.8	95.8
REGO (N = 3)	60.0	63.1 ± 3.3	5.2	105
	1500	1469 ± 32	2.2	97.9
	6000	5813 ± 85	1.5	96.9
oxREGO (N = 3)	60.0	53.6 ± 0.8	1.4	89.4
	750	672 ± 10	1.5	89.6
	3000	2696 ± 84	3.1	89.9
des-oxREGO (N = 3)	60.0	58.1 ± 0.6	1.0	96.8
	750	710 ± 18	2.6	94.7
	3000	2691 ± 88	3.3	89.7

Moreover, a preliminary test to evaluate the difference between two storage conditions (*i.e.,* -80 °C and room temperature in the dryer for 8 months) was performed analyzing 8 patients' DBS samples for SORA and 6 samples for REGO. As report in Table 37 and Table 38, SORA, REGO and their metabolites seemed to be stable in both the tested storage conditions (des-ox-REGO is the only compound that showed 1 out of 6 value of percentage of difference outside the acceptance criteria). To properly verify these preliminary results, triplicates of DBS samples at each QC concentration level stored in the two conditions will be analyzed in triplicate. The two storage conditions can be considered similar in terms of percentage of difference between the two measurements for both SORA (slightly better) and oxSORA, as reported in Table 37.

Table 37. Percentage difference between the determined concentration (conc.) for SORA and oxSORA in patients' DBS samples for both the storage conditions.

PT sample	Conc. at -80°C (ng/mL)	Conc. at RT (ng/mL)	% difference
SORA			
4.15	2283	2325	-1.8
4.16	913	906	0.8
4.17	1800	1752	2.7
4.18	1776	1776	0.0
4.19	1891	1875	0.8
10.1	2733	2763	-1.1
10.2	2680	2582	3.7
11.1	4451	4517	-1.5
oxSORA			
4.15	158	165	-4.3
4.16	34.1	34.7	-1.7
4.17	167	164	1.8
4.18	115	114	0.9
4.19	105	106	-0.9
10.1	297	268	10
10.2	342	332	3.0
11.1	834	741	12

*Table 38.*Percentage difference between the determined concentration (conc.) for REGO and its active metabolites in patients' DBS samples for both the storage conditions.

PT sample	Conc. at -80°C (ng/mL)	Conc. at RT (ng/mL)	% difference
REGO			
5.14	914	937	-2.5
5.15	909	1007	-10
13.1	1005	968	3.8
13.2	760	762	-0.3
14.1	1185	1183	0.2
16.1	2685	2739	-2.0
oxREGO			
5.14	183	192	-4.8
5.15	515	595	-14
13.1	471	445	5.7
13.2	304	282	7.5
14.1	529	519	1.9
16.1	1633	1566	4.2
des-oxREGO			

PT sample	Conc. at -80°C (ng/mL)	Conc. at RT (ng/mL)	% difference
5.14	97.0	110	-13
5.15	291	319	-9.2
13.1	334	418	-22
13.2	210	249	-17
14.1	217	236	-8.4
16.1	1306	1358	-3.9

*Not accepted value according to acceptance criteria

4.2.1.3. Incurred samples reanalysis

The good reproducibility and robustness of the presented method were further demonstrated with the reanalysis of 15 patients' DBS samples stored at room temperature in dryer (8 samples from patients treated with SORA and 7 samples from patients treated with REGO). The percentage difference of the two quantifications were within ±20% in all the 8 samples tested for SORA, in ≥ 87.5% of the re-analyzed samples for ox-SORA, in all the 7 samples tested for both REGO and ox-REGO and in ≥ 71.4% for des-oxREGO, as reported in Figure 39.

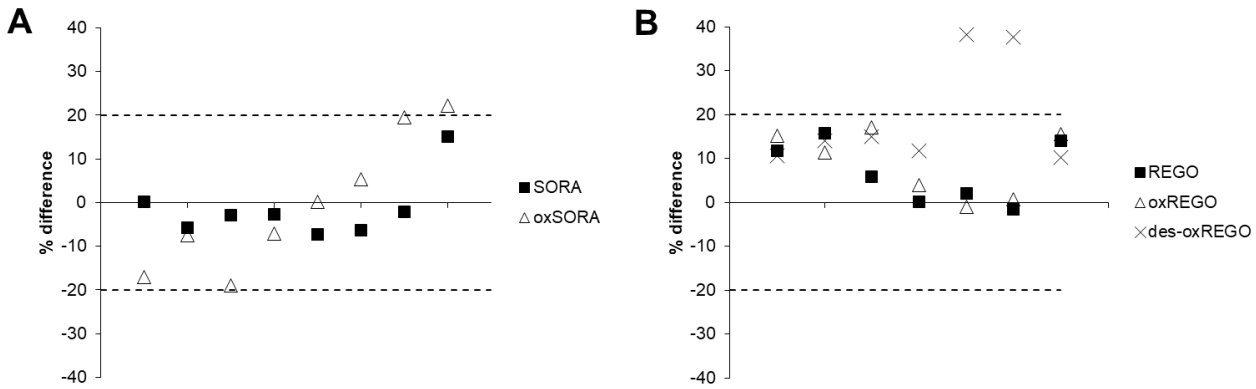

Figure 39. Percentage difference between the first and the second analysis for: (A) patients under treatment with SORA (N. 8 samples). (■) corresponds to SORA, (Δ) to oxSORA quantifications. (B) patients under treatment with REGO (N. 8 samples). (■) corresponds to REGO, (Δ) to oxREGO and (X) to des-oxREGO quantifications. The dotted lines represent the ±20% deviation limits.

4.2.2. Clinical application of LC-MS/MS quantification method in DBS

After validation, this LC-MS/MS method was applied for the quantification of SORA or REGO and their metabolites in DBS samples collected from patients and stored at room temperature in dryer.

Due to the method necessity to analyze a specific spot volume in order to obtain reliable data, it was not possible to quantify patients' DBS samples obtained from finger prick, which are obviously characterized by

variable volumes deposited on the filter paper. Thus, only the venous DBS samples (obtained depositing with a pipette 5 µL-blood drops on the filter paper) were quantified.

Patients' DBS samples were analyzed with a calibration curves and triplicate of each QC concentration levels freshly prepared as reported in section 4.2.1.4. Patients' samples were processed as follows: 5 µL spots were punched with a manually device to take the entire spot, thus getting 6 mm discs. Then, the discs were extracted adding 375 µL (75 volumes) of the extracting solvent (20 ng/mL of SORA-L4 and REGO-D_3 in MeOH + 0.10% of HCOOH (v/v)). After 1 h of gentle mixing, supernatant (200 µL) were transferred to a polypropylene autosampler vial for the analysis.

In Figure 40, the obtained chromatograms of extracted DBS samples from patients treated with SORA (Figure 40 A) and REGO (Figure 40 B) are reported.

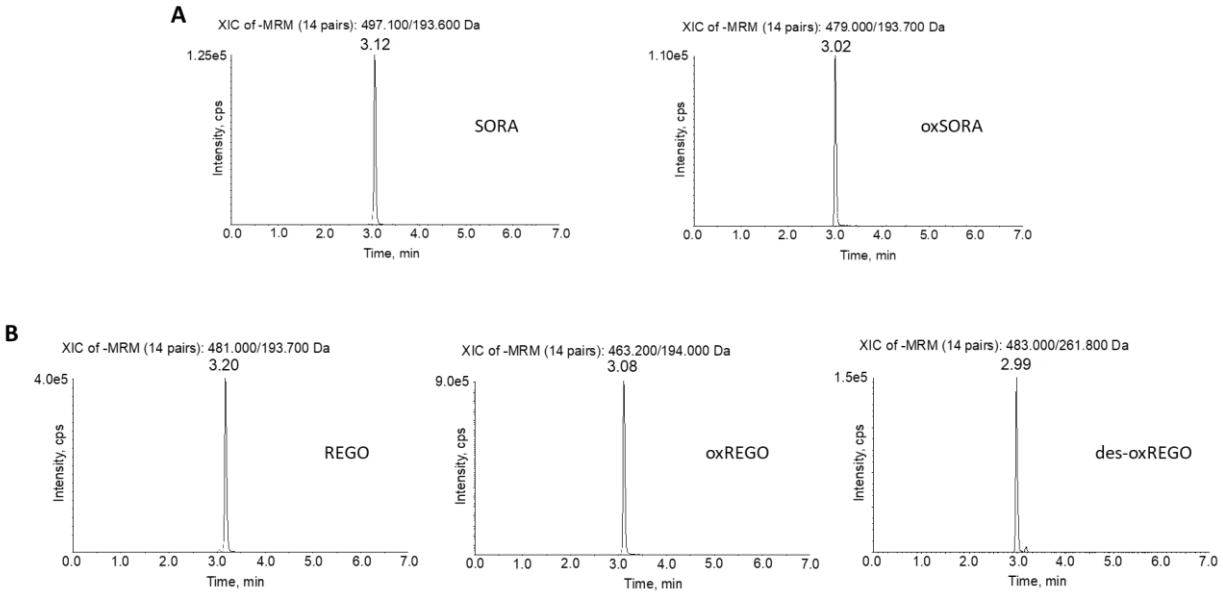

Figure 40. MRM chromatograms of patients' DBS samples. (A) patient treated with SORA (800 mg/day) showing the drug at the concentration of 2424 ng/mL and the metabolite oxSORA at a concentration of 288 ng/mL; (B) patient treated with REGO (160 mg/day) showing the drug at the concentration of 1490 ng/mL, and the metabolites at a concentration of 1187 ng/mL for oxREGO and 1125 ng/mL for des-oxREGO.

Overall, 63 DBS samples from 16 patients were quantifiable Table 39. Patients' demographic and clinical characteristics were the same reported in Table 17 for the corresponding plasma samples.

Table 39. Number of collected samples (total samples#), pathology and treatment received (SORA or REGO) for each enrolled patient for DBS sample (CRC: colorectal cancer; GIST: gastrointestinal stromal tumor; HCC: hepatocellular carcinoma; Pt: patient).

Pt #	Total sample #	Pathology	SORA (mg/day)				REGO (mg/day)		
			200	400	600	800	80	120	160
1	4	HCC	4	-	-	-	-	-	-

Pt #	Total sample #	Pathology	SORA (mg/day)				REGO (mg/day)		
			200	400	600	800	80	120	160
2	2	HCC	-	-	-	2	-	-	-
3	5	HCC	-	1	1	3	-	-	-
4	18	HCC	14	4	-	-	-	-	-
5	10	HCC	-	3	4	-	3	-	-
6	1	HCC	-	1	-	-	-	-	-
7	5	HCC	-	-	2	1	1	-	1
8	1	HCC	-	1	-	-	-	-	-
9	5	HCC	3	1	-	1	-	-	-
10	2	HCC	-	2	-	-	-	-	-
11	1	HCC	-	1	-	-	-	-	-
12	3	HCC	-	-	-	-	-	2	1
13	3	CRC	-	-	-	-	3	-	-
14	1	CRC	-	-	-	-	-	1	-
15	1	GIST	-	-	-	-	-	1	-
16	1	GIST	-	-	-	-	-	1	-

The determined DBS C_{min} values for SORA and oxSORA and REGO and its active metabolites are reported in Table 40 and Table 41, respectively.

Table 40. C_{min} values for SORA and oxSORA determined from the quantification of 49 HCC patients' DBS samples (conc.: concentration).

Patient sample	SORA dose (mg/day)	Timing (hh:mm)[a]	SORA conc. (ng/mL)	oxSORA conc. (ng/mL)
1.1	200	27:40	2347	268
1.2	200	26:00	2990	374
1.3	200	26:25	1758	143
1.4	200	26:30	1323	83.7
2.3	800	14:15	2086	205
2.4	800	98:20	431	116
3.1	400	16:15	4727	412
3.2	800	17:50	5289	725
3.3	800	12:30	6137	1029
3.4	800	06:05	2424	288
3.5	600	16:30	2364	317
4.2	200	24:30	3047	186

Patient sample	SORA dose (mg/day)	Timing (hh:mm)[a]	SORA conc. (ng/mL)	oxSORA conc. (ng/mL)
4.3	200	18:05	2949	232
4.4	200	26:05	2954	278
4.5	400	15:15	3927	545
4.6	400	11:45	7343	1000
4.7	400	14:23	5881	966
4.8	400	15:00	3958	440
4.9	200	26:00	3708	716
4.10	200	26:45	565	428
4.11	200	28:10	2389	321
4.12	200	27:27	2603	155
4.13	200	28:10	2048	172
4.14	200	27:40	989	106
4.15	200	27:32	2320	195
4.16	200	27:30	959	37.4
4.17	200	28:20	1805	198
4.18	200	28:25	1824	122
4.19	200	27:30	2018	106
5.1	400	13:30	2123	418
5.2	600	13:35	2330	687
5.3	600	13:01	2545	544
5.4	600	12:50	6769	1422
5.5	600	13:00	3844	776
5.6	400	13:45	2013	243
5.7	400	14:30	3085	368
6.1	400	03:00	1656	196
7.1	800	07:40	4887	849
7.2	600	20:30	3680	444
7.3	600	15:10	2937	410
8.1	400	14:26	3407	337
9.1	800	16:15	9146*	3948*
9.2	400	13:40	5656	1693
9.3	200	26:00	2693	338
9.4	200	27:30	1311	110
9.5	200	28:30	925	117
10.1	400	14:47	2947	268
10.2	400	17:00	2637	273
11.1	400	06:10	3885	593

[a]: time from the last pill intake expressed in hours; *: value obtained after dilution (dilution factor 1:10).

Table 41. C_{min} values for REGO, oxREGO and des-oxREGO determined from the quantification of 14 patients' DBS samples (conc.: concentration).

Patient sample	REGO dose (mg/day)	Timing (hh:mm)[a]	REGO conc. (ng/mL)	oxREGO conc. (ng/mL)	des-oxREGO conc. (ng/mL)
5.8	80	25:55	1263	570	248
5.9	80	25:20	912	396	264
5.10	80	26:20	705	255	134
7.4	80	28:45	1613	1072	597
7.5	160	N/A	1490	1187	1125
12.1	160	49:15	854	343	452
12.2	120	14:30	1646	841	863
12.3	120	26:00	714	597	904
13.1	80	23:20	825	150	81.5
13.2	80	27:10	891	473	235
13.3	80	01:50	1367	429	234
14.1	120	24:20	1053	519	212
15.1	120	05:00	1429	1223	1449
16.1	120	03:00	2340	1397	1179

[a]: time from the last pill intake expressed in hours; N/A: not available.

4.3. Cross-validation study for sorafenib, regorafenib and their active metabolites DBS method

The cross-validation study was conducted to verify whether DBS can replace the traditional plasma samples for the quantification of SORA, REGO, and their metabolites. As reported more in detail in section 3.9, usually it is necessary to apply a conversion method (*i.e.,* a mathematical equation) to obtain the expected plasma concentration (EC_{pla}) starting from the measured DBS value (C_{DBS}). Thus, as reported in section 3.9, several DBS-to-plasma conversion methods were applied. Firstly, the red blood cells-to-plasma partitioning coefficient ($K_{BC/pla}$), the plasmatic fraction (F_p), and the correction factor (CF) were calculated as reported in section 3.9. The obtained EC_{pla} values for each compound are reported in Table 42. Then, the percentage differences between EC_{pla} and the actual C_{pla} measured in plasma samples (used as reference values) were calculated using the guidelines equation (Equation 26).

$$\%\ difference = \frac{(EC_{pla} - C_{pla})}{mean\ of\ EC_{pla} and\ C_{pla}} x\ 100$$

Equation 26. Percentage difference equation for EC_{pla}.

In Table 42 for each conversion method, the percentage of paired samples that satisfied guideline requirement (percentage difference within ±20%) is reported. This percentage needs to be ≥ 67% to define

the two measurements (EC_{pla} obtained from the DBS analysis and C_{pla} measured in plasma samples) equivalent.

Table 42. F_p, CF and $K_{BC/pla}$ employed for DBS-conversion.

Analyte	F_p	% EC_{pla}-C_{pla} equivalence	CF	% EC_{pla}-C_{pla} equivalence	$K_{BC/pla}$	% EC_{pla}-C_{pla} equivalence
SORA	0.76	70%	1.29	70%	0.32	76%
oxSORA	0.94	53%	1.58	49%	0.15	76%
REGO	0.77	50%	1.25	78%	0.01	29%
oxREGO	0.94	0%	1.53	78%	0.51	71%
des-oxREGO	0.85	0%	1.38	64%	0.13	57%

Taking into account the calculated F_p values, the two drugs seemed to have similar behavior: concentrations of the drugs and their metabolites are expected to be higher in plasma fraction than in whole blood (or DBS) showing F_p values (ranging from 0.76 for SORA to 0.94 for OXSORA and OXREGO) lower than 1 (drug equally partitioned into blood cells and plasma), which indicates that the drug is more concentrated in plasma. This result seemed to be confirmed by the $K_{BC/pla}$ values, especially for REGO that showed a $K_{BC/pla}$ (0.01) very close to 0 ($K_{BC/pla}$ is equal or near to 0 if the drug is isolated in plasma).

As related to SORA, OXSORA, REGO, and OXREGO percentages of equivalence between EC_{pla} and C_{pla} higher than the acceptance criteria (67%) were obtained ranging from 76 to 78%. The best predictive performance (76%) was obtained with the application of the conversion method based on $K_{BC/pla}$ (Equation 21, where $K_{BC/pla}$ = 0.32 and 0.15 for SORA and oxSORA, respectively) for SORA and its metabolite, while for REGO and osREGO the higher percentage of equivalence (78%) was obtained with the CF-based conversion method (Equation 20, where CF = 1.25 and 1.53 for REGO and oxREGO).

Only for des-oxREGO no conversion method allowed an acceptable predictive performance: the highest percentage of equivalence (64%) was obtained with the application of the CF-based method (as for REGO and OXREGO) but was lower than the acceptance criteria.

Results obtained from the conversion method showing the best performance to predict the C_{pla} are discussed more in detail in the following sections.

4.3.1. SORA and oxSORA

DBS samples concentrations were on average 0.8 and 0.6 fold lower than the corresponding plasma samples for SORA and oxSORA, respectively. These data are in line with the calculated $K_{BC/pla}$ (0.32 and 0.15 for SORA and oxSORA, respectively): when this coefficient is near or equal to 0 it means that the drug is isolated in plasma fraction. Thus, from the obtained $K_{BC/pla}$ we expected to have a higher concentration of both analytes in plasma than in DBS and this distribution was expected to be more prominent in the metabolite. The

comparison between DBS and plasma concentrations was characterized by a high variability among the paired samples, as shown by the standard deviations obtained (0.8 ± 0.2 and 0.6 ± 0.1 for SORA and oxSORA, respectively) and the data range (0.6-1.2 and 0.4-1.0 for SORA and oxSORA, respectively). Correlation graphs between C_{pla} and C_{DBS} (Figure 41) showed a moderate to very good linearity between the paired data with R^2= 0.9312 for SORA and R^2= 0.9838 for oxSORA.

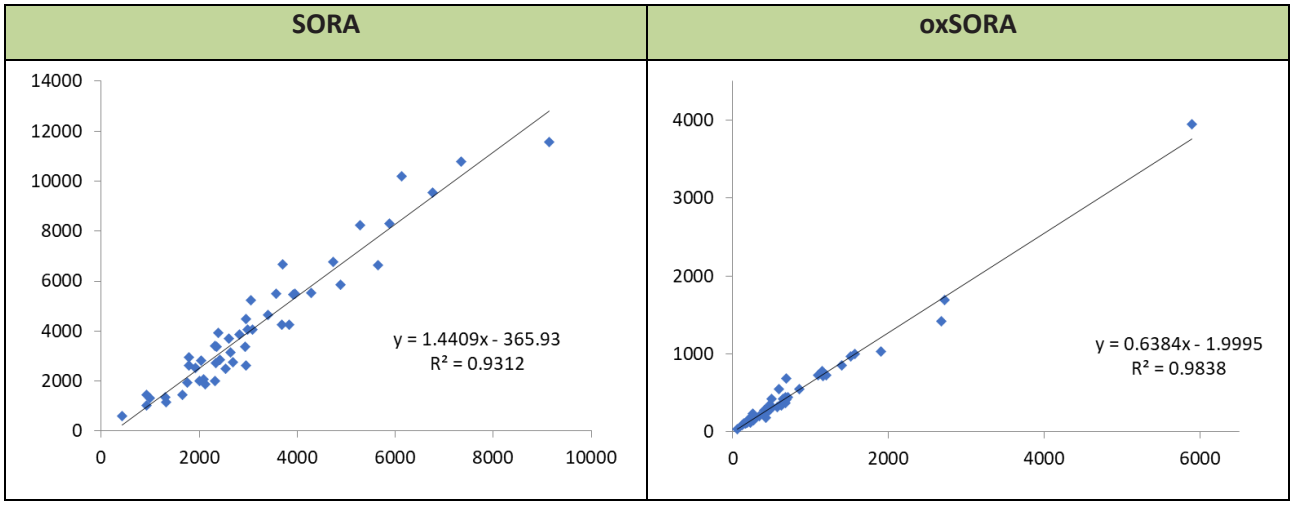

Figure 41. Correlation obtained for SORA and oxSORA by comparing the results on DBS from venous blood (x-axes) and plasma samples (y-axes).

The EC_{pla} values of SORA and oxSORA estimated by the $K_{BC/pla}$-based mathematical processing were equivalent to the real concentrations detected in plasma in 38 (SORA) and 37 (oxSORA) out of 49 cases (76% of the samples for both the analytes). Statistical agreement and bias were evaluated for each analyte by means of Passing-Bablok, Bland-Altman, and Lin's CCC analyses. Results and graphic data processing are reported in Table 43 and Figure 42.

Table 43. Comparison between actual and estimated plasma concentrations applying DBS-conversion based on $K_{BC}/_{pla}$.

Analyte	DBS conversion method	Passing-Bablok regression				Lin's CCC	Bland-Altman analysis	
		Slope	95% CI	Intercept	95% CI		ρs	p-value
SORA	$K_{BC/pla}$	0.92	0.83-1.00	585.5	211.7-823.4	0.96	-0.30	0.03
oxSORA	$K_{BC/pla}$	0.91	0.85-1.00	7.4	-15.5-33.7	0.99	-0.22	0.12

$K_{BC/pla}$: red blood cells-to-plasma partitioning coefficient, CI: confidence interval, Lin's CCC: Lin's concordance correlation coefficient, ρs: Spearman's correlation coefficient between the difference and the mean of the two measures

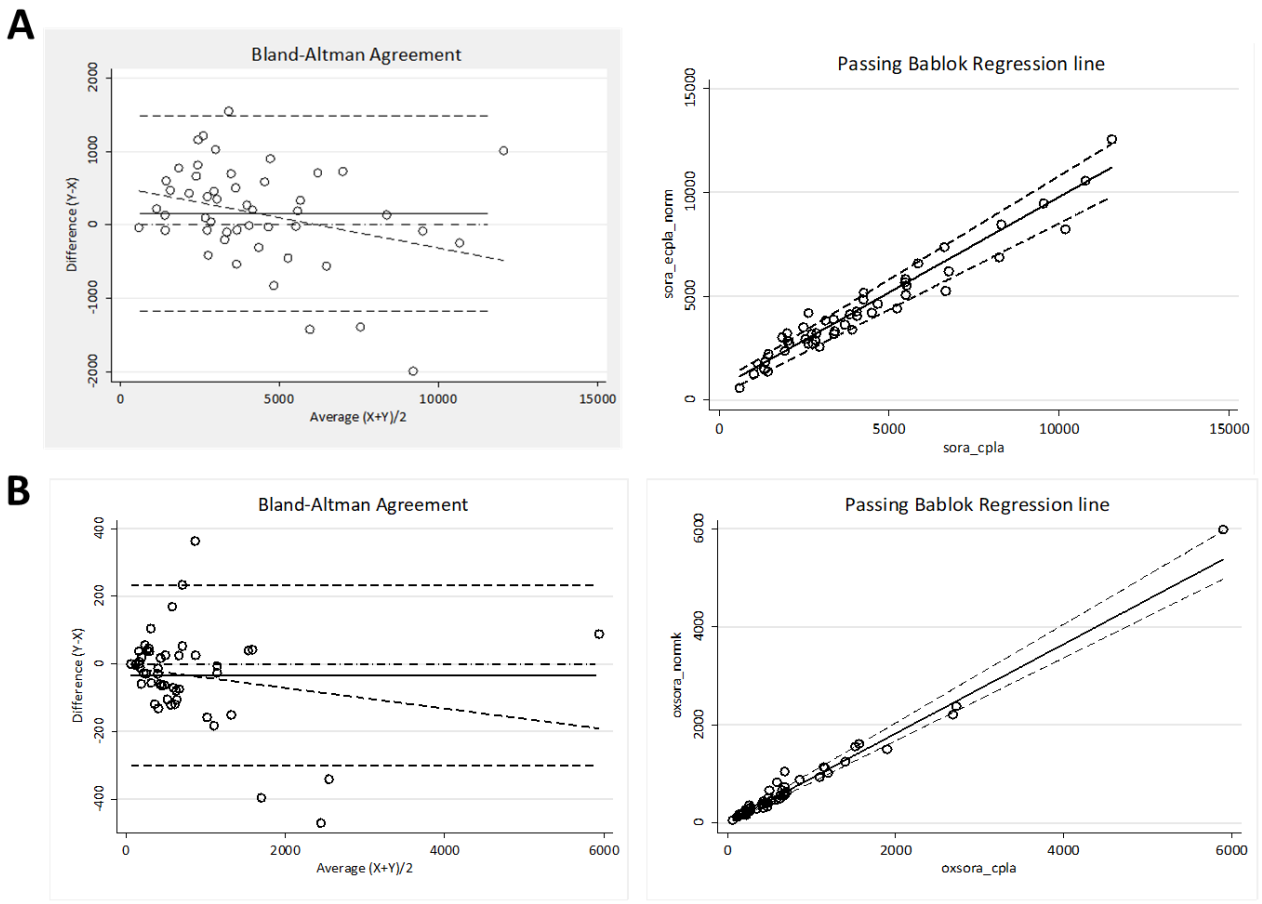

Figure 42. Correlation between SORA and oxSORA concentration in DBS samples after $K_{BC}/_{pla}$ normalization and those obtained from plasma samples. Bland-Altman plot is reported on the left, while Passing-Bablok regression is reported on the right for (A) SORA and (B) oxSORA.

Bland-Altman analyses showed the presence of a low proportional error for both the analytes meaning that lower values are overestimated while higher values are underestimated. This phenomenon is negligible since the correlations are weak (-.030 and -0.22 for SORA and oxSORA, respectively) and only for SORA statistically significant ($p \leq 0.05$). The mean differences (bias) were 160.8 (95% CI: -33.5 to 355.1) and -33.4 (95% CI: -72.6 to 5.8) for SORA and oxSORA, respectively. Since the bias should be as close as possible to 0, a better performance was obtained for oxSORA. This result was confirmed by Passing-Bablok analysis, being the slope 95% CI containing the 1 and the intercept 95% CI containing the 0 only in the case of oxSORA.

4.3.2. REGO and oxREGO

Regarding REGO and oxREGO, DBS samples concentrations were on average 0.8 and 0.7 fold lower than the corresponding plasma samples, respectively. Contrary to what was observed for SORA and its metabolite, the DBS-to-plasma concentration ratio found in REGO and oxREGO were not completely expected from the calculated $K_{BC/pla}$ (0.01 and 0.51 for REGO and oxREGO, respectively): these values suggested that nearly the total amount of REGO was in plasma while oxREGO plasma concentration was 2 fold higher than DBS

measurement. We hypothesized that the difference between the behavior of the analytes expected based on the calculated $K_{BC/pla}$ values compared to the effective concentrations found in DBS explained the better predictive performance of the CF-based conversion method than the $K_{BC/pla}$-based one for REGO and its metabolite.

The comparison between DBS and plasma concentrations was characterized by a high variability among the paired samples, as shown by the standard deviations obtained (0.8 ± 0.1 and 0.7 ± 0.1 for REGO and oxREGO, respectively) and the data range (0.6-1.0 and 0.5-0.8 for REGO and oxREGO, respectively). Correlation graphs between C_{pla} and C_{DBS} (Figure 43) showed good linearity between the paired data with R^2= 0.9445 for OXREGO, while a R^2= 0.8661 was obtained for REGO.

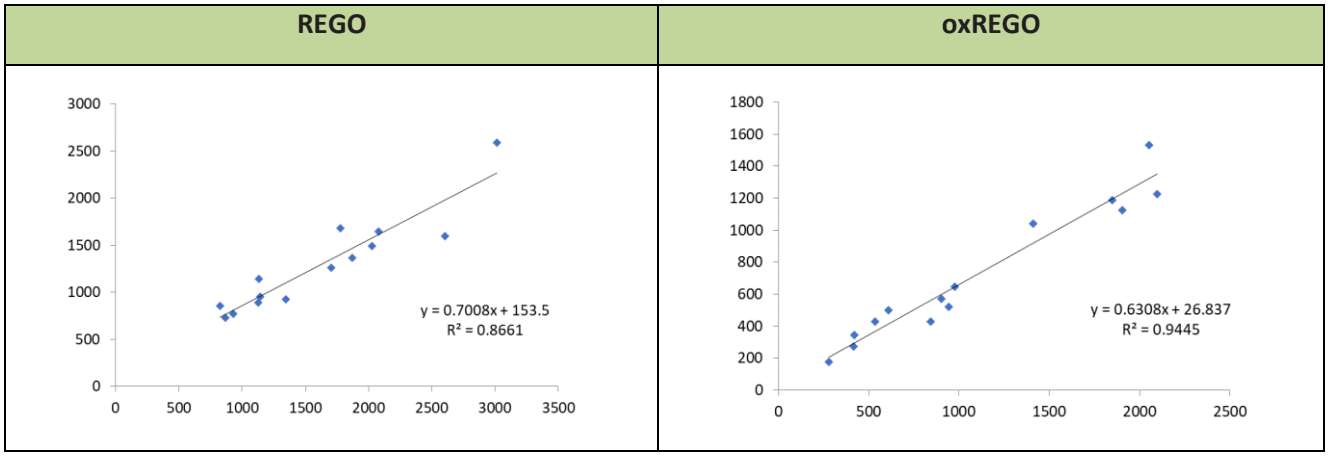

Figure 43. Correlation obtained for REGO and oxREGO by comparing the results on DBS from venous blood (x-axes) and plasma samples (y-axes).

As related to REGO and its metabolite, the EC_{pla} values estimated by the CF-based mathematical processing were equivalent to the real concentrations detected in plasma in 11 (78% of the samples) out of 14 cases for both REGO and oxREGO. Statistical agreement and bias were evaluated for each analyte by means of Passing-Bablok, Bland-Altman, and Lin's CCC analyses. Results and graphic data processing are reported in Table 44 and Figure 44.

Table 44. Comparison between actual and estimated plasma concentrations applying DBS-conversion based on CF.

Analyte	DBS conversion method	Passing-Bablok regression				Lin's CCC	Bland-Altman analysis	
		Slope	95% CI	Intercept	95% CI		ρs	p-value
REGO	CF	0.87	0.67-1.00	115.3	-73.39-450.7	0.94	-0.53	0.05
OXREGO	CF	0.93	0.80-1.13	67.7	-48.2-197.2	0.97	-0.19	0.52

CF: correction factor, CI: confidence interval, Lin's CCC: Lin's concordance correlation coefficient, ρs: Spearman's correlation coefficient between the difference and the mean of the two measures

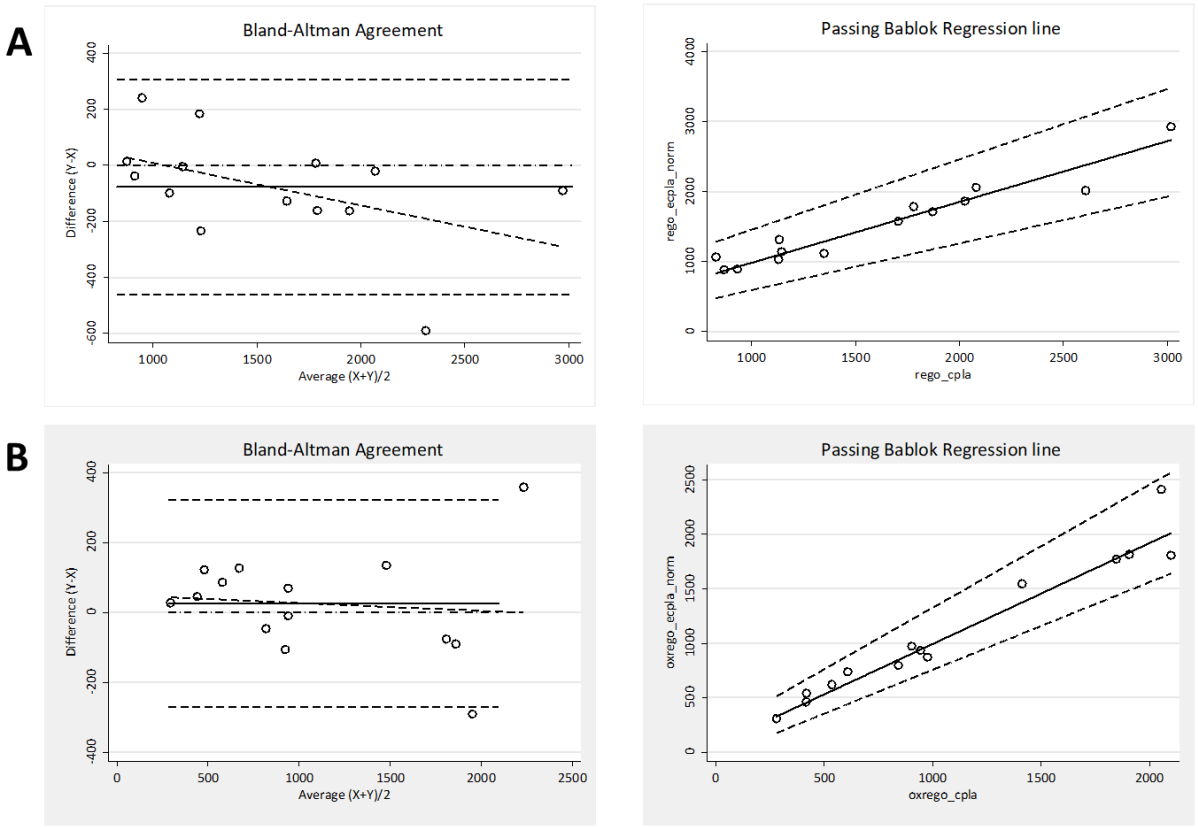

Figure 44.Correlation between REGO and oxREGO concentration in DBS samples after CF normalization and those obtained from plasma samples. Bland-Altman plot is reported on the left, while Passing-Bablok regression is reported on the right for (A) REGO and (B) oxREGO.

Also in this case, Bland-Altman analyses showed the presence of a low proportional error for both the analytes meaning that lower values are overestimated while higher values are underestimated. This phenomenon is negligible since the correlations are weak (-0.53 and -0.18 for REGO and oxREGO, respectively) and only for REGO statistically significant ($p \leq 0.05$). The biases were -77.8 (95% CI: -190.9 to 35.6) and 24.9 (95% CI: -62.3 to 112.0) for REGO and oxREGO, respectively. Contrary to what was observed for SORA and its metabolite, the performances of REGO and oxREGO were similar, being the biases close to 0 for both the analytes. This result was confirmed by Passing-Bablok analysis, being the slope 95% CI containing the 1 and the intercept 95% CI containing the 0 for both the analytes. The 95% CIs were quite broad due to the paucity of samples containing REGO and its metabolite (14 *vs* 49 samples containing SORA). For this reason, the correlation between EC_{pla} and C_{pla} of REGO and its metabolites should be re-evaluated with a higher number of samples and the presented data should be considered as preliminary results.

4.4. LC-MS/MS method for the quantification of lenvatinib in human plasma

To apply TDM in the clinical routine, the development of sensitive and robust quantification method is essential. To the best of our knowledge, the already published LC-MS/MS methods for LENVA quantification in human plasma are reported in Table 45.

Dubbelman et al. [73] quantified LENVA and four metabolites in three different matrices (human plasma, urine, and feces) and LENVA alone in whole blood. The validated analytical range in plasma was 0.25-50 ng/mL, which was lower than the target C_{min} (51.5 ng/mL) and thus not suitable for our purpose. Moreover, this method is time-consuming (twenty-one min of runtime and a sample preparation based on PP followed by supernatant evaporation and re-dissolution steps) and requires a large sample volume (250 µL).

Ogawa-Morita and colleagues partially modified Dubbelman's method extending the linear range (9.6-200 ng/mL) [238] and reducing analysis run time (15 min) but sample preparation remained time-consuming.

Srikanth et al.'s method [239] was relatively fast (8 min), but required a large sample volume (200 µL), a complex sample preparation (LLE) and the validated analytical range (10.20-501.6 pg/mL) was below the target LENVA C_{min}.

Recently, Sueshige and colleagues [240] developed a LC-MS/MS quantification method for LENVA with a reduced sample volume (100 µL), short runtime (4 min), and adequate range for TDM application (0.2-1000 ng/mL). Nonetheless, the sample preparation was based on SPE that could make this method complex and laborious.

In the literature three other methods were reported for LENVA quantification with other 8, 9 or 2 kinase inhibitors, respectively [241–243]. These methods overcome the above-mentioned limitations: they required a small sample volume (50/100 µL), had a fast chromatographic run (between 3.5 and 7min) and a simple sample preparation (PP). Concentration ranges were suitable for the target C_{min} of 51.5 ng/mL except for the method developed by Ye et al. [243] (1.25-40 ng/mL).

However, the quantification of other kinase inhibitors was not necessary for our purpose and we considered of interest the possibility to have a wider concentration range in order to obtain a method useful not only for LENVA C_{min} monitoring in patients with HCC but also for PK investigations in patients affected by other pathologies and treated with LENVA at higher doses (*e.g.,* LENVA is administered at the dose of 24 mg/day in patients with DTC). For these reasons, we developed and validated according to EMA and FDA guidelines, a LC-MS/MS method for the quantification of LENVA in a wide concentration range to be used for cancer patients' plasma samples. It required a relatively low sample volume, an easy and quick sample processing based on PP, and a reasonable runtime.

4.4.1. Mass spectrometric conditions optimization

4.4.1.1. Compound dependent parameters optimization

The optimization of the compound dependent parameters for LENVA and its IS was performed in positive ion mode, thus LENVA and IS mainly produced protonated molecules $[M+H]^+$ for the presence of amino groups.

Table 45. LC-MS/MS methods for the quantification of LENVA in human plasma reported in the literature.

Ref.	Analyte(s)	Sample Volume (µL)	Extraction Method	Runtime (min)	Linearity Range
[73]	LENVA and 4 metabolites (M1: Decyclopropylation; M2: demethylation; M3: N-oxidation; M5 O-dearylation), ER-227326 (IS)	250	PP with supernatant evaporation and re-dissolution	21	0.25-50 ng/mL
[239]	LENVA and LENVA-D_4 (IS)	200	LLE	8	10.20-501.6 pg/mL
[238]	LENVA, propanolol (IS)	250	PP with supernatant evaporation and re-dissolution	15	9.6-200 ng/mL
[241]	alectinib, cobimetinib, LENVA, nintedanib, osimertinib, palbociclib, ribociclib, vismodegib, vorinostat, alectinib-D_8(IS), LENVA-D_5 (IS), nintedani-$^{13}C,D_3$(IS), osimertinib-$^{13}C,D_3$ (IS), palbociclib-D_8 (IS), ribociclib-D_6 (IS), vismodegib-$^{13}C_7$ (IS), vorinostat-$^{13}C_6$ (IS), cobimetinib-$^{13}C_6$ (IS)	50	PP	4	10–200 ng/mL
[240]	LENVA and LENVA-D_4 (IS)	100	SPE	6	0.2-1000 ng/mL
[242]	axitinib, LENVA, afatinib, bosutinib, cabozantinib, dabrafenib, osimertinib, ruxolitinib, nilotinib, trametinib, afatinib-D_6 (IS), bosutinib-D_9(IS), dabrafenib-D_9(IS), LENVA-D_5 (IS), osimertinib-$^{13}C,D_3$ (IS), trametinib-$^{13}C,D_6$ (IS), axitnib-$^{13}C,D_3$ (IS), cabozantinib-D_4 (IS), nilotinib-D_6 (IS) and ruxolitinib-D_4 (IS)	50	PP	7	2-500 ng/mL
[243]	SORA, LENVA, apatinib, SORA-D_3 (IS), LENVA-D_4 (IS), apatinib-D_8 (IS)	100	PP with dilution in MP A	3.5	1.25-40 ng/mL

IS: internal standard; LLE: liquid-liquid extraction; MP A: mobile phase A; PP: protein precipitation; SPE: solid-phase extraction.

The monoisotopic masses of LENVA and LENVA-D_4 are 426.6 and 430.6 Da, respectively. The presence of the analyte of interest was confirmed in Q1 full scan from 300 to 600 Da by the detection of the corresponding protonated molecule $[M+H]^+$ at 427.1 and 431.7 m/z, respectively (Figure 45)

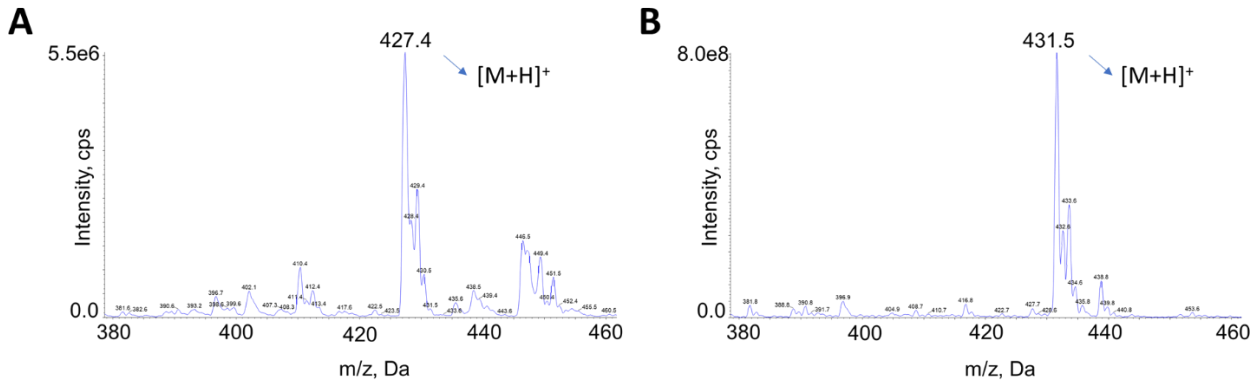

Figure 45. Spectra obtained in positive ion mode with a Q1 scan, which confirm the presence of (A) LENVA and (B) LENVA-D4.

As reported in section 3.5.1.1., DP and EP optimization of LENVA and LENVA-D_4 precursor ion was performed in Q1MI scan: by ramping DP value from 0 to 400 V and EP from 2 to 15 V, the highest LENVA XIC intensity was reached with DP set at 140 V and EP set at 10 V; the optimized DP and EP value for LENVA-D_4 were 120 V and 10 V, respectively. The results for DP value optimization were reported in Figure 46.

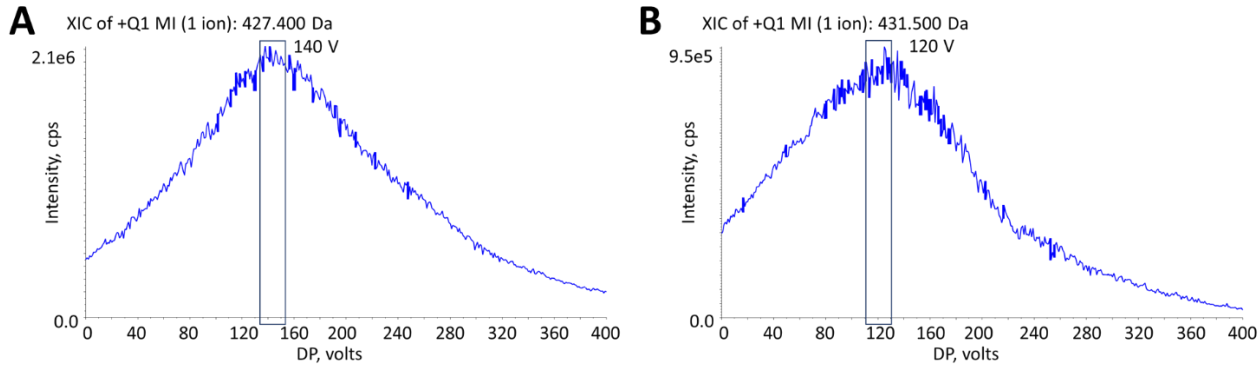

Figure 46. Spectra obtained ramping DP value in positive ion mode with Q1MI scan mode of (A) LENVA, and (B) LENVA-D4. The apex of the each XIC trend was chosen as the optimal DP value

In MS2 mode, the fragmentation pattern of each analyte precursor ion was evaluated by ramping the CE values from 5 V to 130 V in the collision cells (second quadrupole). For each protonated molecule, two product ions were found and identified as reported in Figure 47.

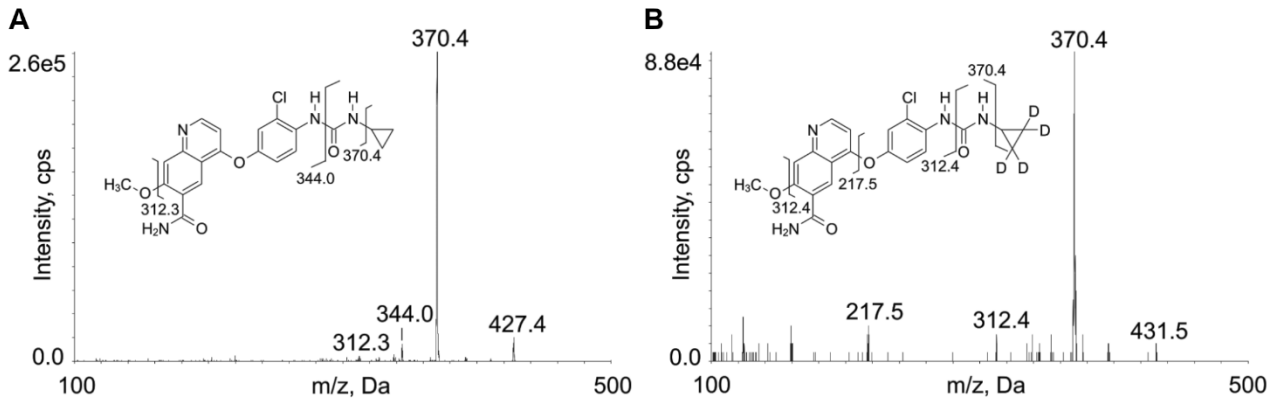

Figure 47. MS/MS mass spectra with chemical structures and identification of the fragment ions of (A) LENVA and (B) LENVA-D_4 (IS); spectra were recorded with CE = 40 V. LENVA fragment at 312.3 m/z derived from 344.0 m/z fragment by the loss of methoxy group.

The signal intensity of each of the three transitions for each compound was monitored through MRM scan mode by ramping CE value from 5 to 130 V, in order to establish its optimal value to generate each fragment. For each analyte, the quantifier fragmentation was selected as the maximum signal intensity (for example, see Figure 61): 427.4 > 370.4 *m/z* for LENVA (CE = 37 V) and 431.5 > 370.4 *m/z* for LENVA-D_4 (CE = 40 V). The other two fragmentations, characterized by a lower XIC, were chosen as qualifiers for analytes identity confirmation: 427.4 > 312.2 *m/z* (CE = 60 V) and 427.4 > 344.0 *m/z* (CE = 40 V) for LENVA, 431.5 > 312.4 *m/z* (CE = 60 V) and 431.5 > 217.5 *m/z* (CE = 30 V) for LENVA-D_4.

In a similar way, the optimal CXP value of 10 V was established for all the fragments for each compound. Furthermore, with the precursor ion scan mode it was possible to confirm the direct derivation of the three selected product ions from the precursor ion for each analyte.

In Table 46 the optimized the compound dependent parameters are summarized.

Table 46. Optimized compound dependent parameters of LENVA and LENVA-D_4.

Compound	Precursor ion			Product ion		
	Q1[a] (*m/z*)	DP[b] (V)	EP[c] (V)	Q3[d] (*m/z*)	CE[e] (V)	CXP[f] (V)
LENVA	427.4	140	10	370.4	37	10
				312.2	60	10
				344.0	40	10
LENVA-D_4	431.5	120	10	370.4	40	10
				312.4	60	10
				217.5	30	10

[a]first quadrupole mass; [b]declustering potential; [c]entrance potential; [d]third quadrupole mass; [e]collision energy; [f]cell exit potential.

4.4.1.2. Source dependent parameters optimization

As reported in section 3.5.1.2., each source dependent parameter was manually varied after 3 consecutive samples with a stable XIC trend (for example, see Figure 62). For each sample was injected 2 µL of methanolic solution containing LENVA at the concentration of 100 ng/mL. In particular, the principal variations applied to each source dependent parameter are summarized below:

- TEM: the optimal value was 550 °C. The tested values were 300 °C, 400 °C, 500 °C and 550 °C;
- ISV: the optimal value was 5500 V. The investigated values were 3000, 4000, 5000 and 5500 V;
- CUR: the optimal value was 35 psi. The tested values were 10 psi, 15 psi, 20 psi, 30 psi, 35 psi, 40 psi, 45 psi and 50 psi;
- CAD: the optimal value was 6 (a medium value), while with Low and High values were observed a decreasing of the XIC intensity;
- GS1 and GS2: the optimal values were 50 and 40 psi, respectively. The GS1-GS2 tested values were 45-45 psi, 50-40 psi, 30-50 psi, 30-60 psi and 50-40 psi.

All the optimized source dependent parameters were summarized in Table 47.

Table 47. Optimized source dependent parameters for LENVA and LENVA-D_4.

Polarity	Positive ion mode
CUR	35 psi
CAD	6
ISV	5000 V
TEM	550 °C
GS1	50 psi
GS2	40 psi

4.4.2. Chromatographic conditions optimization

In this case, no separation degree between analytes was required and a very short column was immediately chosen in order to obtain a method with a short total runtime.

Furthermore, according to the physicochemical properties of LENVA, a C18 SP was identified to be the most suitable one to ensure its retention. A good compromise between these two characteristics (short runtime and adequate analyte retention) was represented by Phenomenex Synergi™ Fusion-RP (4 µm, 30 x 2.0 mm, 80 Å), a very versatile column characterized by a polar embedded C18 SP that offers balanced polar and hydrophobic selectivity. The column was also equipped with a Fusion-RP SecurityGuard™ pre-column (4.0 x 2.0 mm), in order to block coarser particles coming from the MPs and the analyzed biological samples.

Different MPs were tested (*e.g.,* ACN with 0.10% HCOOH (v/v) or MeOH plus 0.10% of HCOOH (v/v) both tested alone or mixed with iPrOH) and the best results in terms of peak shape and sensitivity were obtained

with MeOH:iPrOH (90:10, v/v) with 0.10% of HCOOH (v/v) as MP B and MilliQ H_2O plus 0.10% HCOOH (v/v) as MP A. To reduce the back-pressure caused by MPs, the column oven was set at 50 °C. In fact, high temperatures allows to lower organic solvent viscosity and to increase analytes interchange between SP and MP.

Since isocratic elution method does not provide a proper washing of the analytical column, a multi-step method was selected to guarantee its cleanness from contaminants carried by biological samples.

The elution phase was the first step to be optimized. At the beginning, a wide elution gradient from 5 to 98% of MP B over 2 min, preceded by a conditioning step of 0.5 min at 5% of MP B, with a total flow rate of 0.4 mL/min was tested to assess the behavior of LENVA. No attempt was made to extend conditioning phase, since the selected duration was sufficient for short column and a longer one would have delayed analytes retention time and lengthened the total runtime. Since LENVA elution happened close to the washing phase beginning, the same method was tested with 0.5 mL/min and 0.6 mL/min flow rates, in order to anticipate LENVA elution and to shorten the total runtime, as reported in Figure 48.

LENVA and its IS co-eluted during the gradient phase increasing the flow rate. Total flow rate of 0.6 mL/min was selected it allowed to obtain a faster analytes elution and a higher method sensitivity (1.03 x 10^5 cps) compared to the lower one (0.4 mL/min). Afterward, since the ideal percentage of MP B for the elution of LENVA was assessed to be at 90%, several methods were explored by changing the starting MP B percentage from 5 to 15, 20, and 30% to further anticipate analytes elution, employing the same gradient slope (*circa* 60% of MP B/min) and conditioning phase duration. The gradient from 5 to 98% provided the best peaks resolution and thus 5% of MP B was chosen as the most promising starting condition.

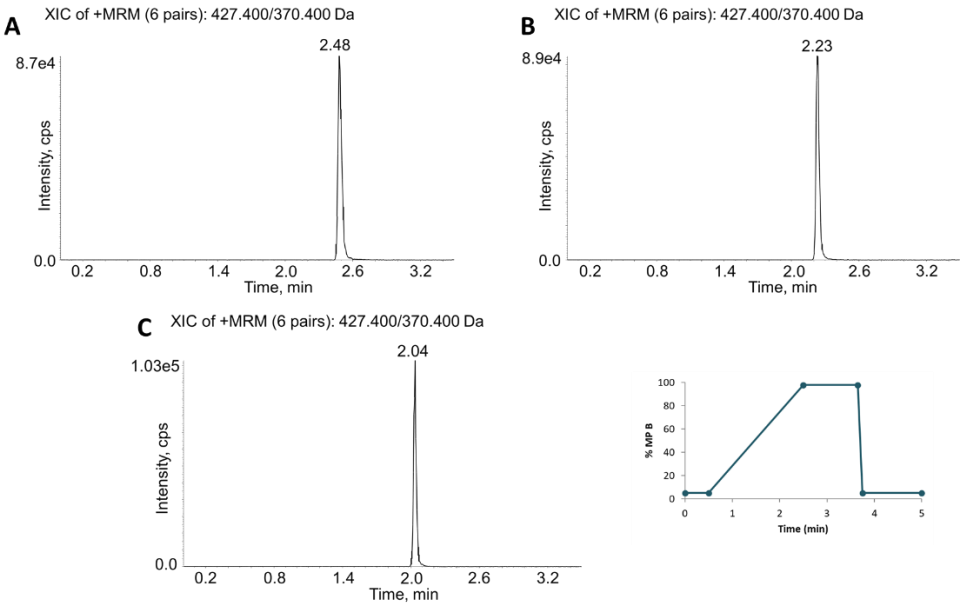

Figure 48. Comparison between LENVA (100 ng/mL in MeOH) chromatogram obtained with (A) 0.4 mL/min, (B) 0.5 mL/min and (C) 0.6 mL/min total flow rate, respectively. The chromatographic method used is reported in the box on the right.

Nevertheless, LENVA retention time was still too delayed compared to the desired short total runtime of the chromatographic method. Therefore, to decrease the retention time, the initial conditioning phase was omitted directly applying the gradient from 5 to 98% of MP B over 2 min. LENVA and LENVA-D_4 eluted 0.5 min earlier and peak shape was symmetrical and narrow, as reported in Figure 49.

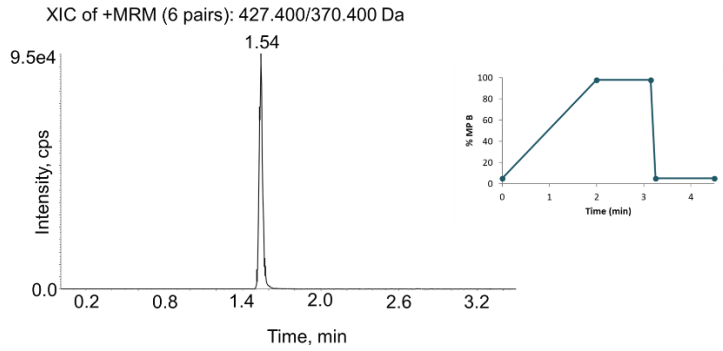

Figure 49. Chromatogram of LENVA (100 ng/mL in MeOH) with the gradient 5-98% of MP B over 2 min without the initial conditioning phase. The chromatographic method used is reported in the box on the right.

Once excluded the initial conditioning phase, the gradient from 5 to 98% of MP B over 1.5 min was compared to 5-98% of MP B over 2 min: with the stepper gradient, LENVA and its IS eluted about 0.14 min earlier, with no differences in term of peak shape. Therefore, a gradient from 5 to 98% of MP B in 1.5 min was selected since it anticipated analytes elution, maintaining at the same time a good peak shape. After analytes elution, 98% of MP B was maintained to perform the column washing for 1.15 min, in order to eliminate lipophilic interferents of the plasmatic matrix, as well as possible analytes residues retained in the column.

Afterward, the MP B initial percentage (5%) was restored in 0.1 min and kept constant for 1.25 min: since the column internal volume was nearly 58 µL, this phase duration at a flow rate of 0.6 mL/min guaranteed the passage of at least 10 column volumes and thus a proper column reconditioning, with no shift in analytes retention time after consecutive runs.

The fully optimized multi-step chromatographic method was composed by the following phases:

- from 5% to 98% of MP B over 1.5 min (elution phase);
- kept constant at 98% of MP B for 1.15 min (washing phase);
- the initial condition was then restored over 0.10 min, and the column was re-equilibrated for 1.25 min (reconditioning phase).

The final LC-MS/MS method was reliable, reproducible, and very fast with a total runtime of 4 min (analyte retention time 1.40 min). The peaks were symmetrical and narrow, described by 18 points (>15) on average applying a dwell time of 85 msec for quantifier transitions and 10 msec for qualifier ones.

Figure 50 displays typical MRM chromatograms of plasma samples: an extracted blank plasma sample (Figure 50 A), a zero blank sample containing IS only (Figure 50 B), an extracted plasma sample at the LLOQ (

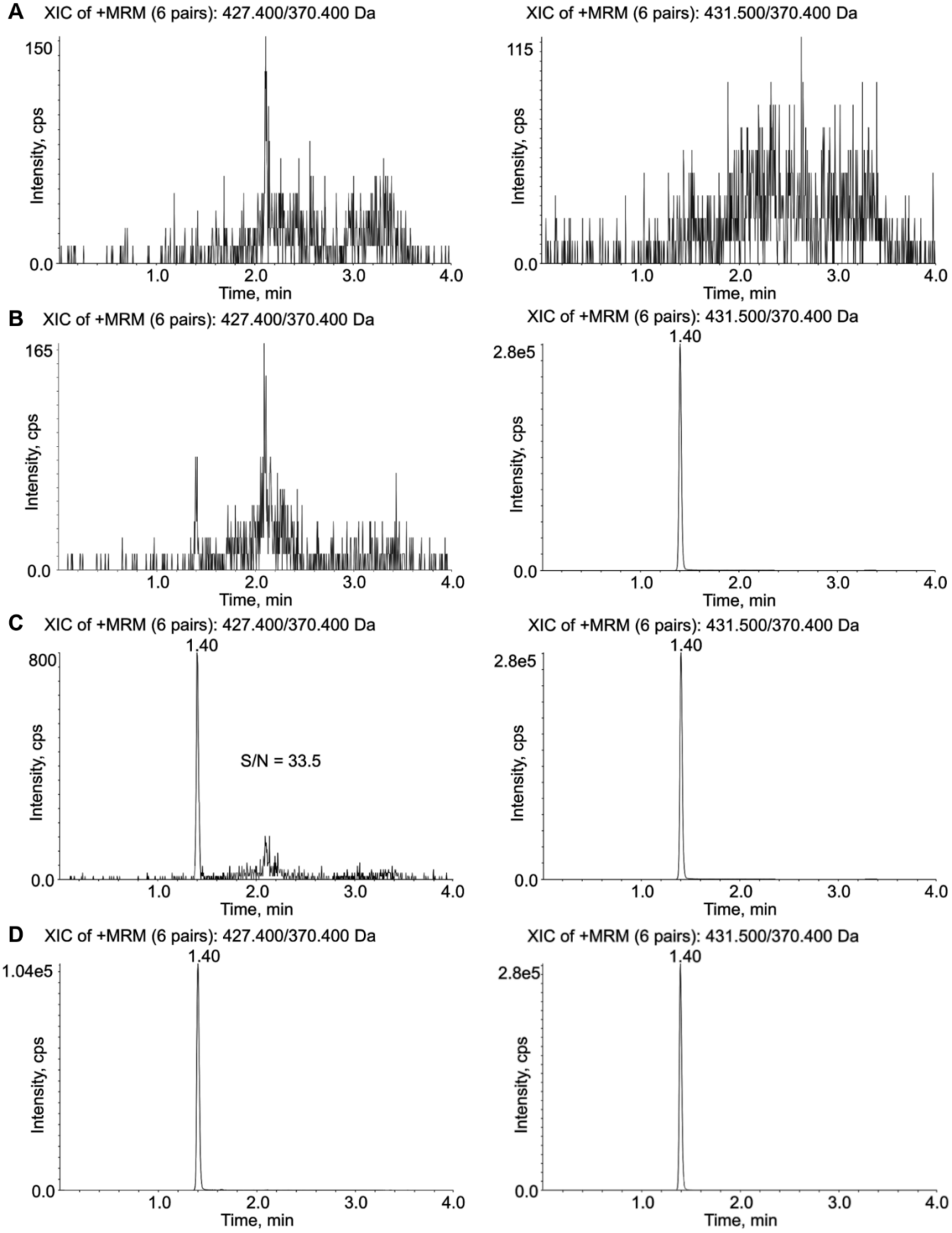

Figure 50. MRM chromatograms for LENVA (left panels) and internal standard (right panels). (A) blank plasma sample; (B) blank plasma sample with IS (50 ng/mL); (C) LLOQ (0.50 ng/mL) with S/N value; (D) plasma sample from a patient treated with 12 mg/day LENVA and showing a drug concentration of 99.6 ng/mL.

Figure 50 C), and a sample from a patient collected 4.5 h after drug intake (dose 12 mg/die) with a measured LENVA concentration of 99.6 ng/mL (Figure 50 D).

Last of all, the carryover phenomenon was assessed and in order to avoid it in the future, the following measures were employed:

- efficient injection-needle washing solution (25% MilliQ H_2O, 25% MeOH, 25% ACN, 25% iPrOH (v/v/v/v) plus 0.10% of HCOOH (v/v));
- strong column washing at 98% of MP B for 1.15 min;
- injection of one MeOH:iPrOH (50:50, v/v) washing run and two blank samples after the ULOQ, QCH and unknow concentration samples.

In Figure 50 A the MRM chromatogram of the second blank sample after one MeOH:iPrOH (50:50, v/v) washing run was reported and shows the absence of residual carryover phenomenon.

4.4.3. Sample preparation for quantitative analysis

4.4.3.1. Plasma sample extraction optimization

PP was chosen to perform the drug extraction from the biological matrix and to eliminate from it any interferents that might alter analyte detection and quantification. This extraction method was appropriate for LENVA detection, since 97.9- 98.6% of circulating drug is bound to human plasma proteins [65,66].

PP was performed by using acidified MeOH (with 0.1% HCOOH, v/v) and acidified ACN (with 0.1% HCOOH, v/v) to extract plasma samples at low concentration (QCL - 1.5 ng/mL) and at high concentration (B -1000 ng/mL), each of them prepared in duplicate. The obtained peak areas were reported in Table 48.

Table 48. Obtained peak areas using acidify MeOH or ACN to perform the protein precipitation.

Sample	Peak area (cps)	
	MeOH with 0.10% HCOOH (v/v)	**ACN with 0.10% HCOOH (v/v)**
QCL (1.50 ng/mL)	3200 - 3210	3150 - 3320
B (1000 ng/mL)	1270000 - 1350000	1260000 - 1250000

Since no significant differences in term of analyte extraction yield had emerged, MeOH was chosen to perform the PP, because it is cheaper and less toxic than ACN. The ratio between the plasma sample volume and IS WS was 1:6 (v/v), *i.e.*, 500 µL IS WS were added to 100 µL of plasma sample: with these proportions, it was possible to concurrently obtain an excellent S/N for LENVA at LLOQ concentration (Figure 50 C) and to avoid the detector saturation (detector limit nearly 3 x 10^6 cps) during the analysis of its ULOQ sample. The 1:20 sample:solvent *ratio* was also tested to perform PP, but LLOQ S/N ratio was to closed to the limit for quantification (S/N nearly 5).

Autosampler temperature was set at 4 °C to minimize MeOH evaporation and to extend the analytes stability.

4.4.3.2. Calibration curve and quality controls preparation

Stock solutions of LENVA and LENVA-D_4 were prepared in DMSO at the concentration of 1 mg/mL and stored at -80 °C. Two different stock solutions were obtained for LENVA: one for the preparation of the calibration curve and the other for QCs. To obtain the WSs for the calibration curve (from A to H), the stock solution of LENVA was diluted with MeOH to achieve the final concentrations of 40.0, 20.0, 10.0, 2.00, 0.80, 0.30, 0.06 and 0.01 µg/mL. The same procedure was applied also to obtain the WSs for the QCs with a final concentration of 30.0, 1.50 and 0.03 µg/mL. Each analyte stock solution, as well as the calibrators and QCs WSs, were kept in polypropylene tubes and stored at -80 °C, while a 500 µL-aliquot of each WS was kept in a polypropylene tube and stored at -20 °C to freshly prepare calibration curve and QC samples during the validation process and quantification of patients' plasma samples. IS stock solution was also diluted in acidified MeOH with 0.10% HCOOH (v/v) to obtain the final concentration of 50.0 ng/mL. This solution was directly used to perform PP during sample processing and stored at -20 °C.

Table 49. Final LENVA concentrations of calibrators and QCs in plasma samples.

Sample	LENVA conc. (ng/mL)
H	0.50
G	3.00
F	15.0
E	40.0
D	100
C	500
B	1000
A	2000
QCL	1.50
QCM	75.0
QCH	1500

Every day, an eight-point calibration curve (A to H) and triplicates of each QC concentration were freshly prepared in plasma. A blank sample (plasma processed without IS) and a zero-blank sample (plasma processed including IS), LLOQ plasma sample were analyzed to verify the proper analytical conditions to allow the beginning of the analytical session. The preparation of calibrators and QCs samples was conducted as follows: 95 µL of pooled blank human plasma were added with 5 µL of proper WSs (dilution 1:20) and vortex-mixed for 10 sec. One hundred µL-aliquots of QCs were prepared and stored at -80°C to allow the assessment of analyte's long-term stability and to be used as controls in future analyses. A hundred µL of each calibrator and QC (95 µL plasma + 5 µL WS) were added with 500 µL of cold IS working solution to precipitate plasma proteins, vortex-mixed for 10 sec and centrifuged for 25 min at 16200 g at 4 °C. Finally, the clean supernatant

was transferred into auto-sampler glass vials and 4 µL were injected in the LC-MS/MS apparatus for the analysis.

Consequently, plasma samples presented the following concentrations for the calibration curve and QCs reported in Table 49.

4.4.4. LC-MS/MS method validation study

A full validation of the proposed method was conducted according to EMA and FDA guidelines, performing the evaluations described below.

4.4.4.1. Recovery

Recovery was assessed in five replicates for each QC concentration level (QCL, QCM, QCH), prepared as reported in section 3.6.1.2. and it was calculated with the Equation 9.

The percentage of LENVA recovery resulted high, ≥ 95.6% (range from 95.6 to 102, CV ≤ 4.6%), and reproducible over the concentrations ranges tested (Table 50). These percentages are the highest (89.5%) among the published methods (Table 45) that used the same sample treatment (PP) [73,238,242,243].

Table 50. Recovery of LENVA from human plasma (conc.: concentration; N: number of replicates; SD: standard deviation).

Analyte	Nominal conc. (ng/mL)	Recovery (%) ± SD	CV (%)
LENVA (N = 5)	1.50	95.6 ± 4.3	4.5
	75.0	97.8 ± 4.5	4.6
	1500	102 ± 1.6	1.6

4.4.4.2. Matrix effect

Both the qualitative test of post-column infusion and the quantitative analysis obtained from the ratio between the analytes peak area in the presence of matrix (single donor plasma) and the peak area in the absence of matrix (MeOH) using QCL and QCH concentrations, demonstrated the presence of a matrix effect. Firstly, the post-column infusion evaluation showed moderate XIC enhancement at the retention time of the analyte, as reported in Figure 51.

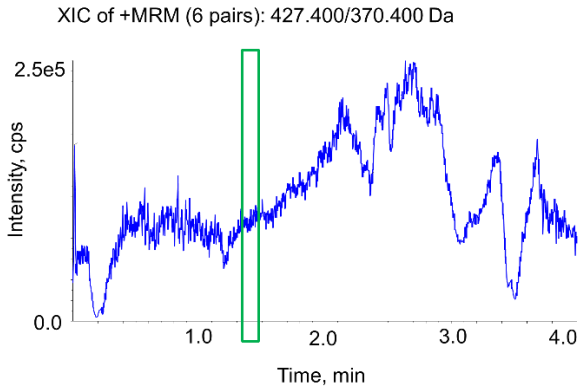

Figure 51. Evaluation of the matrix effect through a post-column infusion. The XIC trend of LENVA shows both ion enhancement and ion suppression areas. These phenomena poorly affected LENVA, whose retention time was highlighted with the green rectangle.

The same XIC enhancement was detected at the retention time of the analyte, comparing the signal in presence of matrix compared to that obtained in pure solvent, as reported inTable 51. A variability on the estimated MF values for LENVA was observed according to the concentration level (157% for QCL and 136% for QCH), whereas, within the concentration levels, results were highly reproducible with a CV always < 2.5%. The MF for LENVA-D_4 resulted 125% with a CV < 5.6%. The IS norm MF was 1.27 with a CV ≤ 2.8% for QCL and 1.09 for QCH with a CV ≤ 2.1%. These data are slightly higher than those reported in the previously published methods (considering only those methods employing PP as sample extraction) but with a much lower CV% values [241–243]. The obtained CV% values were lower within the guidelines requirements (<15%) and so the matrix effect was considered negligible in affecting analyses results.

Table 51. Estimated matrix factor (MF) and IS normalized MF (IS norm MF) of each analyte and ISs in deproteinized human plasma. (conc.: concentration; N: number of replicates; SD: standard deviation).

Analyte	Nominal conc. (ng/mL)	MF (%) ± SD	CV (%)	IS norm MF (%) ± SD	CV (%)
LENVA (N = 6)	1.50	157 ± 3.9	2.5	1.27 ± 0.03	2.8
	1500	136 ± 3.1	2.3	1.09 ± 0.02	2.1
LENVA-D_4 (N = 6)	50	125 ± 7.0	5.6	-	-

Furthermore, the negligible effect of this phenomenon was also proved through the analysis of 6 LLOQ samples from different donors (3 males and 3 females), being the obtained accuracy and precision (as CV%), respectively: 99.8% and 4.8%.

4.4.4.3. Linearity

The linearity of the method was demonstrated over the chosen concentrations (0.50-2000 ng/mL) preparing calibration curves on 8 different working days (Figure 52). The calibration curves were generated plotting the peak area ratios between the analyte and the IS (y) against their nominal concentration (x) and a weighted ($1/x^2$) linear regression model was applied. The Pearson's correlation coefficient (r) was 0.9988±0.0010 (CV ≤ 0.10%).

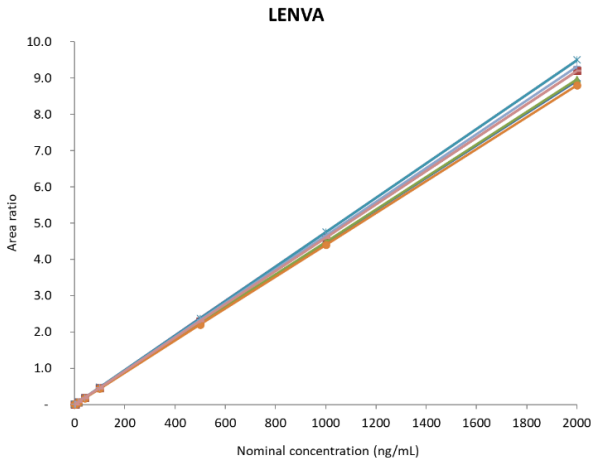

Figure 52. Calibration curves (N = 8) obtained for LENVA in human plasma. For each calibrator the area ratio between the analyte and the IS peaks are plotted against the nominal concentration value.

Moreover, the calculated accuracy was between 95.9 and 105%, and precision (CV) was ≤ 5.0%. In Table 52 the complete list of accuracy and precision data is reported.

Table 52. Accuracy (%) and precision (CV%) data of LENVA calibration curves in human plasma (conc.: concentration; N: number of replicates; SD: standard deviation).

LENVA (N = 8)			
Nominal conc.(ng/mL)	**Mean ± SD (ng/mL)**	**CV%**	**Accuracy%**
0.50	0.50 ± 0.0	0.9	99.5
3.00	3.08 ± 0.2	5.0	103
15.0	15.7 ± 0.8	4.8	105
40.0	41.5 ± 0.8	2.0	104
100	102 ± 2.4	2.4	102
500	489 ± 15	3.1	97.9
1000	959 ± 36	3.7	95.9
2000	1918 ± 89	4.7	95.9

4.4.4.4. Intra-day and inter-day precision and accuracy

The intra-day precision and accuracy for LENVA, in 6 samples at each QC level and at the LLOQ, resulted to be ≤ 10% and between 96.3 and 109%, respectively. At the same time, inter-day precision and accuracy, tested on 5 different working days in triplicate at each QC level and at the LLOQ, were ≤ 11% and between 98.0 and 108%, respectively.

The obtained data of intra- and inter-day precision and accuracy, reported in Table 53, complied with EMA and FDA requirements.

Table 53. Intra- and inter-day precision (CV%) and accuracy (%) for LENVA in human plasma (conc.: concentration; N: number of replicates; SD: standard deviation).

Intra-day (N = 6)			
Nominal conc. (ng/mL)	**Mean ± SD (ng/mL)**	**CV%**	**Accuracy%**
0.50	0.49 ± 0.1	10	98.4
1.50	1.59 ± 0.0	1.7	106
75.0	81.7 ± 2.2	2.7	109
1500	1445 ± 35	2.4	96.3
Inter-day (N = 15)			
Nominal conc. (ng/mL)	**Mean ± SD (ng/mL)**	**CV%**	**Accuracy%**
0.50	0.50 ± 0.1	11	101
1.50	1.60 ± 0.1	4.9	107
75.0	80.6 ± 3.7	4.5	108
1500	1469 ± 98	6.7	98.0

4.4.4.5. Limit of quantification and selectivity

Concerning the method sensitivity, mean accuracy and precision (CV%) obtained for the 6 LLOQ samples (0.50 ng/mL) prepared in pooled blank human plasma were 98.4% and 10.0%, respectively. The obtained S/N ratio was always > 21 (Figure 50 C).

Furthermore, the method proved to be selective since no interferences were detected analyzing six blank plasma samples from different donors, especially at LENVA retention time.

4.4.4.6. Dilution integrity

As reported in section 3.6.6.2, the dilution integrity of plasma samples was assessed at two dilution factors: 1:10 and 1:100. The dilution integrity was verified with a very good precision and accuracy (Table 54): ≤ 4.0% and between 99.9 and 102%, respectively. The results demonstrated that samples having a concentration higher than the established ULOQ can be quantified after appropriate dilution, without affecting precision and accuracy of the analysis.

Table 54. Precision (CV%) and accuracy (%) data obtained with 1:10 and 1:100 dilution factors in plasma samples (conc.: concentration; N: number of replicates; SD: standard deviation).

Analyte	Nominal conc. (ng/mL)	Mean (ng/mL) ± SD	CV%	Accuracy%
LENVA (N = 5)	30.0	30.6 ± 1.2	4.0	102
	300	300 ± 11	3.5	99.9

4.4.4.7. Stability

As reported in section 3.6.7, analyte stability was assessed by analyzing QC plasma samples at the three concentrations (QCL, QCM, QCH) under different conditions (Table 55):

- after extraction, LENVA was stable in autosampler at 4 °C for 94 h after the first injection being accuracy between 89.3-103% and a CV ≤ 4.6%;
- bench-top stability was verified after 4 h at room temperature (25 °C) with an accuracy between 95.1-109% and a CV ≤ 11%;
- freeze (-80 °C)-thaw stability was verified after three cycles with an accuracy between 93.1-103% and a CV ≤ 6.3%;
- long-term stability of plasma samples stored at -80 °C was verified up to 418 days with accuracy between 90.4 and 103% and a CV ≤ 9.9%. These data are in line with those reported by the other methods presented in Table 45. With the proposed method, the long-term stability in human plasma was tested and verified for a longer period (418 days *versus* 6 months);
- long term stability of analyte in DMSO solution stored at -80 °C was verified up to 174 days with accuracy between 95.8 and 109% and a CV ≤ 5.6%;
- long term stability of analyte in MeOH solution stored at -80 °C was verified up to 174 days with accuracy between 89.1 and 105% and a CV ≤ 4.4%.

Stability tests in plasma, MeOH, and DMSO are still ongoing to assess longer time.

Table 55. Short and long-term stability with precision (CV%) and accuracy % obtained for LENVA (conc.: concentration; FTC: freeze-thaw cycle; N: number of replicates; RT: room temperature; SD: standard deviation).

Short term stability of LENVA in human plasma				
N = 3	**Nominal conc.(ng/mL)**	**Mean ± SD (ng/mL)**	**CV%**	**Accuracy %**
4 h at RT	1.50	1.56 ± 0.2	11	104
	75.0	81.7 ± 2.1	2.6	109
	1500	1427 ± 31	2.1	95.1
3° FTC	1.50	1.43 ± 0.0	1.8	95.6
	75.0	77.4 ± 1.2	1.5	103
	1500	1397 ± 87	6.3	93.1
	1.50	1.39 ± 0.1	4.4	92.7

94 h at 4°C	75.0	76.7 ± 3.5	4.6	102
	1500	1340 ± 46	3.4	89.3
Long-term stability of LENVA				
N= 3	**Nominal conc. (ng/mL)**	**Mean ± SD (ng/mL)**	**CV%**	**Accuracy %**
418 days at -80 °C (plasma)	1.50	1.55 ± 0.2	9.9	103
	75.0	78.3 ± 3.1	3.9	104
	1500	1357 ± 98	7.2	90.4
174 days at -80 °C (DMSO)	1.50	1.63 ± 0.1	2.9	109
	75.0	82.1 ± 0.6	0.8	109
	1500	1437 ± 81	5.6	95.8
174 days at -20 °C (MeOH)	1.50	1.58 ± 0.1	2.9	105
	75.0	73.5 ± 3.2	4.4	98.0
	1500	1337 ± 21	1.6	89.1

4.4.4.8. Incurred samples reanalysis

This new quantification method was also reproducible, as demonstrated by the percentage difference between the two measurements of 14 plasma samples from 6 patients treated with LENVA and analyzed in two different working days. Overall, the percentage difference was between -9.20% and 17.5% (Figure 53), thus within the ±20% requirements of EMA and FDA guidelines.

Even if the ISR is not requested by FDA guideline, we considered it an important test to verify the method reproducibility in "real" samples. Anyway, only the method proposed by Ye et al. [243] performed the ISR on 24 clinical samples with a very good percentage difference (-4.5% to 3.1%).

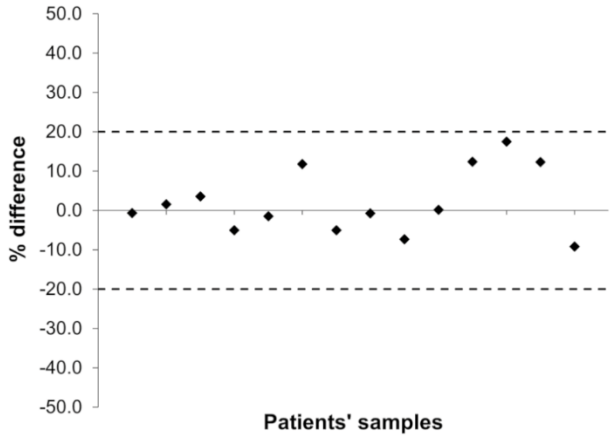

Figure 53. Incurred samples reanalysis: percentage difference between the first and the second analysis for 14 plasma samples from 6 patients. The dotted lines represent the ±20% deviation limits imposed by EMA and FDA guidelines.

4.4.5. Clinical application of LC-MS/MS quantification method

The presented method was used to successfully quantify 24 plasma samples from 6 patients affected by HCC, treated with LENVA, and recruited in the ongoing above-mentioned analytical cross-validation study (internal protocol code: CRO-2018-83).

Patients' plasma samples were analyzed with a calibration curves and triplicates of each QC concentration levels freshly prepared as reported in section 4.4.3.2. The patients' samples were thawed at room temperature, vortexed for 10 sec and centrifuged for 10 min at 3000 g and 4 °C. Subsequently, 100 µL of plasma were precipitated with 500 µL of cold IS WS, vortexed, centrifuged (25 min at 16200 g and 4 °C) and 200 µL of the supernatant was transferred in glass vial for the analysis.

The patients' characteristics and the drug dosage are reported in Table 56.

Table 56. Principal demographic and clinical patients' characteristics.

Patients characteristics	N
Sex	4 males (66.7%)
	2 females (33.3%)
Mean age (range)	74 (61-82) years
Therapy	7 samples at 4 mg/day
	16 samples at 8 mg/day
	1 sample at 12 mg/day

Blood samples were taken between 1.5 and 25.5 h from the last drug assumption. The concentrations found in the samples are reported in Table 57. In all the samples collected LENVA concentration was at the steady-state.

Also in this case, for privacy protection each patient was identified with a progressive number based on the enrolment data, and each plasma sample was named in a univocal way with an ID composed by the patient identification number followed by the sampling number. As an example, ID 6.3 indicates the plasma obtained from patient number 6 at the third blood sampling.

The linear range of the calibration curve demonstrated to be suitable for clinical application since all the quantified samples were within the LLOQ and ULOQ. Due to the paucity of the collected samples, no conclusive considerations can be drawn. However, a certain inter-patients variability in drug concentration can be hypothesized by comparing samples of patients treated at the same dosage and collected at comparable times. For instance, considering patients treated with LENVA at 8 mg/day, 10 samples (2.2, 2.4, 3.3 – 3.6, 4.1 – 4.4), collected around the C_{min} (at 24 ± 1.5 h), displayed a concentration value that spans from 9.1 ng/mL (sample 3.3) to 91.6 ng/mL (sample 2.4) and just two of them were above the proposed C_{min} target of 51.5 ng/mL; three samples (1.2, 3.1 and 3.2) collected at about 17 (±0.5) h since last drug intake showed a comparable variability (17.3-66.7 ng/mL), while two samples (1.3 and 2.1) collected at 4.50 h from last drug

administration, exhibited a lower variability (90.7 ng/mL and 77.6 ng/mL). As regards the dosage of 4 mg/day, the concentration of four samples from 2 patients collected approximately at the C_{min} (24±1.5 h) can be described: within patient variability was low, while mean concentration between the two patients is slightly different (10.7 ng/mL *versus* 18.4 ng/mL).

Table 57. LENVA concentration determined in 24 plasma samples from 6 patients (conc.: concentration; N/A: not available).

Sample	Patient sample	LENVA dose (mg/day)	Hours from last intake (hh:mm)	LENVA conc. (ng/mL)
1	1.1	12	04:37	99.6
2	1.2	8	17:35	66.7
3	1.3	8	04:25	77.6
4	1.4	4	24:45	12.6
5	1.5	4	22:25	8.70
6	2.1	8	04:30	90.7
7	2.2	8	23:20	81.5
8	2.3	8	N/A	81.0
9	2.4	8	24:23	91.6
10	3.1	8	17:32	27.2
11	3.2	8	16:35	17.3
12	3.3	8	23:55	9.10
13	3.4	8	24:45	11.0
14	3.5	8	25:15	11.4
15	3.6	8	24:40	12.6
16	4.1	8	23:50	28.5
17	4.2	8	24:15	42.6
18	4.3	8	23:15	28.5
19	4.4	8	24:03	41.6
20	5.1	4	12:45	39.0
21	6.1	4	23:20	18.0
22	6.2	4	24:45	18.7
23	6.3	4	01:25	21.5
24	6.4	4	24:35	17.7

Generally, a certain intra-patient stability of concentrations was observed when comparing multiple samplings at the same drug dosage collected at comparable times. This observation, even descriptive, corroborates the suitability of LENVA as a candidate for TDM [244,245]. The wide analytical range of the new proposed method represents an advantage respect the method developed by Janssen et al. [241], that quantified simultaneously other different kinase inhibitors and with a comparable run time (4 min). In fact, 2 out of 24 patients' plasma samples that we quantified had a LENVA concentration lower than their LLOQ (10 ng/mL).

4.5. LC-MS/MS method for the quantification of lenvatinib in DBS

To the best of our knowledge, no LC-MS/MS method has been published until now for the quantification of LENVA in DBS matrix. Therefore, a new LC-MS/MS method for the quantification of LENVA in DBS was developed and validated according to EMA [200] and FDA [201] guidelines, EBF recommendation [182,183] and IATDMCT guideline [181].

Also in this case, the LC-MS/MS methods used for the quantification of plasma and DBS samples are the same. In particular, the mass spectrometer conditions are described in section 4.4.1., while the chromatographic conditions are reported in section 4.4.2. Shortly, the mass spectrometer worked in positive ion mode, MP A was MilliQ H_2O with 0.10% of HCOOH (v/v), while MP B was MeOH:iPrOH (90:10, v/v) with 0.10% of HCOOH (v/v), the used column was Synergi™ Fusion-RP column (4 µm, 30 x 2.0 mm, 80 Å) with Fusion-RP Security Guard™ pre-column, column temperatures was set at 50 °C and the total runtime was 4 min. In this case, the injection volume was 5 µL, while the autosampler temperature was set at 15 °C.

The analytical range was slightly reduced respect the plasma method (0.50-2000 ng/mL) because the original LLOQ (0.5 ng/mL) was no longer quantifiable in DBS matrix. The calibration curve was thus fixed at 5-2000 ng/mL.

4.2.3. Optimization of DBS parameters

4.2.3.1. Type of the paper

Initially, the chosen filter paper was the cheaper Whatman 31 ET CHR, for the reason already reported in the previous DBS-based method for the quantification of SORA and REGO. Thus, drug extraction optimization was exclusively conducted on DBS samples deposited on Whatman 31 ET CHR. When the Hct and spot volume effects were tested during the validation process, it was observed that both Hct and spot volume did affect the quantification results and, to overcome this problem, we decided to quantify the entire spot volume. Thus, the extraction process needed to be re-evaluated with the volumetric system and it was also decided to repeat these tests using DBS samples deposited in both Whatman 31 ET CHR and Whatman 903. This choice was made to compare the performance of the two filter papers on LENVA quantification.

For this reason, in the following paragraphs the results obtained with the 3mm-punch of the 20 µL-spot (deposited on Whatman 31 ET CHR) along with those obtained using the volumetric system (8mm-punch of 10 µL-spot deposited on both Whatman 31 ET CHR and Whatman 903) are reported.

4.2.3.2. Drug extraction optimization

Optimization of LENVA extraction from DBS sample involves testing different solvents, volume and extraction time. Standard conditions (1 h of incubation at 37 °C) were applied for these tests. With regard to the 3 mm disc (20 µL-spot deposited on Whatman 31 ET CHR), DBS samples at each QC levels in triplicates were extracted through 1 h mixing in mechanic stirrer with 75 µL of MeOH, ACN, MeOH + 0.10% of HCOOH (v/v), ACN + 0.10% of HCOOH (v/v), MeOH:iPrOH (50:50, v/v) or mixture of MeOH:MilliQ H_2O (90:10, v/v) with 0.10% of HCOOH (v/v). The QCL samples extracted with ACN and ACN + 0.10% of HCOOH (v/v) were not quantifiable, thus these solvents were discarded. The results obtained with the other extraction solvents are reported in Table 58. The selected extraction solvent was MeOH +0.10% of HCOOH (v/v) because the % extraction yield was higher than that obtained with the other mixture and comparable within the concentration tested.

Table 58. Optimization of solvent for LENVA extraction from DBS matrix (N: number of replicates; SD: standard deviation).

Analyte	SAMPLE (N = 3)	% extraction yield (mean ± SD)			
		A	B	C	D
LENVA	QCL	70.6 ± 4.1	72.6 ± 2.7	76.7 ± 4.9	69.9 ± 5.9
	QCM	65.2 ± 2.3	67.9 ± 2.9	65.0 ± 7.0	59.3 ± 2.6
	QCH	63.3 ± 1.5	71.7 ± 4.5	66.7 ± 3.3	58.9 ± 1.6

A: MeOH; B: MeOH + 0.10% of HCOOH (v/v); C: MeOH:iPrOH (50:50, v/v); D: MeOH:MilliQ H_2O (90:10, v/v) with 0.10% of HCOOH (v/v).

The tested volumes of MeOH + 0.10% of HCOOH (v/v) were 45, 60, 75 and 120 µL and the obtained results are reported in Table 59. Also in this case, samples were extracted applying 1 h of mechanic stirrer. The chosen volume was 45 µL because showed an extraction yield similar within the concentrations tested and it was the lowest volume of organic solvent.

Table 59. Optimization of extraction solvent volume of LENVA from DBS matrix (N: number of replicates; SD: standard deviation).

Analyte	SAMPLE (N = 3)	% extraction yield (mean ± SD)			
		45 µL	60 µL	75 µL	120 µL
LENVA	QCL	69.9 ± 5.1	76.7 ± 4.8	73.0 ± 3.5	83.3 ± 2.8
	QCM	64.6 ± 1.8	65.0 ± 1.3	65.2 ± 4.2	65.4 ± 1.5
	QCH	63.0 ± 1.3	64.1 ± 1.4	64.7 ± 2.6	59.7 ± 2.5

At the end, different extraction times were evaluated ranging from 30 min to 4 h and the obtained results are reported in Table 60. All the samples were extracted with 45 µL of MeOH+0.10% of HCOOH (v/v). The chosen extraction time was 1 h.

Table 60. Optimization of extraction time of LENVA from DBS matrix (N: number of replicates; SD: standard deviation).

Analyte	SAMPLE (N = 3)	% extraction yield (mean ± SD)			
		30 min	1 h	2 h	4 h
LENVA	QCL	75.1 ± 3.1	71.5 ± 2.6	73.0 ± 4.0	65.7 ± 3.6
	QCM	67.4 ± 6.7	61.1 ± 3.7	63.8 ± 6.0	59.7 ± 2.1
	QCH	57.4 ± 2.9	59.8 ± 3.6	52.0 ± 0.8	55.8 ± 2.5

As anticipated, sample preparation was successively modified and a volumetric system was introduced in order to avoid the Hct and spot volume effects. Thus, solvents type, volume and extraction time were re-evaluated using 8 mm-punch of 10 µL spot deposited both on Whatman 31 ET CHR and Whatman 903. As related to the solvents type, no modification was required because the results were identical as compared to those reported in Table 58 and MeOH + 0.10% of HCOOH (v/v) provided the higher extraction percentage. Thus, to define the proper extraction volume, the entire 10 µL spot was extracted with 300, 400 and 500 µL of MeOH + 0.10% of HCOOH (v/v). The obtained results are reported in Table 61. A volume minor than 300 µL was not applicable because 8 mm disc was not completely immersed in the extraction solvent.
The selected volume was 300 µL because it used the lowest organic volume and with a comparable results among different concentration levels. Moreover, the extraction yield was comparable between the two filter papers.

Table 61. Optimization of solvent volume for LENVA extraction from entire DBS sample on both Whatman 31 ET CHR and Whatman 903 (N: number of replicates; SD: standard deviation).

Whatman 31 ET CHR				
Analyte	SAMPLE (N = 3)	% extraction yield (mean ± SD)		
		300 µL	400 µL	500 µL
LENVA	QCL	77.1 ± 2.6	85.3 ± 4.3	77.3 ± 2.8
	QCM	81.8 ± 2.1	77.7 ± 3.8	77.3 ± 3.1
	QCH	71.7 ± 0.6	75.2 ± 1.3	72.2 ± 0.7
Whatman 903				
Analyte	SAMPLE (N = 3)	% extraction yield (mean ± SD)		
		300 µL	400 µL	500 µL
LENVA	QCL	79.7 ± 5.6	86.0 ± 7.0	78.9 ± 5.4
	QCM	77.4 ± 3.5	74.9 ± 4.4	76.2 ± 0.8
	QCH	73.2 ± 2.3	74.3 ± 0.4	77.9 ± 3.9

Data obtained from the re-evaluation of the extraction time (from 30 min to 4 h) necessary for the volumetric system are reported in Table 62 and they showed the possibility to reduce the agitation time from 1 h to 30 min. Also in this case, the extraction yield was comparable between the two filter papers and are even slightly higher compared to the previous results.

Table 62. Optimization of LENVA extraction time from entire DBS sample on both Whatman 31 ET CHR and Whatman 903 (N: number of replicates; SD: standard deviation).

Whatman 31 ET CHR					
Analyte	**SAMPLE (N = 3)**	**% extraction yield *vs* MeOH samples (mean ± SD)**			
		30 min	**1 h**	**2 h**	**4 h**
LENVA	QCL	80.3 ± 0.6	79.2 ± 0.7	78.4 ± 3.9	76.4 ± 2.8
	QCM	83.0 ± 1.2	82.8 ± 3.3	80.2 ± 1.8	82.3 ± 2.5
	QCH	75.6 ± 2.2	75.4 ± 0.7	74.8 ± 2.7	73.5 ± 1.3
Whatman 903					
Analyte	**SAMPLE (N = 3)**	**% extraction yield *vs* MeOH samples (mean ± SD)**			
		30 min	**1 h**	**2 h**	**4 h**
LENVA	QCL	82.5 ± 1.7	80.9 ± 1.8	77.7 ± 0.0	79.0 ± 2.6
	QCM	81.0 ± 4.0	83.9 ± 3.7	80.8 ± 2.1	83.5 ± 3.0
	QCH	77.8 ± 4.3	75.7 ± 1.9	76.7 ± 1.6	74.4 ± 2.8

Overall. the final sample extraction procedure for the volumetric system was characterized by 300 µL of MeOH + 0.10% of HCOOH (v/v) and by 30 min of shacking.

4.2.3.3. Incubation time optimization

Also in this case, the incubation time optimization was conducted firstly on 3 mm disc of 20 µL spot deposited on Whatman 31 ET CHR extracted with 45 µL of MeOH + 0.10% of HCOOH (v/v). The obtained data are reported in Table 63 and the chosen time was 1 h instead of 30 min due to the lower SD.

Table 63. Optimization of incubation time of LENVA in DBS matrix (N: number of replicates; SD: standard deviation).

Analyte	**SAMPLE (N = 3)**	**% extraction yield (mean ± SD)**					
		30 min	**1 h**	**2 h**	**4 h**	**8 h**	**24 h**
LENVA	QCL	67.2 ± 3.5	64.0 ± 2.8	59.0 ± 4.2	56.0 ± 2.2	50.0 ± 3.5	37.0 ± 2.9
	QCM	65.3 ± 3.3	65.6 ± 2.2	63.1 ± 3.3	54.1 ± 2.8	42.5 ± 4.4	33.0 ± 0.4
	QCH	67.1 ± 2.0	63.1 ± 1.6	64.5 ± 4.7	57.6 ± 3.0	42.2 ± 2.6	31.9 ± 1.3

Then, the same experiment was conducted on 8 mm disc of 10 µL spot deposited on both Whatman 31 ET CHR and Whatman 903 and extracted with 300 µL of MeOH + 0.10% of HCOOH (v/v). Results are reported in Table 64 and the selected time was 30 min. Extraction yields were comparable between Whatman 31 ET CHR and Whatman 903 filter papers.

The optimized sample preparation workflow was: 30 min of incubation followed by extraction obtained with 300 µL of MeOH + 0.10% of HCOOH (v/v) and 30 min of shacking.

Table 64. Optimization of incubation time of LENVA in DBS matrix on both Whatman 31 ET CHR and Whatman 903 (N: number of replicates; SD: standard deviation).

Whatman 31 ET CHR							
Analyte	**SAMPLE (N = 3)**	**% extraction yield *vs* MeOH samples (mean ± SD)**					
		30 min	**1 h**	**2 h**	**4 h**	**8 h**	**24 h**
LENVA	QCL	81.3 ± 5.1	74.7 ± 6.0	71.1 ± 3.5	60.7 ± 2.2	49.5 ± 3.8	38.4 ± 2.0
	QCM	86.5 ± 2.9	81.7 ± 3.4	77.2 ± 3.4	65.0 ± 1.3	54.8 ± 3.9	38.3 ± 3.3
	QCH	79.2 ± 2.3	77.5 ± 1.6	75.1 ± 1.0	65.6 ± 2.1	54.3 ± 2.0	36.3 ± 3.9
Whatman 903							
Analyte	**SAMPLE (N = 3)**	**% extraction yield *vs* MeOH samples (mean ± SD)**					
		30 min	**1 h**	**2 h**	**4 h**	**8 h**	**24 h**
LENVA	QCL	82.8 ± 5.5	78.5 ± 2.6	70.6 ± 1.8	64.0 ± 4.6	49.6 ± 3.1	34.8 ± 1.6
	QCM	86.1 ± 1.2	81.1 ± 1.7	74.6 ± 3.2	63.3 ± 1.7	52.6 ± 2.0	38.8 ± 1.3
	QCH	81.9 ± 6.0	76.6 ± 3.8	71.3 ± 1.5	62.5 ± 2.6	53.2 ± 1.4	36.4 ± 2.3

4.2.3.4. Calibration curve and quality controls preparation

The stock solution of LENVA and LENVA-D_4 were the same used for the corresponding plasma-based method (1 mg/mL in DMSO stored at -80 °C). To obtain the WSs for the calibration curve (from A to H), the stock solution of LENVA was diluted with MeOH to achieve the final concentrations of 40.0, 20.0, 10.0, 2.00, 0.80, 0.40, 0.20 and 0.10 µg/mL. The same procedure was also applied to obtain the QC WSs with a final concentrations of 30.0, 1.50 and 0.30 µg/mL. Each analyte stock solution, as well as the calibrators and QCs WSs, were kept in polypropylene tubes and stored at -80 °C, while a 1000 µL-aliquot of each WS was kept in a polypropylene tube and stored at -20 °C to freshly prepare calibration curve and QC samples during the validation process and quantification of patients' DBS samples. The IS WS was the same used for the plasma-based method, see section 4.4.3.2.

Every day, an eight-point calibration curve (A to H) and triplicates of each QC concentration were freshly prepared in DBS matrix. A blank sample (DBS processed without IS), a zero-blank sample (DBS processed including IS), and a LLOQ DBS sample were analyzed before each run to verify the system performance. Preparation of calibrators and QCs samples was conducted as follows: 1) 10 µL of proper WS were added to 190 µL of blank human blood containing EDTA (dilution 1:20) and gently mixed for 10 s; 2) the spiked blood was incubated at 37 °C for 30 min; 3) after incubation the spiked blood was newly gently mixed and 10 µL blood spots were performed on both Whatman 31 ET CHR and Whatman 903 paper; 4) the spots were let dry in the air for at least 3 h; 5) after drying, a 8 mm diameter punch was manually performed for every spot; 6) the punch was extracted by adding 300 µL of IS WS and mixed for 30 min in a mechanical stirrer, 7) 100 µL of the supernatant were diluted with 50 µL of MP A and vortexed for 10 s; 8) 130 µL were transferred to a glass autosampler vial for the analysis.

Therefore, concentrations of the calibration curve and QCs DBS samples are reported in Table 65.

Table 65. Final LENVA concentrations of calibrators and QCs in DBS samples (conc.: concentration).

Sample	LENVA conc. (ng/mL)
H	5.00
G	10.0
F	20.0
E	40.0
D	100
C	500
B	1000
A	2000
QCL	15.0
QCM	75.0
QCH	1500

4.2.4. LC-MS/MS method validation study in DBS

Once the necessity to quantify the entire volume of the DBS sample was defined due to the presence of Hct and spot volume effect on LENVA quantification of DBS samples, the extraction procedure was accordingly modified and the analytical LC-MS/MS method was fully validated in both Whatman 31 ET CHR and Whatman 903 filter paper according to EMA [200] and FDA [201] guidelines, EBF recommendation[182,183] and IATDMCT guideline[181].

4.2.4.1. Effect of hematocrit and spot volume

A first attempt to evaluate the effect of Hct and spot volume was conducted by simultaneously quantifying samples on a calibration curve with 40.4% as Hct and 20 µL as spot volume. As reported in Table 66, the analyzed samples were underestimated for 5 µL and 10 µL spots for at almost each Hct tested. Moreover, increasing the spot volume also the accuracy seemed to increase. These data were not acceptable according to the guidelines criteria meaning that the extraction of 3 mm disc (i.e. only a part of the entire spot) on Whatman 31 ET CHR was not possible due to unacceptable effect of Hct and spot volume.

Table 66. Hct and spot volume effect on LENVA extracted from 3 mm punch of LENVA in DBS samples (conc.: concentration; Hct: hematocrit; N: number of replicates).

Analyte	Sample	Spot volume (µL)	Hct 25.0%	Hct 35.1%	Hct 40.4%	Hct 45.0%	Hct 54.9%
			Accuracy% (CV%)	Accuracy% (CV %)	Accuracy% (CV%)	Accuracy% (CV %)	Accuracy% (CV%)
LENVA (N = 3)	QCL	5	69.8 (6.3)	85.7 (0.2)	70.4 (10)	84.5 (2.9)	90.0 (1.4)
		10	79.5 (2.6)	92.1 (5.0)	83.0 (2.8)	88.2 (7.9)	96.0 (4.6)
		20	94.7 (8.3)	96.1 (4.8)	99.3 (1.9)	103 (8.0)	112 (2.7)
		40	105 (9.6)	103 (7.7)	98.8 (1.9)	102 (6.1)	118 (2.6)
	QCH	5	69.8 (12)	76.0 (2.5)	71.5 (11)	80.2 (3.2)	85.2 (0.4)

Analyte	Sample	Spot volume (µL)	Hct 25.0% Accuracy% (CV%)	Hct 35.1% Accuracy% (CV %)	Hct 40.4% Accuracy% (CV%)	Hct 45.0% Accuracy% (CV %)	Hct 54.9% Accuracy% (CV%)
		10	70.7 (2.50)	77.8 (2.2)	82.0 (5.3)	87.0 (0.5)	95.8 (3.8)
		20	88.7 (5.3)	90.2 (0.9)	96.9 (4.0)	102 (5.0)	111 (2.3)
		40	90.3 (0.5)	92.2 (6.5)	101 (2.1)	100 (4.4)	114 (1.2)

*Not accepted value according to acceptance criteria

To avoid these phenomena, a volumetric sampling was performed on both Whatman 31 ET CHR and Whatman 903 paper and the entire 10 µL spot was punched, generating a 8 mm disc. In this way, the spot volume was fixed and an acceptable impact of Hct (within the range of 25-55%) was obtained, as reported in Table 67.

In fact, accuracy was between 103 and 112% with a CV ≤ 6.2 % for Whatman 31 ET CHR, while it was between 96-105% with a CV% ≤ 5.5% for Whatman 903. These results showed a slightly better performance of Whatman 903 as compared to Whatman 31 ET CHR paper. For this reason, from this point on the validation process was performed extracting the entire 10 µL DBS sample with 300 µL of MeOH + 0.10% of HCOOH (v/v) containing 50 ng/mL of LENVA-D_4.

Table 67. Hct effect on LENVA extracted from DBS samples with a 8 mm punch (conc.: concentration; Hct: hematocrit; N: number of replicates; SD: standard deviation).

Whatman 31 ET CHR					
Analyte	**Nominal conc. (ng/mL)**	**Hct**	**Mean ± SD**	**Accuracy%**	**CV%**
LENVA (N = 5)	15.0	25%	16.1 ± 0.6	107	3.8
		39.7%	16.1 ± 0.9	107	5.4
		55%	15.4 ± 1.0	103	6.2
	1500	25%	1588 ± 52	106	3.3
		39.7%	1594 ± 50	106	3.1
		55%	1680 ± 36	112	2.1
Whatman 903					
Analyte	**Nominal conc. (ng/mL)**	**Hct**	**Mean ± SD**	**Accuracy%**	**CV%**
LENVA (N = 5)	15.0	25%	15.2 ± 0.7	102	5.5
		39.7%	14.5 ± 0.5	97	3.6
		55%	15.0 ± 0.6	100	4.1
	1500	25%	1572 ± 42	104	2.8
		39.7%	1438 ± 48	96	3.3
		55%	1598 ± 82	105	3.9

4.2.4.2. Recovery

Recovery was assessed in triplicate for each QC concentration level (QCL, QCM, QCH) using 6 different donors (3 males and 3 females), of which 1 donor at 3 Hct levels, prepared as reported in section 3.7.2 and it was calculated with the Equation 9.

The recovery percentage was very good for both the filter papers. In particular, the recovery percentage of LENVA was consistent among the three concentrations tested on Whatman 903 (showing values between 82.3% and 88.5%), as reported in Table 68. Very similar recovery percentages were observed for QCM and QCH samples deposited on Whatman 31 ET CHR (84.0% and 81.6%, respectively), while the percentage for QCL sample was higher (108%).

Table 68. Recovery of LENVA from DBS samples deposited on Whatman 31 ET CHR and Whatman 903 (conc.: concentration; N: number of replicates; SD: standard deviation).

Whatman 31 ET CHR			
Analyte	**Nominal conc. (ng/mL)**	**Recovery (%) ± SD**	**CV (%)**
LENVA (N = 24)	15.0	108 ± 11	10
	75.0	84.0 ± 3.9	4.7
	1500	81.6 ± 5.8	7.1
Whatman 903			
Analyte	**Nominal conc. (ng/mL)**	**Recovery (%) ± SD**	**CV (%)**
LENVA (N = 24)	15.0	88.5 ± 8.2	9.2
	75.0	82.3 ± 5.8	7.0
	1500	86.7 ± 4.6	5.4

To verify, whether the greater recovery for QCL samples depended on an instrumental variation, the recovery was calculated using the area ratio (area of the analyte over the area of IS) of the analyte in DBS samples and the analyte in extracted matrix. In this case, a lower variability in recovery percentage was observed among the concentration levels and between the two filter paper type, as reported in Table 69.

Table 69. Recovery of LENVA from DBS samples deposited on Whatman 31 ET CHR and Whatman 903 and calculated using area ratio (conc.: concentration; N: number of replicates; SD: standard deviation).

Whatman 31 ET CHR			
Analyte	**Nominal conc. (ng/mL)**	**Recovery (%) ± SD**	**CV (%)**
LENVA (N = 24)	15.0	85.8 ± 5.0	5.8
	75.0	77.2 ± 2.6	3.4
	1500	76.6 ± 3.1	4.1
Whatman 903			
Analyte	**Nominal conc. (ng/mL)**	**Recovery (%) ± SD**	**CV (%)**
LENVA (N = 24)	15.0	82.7 ± 5.6	6.7
	75.0	77.3 ± 2.5	3.2
	1500	80.1 ± 2.6	3.3

4.2.4.3. Matrix effect

A quantitative determination of MF was assessed following the procedure described in section 3.7.3.2 and the obtained data are reported in Table 70. In particular, the MF and IS norm MF were slightly higher on Whatman 903 than Whatman 31 ET CHR, with a similar CV%. The CV of IS norm MF for both filter paper were abundantly within the criteria imposed by the guidelines (≤ 5.6% for Whatman 31 ET CHR and ≤ 6.1% for Whatman 903), so the matrix effect was considered negligible in affecting analyses results.

Table 70. Estimated matrix factor (MF) and IS normalized MF (IS norm MF) of LENVA and IS in extracted DBS matrix. (conc.: concentration; N: number of replicates; SD: standard deviation).

Whatman 31 ET CHR					
Analyte	**Nominal conc. (ng/mL)**	**MF (%) ± SD**	**CV (%)**	**IS norm MF (%) ± SD**	**CV (%)**
LENVA (N = 24)	15.0	58.7 ± 2.3	4.0	0.94 ± 0.04	3.9
	75.0	55.2 ± 3.1	5.6	0.88 ± 0.05	5.6
	1500	55.9 ± 2.6	4.7	0.90 ± 0.04	4.7
LENVA-D_4 (N = 24)	50	62.4 ± 3.3	5.3	-	-
Whatman 903					
Analyte	**Nominal conc. (ng/mL)**	**MF (%) ± SD**	**CV (%)**	**IS norm MF (%) ± SD**	**CV (%)**
LENVA (N = 24)	15.0	70.6 ± 4.3	6.1	1.00 ± 0.06	6.1
	75.0	68.5 ± 3.6	5.2	0.97 ± 0.05	5.2
	1500	64.5 ± 3.7	5.7	0.91 ± 0.05	5.7
LENVA-D_4 (N = 24)	50	70.6 ± 3.8	5.4	-	-

Furthermore, the negligible effect of this phenomenon was also proved through the analysis of 6 LLOQ samples from different donors (3 males and 3 females), being the obtained accuracy and precision (as CV), respectively: 101% and 8.7% for Whatman 31 ET CHR and 100% and 6.4% for Whatman 903.

4.2.4.4. Process efficiency

The process efficiency was evaluated, as described in section 3.7.4.2. and results are reported in Table 71. The obtained values were similar among the concentrations range (QCL-QCH) and between the two tested filter papers. In fact, process efficiency was within 68.7 and 77.5% for Whatman 31 ET CHR and within 75.1 and 79.8% for Whatman 903.

Table 71. Process efficiency of the extraction method of LENVA from DBS samples deposited on both Whatman 31 ET CHR and Whatman 903 (conc.: concentration; N: number of replicates; SD: standard deviation).

Whatman 31 ET CHR			
Analyte	**Nominal conc. (ng/mL)**	**Process efficiency (%) ± SD**	**CV (%)**
LENVA (N = 24)	15.0	77.5 ± 4.5	5.8
	75.0	68.7 ± 2.3	3.4
	1500	71.6 ± 2.9	4.1
Whatman 903			
Analyte	**Nominal conc. (ng/mL)**	**Process efficiency (%) ± SD**	**CV (%)**
LENVA (N = 24)	15.0	79.8 ± 5.7	7.2
	75.0	75.7 ± 2.5	3.2
	1500	75.1 ± 2.5	3.3

4.2.4.5. Linearity

The linearity of the method was demonstrated over the selected concentrations (5.00-2000 ng/mL) preparing calibration curves during 4 different working days (Figure 54). The applied linear regression model was weighted ($1/x^2$). The Pearson's correlation coefficient (r) was 0.9983 ± 0.0014 (CV ≤ 0.14%) for Whatman 31 ET CHR and 0.9987 ± 0.0005 (CV ≤ 0.05%) for Whatman 903.

The calculated accuracy and precision of the calibration curve obtained for the two filter papers are reported in Table 72. The obtained results between the filter papers were similar: accuracy and precision were between 96.0 and 104% and ≤ 6.8 % for Whatman 31 ET CHR and 95.6-102% and ≤ 5.6 % for Whatman 903, respectively.

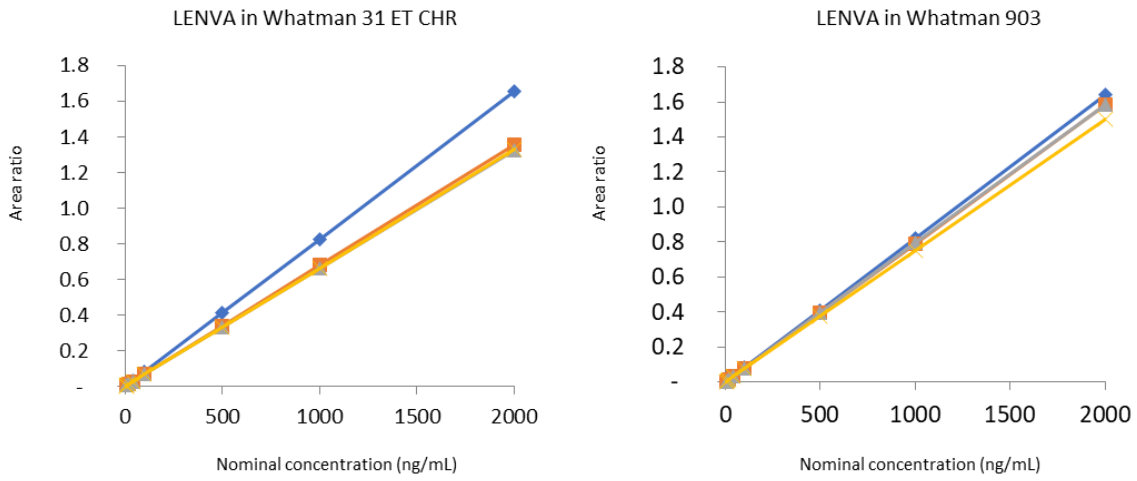

Figure 54. Calibration curves (N = 4) for the quantification of LENVA in DBS samples. For each calibrator the area ratio of LENVA peak area over IS peak area was plotted against the nominal concentration value.

Table 72. Accuracy (%) and precision (CV%) data of LENVA calibration curves in DBS samples (conc.: concentration; N: number of replicates; SD: standard deviation).

LENVA in Whatman 31 ET CHR (N = 4)			
Nominal conc.(ng/mL)	**Mean ± SD (ng/mL)**	**CV%**	**Accuracy%**
5.00	4.90 ± 0.2	3.6	98.1
10.0	10.4 ± 0.7	6.8	104
20.0	19.8 ± 1.4	6.8	98.9
40.0	40.8 ± 1.1	2.8	102
100	101 ± 2.2	2.1	101
500	500 ± 16	3.3	100
1000	993 ± 6.0	0.6	99.3
2000	1920 ± 98	5.1	96.0
LENVA in Whatman 903 (N = 4)			
Nominal conc.(ng/mL)	**Mean ± SD (ng/mL)**	**CV%**	**Accuracy%**
5.00	5.03 ± 0.1	2.7	101
10.0	10.1 ± 0.5	4.6	101
20.0	19.1 ± 0.6	2.9	95.6
40.0	39.4 ± 0.7	1.8	98.6
100	102 ± 3.1	3.1	102
500	499 ± 22	4.4	99.8
1000	1057 ± 55	5.2	106
2000	1970 ± 110	5.6	98.5

4.2.4.6. Intra-day and inter-day precision and accuracy

The obtained data of intra- and inter-day precision and accuracy are reported in Table 73 and Table 74, respectively, and they complied with EMA and FDA requirements for both filter papers.

Table 73. Intra-day precision (CV%) and accuracy (%) for LENVA in DBS samples (conc.: concentration; N: number of replicates; SD: standard deviation).

Intra-day in Whatman 31 ET CHR (N = 5)			
Nominal conc. (ng/mL)	**Mean ± SD (ng/mL)**	**CV%**	**Accuracy%**
5.00	4.75 ± 0.1	2.2	94.9
15.0	13.9 ± 0.7	4.8	92.8
75.0	71.4 ± 2.1	2.9	95.2
1500	1408 ± 46	3.3	93.9
Intra-day in Whatman 903 (N = 5)			
Nominal conc. (ng/mL)	**Mean ± SD (ng/mL)**	**CV%**	**Accuracy%**
5.00	4.80 ± 0.3	6.2	96.0
15.0	14.5 ± 0.5	3.6	96.8
75.0	75.8 ± 3.0	3.9	101
1500	1438 ± 48	3.3	95.9

In fact, intra- and inter-day precision were ≤ 7.0% for Whatman 31 ET CHR and ≤ 8.8% for Whatman 903, while the intra- and inter-day accuracy were between 92.8-108% for Whatman 31 ET CHR and 95.9-104% for Whatman 903. Also in this case, accuracy and precision data were comparable between the two filter papers.

Table 74. Inter-day precision (CV%) and accuracy (%) for LENVA in DBS samples (conc.: concentration; N: number of replicates; SD: standard deviation).

Inter-day in Whatman 31 ET CHR (N = 15)			
Nominal conc. (ng/mL)	**Mean ± SD (ng/mL)**	**CV%**	**Accuracy%**
5.00	5.27 ± 0.4	7.0	105
15.0	16.1 ± 0.9	5.5	107
75.0	79.7 ± 2.3	2.9	106
1500	1615 ± 73	4.5	108
Inter-day in Whatman 903 (N = 15)			
Nominal conc. (ng/mL)	**Mean ± SD (ng/mL)**	**CV%**	**Accuracy%**
5.00	4.90 ± 0.4	8.8	98.0
15.0	15.2 ± 0.8	5.3	101
75.0	78.0 ± 3.3	4.2	104
1500	1522 ± 72	4.7	102

4.2.4.7. Limit of quantification and selectivity

Regarding the method sensitivity, the accuracy and precision (CV%) obtained for the 6 LLOQ samples (5.00 ng/mL) prepared in DBS matrix were 94.9% and 2.2%, respectively, for Whatman 31 ET CHR and 96.0% and 6.2%, respectively, for Whatman 903. Moreover, the S/N ratio obtained for Whatman 31 ET CHR and Whatman 903 was always > 48 and > 57, respectively (Figure 55 B and Figure 56 B).

Furthermore, the method proved to be selective since no interferences were detected analyzing 6 blank DBS samples from 6 different donors, especially at LENVA retention times ((Figure 55 A and Figure 56 A).

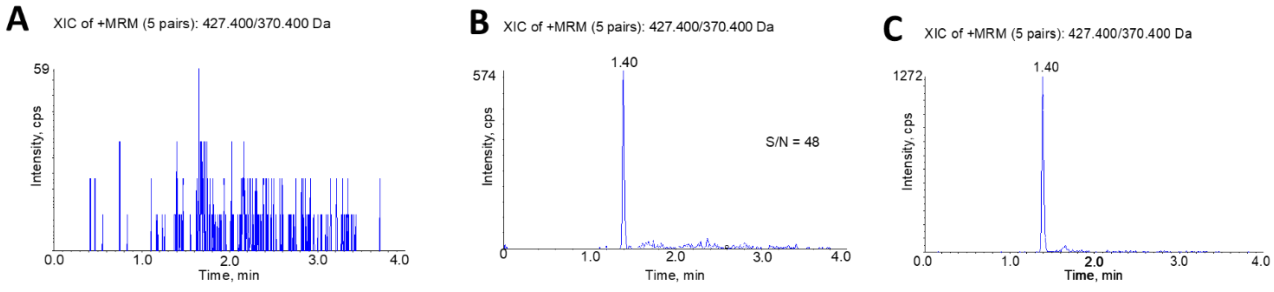

Figure 55. MRM chromatograms for LENVA in DBS samples deposited on Whatman 31 ET CHR. A: blank plasma sample; B: LLOQ (5.0 ng/mL) with S/N value; C: plasma sample from a patient treated with 8 mg/day LENVA and showing a drug concentration of 7.70 ng/mL.

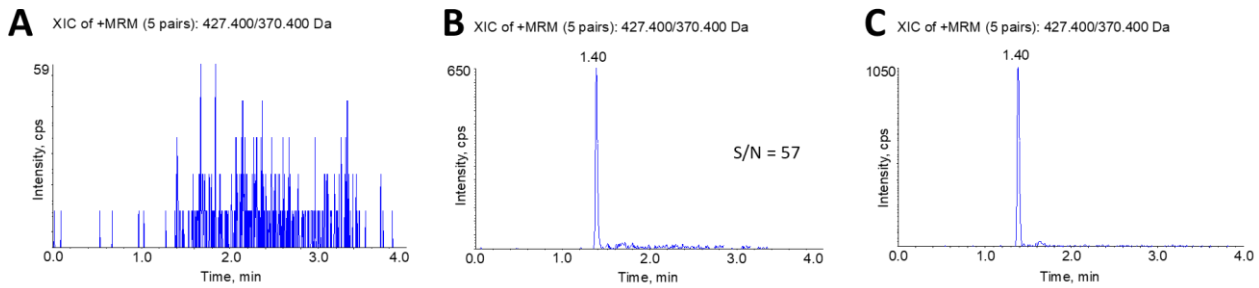

Figure 56. MRM chromatograms for LENVA in DBS samples deposited on Whatman 903. A: blank plasma sample; B: LLOQ (5.0 ng/mL) with S/N value; C: plasma sample from a patient treated with 8 mg/day LENVA and showing a drug concentration of 8.31 ng/mL.

4.2.4.8. Stability

LENVA stability tests on both Whatman 31 ET CHR and Whatman 903 were evaluated analyzing QCL and QCH DBS samples in quintuplicate under different conditions, as reported in section 3.7.9.

The results obtained for Whatman 31 ET CHR are reported in Table 75 and summarized below:

- after extraction, LENVA was stable in autosampler at 15 °C for at least 94 h after the first injection being accuracy between 104-106% and a CV ≤ 6.3%;
- freeze (-80 °C)-thaw stability was verified after two cycles with an accuracy between 94.0-95.5% and a CV ≤ 7.8%;
- stability under elevated temperatures (50 °C) was verified up to 4 days with accuracy between 107 and 108% and a CV ≤ 2.9%;
- long term stability of DBS stored in paper envelopes inside the dryer at room temperature was verified up to 98 days with accuracy between 99.6-101% and a CV ≤ 5.4%;
- long term stability of DBS stored at -80 °C in plastic envelops was verified up to 25 days with accuracy between 98.5-98.7% and a CV ≤ 2.6%;

Table 75. Short and long-term stability of DBS samples deposited on Whatman 31 ET CHR with precision (CV%) and accuracy % obtained for LENVA (conc.: concentration; FTC: freeze-thaw cycle; N: number of replicates; RT: room temperature; SD: standard deviation).

Short term stability of LENVA in Whatman 31 ET CHR				
N = 5	**Nominal conc.(ng/mL)**	**Mean ± SD (ng/mL)**	**CV%**	**Accuracy %**
94 h at 15 °C	15.0	15.6 ± 1.0	6.3	104
	1500	1590 ± 47	3.0	106
2° FTC	15.0	14.3 ± 1.1	7.8	95.5
	1500	1410 ± 20.0	1.4	94.0
4 days at 50 °C	15.0	16.1 ± 0.5	2.9	107
	1500	1626 ± 5.5	0.3	108
Long-term stability of LENVA in Whatman 31 ET CHR				

N = 5	Nominal conc. (ng/mL)	Mean ± SD (ng/mL)	CV%	Accuracy %
98 days at RT in dryer (DBS)	15.0	14.9 ± 0.8	5.4	99.6
	1500	1517 ± 68	4.5	101
25 days at -80°C (DBS)	15.0	14.8 ± 0.4	2.6	98.5
	1500	1480 ± 19	1.3	98.7

The results obtained for Whatman 903 are reported in Table 76 and briefed below:

- after extraction, LENVA was stable in autosampler at 15 °C for at least 94 h after the first injection being accuracy between 105-107% and a CV ≤ 4.4%;
- freeze (-80 °C)-thaw stability was verified after two cycles with an accuracy between 89.3-91.0% and a CV ≤ 2.4%;
- stability at elevated temperatures (50 °C) was verified up to 4 days with accuracy between 94.2 and 101% and a CV ≤ 6.3%;
- long term stability of DBS stored in paper envelopes inside the dryer at room temperature was verified up to 98 days with accuracy between 88.2-94.3% and a CV ≤ 5.0%;
- long term stability of DBS stored at -80 °C in plastic envelops was verified up to 25 days with accuracy between 94.9-99.6% and a CV ≤ 3.0%;

Table 76. Short and long-term stability of DBS samples deposited on Whatman 903 with precision (CV%) and accuracy % obtained for LENVA (conc.: concentration; FTC: freeze-thaw cycle; N: number of replicates; RT: room temperature; SD: standard deviation).

Short term stability of LENVA in Whatman 903				
N = 5	**Nominal conc.(ng/mL)**	**Mean ± SD (ng/mL)**	**CV%**	**Accuracy %**
94 h at 15 °C	15.0	16.1 ± 0.7	4.4	107
	1500	1570 ± 54	3.5	105
2' FTC	15.0	13.7 ± 0.1	0.4	91.0
	1500	1340 ± 32	2.4	89.3
4 days at 50 °C	15.0	14.1 ± 0.9	6.3	94.2
	1500	1520 ± 20	1.3	101
Long-term stability of LENVA in Whatman 903				
N = 5	**Nominal conc. (ng/mL)**	**Mean ± SD (ng/mL)**	**CV%**	**Accuracy %**
98 days at RT in dryer (DBS)	15.0	13.2 ± 0.7	5.0	88.2
	1500	1415 ± 50	3.5	94.3
25 days at -80°C (DBS)	15.0	14.9 ± 0.5	3.0	99.6
	1500	1424 ± 22	1.5	94.9

LENVA proved to be stable under the several tested conditions with no substantial difference between Whatman 31 ET CHR and Whatman 903. Long-term stability tests are still ongoing to further extend the possible storage period of DBS samples.

4.2.4.9. Incurred samples reanalysis

The reproducibility of this new quantification method was preliminary tested on only 4 venous DBS samples from 2 patients enrolled in the cross-validation study (internal protocol code: CRO-2018-83). Samples collected on both Whatman 31 ET CHR and Whatman 903, were stored in dryer (at room temperature) and at -80 °C.

The LC-MS/MS resulted reproducible in all the conditions tested satisfying the ±20% requirements of EMA and FDA guidelines. In particular, the percentage difference was between -10 and 18% for Whatman 31 ET CHR stored at room temperature in dryer, while within -16% and 6.9% for Whatman 31 ET CHR stored at -80°C, as reported in Figure 57.

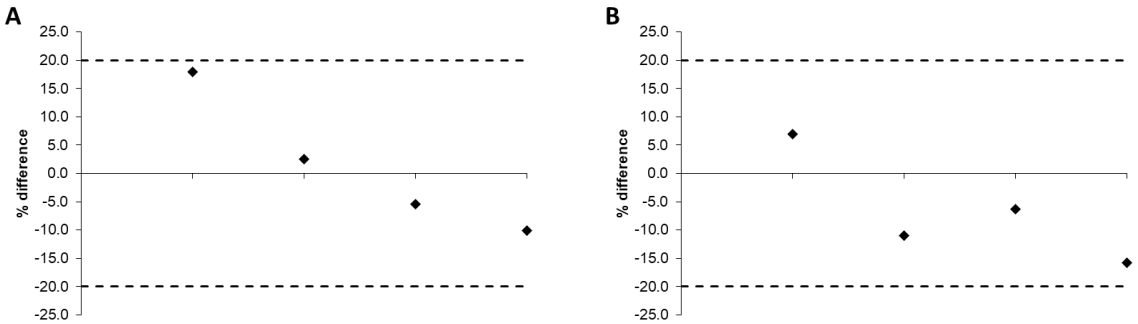

Figure 57. Incurred samples reanalysis: percentage difference between the first and the second analysis of 4 venous DBS samples from 2 patients in Whatman 31 ET CHR: A) DBS samples stored at room temperature in dryer and B) DBS samples stored at -80°C. The dotted lines represent the ±20% deviation limits imposed by EMA and FDA guidelines.

The obtained results on Whatman 903 was slight better than the other paper. In fact, the % difference was between -9.8 and -1.4% for samples stored at room temperature in dryer, while within -10% and 3.0% for samples stored at -80°C, as reported in Figure 58.

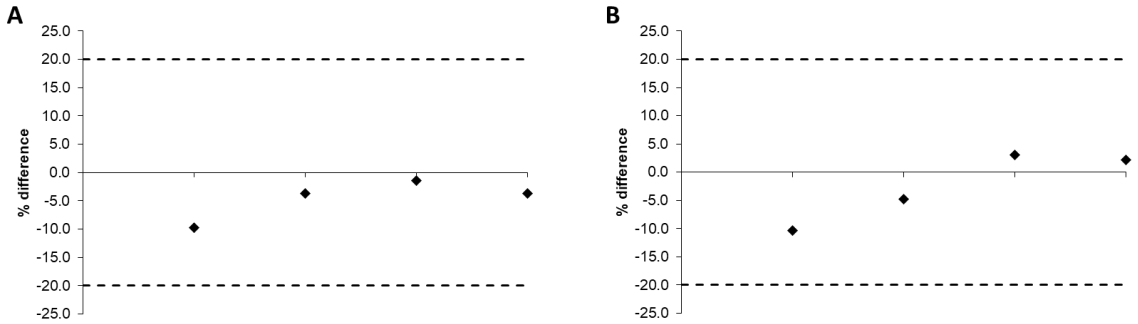

Figure 58. Incurred samples reanalysis: percentage difference between the first and the second analysis of 4 venous DBS samples from 2 patients in Whatman 903: A) DBS samples stored at room temperature in dryer and B) DBS samples stored at -80°C. The dotted lines represent the ±20% deviation limits imposed by EMA and FDA guidelines

As, reported above, these are very preliminary results and more patients samples need to be analyzed to verify the method reproducibility.

4.2.5. Clinical application of DBS-based LC-MS/MS quantification method

The presented method was used to quantify 4 DBS samples from 2 patients affected by HCC, treated with LENVA, and recruited in the ongoing aforementioned analytical cross-validation study (internal protocol code: CRO-2018-83). Finger prick DBS samples collected from patients were no longer quantifiable because they are characterized by variable spot volumes while the sample preparation was based on a specific blood spot volume (10 µL). Thus, only venous DBS samples (see section 3.8.2) collected from patients were quantified.

As reported in section 3.8, DBS samples were analyzed with a calibration curve and triplicates of each QC concentration levels freshly prepared.

Patients' samples were thawed at room temperature, a 8 mm diameter punch was manually performed for 10 µL spot. After that, the entire spot was extracted by adding 300 µL of IS WS and mixed for 30 min in a mechanical stirrer. One-hundred µL of the supernatant were diluted with 50 µL of MP A, vortexed for 10 sec and 130 µL were transferred to a glass autosampler vial for the analysis.

Patients' characteristics and the drug dosage are reported in Table 77, while an example of obtained chromatogram is reported in Figure 55 C and Figure 56 C.

Table 77. Principal demographic and clinical patients' characteristics.

Patients characteristics	N
Sex	1 male
	1 female
Mean age (range)	71 (61-81) years
Therapy	2 samples at 4 mg/day
	2 samples at 8 mg/day

Concentrations found in DBS samples are reported in Table 78. In generally, these quantifications are about 70% of those obtained in the paired plasma samples. The two storage conditions seemed to be similar since the percentage difference between these patients' samples was in the range from -2.9 to 7.7 for Whatman 31 ET CHR and from -9.7 to 6.9 for Whatman 903. Moreover, these preliminary data indicated a good correlation between LENVA concentrations determined in DBS (stored at 80°C) and plasma samples, since the R^2 was 0.984 and 0.987 for Whatman 31 ET CHR and Whatman 903, respectively.

Unfortunately, no further consideration was attempted due to the paucity of the available paired DBS-plasma samples.

Table 78. LENVA concentration determined in 4 venous DBS samples from 2 patients (conc.: concentration; RT: room temperature in the dryer).

Patient sample	LENVA dose (mg/day)	Hours from last intake (hh:mm)	Whatman 31 ET CHR (ng/mL)		Whatman 903 (ng/mL)	
			LENVA conc. at RT	LENVA conc. at -80 °C	LENVA conc. at RT	LENVA conc. at -80 °C
3.5	8	25:15	7.70	8.32	8.31	7.54
3.6	8	24:40	8.70	9.16	8.37	8.97
6.3	4	01:25	16.0	15.5	14.4	14.6
6.4	4	24:35	13.0	13.7	12.2	11.6

For future application of the proposed method in clinical practice, an interesting blood collection device that allows to deposit specific volume of blood drop on the filter paper is represented by HemaXis DB 10 (DBS system SA, Switzerland). Since this commercially available device uses Whatman 903, the implementation of this collection system into our developed method, validated also using this filter paper, will be extremely easy.

4.6. LC-MS/MS method for the quantification of idarubicin and idarubicinol in human plasma

A phase II clinical trial for the evaluation of efficacy and safety of metronomic treatment with IDA for patients affected by HCC to include it as a third-line therapeutic option is ongoing at *C.R.O. di Aviano* (internal protocol code: CRO-2017-42). This trial also requires the quantification of IDA and IDOL C_{min} in the enrolled patients. In the literature three analytical LC-MS/MS method for the quantification of IDA (with or without its active metabolite, IDOL) are reported [246–248]. Among them, only the method proposed by Vail et al. simultaneously quantified IDA and IDOL in dog plasma. Unfortunately, its analytical range was inadequate to cover the plasma concentrations found in human patients (range: 0.5-2000 ng/mL for IDA and 0.1-2000 ng/mL for IDOL) [246].

On this basis, a new LC-MS/MS method for the simultaneously quantification of IDA and IDOL in human plasma was developed.

4.6.1. Mass spectrometric conditions optimization

4.6.1.1. Compound dependent parameters optimization

The monoisotopic masses of IDA, IDOL and DAUNO (IS) are 497.5, 499.5 and 527.5 Da, respectively. The presence of each analyte was verified in Q1 full scan from 300 to 600 Da in positive ion mode with ESI source

detecting the corresponding protonated molecule $[M+H]^+$ at 498.5, 500.4 and 528.5 *m/z*, respectively, as reported in Figure 59.

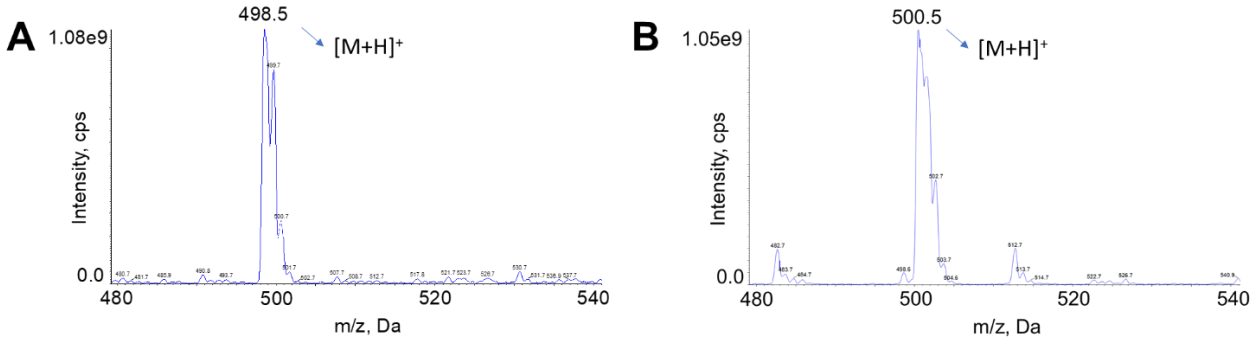

Figure 59. Spectra obtained in positive ion mode with a Q1 scan, which confirm the presence of (A) IDA and (B) IDOL.

Successively, XIC of each protonated molecule was monitored through Q1MI scan mode ramping DP from 0 to 250 V. The optimal DP value for IDA was 65 V, which represents also the maximum XIC intensity. Nonetheless, the maximum XIC intensity for IDOL and DAUNO was at 180 V, but the XIC signals were very unstable. For this reason, optimized DP value for IDOL and DAUNO was set at 65 V, where the signal was sufficiently high and more stable. Figure 60 reported the mass spectra with DP ramping.

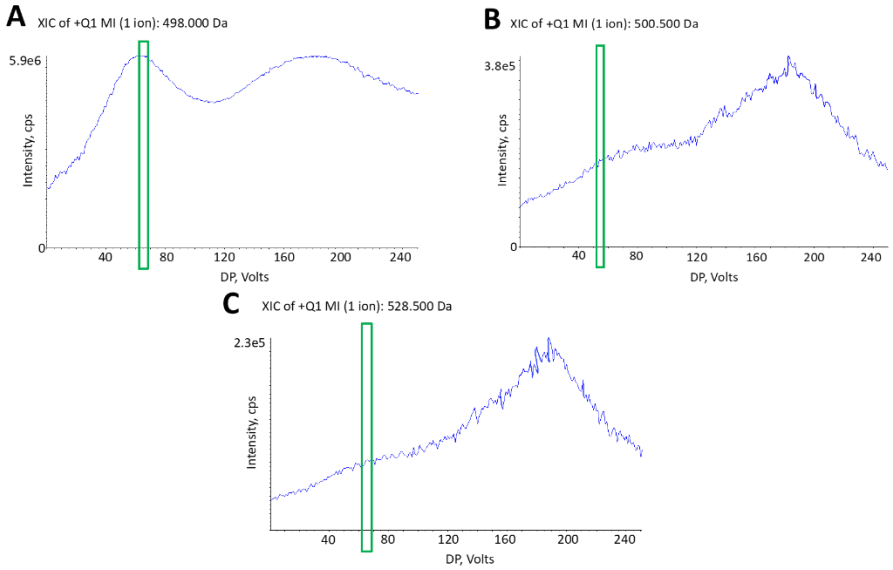

Figure 60. Spectra obtained ramping DP value in positive ion mode with Q1MI scan mode of (A) IDA, (B) IDOL, and (C) DAUNO.

Similarly, the optimization of the EP value was performed by ramping it from 2 to 15 V. Ten V was selected as optimal EP value for each analyte.

Subsequently, the analyte fragmentation pattern was evaluated by ramping CE from 5 to 130 V in the second quadrupole over the MS2 scan mode. For each analyte, the three most representative product ions were identified and selected.

The optimal CE value for each fragment was determined through MRM scan mode by ramping CE value from 5 to 130 V. In particular, the quantifier transition was 498.0 > 130.3 *m/z* for IDA (CE = 20 V), 500.5 > 353.1 *m/z* for IDOL (CE = 15 V) and 528.6 > 321.2 *m/z* for DAUNO (CE = 35 V). While the fragment used to confirm the analyte identity (qualifier) were 498.0 > 291.3 *m/z* (CE = 45 V) and 498.0 > 333.3 *m/z* (CE = 23 V) for IDA, 500.5 > 291.4 *m/z* (CE = 30 V) and 500.5 > 130.1 *m/z* (CE = 22 V) for IDOL, 528.6 > 363.4 *m/z* (CE = 20 V) and 528.6 > 381.4 *m/z* (CE = 15 V) for DAUNO, as reported in Figure 61..

Analogously, the optimal CXP value for all the analytes fragments was 10 V. Moreover, with the precursor ion scan mode it was possible to confirm the direct derivation of the three selected product ions from the precursor ion for each analyte.

In Table 79 the optimized compound dependent parameters are summarized.

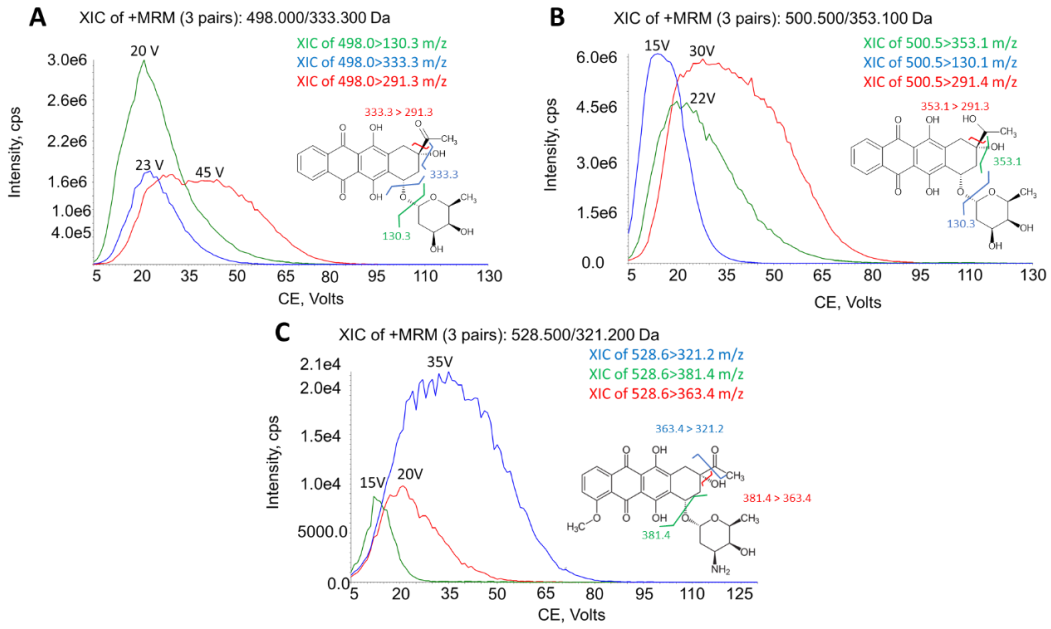

Figure 61. Spectra obtained ramping CE value in positive ion mode in MRM scan mode of (A) IDA, (B) IDOL and (C) DAUNO.

Table 79. Optimized compound dependent parameters of IDA, IDOL and DAUNO (IS).

Compound	Precursor ion			Product ion		
	Q1[a] (*m/z*)	DP[b] (V)	EP[c] (V)	Q3[d] (*m/z*)	CE[e] (V)	CXP[f] (V)
IDA	498.0	65	10	130.3	20	10
				291.3	45	10
				333.3	23	10
IDOL	500.5	65	10	353.1	15	10

Compound	Precursor ion			Product ion		
	Q1[a] (*m/z*)	DP[b] (V)	EP[c] (V)	Q3[d] (*m/z*)	CE[e] (V)	CXP[f] (V)
				291.4	30	10
				130.1	22	10
DAUNO	528.6	65	10	321.2	35	10
				363.4	20	10
				381.4	15	10

[a]first quadrupole mass; [b]declustering potential; [c]entrance potential; [d]third quadrupole mass; [e]collision energy; [f]cell exit potential.

4.6.1.2. Source dependent parameters optimization

The source dependent parameters were optimized in order to reach the maximum possible sensitivity for IDA that was the interested analyte following the procedure reported in section 3.5.1.2.

Specifically, the principal modifications evaluated to each source dependent parameter are reported below:

- TEM: the optimal value was 450 °C. The tested values were 350 °C, 450 °C, 500 °C and 550 °C, as reported in Figure 62;
- ISV: the optimal value was 5000 V. The investigated values were 4000, 5000 and 550 V;
- GS1 and GS2: the optimal values were 30 and 60 psi, respectively. The GS1-GS2 tested values were 40-50 psi, 45-45 psi, 30-50 psi and 30-60 psi;
- CUR: the optimal value was 30 psi. The tested values were 20 psi, 30 psi, 35 psi, 40 psi, 45 psi and 50 psi;
- CAD: the optimal value was Medium, while with Low and High values were observed a decreasing of the XIC intensity.

All the optimized source dependent parameters were summarized in Table 80.

Table 80. Optimized source dependent parameters for IDA, IDOL and DAUNO.

Polarity	Positive ion mode
CUR	30 psi
CAD	Medium
ISV	5500 V
TEM	450°C
GS1	30 psi
GS2	60 psi

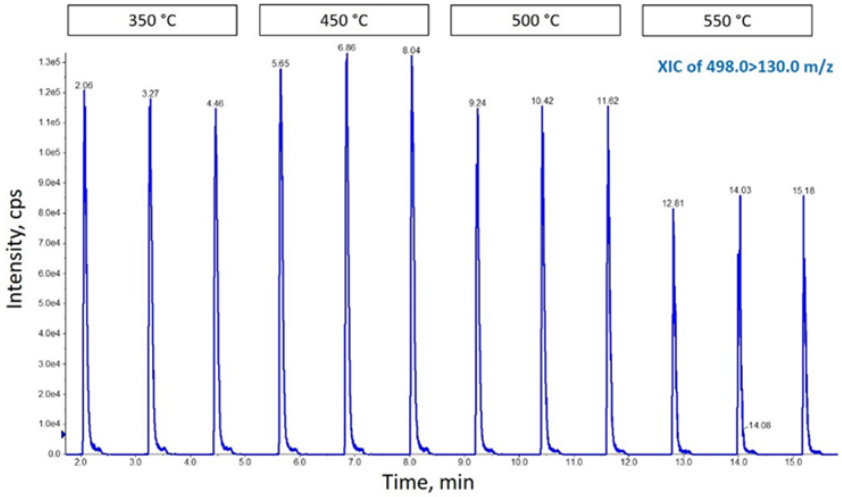

Figure 62. MS/MS spectra representing the XIC trend of IDA quantifier transition during TEM optimization

4.6.2. Chromatographic conditions optimization

Based on the physicochemical properties of the analytes, several columns were tested and Luna Omega Polar C18 (3 µm, 50 x 2.1 mm, 100 Å, Phenomenex) was selected. This SP is characterized by polar groups on its surface. In particular, the interested analytes differ only in methoxy- or a hydroxyl- group and this column gave the best results in terms of peak resolution, thanks its good hydrophobic and hydrophilic selectivity. To lengthen the column life, a Polar C18 Security Guard™ pre-column (4.0 x 2.0 mm, Phenomenex) was used.

Regarding the MPs, both acidified MeOH and ACN were tested as MP B, while acidified MilliQ H_2O was used as MP A (acidification of MPs was used to facilitate the analytes ionization). The peaks shape was less indented using acidified ACN, so it was selected as MP B. Moreover, lower noise background and more symmetrical smoothed peaks were obtained with 0.10% of CH_3COOH (v/v), instead 0.10% of HCOOH (v/v). For this reason, the selected MPs were MilliQ H_2O with 0.10% of CH_3COOH (v/v) as MP A and ACN plus 0.10% of CH_3COOH (v/v) as MP B. The column oven temperature was set at 50 °C.

Subsequently, a multi-step chromatographic method was chosen to guarantee the constant column regeneration necessary due to low purity of the injected samples. The most relevant tested methods were summarized below.

Initially, a linear gradient from 10% to 50% of MP B over 6 min (6.7% of MP B/min) was tested to determine both analytes chromatographic behaviour and the theoretical percentage of MP B necessary to analytes elution (40% of MP B). This gradient was followed by a washing phase at 98% of MP B for 1 min, in order to remove lipophilic contaminants of the plasmatic matrix, as well as possible residues of analytes held in the column. Afterward, a reconditioning phase was set at 10% of MP B for 1.8 min to equilibrate the column. This time corresponds to about 7 column volumes (column volume is about 0.1 mL and the flow rate was 0.4 mL/min), but it was sufficient to ensure method reproducibility since no shift of analytes retention time after

consecutives runs was observed. The peaks obtained with this method were baseline separated (0.30 min), symmetrical and narrow, as reported in Figure 63.

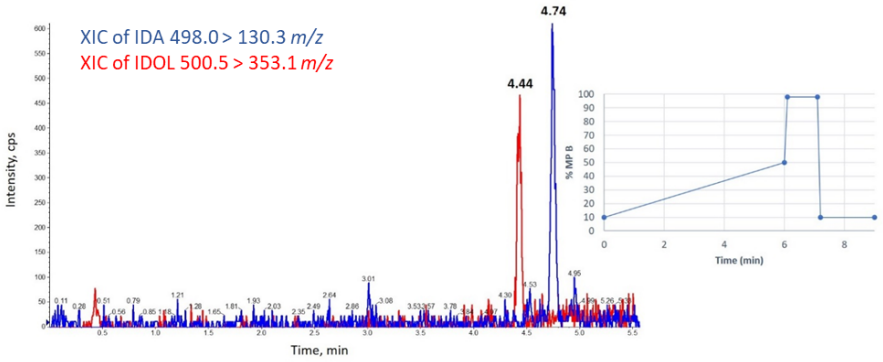

Figure 63. MRM chromatogram from 0.0 to 5.5 min of 0.20 ng/mL of IDA and IDOL in solvent sample. The time program is reported on the right.

This method was used to determine the best sample preparation (for more details see section 4.6.3). Once the sample processing was defined, the initial chromatographic method was re-evaluated and optimized to obtain the final one.

To reduce the total runtime, shorter and steeper gradients were evaluated preserving as much as possible the baseline separation of the peaks and maintaining the same duration for the washing and reconditioning phases (1.0 and 1.8 min, respectively).

In Figure 64 the three tested gradients are reported. The analyzed sample was IDA and IDOL at the concentration of 0.20 ng/mL in solvent. In the first case the gradient started from 10% to 50% of MP in 4 min (10% of MP B/min with a total run time of 7 min). The analytes retention time was anticipated of *circa* 1 min without differences in terms of peaks and symmetry but with a slightly lower separation degree (0.23 *versus* 0.30 min), as reported in Figure 64 A. Nevertheless, the sensitivity was poor with a S/N of 9-10 for both IDA and IDOL at the concentration of 0.02 ng/mL, thus the LLOQ (0.10 ng/mL for IDA and IDOL) was not quantifiable, and the analytes eluted too closed to the washing phase. To anticipate the analytes elution, a steeper gradient was tested (10-60% of MP B over 4 min; 12.5% of MP B/min with a total run time of 7 min). In this case, the analytes retention time was about 0.4 min earlier without differences in separation degree and peaks shape, but with a better sensitivity (S/N of 10-15 for both IDA and IDOL), as described in Figure 64 B.

Moreover, a steeper gradient from 10% to 60% of MP B in 3.5 min (14.3% of MP B/min with a total run time of 6.5 min) was tested to further anticipated analyte elution. IDOL retention time was the same of the previous method, while IDA was slightly anticipated (0.08 min) inducing a lower separation degree (0.15 min), as reported in Figure 64 C.

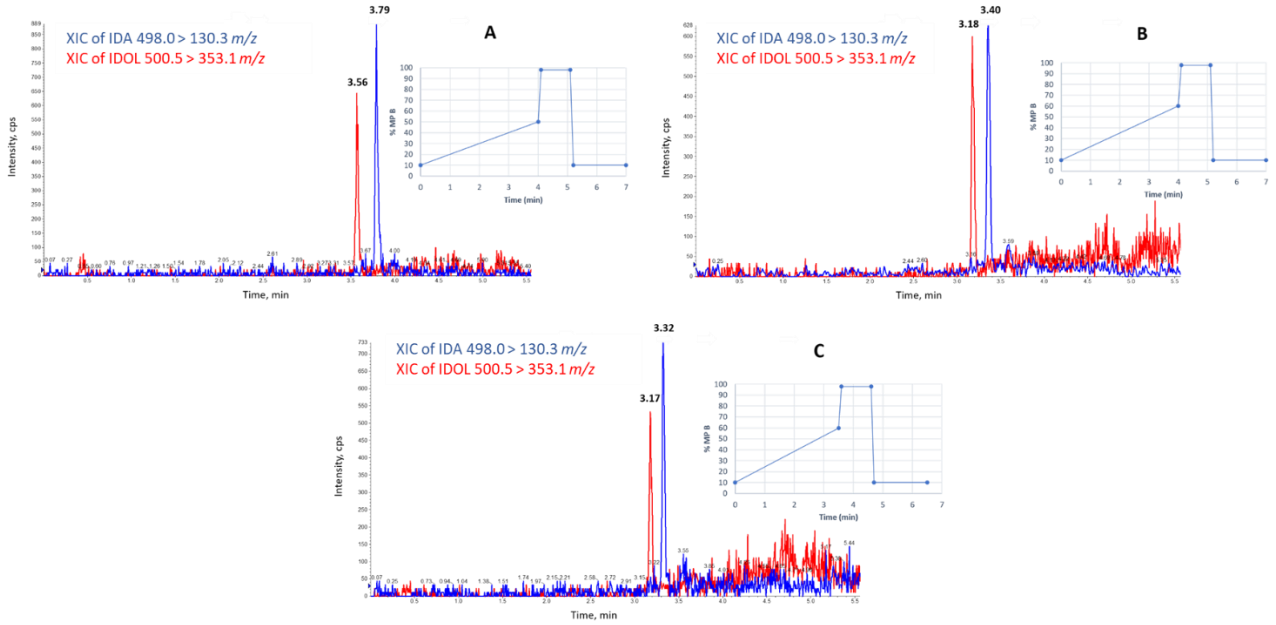

Figure 64. MRM chromatogram (from 0 to 5.5 min) obtained by the analysis of a solvent sample containing 0.20 ng/mL for IDA and IDOL with elution gradient (A) from 10 to 50% of MPB in 4 min, (B) from 10 to 60% of MPB in 4 min, and (C) from 10 to 60% of MPB in 3.5 min.

Hence, the gradient from 10 to 60% of MP B over 4 min was selected because it allowed to obtain narrow, symmetrical, well separated peaks, together with the best method sensitivity, in a reasonable total runtime (7 min).

The final multi-step chromatographic method was characterized by the following phases:

- from 10 to 60% of MP B over 4 min (elution phase);
- from 60% to 98% of MP B over 0.1 min and kept constant for 1.0 min (washing phase);
- MP B initial condition was restored in 0.1 min and kept constant for 1.8 min (reconditioning phase).

Afterward, to establish the optimal initial MP B percentage, 5% and 15% were tested, evaluating the same gradient up to 60% of MP B reached in 4.4 and 3.6 min, respectively, to maintain the same slope of the chromatographic method previously selected (12.5% of MP B/min). Both the methods did not introduce any significant improvements thus gradient from 10 to 60% over 4 min was preserved.

In all the experiments executed until now, 4 µL of injection volume was used, but unfortunately, LLOQ samples at 0.10 ng/mL for both IDA and IDOL were not quantifiable since S/N was minor than 5. To obtain a quantifiable LLOQ, 5 and 6 µL as injection volume were tested. No significant improvement was reached using 5 µL, while with 6 µL the S/N of IDA and IDOL was *circa* 8 and 11, respectively, achieving the purpose.

Finally, the carryover phenomenon was investigated as reported for the other methods presented in this thesis and the employed precautions were:

- efficient injection needle washing solution: MilliQ H_2O:ACN:MeOH:iPrOH (25:25:25:25, v/v/v/v) with 0.10% of HCOOH (v/v);
- strong column washing at 98% of MP B for 1 min;

- injection of two MeOH:iPrOH (50:50, v/v) and two blank samples after ULOQ and QCH analysis.

In this way, no analytes or IS peak higher than 20% of LLOQ or 5% of IS, respectively, were observed in the second cleaning blank sample after the analysis of a high IDA and IDOL concentration plasma sample, as reported in Figure 65.

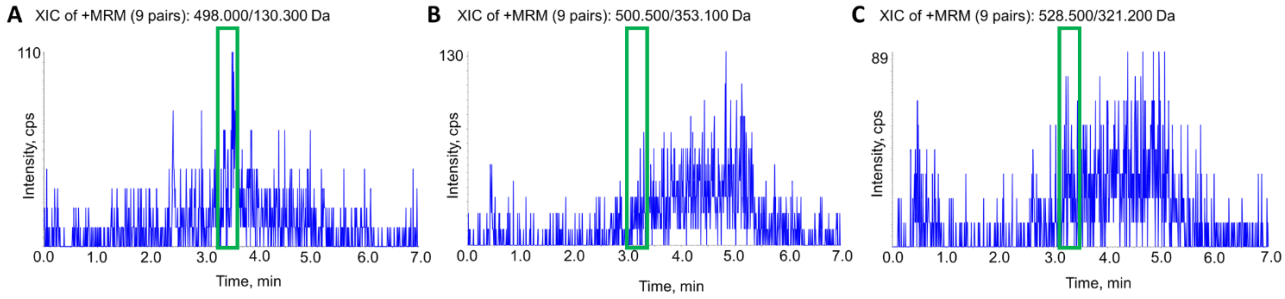

Figure 65. MRM chromatogram (from 0 to 7 min) obtained by injecting a blank sample after two MeOH:iPrOH (50:50, v/v) washing run and another blank sample. The XIC trend of (A) IDA, (B) IDOL, and (C) DAUNO.

4.6.3. Sample preparation for quantitative analysis

4.6.3.1. Plasma sample extraction optimization

A simple and rapid sample extraction procedure was our purpose, and for this reason the PP was selected. Moreover, it was compatible with the total amount of circulating IDA and IDOL bound to plasma protein, which is 97% and 94%, respectively [108].

The sample extraction optimization was performed using a plasma sample with our prefixed LLOQ concentration (0.10 ng/mL for both IDA and IDOL) based on IDA plasma concentration reported in the literature [104].

To perform the PP, DAUNO solutions of 50 ng/mL in both MeOH and ACN were tested with three different plasma:solvent *ratios* (1:3, 1:4 and 1:5). The optimal solvent was ACN, while the best *ratio* was 1:5 because they allowed the best analytes extraction. Unfortunately the LLOQ sample was not quantifiable (S/N < 5).

To obtain a quantifiable LLOQ, a concentration step was introduced through sample evaporation, although it increased duration and complexity of the sample preparation workflow. In detail, 1000 µL of supernatant obtained after the PP step were transferred in polypropylene tubes and evaporated to dryness at 25 °C under vacuum conditions. The duration of the evaporation step was 22-24 h for samples extracted with MeOH and 4-6 h when CAN was used, because it allowed to obtain a cleaner supernatant as compare to that obtained using MeOH. This was another important point that corroborated the choice of ACN to perform the PP.

Subsequently, the optimal solvent for the re-dissolution of the dry residue was investigated. The dry residue was reconstituted with 100 µL of 0.10% of HCOOH in MeOH (v/v), 0.10% of HCOOH in ACN (v/v), 0.10% of HCOOH in iPrOH (v/v), and 0.10% of HCOOH in MilliQ H_2O (v/v) for both the samples extracted with MeOH

and ACN. Unfortunately, coarse suspensions were obtained for all the samples. Thus, mixture of these solvents were tested to try to get a cleaner solution: MilliQ H_2O:MeOH (50:50, v/v) with 0.10% of HCOOH (v/v), MilliQ H_2O:MeOH (50:50, v/v) with 0.10% of HCOOH (v/v), MilliQ H_2O:ACN (50:50, v/v) with 0.10% of HCOOH (v/v), MilliQ H_2O:iPrOH (50:50, v/v) with 0.10% of HCOOH (v/v).

After 30 sec of vortex mixing, a qualitatively limpid solution was obtained for:

- MilliQ H_2O:iPrOH (50:50, v/v) with 0.10% of HCOOH (v/v) for both samples extracted with MeOH and ACN;
- MilliQ H_2O:ACN (50:50, v/v) with 0.10% of HCOOH (v/v) only for samples extracted with ACN;
- MilliQ H_2O:MeOH (50:50, v/v) with 0.10% of HCOOH (v/v) after also centrifugation at 16200 g and 4 °C for 10 min only for samples extracted with ACN.

After that, different volumes of these mixtures were tested (50, 100, 200, and 400 µL) only for limpid solutions, and 50 µL was selected since no suspension was observed and in order to keep analytes more concentrated.

Unfortunately, a white residue at the bottom of the glass vial was notice after storage in AS at 4 °C. In particular, samples extracted with MeOH precipitated after 24 h, while samples extracted with ACN precipitated after 48 h, with the exception of samples re-dissolved with MilliQ H_2O:ACN (50:50, v/v) with 0.10% of HCOOH (v/v) which precipitated after 24 h. The presence of this phenomenon was very limiting because it cannot ensure the quality of the analyzed samples and can clogged the LC system and the column. For this reason, only MilliQ H_2O:iPrOH (50:50, v/v) with 0.10% of HCOOH (v/v) for both samples extracted in MeOH and ACN and MilliQ H_2O:MeOH (50:50, v/v) with 0.10% of HCOOH (v/v) only for samples extracted with ACN were considered for further analysis, while the other mixture were discarded.

Moreover, the following solvent were excluded in order to reduce the time of the samples preparation:

- MeOH to perform the PP due to the longer time necessary to evaporate the supernatant;
- H_2O:MeOH (50:50, v/v) with 0.10% of HCOOH (v/v) to re-dissolve samples extracted with ACN due to the additional centrifugation step.

To summarize, ACN was used to perform drug extraction (PP) from plasma samples thanks to its higher efficiency and its shorter duration of the evaporation step, while 50 µL of MilliQ H_2O:iPrOH (50:50, v/v) with 0.10% of HCOOH (v/v) was selected to re-dissolve the dry sample.

4.6.3.2. Calibration curve and quality controls preparation

Two different stock solutions (one for calibrators and one for QCs) were prepared in DMSO at the concentration of 1 mg/mL and stored at -80 °C for each analyte. To prepare the calibrators, two intermediate solutions in MeOH with both IDA and IDOL were prepared at 10 µg/mL and 100 ng/mL diluting the stock solutions. These intermediate solutions were again diluted with MilliQ H_2O:MeOH (50:50, v/v) to obtain the

calibrators final concentrations (from A to H) of 4000, 2000, 1000, 500, 100, 20, 4 and 2 ng/mL. Analogously, stock solutions for QCs (QCH, QCM and QCL) were mixed together to achieve the intermediate concentration of 10 µg/mL in MeOH. After that, this solution was diluted in MilliQ H_2O:MeOH (50:50, v/v) to reach the final concentration of 3000, 300 and 6 ng/mL. For all the WSs, 1-mL aliquots were stored at -20 °C to use for the samples preparation and the remaining WSs were kept in polypropylene tubes and stored at -80 °C.

IS stock solution was prepared in DMSO at the concentration of 1 mg/mL and further diluted in ACN to obtain the final concentration of 50 ng/mL. This solution was directly used to precipitate plasma proteins during the sample processing. The stock and intermediate solutions were kept in polypropylene tubes and stored at -80 °C, while the WSs were stored at -20 °C until use.

Calibration curve and QCs were freshly prepared through the following steps: 10 µL of proper WS were added to 190 µL of blank pooled human plasma (dilution 1:20) and vortexed for 10 sec, after that 1000 µL of IS WS (dilution 1:6) were added to perform PP, vortexed and then centrifuged for 15 min at 16200 g and 4 °C. One-thousand µL of clean supernatant were transferred to a polypropylene tube and evaporated to dryness under vacuum conditions at 25 °C for 4-6 h. Each dry residue was re-dissolved by adding 50 µL of Milli H_2O:iPrOH (50:50, v/v) plus 0.10% of HCOOH (v/v); the resulting limpid solution was mechanically shaken for 30 min and finally transferred in a glass vial until the LC-MS/MS analysis.

Consequently, plasma samples presented the following concentrations for the calibration curve and QCs reported in Table 81.

Table 81. Final concentrations of calibrators and QCs in plasma samples for IDA and IDOL.

Sample	IDA and IDOL conc. (ng/mL)
H	0.10
G	0.20
F	1.00
E	5.00
D	25.0
C	50.0
B	100
A	200
QCL	0.30
QCM	15.0
QCH	150

4.6.4. LC-MS/MS method validation study for idarubicin and idarubicinol

Due to the breakdown of the evaporator, it was not possible to complete the validation study for this method. The validation process will follow the procedures reported in section 3.6 it will be performed in the next months.

5. CONCLUSIONS

The introduction of SORA and LENVA as alternative first-line therapy, and REGO as second-line therapy in patients affected by advanced HCC has led to improvements in their clinical outcomes. However, high inter-individual variability in plasma concentrations is reported for these oral anticancer agents and TDM could represent a useful tool to personalize patients' therapy and maximize treatment benefits. LC-MS/MS methods are the gold standard technique to quantify drugs in human fluids (usually plasma) for TDM application in clinical practice. Nonetheless, this technique has some limitations that can be overcome by the use of DBS as a matrix. In fact, the use of DBS could increase patient compliance, reduce analysis costs and facilitate samples storage. For this reason, LC-MS/MS for the quantification of SORA, LENVA, and REGO in both plasma and DBS samples were developed, validated, and applied.

Firstly, a novel LC-MS/MS method for the simultaneous quantification of SORA, REGO, and their active metabolites in human plasma has been developed and fully validated according to EMA and FDA guidelines. Thanks to the wide concentration range for all the analytes, the short run time (7 min), the low amount of plasma necessary for the analysis (5 µL), and the rapid and simple sample processing based on PP, this method overcame some limitations of the already published methods. Moreover, the negative ionization mode, instead of the positive one applied in a previously published paper [234], allowed to considerably increase the sensitivity making the proposed method a useful choice for anyone who has a sensitivity problem. Linearity was defined ($R \geq 0.998$) over the concentration ranges of 50-8000 ng/mL for SORA and REGO, and 30-4000 ng/mL for their metabolites, appropriately covering the therapeutic plasma concentrations. The presented method also showed adequate results in terms of intra- and inter-day precision (CV ≤ 7.2%) and accuracy (between 89.4% and 109%), sensitivity, selectivity, and reproducibility. Once successfully validated, this method was applied to quantify the C_{min} of SORA, REGO, and their active metabolites in 66 plasma samples collected from 16 patients affected by HCC and enrolled in an ongoing cross-validation study (internal protocol code: CRO-2018-83). Although the patients' paucity, some preliminary considerations could be performed, as less than 50% (42.5% for SORA and 25.0% for REGO) of the plasma samples collected at the C_{min} has a concentration above the threshold proposed for the TDM (3750 ng/mL for SORA and 1400 ng/mL for REGO). More considerations can be drawn by expanding the sample size.

The same LC-MS/MS was also used to quantify SORA, REGO, and their active metabolites in DBS samples collected on Whatman 31 ET CHR filter paper. Due to the presence of Hct and volume spot effects on the quantification, a volumetric sampling system was necessary. For this reason, the method was fully validated according to EMA and FDA guidelines and EBF recommendation analyzing the whole DBS spot (5 µL) assessing recovery (≥ 51.7%), the absence of matrix effect, process efficiency (near 80% for SORA and REGO, near 50%, 70% and 30% for oxSORA, oxREGO, and des-oxREGO, respectively), Hct effect (CV ≤ 9% and accuracy within 89.9-114%), linearity ($R \geq 0.998$), intra- and inter-day precision (CV ≤ 10%) and accuracy (92.1 - 108%), selectivity and sensitivity, dilution integrity, reproducibility with ISR, and stability. After the validation, this

method was applied for the quantification of 63 DBS samples from 16 patients treated with SORA or REGO and collected within the cross-validation study (*i.e.,* the paired samples of the corresponding and already analyzed plasma samples). The analyzed patients' samples were obtained from venous blood because a volumetric system to collect the finger prick blood drops was not available and not planned by the clinical protocol. To verify the possibility to use DBS as alternative samples for the quantification of these analytes, firstly it was necessary to apply a mathematical conversion to the DBS measurement to obtain the expected plasma concentration. Then, the expected plasma concentration was compared to the actual plasma measurement through a cross-validation study to verify if the two analytical methods were equivalent and the same drug plasma levels were determined in patients. DBS samples concentrations were on average slightly lower than the plasma levels, with a DBS-to-plasma ratio ranging from 0.6 (for oxSORA) to 0.8 (for SORA and REGO). Several conversion methods were applied to the measured DBS values to obtain the expected plasma concentrations. The best predictive performance (76%) was obtained with the application of the conversion method based on $K_{BC/pla}$ for SORA and its metabolite, while for REGO and oxREGO the highest percentage of equivalence (78%) was obtained with the CF-based conversion method. Only for des-oxREGO no conversion method allowed an acceptable predictive performance. Although the DBS-based method works analytically, nevertheless the correlation with the plasma values would have to be improved especially for des-oxREGO. Thanks to the better knowledge acquired by our group with the following DBS-based methods development and with the introduction of the IATDMCT validation guidelines for the DBS method (introduced after the development of this method), this method could be re-evaluated especially as regards the hematocrit and spot volume effects to improve the DBS-to-plasma correlation. Anyway, to the best of our knowledge, it is the first LC-MS/MS method for the simultaneous quantification of these analytes in DBS matrix.

Then, a new LC-MS/MS method for the quantification of LENVA in human plasma was developed and fully validated according to EMA and FDA guidelines. Its characteristics include a wide analytical range, a short run time (4 min), a low plasma volume necessary for the analysis (100 µL), and a simple and rapid sample preparation based on PP. The linearity was defined ($R \geq 0.997$) over LENVA concentration range of 0.5-2000 ng/mL. This analytical range not only properly covered the therapeutic plasma concentrations of HCC patients but also makes the method applicable for PK investigations in patients affected by other pathologies which require higher doses (24 mg/day) of LENVA. The method showed adequate results in terms of intra- and inter-day precision and accuracy (CV ≤ 11% and within 93.6-109%), analyte recovery from the matrix (≥ 95.6%), sensitivity, selectivity, dilutional integrity, reproducibility with ISR, absence of matrix effect and stability under various conditions that can be encountered in the laboratory practice.

Once successfully validated, the presented method was applied to quantify LENVA in 24 samples collected from 6 patients affected by advanced HCC enrolled in the ongoing cross-validation study (internal protocol code: CRO-2018-83). Due to the paucity of the collected samples, no conclusive considerations could be

drawn. However, a certain inter-patients variability in drug concentration was observed. As the case of the previous method, the proposed LC-MS/MS assay was used as a reference method to clinically validate the corresponding DBS-based method. In fact, the same developed LC-MS/MS method to quantify LENVA in plasma was applied to measure the drug also in DBS samples, with a slightly reduced analytical range (5-2000 ng/mL) due to sensitivity problems. Also in this case, a volumetric sampling was required to avoid the Hct effect. This method was fully validated according to EMA and FDA guidelines, EBF recommendation, and IATDMCT guidelines in both Whatman 31 ET CHR and Whatman 903 as filter papers obtaining similar results. The parameters evaluated during the validation was Hct effect (CV ≤ 6.2% and accuracy within 103-112% and CV ≤ 5.5% and accuracy within 96-105% for Whatman 31 ET CHR and Whatman 903, respectively), recovery (≥ 77% for both filter papers), the absence of matrix effect, process efficiency (near 72% for Whatman 31 ET CHR and near 77% for Whatman 903), linearity (R ≥ 0.998 for Whatman 31 ET CHR and R ≥ 0.999 for Whatman 903), intra- and inter-day precision (CV ≤ 7% and 8.8% for Whatman 31 ET CHR and Whatman 903, respectively) and accuracy (92.8 - 108% and 95.9 – 104% for Whatman 903), selectivity and sensitivity, reproducibility with ISR and stability. Due to the paucity of the samples, no consideration and cross-validation test can be performed yet. Preliminary evaluation showed that DBS concentrations were on average 70% than plasma measurements. In the next months, a volumetric device (HemaXis) to collect 10 µL of whole blood from finger-prick will be tested to quantify LENVA in finger-prick DBS samples. This solution can be a possible strategy to perform TDM in DBS samples for those drugs, like LENVA, SORA, and REGO, that require a volumetric collection system.

Lastly, to support the phase II clinical trial entitled "*Studio di Fase II che valuta l'efficacia e la sicurezza del trattamento metronomico orale con Idarubicina in pazienti affetti da Epatocarcinoma allo stadio intermedio-avanzato dopo fallimento o intolleranza a Sorafenib e Regorafenib*" ongoing at the *C.R.O. di Aviano,* a new LC-MS/MS for the simultaneous quantification of IDA and IDOL in human plasma was developed. This method was characterized by a good chromatographic resolution and a fast runtime (7 min) and it showed a good preliminary result of linearity (analytical range: 0.10-200 ng/mL for both IDA and IDOL). In order to guarantee an adequate sensitivity (S/N ≥ 5) for LLOQ (0.10 ng/mL for both IDA and IDOL) quantification, an evaporation step turned out to be essential in sample preparation workflow, which in complex resulted to be simple and reliable. Based on these results achieved up to now, the next step will be a complete validation of the obtained analytical method according to EMA and FDA guidelines. Once the analytical method will be validated, the future outlooks include the quantification of IDA and IDOL C_{min} in patients affected by advanced HCC enrolled in the aforementioned phase II clinical trial (internal protocol code: CRO-2017-42), which evaluates the efficacy and safety of metronomic treatment with IDA in order to include it as a third-line therapeutic option.

The application of these newly developed methods will help to deepen the knowledge about intra- and inter-patient drug exposure of SORA, REGO, LENVA, and IDA-IDOL and to further evaluate their possible

correlations with response to therapy or toxicity development in the perspective of TDM application in clinical practice.

REFERENCES

1. Cancer today, all cancer fact sheet. Available: https://gco.iarc.fr/today/data/factsheets/cancers/39-All-cancers-fact-sheet.pdf

2. Global Cancer Statistics 2020: GLOBOCAN Estimates of Incidence and Mortality Worldwide for 36 Cancers in 185 Countries - Sung - 2021 - CA: A Cancer Journal for Clinicians - Wiley Online Library. Available: https://acsjournals.onlinelibrary.wiley.com/doi/full/10.3322/caac.21660

3. Cancer today. Available: http://gco.iarc.fr/today/home

4. El–Serag HB, Rudolph KL. Hepatocellular Carcinoma: Epidemiology and Molecular Carcinogenesis. Gastroenterology. 2007;132: 2557–2576. doi:10.1053/j.gastro.2007.04.061

5. Global Burden of Disease Liver Cancer Collaboration, Akinyemiju T, Abera S, Ahmed M, Alam N, Alemayohu MA, et al. The Burden of Primary Liver Cancer and Underlying Etiologies From 1990 to 2015 at the Global, Regional, and National Level: Results From the Global Burden of Disease Study 2015. JAMA Oncol. 2017;3: 1683. doi:10.1001/jamaoncol.2017.3055

6. El-Serag HB. Epidemiology of Viral Hepatitis and Hepatocellular Carcinoma. Gastroenterology. 2012;142: 1264-1273.e1. doi:10.1053/j.gastro.2011.12.061

7. White DL, Thrift AP, Kanwal F, Davila J, El-Serag HB. Incidence of Hepatocellular Carcinoma in All 50 United States, From 2000 Through 2012. Gastroenterology. 2017;152: 812-820.e5. doi:10.1053/j.gastro.2016.11.020

8. Galle PR, Forner A, Llovet JM, Mazzaferro V, Piscaglia F, Raoul J-L, et al. EASL Clinical Practice Guidelines: Management of hepatocellular carcinoma. J Hepatol. 2018;69: 182–236. doi:10.1016/j.jhep.2018.03.019

9. Bosetti C, Levi F, Boffetta P, Lucchini F, Negri E, La Vecchia C. Trends in mortality from hepatocellular carcinoma in Europe, 1980-2004. Hepatology. 2008;48: 137–145. doi:10.1002/hep.22312

10. Ghouri YA, Mian I, Rowe JH. Review of hepatocellular carcinoma: Epidemiology, etiology, and carcinogenesis. J Carcinog. 2017;16. doi:10.4103/jcar.JCar_9_16

11. Jindal A, Thadi A, Shailubhai K. Hepatocellular Carcinoma: Etiology and Current and Future Drugs. J Clin Exp Hepatol. 2019;9: 221–232. doi:10.1016/j.jceh.2019.01.004

12. McGlynn KA, London WT. The Global Epidemiology of Hepatocellular Carcinoma: Present and Future. Clin Liver Dis. 2011;15: 223–243. doi:10.1016/j.cld.2011.03.006

13. Sanyal AJ, Yoon SK, Lencioni R. The Etiology of Hepatocellular Carcinoma and Consequences for Treatment. The Oncologist. 2010;15: 14–22. doi:10.1634/theoncologist.2010-S4-14

14. Weltman MD, Brotodihardjo A, Crewe EB, Farrell GC, Bilous M, Grierson JM, et al. Coinfection with hepatitis B and C or B, C and delta viruses results in severe chronic liver

disease and responds poorly to interferon-alpha treatment. J Viral Hepat. 1995;2: 39–45. doi:10.1111/j.1365-2893.1995.tb00070.x

15. Soriano V, Vispo E, Labarga P, Medrano J, Barreiro P. Viral hepatitis and HIV co-infection. Antiviral Res. 2010;85: 303–315. doi:10.1016/j.antiviral.2009.10.021

16. Tsilidis KK, Kasimis JC, Lopez DS, Ntzani EE, Ioannidis JPA. Type 2 diabetes and cancer: umbrella review of meta-analyses of observational studies. BMJ. 2015;350: g7607. doi:10.1136/bmj.g7607

17. Calle EE, Rodriguez C, Walker-Thurmond K, Thun MJ. Overweight, Obesity, and Mortality from Cancer in a Prospectively Studied Cohort of U.S. Adults. N Engl J Med. 2003;348: 1625–1638. doi:10.1056/NEJMoa021423

18. Younossi ZM, Blissett D, Blissett R, Henry L, Stepanova M, Younossi Y, et al. The economic and clinical burden of nonalcoholic fatty liver disease in the United States and Europe. Hepatology. 2016;64: 1577–1586. doi:10.1002/hep.28785

19. Welzel TM, Graubard BI, Quraishi S, Zeuzem S, Davila JA, El-Serag HB, et al. Population-Attributable Fractions of Risk Factors for Hepatocellular Carcinoma in the United States: Am J Gastroenterol. 2013;108: 1314–1321. doi:10.1038/ajg.2013.160

20. Nahon P, Sutton A, Rufat P, Ziol M, Akouche H, Laguillier C, et al. Myeloperoxidase and superoxide dismutase 2 polymorphisms comodulate the risk of hepatocellular carcinoma and death in alcoholic cirrhosis. Hepatology. 2009;50: 1484–1493. doi:10.1002/hep.23187

21. Shen H-M, Ong C-N. Mutations of the p53 tumor suppressor gene and ras oncogenes in aflatoxin hepatocarcinogenesis. Mutat Res Genet Toxicol. 1996;366: 23–44. doi:10.1016/S0165-1110(96)90005-6

22. Deugnier YM, Guyader D, Crantock L, Lopez J-M, Turlin B, Yaouanq J, et al. Primary liver cancer in genetic hemochromatosis: A clinical, pathological, and pathogenetic study of 54 cases. Gastroenterology. 1993;104: 228–234. doi:10.1016/0016-5085(93)90856-8

23. Forner A, Reig M, Bruix J. Hepatocellular carcinoma. The Lancet. 2018;391: 1301–1314. doi:10.1016/S0140-6736(18)30010-2

24. Yang JD, Hainaut P, Gores GJ, Amadou A, Plymoth A, Roberts LR. A global view of hepatocellular carcinoma: trends, risk, prevention and management. Nat Rev Gastroenterol Hepatol. 2019;16: 589–604. doi:10.1038/s41575-019-0186-y

25. Papatheodoridis GV, Idilman R, Dalekos GN, Buti M, Chi H, van Boemmel F, et al. The risk of hepatocellular carcinoma decreases after the first 5 years of entecavir or tenofovir in Caucasians with chronic hepatitis B. Hepatology. 2017;66: 1444–1453. doi:10.1002/hep.29320

26. Morgan RL, Baack B, Smith BD, Yartel A, Pitasi M, Falck-Ytter Y. Eradication of hepatitis C virus infection and the development of hepatocellular carcinoma: a meta-analysis of observational studies. Ann Intern Med. 2013;158: 329–337. doi:10.7326/0003-4819-158-5-201303050-00005

27. Furlan A, Marin D, Cabassa P, Taibbi A, Brunelli E, Agnello F, et al. Enhancement pattern of small hepatocellular carcinoma (HCC) at contrast-enhanced US (CEUS), MDCT, and MRI: intermodality agreement and comparison of diagnostic sensitivity between 2005 and 2010 American Association for the Study of Liver Diseases (AASLD) guidelines. Eur J Radiol. 2012;81: 2099–2105. doi:10.1016/j.ejrad.2011.07.010

28. Singal A, Volk ML, Waljee A, Salgia R, Higgins P, Rogers M a. M, et al. Meta-analysis: surveillance with ultrasound for early-stage hepatocellular carcinoma in patients with cirrhosis. Aliment Pharmacol Ther. 2009;30: 37–47. doi:10.1111/j.1365-2036.2009.04014.x

29. Llovet JM, Montal R, Sia D, Finn RS. Molecular therapies and precision medicine for hepatocellular carcinoma. Nat Rev Clin Oncol. 2018;15: 599–616. doi:10.1038/s41571-018-0073-4

30. Bressac B, Kew M, Wands J, Ozturk M. Selective G to T mutations of p53 gene in hepatocellular carcinoma from southern Africa. Nature. 1991;350: 429–431. doi:10.1038/350429a0

31. Jablkowski M, Bocian A, Bialkowska J, Bartkowiak J. A comparative study of P53/MDM2 genes alterations and P53/MDM2 proteins immunoreactivity in liver cirrhosis and hepatocellular carcinoma. J Exp Clin Cancer Res CR. 2005;24: 117–125.

32. Llovet JM, Chen Y, Wurmbach E, Roayaie S, Fiel MI, Schwartz M, et al. A molecular signature to discriminate dysplastic nodules from early hepatocellular carcinoma in HCV cirrhosis. Gastroenterology. 2006;131: 1758–1767. doi:10.1053/j.gastro.2006.09.014

33. Higashitsuji H, Higashitsuji H, Itoh K, Sakurai T, Nagao T, Sumitomo Y, et al. The oncoprotein gankyrin binds to MDM2/HDM2, enhancing ubiquitylation and degradation of p53. Cancer Cell. 2005;8: 75–87. doi:10.1016/j.ccr.2005.06.006

34. Higashitsuji H, Itoh K, Nagao T, Dawson S, Nonoguchi K, Kido T, et al. Reduced stability of retinoblastoma protein by gankyrin, an oncogenic ankyrin-repeat protein overexpressed in hepatomas. Nat Med. 2000;6: 96–99. doi:10.1038/71600

35. Azechi H, Nishida N, Fukuda Y, Nishimura T, Minata M, Katsuma H, et al. Disruption of the p16/Cyclin D1/Retinoblastoma Protein Pathway in the Majority of Human Hepatocellular Carcinomas. Oncology. 2001;60: 346–354. doi:10.1159/000058531

36. Yamada T, Souza ATD, Finkelstein S, Jirtle RL. Loss of the gene encoding mannose 6-phosphate/insulin-like growth factor II receptor is an early event in liver carcinogenesis. Proc Natl Acad Sci. 1997;94: 10351–10355. doi:10.1073/pnas.94.19.10351

37. Daher S, Massarwa M, Benson AA, Khoury T. Current and Future Treatment of Hepatocellular Carcinoma: An Updated Comprehensive Review. J Clin Transl Hepatol. 2018;6: 1–10. doi:10.14218/JCTH.2017.00031

38. Nishida N, Kudo M. Oncogenic Signal and Tumor Microenvironment in Hepatocellular Carcinoma. Oncology. 2017;93: 160–164. doi:10.1159/000481246

39. Liu Z, Lin Y, Zhang J, Zhang Y, Li Y, Liu Z, et al. Molecular targeted and immune checkpoint therapy for advanced hepatocellular carcinoma. J Exp Clin Cancer Res. 2019;38. doi:10.1186/s13046-019-1412-8

40. Okuda K, Ohtsuki T, Obata H, Tomimatsu M, Okazaki N, Hasegawa H, et al. Natural history of hepatocellular carcinoma and prognosis in relation to treatment study of 850 patients. Cancer. 1985;56: 918–928. doi:10.1002/1097-0142(19850815)56:4<918::AID-CNCR2820560437>3.0.CO;2-E

41. Llovet JM, Bustamante J, Castells A, Vilana R, Ayuso MDC, Sala M, et al. Natural history of untreated nonsurgical hepatocellular carcinoma: Rationale for the design and evaluation of therapeutic trials. Hepatology. 1999;29: 62–67. doi:10.1002/hep.510290145

42. Cabibbo G, Enea M, Attanasio M, Bruix J, Craxì A, Cammà C. A meta-analysis of survival rates of untreated patients in randomized clinical trials of hepatocellular carcinoma. Hepatology. 2010;51: 1274–1283. doi:10.1002/hep.23485

43. Llovet JM, Kelley RK, Villanueva A, Singal AG, Pikarsky E, Roayaie S, et al. Hepatocellular carcinoma. Nat Rev Dis Primer. 2021;7: 6. doi:10.1038/s41572-020-00240-3

44. Jiao Q, Bi L, Ren Y, Song S, Wang Q, Wang Y. Advances in studies of tyrosine kinase inhibitors and their acquired resistance. Mol Cancer. 2018;17. doi:10.1186/s12943-018-0801-5

45. Giamas G, Man YL, Hirner H, Bischof J, Kramer K, Khan K, et al. Kinases as targets in the treatment of solid tumors. Cell Signal. 2010;22: 984–1002. doi:10.1016/j.cellsig.2010.01.011

46. Widmer N, Bardin C, Chatelut E, Paci A, Beijnen J, Levêque D, et al. Review of therapeutic drug monitoring of anticancer drugs part two – Targeted therapies. Eur J Cancer. 2014;50: 2020–2036. doi:10.1016/j.ejca.2014.04.015

47. Wang Z, Cole PA. Catalytic Mechanisms and Regulation of Protein Kinases. Methods in Enzymology. Elsevier; 2014. pp. 1–21. doi:10.1016/B978-0-12-397918-6.00001-X

48. Doycheva I, Thuluvath PJ. Systemic Therapy for Advanced Hepatocellular Carcinoma: An Update of a Rapidly Evolving Field. J Clin Exp Hepatol. 2019;9: 588–596. doi:10.1016/j.jceh.2019.07.012

49. Garuti L, Roberti M, Bottegoni G. Non-ATP Competitive Protein Kinase Inhibitors. Curr Med Chem. 2010;17: 2804–2821. doi:10.2174/092986710791859333

50. Liu L, Cao Y, Chen C, Zhang X, McNabola A, Wilkie D, et al. Sorafenib blocks the RAF/MEK/ERK pathway, inhibits tumor angiogenesis, and induces tumor cell apoptosis in hepatocellular carcinoma model PLC/PRF/5. Cancer Res. 2006;66: 11851–11858. doi:10.1158/0008-5472.CAN-06-1377

51. Adnane L, Trail PA, Taylor I, Wilhelm SM. Sorafenib (BAY 43-9006, Nexavar), a dual-action inhibitor that targets RAF/MEK/ERK pathway in tumor cells and tyrosine kinases VEGFR/PDGFR in tumor vasculature. Methods Enzymol. 2006;407: 597–612. doi:10.1016/S0076-6879(05)07047-3

52. Wilhelm SM, Carter C, Tang L, Wilkie D, McNabola A, Rong H, et al. BAY 43-9006 exhibits broad spectrum oral antitumor activity and targets the RAF/MEK/ERK pathway and receptor tyrosine kinases involved in tumor progression and angiogenesis. Cancer Res. 2004;64: 7099–7109. doi:10.1158/0008-5472.CAN-04-1443

53. Wilhelm S, Carter C, Lynch M, Lowinger T, Dumas J, Smith RA, et al. Discovery and development of sorafenib: a multikinase inhibitor for treating cancer. Nat Rev Drug Discov. 2006;5: 835–844. doi:10.1038/nrd2130

54. Llovet JM, Hilgard P, de Oliveira AC, Forner A, Zeuzem S, Galle PR, et al. Sorafenib in Advanced Hepatocellular Carcinoma. N Engl J Med. 2008; 13.

55. Cheng A-L, Kang Y-K, Chen Z, Tsao C-J, Qin S, Kim JS, et al. Efficacy and safety of sorafenib in patients in the Asia-Pacific region with advanced hepatocellular carcinoma: a phase III randomised, double-blind, placebo-controlled trial. Lancet Oncol. 2009;10: 25–34. doi:10.1016/S1470-2045(08)70285-7

56. FDA. Nexavar (sorafenib) prescribing information. Available: https://www.accessdata.fda.gov/drugsatfda_docs/label/2018/021923s020lbl.pdf.

57. Villarroel MC, Pratz KW, Xu L, Wright JJ, Smith BD, Rudek MA. Plasma protein binding of sorafenib, a multi kinase inhibitor: in vitro and in cancer patients. Invest New Drugs. 2012;30: 2096–2102. doi:10.1007/s10637-011-9767-5

58. EMA. Nexavar (sorafenib), summary of product characteristics. Available: https://www.ema.europa.eu/en/documents/product-information/nexavar-epar-product-information_en.pdf

59. Josephs DH, Fisher DS, Spicer J, Flanagan RJ. Clinical Pharmacokinetics of Tyrosine Kinase Inhibitors: Implications for Therapeutic Drug Monitoring. Ther Drug Monit. 2013;35: 26. doi:10.1097/FTD.0b013e318292b931

60. Bellmunt J, Eisen T, Fishman M, Quinn D. Experience with sorafenib and adverse event management. Crit Rev Oncol Hematol. 2011;78: 24–32. doi:10.1016/j.critrevonc.2010.03.006

61. Chen J, Jin R, Zhao J, Liu J, Ying H, Yan H, et al. Potential molecular, cellular and microenvironmental mechanism of sorafenib resistance in hepatocellular carcinoma. Cancer Lett. 2015;367: 1–11. doi:10.1016/j.canlet.2015.06.019

62. Nishida N, Kitano M, Sakurai T, Kudo M. Molecular Mechanism and Prediction of Sorafenib Chemoresistance in Human Hepatocellular Carcinoma. Dig Dis. 2015;33: 771–779. doi:10.1159/000439102

63. Yamamoto Y, Matsui J, Matsushima T, Obaishi H, Miyazaki K, Nakamura K, et al. Lenvatinib, an angiogenesis inhibitor targeting VEGFR/FGFR, shows broad antitumor activity in human tumor xenograft models associated with microvessel density and pericyte coverage. Vasc Cell. 2014;6: 18. doi:10.1186/2045-824X-6-18

64. Suyama K, Iwase H. Lenvatinib: A Promising Molecular Targeted Agent for Multiple Cancers. Cancer Control. 2018;25: 107327481878936. doi:10.1177/1073274818789361

65. EMA. Lenvima (lenvatinib), summary of product characteristics. Available: l https://www.ema.europa.eu/en/documents/product-information/lenvima-epar-product-information_en.pdf.

66. FDA. Lenvima (lenvatinib), prescribing information. Available: https://www.accessdata.fda.gov/drugsatfda_docs/label/2019/206947s011lbl.pdf.

67. Kudo M, Finn RS, Qin S, Han K-H, Ikeda K, Piscaglia F, et al. Lenvatinib versus sorafenib in first-line treatment of patients with unresectable hepatocellular carcinoma: a randomised phase 3 non-inferiority trial. The Lancet. 2018;391: 1163–1173. doi:10.1016/S0140-6736(18)30207-1

68. Kim JJ, McFarlane T, Tully S, Wong WWL. Lenvatinib Versus Sorafenib as First-Line Treatment of Unresectable Hepatocellular Carcinoma: A Cost–Utility Analysis. The Oncologist. 2020;25. doi:10.1634/theoncologist.2019-0501

69. Pan-Canadian Oncology Drug Review. Pan-Canadian Oncology Drug Review. pCODR expert review committee (pERC) final recommendation. Available: https://www.cadth.ca/sites/default/files/pcodr/pcodr_sorafenib_nexavar_dtc_fn_rec.pdf

70. Pan-Canadian Oncology Drug Review. pCODR expert review committee (pERC) initial recommendation. Available: https://cadth.ca/sites/default/files/pcodr/pcodr_lenvatinib_lenvima_rcc_in_rec.pdf

71. Overview of the patent expiry of (non-)tyrosine kinase inhibitors approved for clinical use in the EU and the US - GaBI Journal. Available: http://gabi-journal.net/overview-of-the-patent-expiry-of-non-tyrosine-kinase-inhibitors-approved-for-clinical-use-in-the-eu-and-usa.html

72. Hussein Z, Mizuo H, Hayato S, Namiki M, Shumaker R. Clinical Pharmacokinetic and Pharmacodynamic Profile of Lenvatinib, an Orally Active, Small-Molecule, Multitargeted Tyrosine Kinase Inhibitor. Eur J Drug Metab Pharmacokinet. 2017;42: 903–914. doi:10.1007/s13318-017-0403-4

73. Dubbelman AC, Rosing H, Thijssen B, Gebretensae A, Lucas L, Chen H, et al. Development and validation of LC–MS/MS assays for the quantification of E7080 and metabolites in various human biological matrices. J Chromatogr B. 2012;887–888: 25–34. doi:10.1016/j.jchromb.2012.01.004

74. Dubbelman A-C, Nijenhuis CM, Jansen RS, Rosing H, Mizuo H, Kawaguchi S, et al. Metabolite profiling of the multiple tyrosine kinase inhibitor lenvatinib: a cross-species comparison. Invest New Drugs. 2016;34: 300–318. doi:10.1007/s10637-016-0342-y

75. Shumaker RC, Aluri J, Fan J, Martinez G, Thompson GA, Ren M. Effect of Rifampicin on the Pharmacokinetics of Lenvatinib in Healthy Adults. Clin Drug Investig. 2014;34: 651–659. doi:10.1007/s40261-014-0217-y

76. Shumaker R, Aluri J, Fan J, Martinez G, Thompson GA, Ren M. Effects of ketoconazole on the pharmacokinetics of lenvatinib (E7080) in healthy participants. Clin Pharmacol Drug Dev. 2015;4: 155–160. doi:10.1002/cpdd.140

77. Tamai T, Hayato S, Hojo S, Suzuki T, Okusaka T, Ikeda K, et al. Dose Finding of Lenvatinib in Subjects With Advanced Hepatocellular Carcinoma Based on Population Pharmacokinetic and Exposure-Response Analyses. J Clin Pharmacol. 2017;57: 1138–1147. doi:10.1002/jcph.917

78. Stivarga efficacy in HCC, US HCP. Available: https://www.hcp.stivarga-us.com/hepatocellular-carcinoma/efficacy-in-resorce

79. Wilhelm SM, Dumas J, Adnane L, Lynch M, Carter CA, Schütz G, et al. Regorafenib (BAY 73-4506): A new oral multikinase inhibitor of angiogenic, stromal and oncogenic receptor tyrosine kinases with potent preclinical antitumor activity. Int J Cancer. 2011;129: 245–255. doi:10.1002/ijc.25864

80. FDA. Stivarga (regorafenib), prescribing information. Available: https://www.accessdata.fda.gov/drugsatfda_docs/label/2017/203085s007lbl.pdf

81. EMA. Stivarga (regorafenib) summary of product characteristics. Available: https://www.ema.europa.eu/en/documents/product-information/stivarga-epar-product-information_en.pdf

82. Bruix J, Qin S, Merle P, Granito A, Huang Y-H, Bodoky G, et al. Regorafenib for patients with hepatocellular carcinoma who progressed on sorafenib treatment (RESORCE): a randomised, double-blind, placebo-controlled, phase 3 trial. The Lancet. 2017;389: 56–66. doi:10.1016/S0140-6736(16)32453-9

83. EMA. Cabometyx (cabozantinib), summary of product characteristics. Available: https://www.ema.europa.eu/en/documents/product-information/cabometyx-epar-product-information_en-0.pdf

84. FDA. Cabometyx (cabozantinib) prescribing information. Available: https://www.accessdata.fda.gov/drugsatfda_docs/label/2021/208692s010lbl.pdf

85. Abou-Alfa GK, Meyer T, Cheng A-L, El-Khoueiry AB, Rimassa L, Ryoo B-Y, et al. Cabozantinib in Patients with Advanced and Progressing Hepatocellular Carcinoma. N Engl J Med. 2018;379: 54–63. doi:10.1056/NEJMoa1717002

86. Personeni N, Pressiani T, Bozzarelli S, Rimassa L. Targeted agents for second-line treatment of advanced hepatocellular carcinoma. World J Gastrointest Oncol. 2019;11: 788–803. doi:10.4251/wjgo.v11.i10.788

87. Burroughs A, Hochhauser D, Meyer T. Systemic treatment and liver transplantation for hepatocellular carcinoma: two ends of the therapeutic spectrum. Lancet Oncol. 2004;5: 409–418. doi:10.1016/S1470-2045(04)01508-6

88. Burney I. Cancer Chemotherapy and Biotherapy. Sultan Qaboos Univ Med J. 2011;11: 424–425.

89. Zwelling LA, Bales E, Altschuler E, Mayes J. Circumvention of resistance by doxorubicin, but not by idarubicin, in a human leukemia cell line containing an intercalator-resistant form of topoisomerase II: evidence for a non-topoisomerase II-mediated mechanism of doxorubicin cytotoxicity. Biochem Pharmacol. 1993;45: 516–520. doi:10.1016/0006-2952(93)90091-A

90. Bachur NR, Yu F, Johnson R, Hickey R, Wu Y, Malkas L. Helicase inhibition by anthracycline anticancer agents. Mol Pharmacol. 1992;41: 993–998.

91. Anthony Greco F. Chronic etoposide administration: overview of clinical experience. Cancer Treat Rev. 1993;19: 35–45. doi:10.1016/0305-7372(93)90046-T

92. Booser DJ, Hortobagyi GN. Anthracycline antibiotics in cancer therapy. Focus on drug resistance. Drugs. 1994;47: 223–258. doi:10.2165/00003495-199447020-00002

93. Gewirtz D. A critical evaluation of the mechanisms of action proposed for the antitumor effects of the anthracycline antibiotics adriamycin and daunorubicin. Biochem Pharmacol. 1999;57: 727–741. doi:10.1016/S0006-2952(98)00307-4

94. Egorin MJ, Clawson RE, Cohen JL, Ross LA, Bachur NR. Cytofluorescence localization of anthracycline antibiotics. Cancer Res. 1980;40: 4669–4676.

95. Twelves CJ. Oral Idarubicin in Solid Tumour Chemotherapy: Clin Drug Investig. 1995;9: 39–54. doi:10.2165/00044011-199500092-00007

96. Borchmann P, Hübel K, Schnell R, Engert A. Idarubicin: a brief overview on pharmacology and clinical use. Int J Clin Pharmacol Ther. 1997;35: 80–83.

97. Cersosimo RJ. Idarubicin: an anthracycline antineoplastic agent. Clin Pharm. 1992;11: 152–167.

98. Boulin M, Guiu S, Chauffert B, Aho S, Cercueil J-P, Ghiringhelli F, et al. Screening of anticancer drugs for chemoembolization of hepatocellular carcinoma. Anticancer Drugs. 2011;22: 741–748. doi:10.1097/CAD.0b013e328346a0c5

99. Park J-G, Lee S-K, Hong I-G, Kim H-S. MDRl Gene Expression: Its Effect on Drug Resistance to Doxorubicin in Human Hepatocellular Carcinoma Cell Lines. J Natl Cancer Inst. 1994;86: 6.

100. Broggini M, Italia C, Colombo T, Marmonti L, Donelli MG. Activity and distribution of iv and oral 4-demethoxydaunorubicin in murine experimental tumors. Cancer Treat Rep. 1984;68: 739–747.

101. Roovers DJ, van Vliet M, Bloem AC, Lokhorst HM. Idarubicin overcomes P-glycoprotein-related multidrug resistance: comparison with doxorubicin and daunorubicin in human multiple myeloma cell lines. Leuk Res. 1999;23: 539–548. doi:10.1016/S0145-2126(99)00041-7

102. Robert J. Clinical Pharmacokinetics of Idarubicin: Clin Pharmacokinet. 1993;24: 275–288. doi:10.2165/00003088-199324040-00002

103. Camaggi CM, Strocchi E, Carisi P, Martoni A, Tononi A, Guaraldi M, et al. Idarubicin metabolism and pharmacokinetics after intravenous and oral administration in cancer

patients: a crossover study. Cancer Chemother Pharmacol. 1992;30: 307–316. doi:10.1007/BF00686301

104. Toffoli G, Sorio R, Aita P, Crivellari D, Corona G, Bearz A, et al. Dose-finding and pharmacologic study of chronic oral idarubicin therapy in metastatic breast cancer patients. Clin Cancer Res Off J Am Assoc Cancer Res. 2000;6: 2279–2287.

105. Crivellari D, Lombardi D, Spazzapan S, Veronesi A, Toffoli G. New oral drugs in older patients: a review of idarubicin in elderly patients. Crit Rev Oncol Hematol. 2004;49: 153–163. doi:10.1016/S1040-8428(03)00120-3

106. Toffoli G, Corona G, Simone F, Gigante M, De Angeli S, Boiocchi M. Cellular pharmacology of idarubicinol in multidrug-resistant LoVo cell lines. Int J Cancer. 1996;67: 129–137. doi:10.1002/(SICI)1097-0215(19960703)67:1<129::AID-IJC21>3.0.CO;2-8

107. Kuffel MJ, Ames MM. Comparative resistance of idarubicin, doxorubicin and their C-13 alcohol metabolites in human MDR1 transfected NIH-3T3 cells. Cancer Chemother Pharmacol. 1995;36: 223–226. doi:10.1007/BF00685850

108. Kessel M, Gieseler F, Woodcock BG. Influence of serum protein binding on the uptake and retention of idarubicin by sensitive and multidrug resistant human leukemic cells. Eur J Clin Pharmacol. 1999;55: 369–373. doi:10.1007/s002280050642

109. Toffoli G, Sorio R, Basso B, Aita P, Corona G, Ruolo G, et al. Pharmacokinetic Comparison of 120-Hour Infusion *Versus* Hyperfractionated Oral Administration of Idarubicin. J Chemother. 2004;16: 193–200. doi:10.1179/joc.2004.16.2.193

110. Crivellari D, Lombardi D, Corona G, Massacesi C, Talamini R, Sorio R, et al. Innovative schedule of oral idarubicin in elderly patients with metastatic breast cancer: comprehensive results of a phase II multi-institutional study with pharmacokinetic drug monitoring. Ann Oncol. 2006;17: 807–812. doi:10.1093/annonc/mdl013

111. Ghiculescu RA. Therapeutic drug monitoring: which drugs, why, when and how to do it. [cited 28 Nov 2021]. doi:10.18773/austprescr.2008.025

112. Zhou J, Wang G, Chen Y, Wang H, Hua Y, Cai Z. Immunogenic cell death in cancer therapy: Present and emerging inducers. J Cell Mol Med. 2019;23: 4854–4865. doi:10.1111/jcmm.14356

113. Obeid M, Panaretakis T, Tesniere A, Joza N, Tufi R, Apetoh L, et al. Leveraging the Immune System during Chemotherapy: Moving Calreticulin to the Cell Surface Converts Apoptotic Death from “Silent” to Immunogenic: Figure 1. Cancer Res. 2007;67: 7941–7944. doi:10.1158/0008-5472.CAN-07-1622

114. Apetoh L, Ghiringhelli F, Tesniere A, Obeid M, Ortiz C, Criollo A, et al. Toll-like receptor 4–dependent contribution of the immune system to anticancer chemotherapy and radiotherapy. Nat Med. 2007;13: 1050–1059. doi:10.1038/nm1622

115. Garg AD, Krysko DV, Vandenabeele P, Agostinis P. Hypericin-based photodynamic therapy induces surface exposure of damage-associated molecular patterns like HSP70 and

calreticulin. Cancer Immunol Immunother. 2012;61: 215–221. doi:10.1007/s00262-011-1184-2

116. EMA. Cyramza (ramucirumab) summary of products characteristics. Available: https://www.ema.europa.eu/en/documents/product-information/cyramza-epar-product-information_en.pdf

117. FDA. Cyramza (ramucirumab) prescribing information. Available: https://www.accessdata.fda.gov/drugsatfda_docs/label/2015/125477s011lbl.pdf

118. Zhu AX, Kang Y-K, Yen C-J, Finn RS, Galle PR, Llovet JM, et al. Ramucirumab after sorafenib in patients with advanced hepatocellular carcinoma and increased α-fetoprotein concentrations (REACH-2): a randomised, double-blind, placebo-controlled, phase 3 trial. Lancet Oncol. 2019;20: 282–296. doi:10.1016/S1470-2045(18)30937-9

119. Finn RS, Qin S, Ikeda M, Galle PR, Ducreux M, Kim T-Y, et al. Atezolizumab plus Bevacizumab in Unresectable Hepatocellular Carcinoma. N Engl J Med. 2020 [cited 22 Nov 2021]. doi:10.1056/NEJMoa1915745

120. AstraZeneca. A Phase III, Randomized, Double-Blind, Placebo-Controlled, Multi Center Study of Durvalumab Monotherapy or in Combination With Bevacizumab as Adjuvant Therapy in Patients With Hepatocellular Carcinoma Who Are at High Risk of Recurrence After Curative Hepatic Resection or Ablation. clinicaltrials.gov; 2021 Oct. Report No.: study/NCT03847428. Available: https://clinicaltrials.gov/ct2/show/study/NCT03847428

121. Research C for DE and. FDA grants accelerated approval to nivolumab for HCC previously treated with sorafenib. FDA. 2019. Available: https://www.fda.gov/drugs/resources-information-approved-drugs/fda-grants-accelerated-approval-nivolumab-hcc-previously-treated-sorafenib

122. Yau T, Park JW, Finn RS, Cheng A-L, Mathurin P, Edeline J, et al. CheckMate 459: A randomized, multi-center phase III study of nivolumab (NIVO) vs sorafenib (SOR) as first-line (1L) treatment in patients (pts) with advanced hepatocellular carcinoma (aHCC). Ann Oncol. 2019;30: v874–v875. doi:10.1093/annonc/mdz394.029

123. Merck Sharp & Dohme Corp. A Phase III Study of Pembrolizumab (MK-3475) vs. Best Supportive Care as Second-Line Therapy in Subjects With Previously Systemically Treated Advanced Hepatocellular Carcinoma (KEYNOTE-240). clinicaltrials.gov; 2021 Nov. Report No.: NCT02702401. Available: https://clinicaltrials.gov/ct2/show/NCT02702401

124. Kelley RK, W Oliver J, Hazra S, Benzaghou F, Yau T, Cheng A-L, et al. Cabozantinib in combination with atezolizumab versus sorafenib in treatment-naive advanced hepatocellular carcinoma: COSMIC-312 Phase III study design. Future Oncol Lond Engl. 2020;16: 1525–1536. doi:10.2217/fon-2020-0283

125. Bristol-Myers Squibb. A Randomized, Multi-center, Phase 3 Study of Nivolumab in Combination With Ipilimumab Compared to Sorafenib or Lenvatinib as First-Line Treatment in Participants With Advanced Hepatocellular Carcinoma. clinicaltrials.gov; 2020 Nov. Report No.: NCT04039607. Available: https://clinicaltrials.gov/ct2/show/NCT04039607

126. Ikeda M, Sung MW, Kudo M, Kobayashi M, Baron AD, Finn RS, et al. A phase 1b trial of lenvatinib (LEN) plus pembrolizumab (PEM) in patients (pts) with unresectable hepatocellular carcinoma (uHCC). J Clin Oncol. 2018;36: 4076–4076. doi:10.1200/JCO.2018.36.15_suppl.4076

127. Yu H, Steeghs N, Nijenhuis CM, Schellens JHM, Beijnen JH, Huitema ADR. Practical Guidelines for Therapeutic Drug Monitoring of Anticancer Tyrosine Kinase Inhibitors: Focus on the Pharmacokinetic Targets. Clin Pharmacokinet. 2014;53: 305–325. doi:10.1007/s40262-014-0137-2

128. Spector R, Park GD, Johnson GF, Vesell ES. Therapeutic drug monitoring. Clin Pharmacol Ther. 1988;43: 345–353. doi:10.1038/clpt.1988.42

129. Reynolds DJ, Aronson JK. ABC of monitoring drug therapy. Making the most of plasma drug concentration measurements. BMJ. 1993;306: 48–51.

130. Hon YY, Evans WE. Making TDM work to optimize cancer chemotherapy: a multidisciplinary team approach. Clin Chem. 1998;44: 388–400.

131. Alnaim L. Therapeutic drug monitoring of cancer chemotherapy. J Oncol Pharm Pract. 2007;13: 207–221. doi:10.1177/1078155207081133

132. Galpin AJ, Evans WE. Therapeutic drug monitoring in cancer management. Clin Chem. 1993;39: 2419–2430.

133. Simsek C, Esin E, Yalcin S. Metronomic Chemotherapy: A Systematic Review of the Literature and Clinical Experience. J Oncol. 2019;2019: 5483791. doi:10.1155/2019/5483791

134. Gross AS. Best practice in therapeutic drug monitoring. Br J Clin Pharmacol. 2001;52: 5S-10S. doi:10.1046/j.1365-2125.2001.0520s1005.x

135. Chatterjee K. Congestive heart failure: what should be the initial therapy and why? Am J Cardiovasc Drugs Drugs Devices Interv. 2002;2: 1–6. doi:10.2165/00129784-200202010-00001

136. Delbaldo C, Chatelut E, Re M, Deroussent A, Seronie-Vivien S, Jambu A, et al. Pharmacokinetic-Pharmacodynamic Relationships of Imatinib and Its Main Metabolite in Patients with Advanced Gastrointestinal Stromal Tumors. Clin Cancer Res. 2006;12: 6073–6078. doi:10.1158/1078-0432.CCR-05-2596

137. von Mehren M, Widmer N. Correlations between imatinib pharmacokinetics, pharmacodynamics, adherence, and clinical response in advanced metastatic gastrointestinal stromal tumor (GIST): An emerging role for drug blood level testing? Cancer Treat Rev. 2011;37: 291–299. doi:10.1016/j.ctrv.2010.10.001

138. Hughes T, Deininger M, Hochhaus A, Branford S, Radich J, Kaeda J, et al. Monitoring CML patients responding to treatment with tyrosine kinase inhibitors: review and recommendations for harmonizing current methodology for detecting BCR-ABL transcripts and kinase domain mutations and for expressing results. Blood. 2006;108: 28–37. doi:10.1182/blood-2006-01-0092

139. Klümpen H-J, Samer CF, Mathijssen RHJ, Schellens JHM, Gurney H. Moving towards dose individualization of tyrosine kinase inhibitors. Cancer Treat Rev. 2011;37: 251–260. doi:10.1016/j.ctrv.2010.08.006

140. Wilkinson GR. Drug metabolism and variability among patients in drug response. N Engl J Med. 2005;352: 2211–2221. doi:10.1056/NEJMra032424

141. Sawyers C. Targeted cancer therapy. Nature. 2004;432: 294–297. doi:10.1038/nature03095

142. Relling MV, Fairclough D, Ayers D, Crom WR, Rodman JH, Pui CH, et al. Patient characteristics associated with high-risk methotrexate concentrations and toxicity. J Clin Oncol Off J Am Soc Clin Oncol. 1994;12: 1667–1672. doi:10.1200/JCO.1994.12.8.1667

143. Evans WE, Relling MV. Clinical pharmacokinetics-pharmacodynamics of anticancer drugs. Clin Pharmacokinet. 1989;16: 327–336.

144. Moore MJ, Erlichman C. Therapeutic drug monitoring in oncology. Problems and potential in antineoplastic therapy. Clin Pharmacokinet. 1987;13: 205–227. doi:10.2165/00003088-198713040-00001

145. DeVita VT, Lawrence TS, Rosenberg SA. DeVita, Hellman, and Rosenberg's cancer: Principles & practice of oncology: Tenth edition. DeVita Hellman Rosenb Cancer Princ Pract Oncol Tenth Ed. 2015; 1–2280.

146. Thomas-Schoemann A, Blanchet B, Bardin C, Noé G, Boudou-Rouquette P, Vidal M, et al. Drug interactions with solid tumour-targeted therapies. Crit Rev Oncol Hematol. 2014;89: 179–196. doi:10.1016/j.critrevonc.2013.08.007

147. Gao B, Yeap S, Clements A, Balakrishnar B, Wong M, Gurney H. Evidence for Therapeutic Drug Monitoring of Targeted Anticancer Therapies. J Clin Oncol. 2012;30: 4017–4025. doi:10.1200/JCO.2012.43.5362

148. Moore MJ, Erlichman C. Therapeutic Drug Monitoring in Oncology. Clin Pharmacokinet. 1987;13: 205–227. doi:10.2165/00003088-198713040-00001

149. Teng JF, Mabasa VH, Ensom MH. The role of therapeutic drug monitoring of imatinib in patients with chronic myeloid leukemia and metastatic or unresectable gastrointestinal stromal tumors. Ther Drug Monit. 2012;34: 85–97.

150. Bardin C, Veal G, Paci A, Chatelut E, Astier A, Levêque D, et al. Therapeutic drug monitoring in cancer – Are we missing a trick? Eur J Cancer. 2014;50: 2005–2009. doi:10.1016/j.ejca.2014.04.013

151. Mueller-Schoell A, Groenland SL, Scherf-Clavel O, van Dyk M, Huisinga W, Michelet R, et al. Therapeutic drug monitoring of oral targeted antineoplastic drugs. Eur J Clin Pharmacol. 2021;77: 441–464. doi:10.1007/s00228-020-03014-8

152. Blanchet B, Billemont B, Cramard J, Benichou AS, Chhun S, Harcouet L, et al. Validation of an HPLC-UV method for sorafenib determination in human plasma and application to cancer patients in routine clinical practice. J Pharm Biomed Anal. 2009;49: 1109–1114. doi:10.1016/j.jpba.2009.02.008

153. Fukudo M, Ito T, Mizuno T, Shinsako K, Hatano E, Uemoto S, et al. Exposure-toxicity relationship of sorafenib in Japanese patients with renal cell carcinoma and hepatocellular carcinoma. Clin Pharmacokinet. 2014;53: 185–196. doi:10.1007/s40262-013-0108-z

154. Shimada M, Okawa H, Kondo Y, Maejima T, Kataoka Y, Hisamichi K, et al. Monitoring Serum Levels of Sorafenib and Its N-Oxide Is Essential for Long-Term Sorafenib Treatment of Patients with Hepatocellular Carcinoma. Tohoku J Exp Med. 2015;237: 173–182. doi:10.1620/tjem.237.173

155. Verheijen RB, Yu H, Schellens JHM, Beijnen JH, Steeghs N, Huitema ADR. Practical Recommendations for Therapeutic Drug Monitoring of Kinase Inhibitors in Oncology. Clin Pharmacol Ther. 2017;102: 765–776. doi:10.1002/cpt.787

156. FDA. Stivarga (regorafenib) clinical pharmacology and biopharmaceutics review(s). Available: https://www.accessdata.fda.gov/drugsatfda_docs/nda/2012/203085Orig1s000ClinPharmR.pdf

157. Committee for Medicinal Products for Human Use (CHMP), European Medicines Agency. Lenvima (lenvatinib) Lenvima European public assessment report. 2015 [cited 28 Nov 2021]. Available: https://www.ema.europa.eu/en/documents/assessment-report/lenvima-epar-public-assessment-report_en.pdf

158. Hayato S, Shumaker R, Ferry J, Binder T, Dutcus CE, Hussein Z. Exposure–response analysis and simulation of lenvatinib safety and efficacy in patients with radioiodine-refractory differentiated thyroid cancer. Cancer Chemother Pharmacol. 2018;82: 971–978. doi:10.1007/s00280-018-3687-4

159. Nagahama M, Ozeki T, Suzuki A, Sugino K, Niioka T, Ito K, et al. Association of lenvatinib trough plasma concentrations with lenvatinib-induced toxicities in Japanese patients with thyroid cancer. Med Oncol Northwood Lond Engl. 2019;36: 39. doi:10.1007/s12032-019-1263-3

160. Adaway JE, Keevil BG. Therapeutic drug monitoring and LC-MS/MS. J Chromatogr B Analyt Technol Biomed Life Sci. 2012;883–884: 33–49. doi:10.1016/j.jchromb.2011.09.041

161. Lakshmy R. Analysis of the Use of Dried Blood Spot Measurements in Disease Screening. J Diabetes Sci Technol. 2008;2: 242–243.

162. Guthrie R, Susi A. A Simple Phenylalanine Method for Detecting Phenylketonuria in Large Populations of Newborn Infants. Pediatrics. 1963;32: 338–343.

163. Zakaria R, Allen KJ, Koplin JJ, Roche P, Greaves RF. Advantages and Challenges of Dried Blood Spot Analysis by Mass Spectrometry Across the Total Testing Process. EJIFCC. 2016;27: 288–317.

164. Chace DH, Spitzer AR, De Jesús VR. Applications of Dried Blood Spots in Newborn and Metabolic Screening. Dried Blood Spots. John Wiley & Sons, Ltd; 2014. pp. 53–75. doi:10.1002/9781118890837.ch6

165. Lehmann S, Delaby C, Vialaret J, Ducos J, Hirtz C. Current and future use of “dried blood spot” analyses in clinical chemistry. Clin Chem Lab Med. 2013;51: 1897–1909. doi:10.1515/cclm-2013-0228

166. Stove CP, Ingels A-SME, De Kesel PMM, Lambert WE. Dried blood spots in toxicology: from the cradle to the grave? Crit Rev Toxicol. 2012;42: 230–243. doi:10.3109/10408444.2011.650790

167. McDade TW, Williams S, Snodgrass JJ. What a drop can do: dried blood spots as a minimally invasive method for integrating biomarkers into population-based research. Demography. 2007;44: 899–925. doi:10.1353/dem.2007.0038

168. Fontaine E, Saez C. Analysis of SARS-CoV-2 antibodies from dried blood spot samples with the Roche Elecsys Immunochemistry method. Pract Lab Med. 2021;25: e00234. doi:10.1016/j.plabm.2021.e00234

169. Weisser H, Steinhagen K, Höcker R, Borchardt-Lohölter V, Anvari Ö, Kern PM. Evaluation of dried blood spots as alternative sampling material for serological detection of anti-SARS-CoV-2 antibodies using established ELISAs. Clin Chem Lab Med CCLM. 2021;59: 979–985. doi:10.1515/cclm-2020-1436

170. Beyerl J, Rubio-Acero R, Castelletti N, Paunovic I, Kroidl I, Khan ZN, et al. A dried blood spot protocol for high throughput analysis of SARS-CoV-2 serology based on the Roche Elecsys anti-N assay. EBioMedicine. 2021;70. doi:10.1016/j.ebiom.2021.103502

171. Mulchandani R, Brown B, Brooks T, Semper A, Machin N, Linley E, et al. Use of dried blood spot samples for SARS-CoV-2 antibody detection using the Roche Elecsys ® high throughput immunoassay. J Clin Virol Off Publ Pan Am Soc Clin Virol. 2021;136: 104739. doi:10.1016/j.jcv.2021.104739

172. Wilhelm AJ, den Burger JCG, Swart EL. Therapeutic drug monitoring by dried blood spot: progress to date and future directions. Clin Pharmacokinet. 2014;53: 961–973. doi:10.1007/s40262-014-0177-7

173. Directive 2010/63/EU of the European Parliament and of the Council of 22 September 2010 on the protection of animals used for scientific purposesText with EEA relevance. Available: https://eur-lex.europa.eu/LexUriServ/LexUriServ.do?uri=OJ:L:2010:276:0033:0079:en:PDF

174. Sharma A, Jaiswal S, Shukla M, Lal J. Dried blood spots: Concepts, present status, and future perspectives in bioanalysis. Drug Test Anal. 2014;6: 399–414. doi:10.1002/dta.1646

175. Enderle Y, Foerster K, Burhenne J. Clinical feasibility of dried blood spots: Analytics, validation, and applications. J Pharm Biomed Anal. 2016;130: 231–243. doi:10.1016/j.jpba.2016.06.026

176. Sagendorph WK. Shipping Guidelines for Dried-Blood Spot Specimens. Available: https://www.cdc.gov/labstandards/pdf/nsqap/Bloodspot_Transportation_Guidelines.pdf.

177. D'Arienzo CJ, Ji QC, Discenza L, Cornelius G, Hynes J, Cornelius L, et al. DBS sampling can be used to stabilize prodrugs in drug discovery rodent studies without the addition of esterase inhibitors. Bioanalysis. 2010;2: 1415–1422. doi:10.4155/bio.10.94

178. Li W, Zhang J, Tse FLS. Strategies in quantitative LC-MS/MS analysis of unstable small molecules in biological matrices. Biomed Chromatogr BMC. 2011;25: 258–277. doi:10.1002/bmc.1572

179. Van Uytfanghe K, Heughebaert L, Stove C. Self-sampling at home using volumetric absorptive microsampling: coupling analytical evaluation to volunteers' perception in the context of a large scale study. Clin Chem Lab Med CCLM. 2020;1. doi:10.1515/cclm-2020-1180

180. Iacuzzi V, Posocco B, Zanchetta M, Gagno S, Poetto AS, Guardascione M, et al. Dried Blood Spot Technique Applied in Therapeutic Drug Monitoring of Anticancer Drugs: a Review on Conversion Methods to Correlate Plasma and Dried Blood Spot Concentrations. Pharm Res. 2021;38: 759–778. doi:10.1007/s11095-021-03036-6

181. Capiau S, Veenhof H, Koster RA, Bergqvist Y, Boettcher M, Halmingh O, et al. Official International Association for Therapeutic Drug Monitoring and Clinical Toxicology Guideline: Development and Validation of Dried Blood Spot–Based Methods for Therapeutic Drug Monitoring. Ther Drug Monit. 2019;41: 22.

182. Timmerman P, White S, Globig S, Lüdtke S, Brunet L, Smeraglia J. EBF recommendation on the validation of bioanalytical methods for dried blood spots. Bioanalysis. 2011;3: 1567–1575. doi:10.4155/bio.11.132

183. Timmerman P, White S, Cobb Z, de Vries R, Thomas E, van Baar B, et al. Update of the EBF recommendation for the use of DBS in regulated bioanalysis integrating the conclusions from the EBF DBS-microsampling consortium. Bioanalysis. 2013;5: 2129–2136. doi:10.4155/bio.13.173

184. Crotti S, Posocco B, Marangon E, Nitti D, Toffoli G, Agostini M. Mass spectrometry in the pharmacokinetic studies of anticancer natural products. Mass Spectrom Rev. 2017;36: 213–251. doi:10.1002/mas.21478

185. Thomson JJ. Bakerian Lecture:—Rays of positive electricity. Proc R Soc Lond Ser Contain Pap Math Phys Character. 1913;89: 1–20. doi:10.1098/rspa.1913.0057

186. Fenn JB, Mann M, Meng CK, Wong SF, Whitehouse CM. Electrospray ionization for mass spectrometry of large biomolecules. Science. 1989;246: 64–71. doi:10.1126/science.2675315

187. Chace DH, Kalas TA, Naylor EW. Use of tandem mass spectrometry for multianalyte screening of dried blood specimens from newborns. Clin Chem. 2003;49: 1797–1817. doi:10.1373/clinchem.2003.022178

188. Grebe SK, Singh RJ. LC-MS/MS in the Clinical Laboratory - Where to From Here? Clin Biochem Rev. 2011;32: 5–31.

189. Soni NR. Improve GC separations with derivatization for selective response and detection in novel matrices. 1: 13.

190. Herviou P, Thivat E, Richard D, Roche L, Dohou J, Pouget M, et al. Therapeutic drug monitoring and tyrosine kinase inhibitors. Oncol Lett. 2016;12: 1223–1232. doi:10.3892/ol.2016.4780

191. Hopfgartner G, Bourgogne E. Quantitative high-throughput analysis of drugs in biological matrices by mass spectrometry. Mass Spectrom Rev. 2003;22: 195–214. doi:10.1002/mas.10050

192. Taylor G. Disintegration of water drops in an electric field. Proceedings of the Royal Society of London A: Mathematical, Physical and Engineering Sciences. The Royal Society; 1964. pp. 383–397.

193. Dülcks Th, Juraschek R. Electrospray as an ionisation method for mass spectrometry. J Aerosol Sci. 1999;30: 927–943. doi:10.1016/S0021-8502(98)00781-2

194. F.R.S LR. XX. On the equilibrium of liquid conducting masses charged with electricity. Lond Edinb Dublin Philos Mag J Sci. 1882;14: 184–186. doi:10.1080/14786448208628425

195. Stauffer E, Dolan JA, Newman R. Gas Chromatography and Gas Chromatography—Mass Spectrometry. Fire Debris Analysis. Elsevier; 2008. pp. 235–293. doi:10.1016/B978-012663971-1.50012-9

196. Chace DH, Millington DS, Terada N, Kahler SG, Roe CR, Hofman LF. Rapid diagnosis of phenylketonuria by quantitative analysis for phenylalanine and tyrosine in neonatal blood spots by tandem mass spectrometry. Clin Chem. 1993;39: 66–71.

197. Yang Z, Peng Y, Wang S. Immunosuppressants: Pharmacokinetics, methods of monitoring and role of high performance liquid chromatography/mass spectrometry. Clin Appl Immunol Rev. 2005;5: 405–430. doi:10.1016/j.cair.2005.12.001

198. Gu J, Soldin SJ. Modification of tandem mass spectrometric method to permit simultaneous quantification of 17 anti-HIV drugs which include atazanavir and tipranavir. Clin Chim Acta Int J Clin Chem. 2007;378: 222–224. doi:10.1016/j.cca.2006.11.004

199. Lennard L. Therapeutic drug monitoring of cytotoxic drugs. Br J Clin Pharmacol. 2001;52: 75S-87S. doi:10.1046/j.1365-2125.2001.0520s1075.x

200. EMA. Guideline on bioanalytical method validation. 2011. Available: https://www.ema.europa.eu/en/documents/scientific-guideline/guideline-bioanalytical-method-validation_en.pdf

201. FDA. Bioanalytical Method Validation Guidance for Industry. 2018. Available: https://www.fda.gov/files/drugs/published/Bioanalytical-Method-Validation-Guidance-for-Industry.pdf

202. Shah VP, Midha KK, Dighe S, McGilveray IJ, Skelly JP, Yacobi A, et al. Analytical methods validation: bioavailability, bioequivalence and pharmacokinetic studies. Conference report. Eur J Drug Metab Pharmacokinet. 1991;16: 249–255. doi:10.1007/BF03189968

203. Internation council for harmonisation (ICH). Bioanalytical method validation M10. Available: https://www.ema.europa.eu/en/documents/scientific-guideline/draft-ich-guideline-m10-bioanalytical-method-validation-step-2b_en.pdf

204. Booth B, Arnold ME, DeSilva B, Amaravadi L, Dudal S, Fluhler E, et al. Workshop Report: Crystal City V—Quantitative Bioanalytical Method Validation and Implementation: The 2013 Revised FDA Guidance. AAPS J. 2014;17: 277–288. doi:10.1208/s12248-014-9696-2

205. Evans C, Arnold M, Bryan P, Duggan J, James CA, Li W, et al. Implementing dried blood spot sampling for clinical pharmacokinetic determinations: considerations from the IQ Consortium Microsampling Working Group. AAPS J. 2015;17: 292–300. doi:10.1208/s12248-014-9695-3

206. Clinical and Laboratory Standard Institute. Liquid Chromatography-Mass Spectrometry Methods. Approved Guideline C62-A. Wayne (PA): Clinical and Laboratory Standard Institute, 2014. https://clsi.org/media/1346/ c62a_sample.pdf.

207. WMA - The World Medical Association-WMA Declaration of Helsinki – Ethical Principles for Medical Research Involving Human Subjects. Available: https://www.wma.net/policies-post/wma-declaration-of-helsinki-ethical-principles-for-medical-research-involving-human-subjects/

208. Abu-Rabie P, Denniff P, Spooner N, Brynjolffssen J, Galluzzo P, Sanders G. Method of Applying Internal Standard to Dried Matrix Spot Samples for Use in Quantitative Bioanalysis. Anal Chem. 2011;83: 8779–8786. doi:10.1021/ac202321q

209. Abu-Rabie P, Denniff P, Spooner N, Chowdhry BZ, Pullen FS. Investigation of different approaches to incorporating internal standard in DBS quantitative bioanalytical workflows and their effect on nullifying hematocrit-based assay bias. Anal Chem. 2015;87: 4996–5003. doi:10.1021/acs.analchem.5b00908

210. Mommers J, Mengerink Y, Ritzen E, Weusten J, van der Heijden J, van der Wal S. Quantitative analysis of morphine in dried blood spots by using morphine-d3 pre-impregnated dried blood spot cards. Anal Chim Acta. 2013;774: 26–32. doi:10.1016/j.aca.2013.03.001

211. Historical review of sample preparation for chromatographic bioanalysis: pros and cons - Chang - 2007 - Drug Development Research - Wiley Online Library. [cited 29 Nov 2021]. Available: https://onlinelibrary.wiley.com/doi/abs/10.1002/ddr.20173

212. Rood JJM, Schellens JHM, Beijnen JH, Sparidans RW. Recent developments in the chromatographic bioanalysis of approved kinase inhibitor drugs in oncology. J Pharm Biomed Anal. 2016;130: 244–263. doi:10.1016/j.jpba.2016.06.037

213. Mei JV, Alexander JR, Adam BW, Hannon WH. Use of Filter Paper for the Collection and Analysis of Human Whole Blood Specimens. J Nutr. 2001;131: 1631S-1636S. doi:10.1093/jn/131.5.1631S

214. Mei JV, Zobel SD, Hall EM, De Jesús VR, Adam BW, Hannon WH. Performance properties of filter paper devices for whole blood collection. Bioanalysis. 2010;2: 1397–1403. doi:10.4155/bio.10.73

215. Vu DH, Koster RA, Alffenaar JWC, Brouwers JRBJ, Uges DRA. Determination of moxifloxacin in dried blood spots using LC–MS/MS and the impact of the hematocrit and blood volume. J Chromatogr B. 2011;879: 1063–1070. doi:10.1016/j.jchromb.2011.03.017

216. Wong P, James CA. Punching and Extraction Techniques for Dried Blood Spot Sample Analysis. In: Li W, Lee MS, editors. Dried Blood Spots. Hoboken, NJ, USA: John Wiley & Sons, Inc.; 2014. pp. 160–167. doi:10.1002/9781118890837.ch13

217. Wong P, Pham R, Whitely C, Soto M, Salyers K, James C, et al. Application of automated serial blood sampling and dried blood spot technique with liquid chromatography–tandem mass spectrometry for pharmacokinetic studies in mice. J Pharm Biomed Anal. 2011;56: 604–608. doi:10.1016/j.jpba.2011.06.022

218. Mei H, Hsieh Y, Nardo C, Xu X, Wang S, Ng K, et al. Investigation of matrix effects in bioanalytical high-performance liquid chromatography/tandem mass spectrometric assays: application to drug discovery. Rapid Commun Mass Spectrom. 2003;17: 97–103. doi:10.1002/rcm.876

219. González O, Blanco ME, Iriarte G, Bartolomé L, Maguregui MI, Alonso RM. Bioanalytical chromatographic method validation according to current regulations, with a special focus on the non-well defined parameters limit of quantification, robustness and matrix effect. J Chromatogr A. 2014;1353: 10–27. doi:10.1016/j.chroma.2014.03.077

220. Matuszewski BK, Constanzer ML, Chavez-Eng CM. Strategies for the Assessment of Matrix Effect in Quantitative Bioanalytical Methods Based on HPLC−MS/MS. Anal Chem. 2003;75: 3019–3030. doi:10.1021/ac020361s

221. Bonfiglio null, King null, Olah null, Merkle null. The effects of sample preparation methods on the variability of the electrospray ionization response for model drug compounds. Rapid Commun Mass Spectrom RCM. 1999;13: 1175–1185. doi:10.1002/(SICI)1097-0231(19990630)13:12<1175::AID-RCM639>3.0.CO;2-0

222. Fast DM, Kelley M, Viswanathan CT, O'Shaughnessy J, King SP, Chaudhary A, et al. Workshop Report and Follow-Up—AAPS Workshop on Current Topics in GLP Bioanalysis: Assay Reproducibility for Incurred Samples—Implications of Crystal City Recommendations. AAPS J. 2009;11: 238–241. doi:10.1208/s12248-009-9100-9

223. Eckmann DM, Bowers S, Stecker M, Cheung AT. Hematocrit, Volume Expander, Temperature, and Shear Rate Effects on Blood Viscosity. Anesth Analg. 2000;91: 539–545. doi:10.1213/00000539-200009000-00007

224. Antunes MV, Charão MF, Linden R. Dried blood spots analysis with mass spectrometry: Potentials and pitfalls in therapeutic drug monitoring. Clin Biochem. 2016;49: 1035–1046. doi:10.1016/j.clinbiochem.2016.05.004

225. De Kesel PM, Sadones N, Capiau S, Lambert WE, Stove CP. Hemato-critical issues in quantitative analysis of dried blood spots: challenges and solutions. Bioanalysis. 2013;5: 2023–2041. doi:10.4155/bio.13.156

226. Yu S, Li S, Yang H, Lee F, Wu J-T, Qian MG. A novel liquid chromatography/tandem mass spectrometry based depletion method for measuring red blood cell partitioning of pharmaceutical compounds in drug discovery. Rapid Commun Mass Spectrom. 2005;19: 250–254. doi:10.1002/rcm.1777

227. Dilo A, Daali Y, Desmeules J, Chalandon Y, Uppugunduri CRS, Ansari M. Comparing Dried Blood Spots and Plasma Concentrations for Busulfan Therapeutic Drug Monitoring in Children. Ther Drug Monit. 2020;42: 111–117. doi:10.1097/FTD.0000000000000673

228. Romański M, Zacharzewska A, Teżyk A, Główka FK. In Vivo Red Blood Cells/Plasma Partition Coefficient of Treosulfan and Its Active Monoepoxide in Rats. Eur J Drug Metab Pharmacokinet. 2018;43: 565–571. doi:10.1007/s13318-018-0469-7

229. Jain L, Gardner ER, Venitz J, Dahut W, Figg WD. Development of a rapid and sensitive LC–MS/MS assay for the determination of sorafenib in human plasma. J Pharm Biomed Anal. 2008;46: 362–367. doi:10.1016/j.jpba.2007.10.027

230. Luethi D, Durmus S, Schinkel AH, Schellens JHM, Beijnen JH, Sparidans RW. Liquid chromatography-tandem mass spectrometric assay for the multikinase inhibitor regorafenib in plasma: LC-MS/MS assay for regorafenib. Biomed Chromatogr. 2014;28: 1366–1370. doi:10.1002/bmc.3176

231. Li L, Zhao M, Navid F, Pratz K, Smith BD, Rudek MA, et al. Quantitation of sorafenib and its active metabolite sorafenib N-oxide in human plasma by liquid chromatography–tandem mass spectrometry. J Chromatogr B. 2010;878: 3033–3038. doi:10.1016/j.jchromb.2010.08.049

232. Hafner F-T, Werner D, Kaiser M. Determination of regorafenib (BAY 73-4506) and its major human metabolites BAY 75-7495 (M-2) and BAY 81-8752 (M-5) in human plasma by stable-isotope dilution liquid chromatography–tandem mass spectrometry. Bioanalysis. 2014;6: 1923–1937. doi:10.4155/bio.14.52

233. Merienne C, Rousset M, Ducint D, Castaing N, Titier K, Molimard M, et al. High throughput routine determination of 17 tyrosine kinase inhibitors by LC–MS/MS. J Pharm Biomed Anal. 2018;150: 112–120. doi:10.1016/j.jpba.2017.11.060

234. Allard M, Khoudour N, Rousseau B, Joly C, Costentin C, Blanchet B, et al. Simultaneous analysis of regorafenib and sorafenib and three of their metabolites in human plasma using LC–MS/MS. J Pharm Biomed Anal. 2017;142: 42–48. doi:10.1016/j.jpba.2017.04.053

235. Mross K, Frost A, Steinbild S, Hedbom S, Buchert M, Fasol U, et al. A Phase I Dose-Escalation Study of Regorafenib (BAY 73-4506), an Inhibitor of Oncogenic, Angiogenic, and Stromal Kinases, in Patients with Advanced Solid Tumors. Clin Cancer Res. 2012;18: 2658–2667. doi:10.1158/1078-0432.CCR-11-1900

236. Sacco R, Granito A, Bargellini I, Zolfino T, Saitta C, Marzi L, et al. Clinical outcomes with long-term sorafenib treatment of patients with hepatocellular carcinoma: a multicenter real-life study. Future Oncol. 2018;14: 3049–3058. doi:10.2217/fon-2018-0281

237. de Wit D, Guchelaar H-J, den Hartigh J, Gelderblom H, van Erp NP. Individualized dosing of tyrosine kinase inhibitors: are we there yet? Drug Discov Today. 2015;20: 18–36. doi:10.1016/j.drudis.2014.09.007

238. Ogawa-Morita T, Sano Y, Okano T, Fujii H, Tahara M, Yamaguchi M, et al. Validation of a Liquid Chromatography-Tandem Mass Spectrometric Assay for Quantitative Analysis of Lenvatinib in Human Plasma. Int J Anal Chem. 2017;2017: 1–6. doi:10.1155/2017/2341876

239. Srikanth I, Prameela Rani A. Development and validation of liquid chromatography coupled with tandem mass spectrometry method for estimation of lenvatinib in human plasma. Asian J Pharm Clin Res. 2017;10: 120. Doi:10.22159/ajpcr.2017.v10i7.18287

240. Sueshige Y, Shiraiwa K, Honda K, Tanaka R, Saito T, Tokoro M, et al. A Broad Range High-Throughput Assay For Lenvatinib Using Ultra-High Performance Liquid Chromatography Coupled To Tandem Mass Spectrometry With Clinical Application In Patients With Hepatocellular Carcinoma. Ther Drug Monit. 2021;Publish Ahead of Print. doi:10.1097/FTD.0000000000000872

241. Janssen JM, de Vries N, Venekamp N, Rosing H, Huitema ADR, Beijnen JH. Development and validation of a liquid chromatography-tandem mass spectrometry assay for nine oral anticancer drugs in human plasma. J Pharm Biomed Anal. 2019;174: 561–566. doi:10.1016/j.jpba.2019.06.034

242. Aghai F, Zimmermann S, Kurlbaum M, Jung P, Pelzer T, Klinker H, et al. Development and validation of a sensitive liquid chromatography tandem mass spectrometry assay for the simultaneous determination of ten kinase inhibitors in human serum and plasma. Anal Bioanal Chem. 2021;413: 599–612. doi:10.1007/s00216-020-03031-7

243. Ye Z, Wu L, Zhang X, Hu Y, Zheng L. Quantification of sorafenib, lenvatinib, and apatinib in human plasma for therapeutic drug monitoring by UPLC-MS/MS. J Pharm Biomed Anal. 2021;202: 114161. doi:10.1016/j.jpba.2021.114161

244. Liefaard L, Chen C. Quantifying the Effectiveness of Dose Individualization by Simulation for a Drug With Moderate Pharmacokinetic Variability. Ther Drug Monit. 2015;37: 641–648. doi:10.1097/FTD.0000000000000194

245. Chatelut E, Bruno R, Ratain MJ. Intraindividual Pharmacokinetic Variability: Focus on Small-Molecule Kinase Inhibitors. Clin Pharmacol Ther. 2018;103: 956–958. doi:10.1002/cpt.937

246. Vail DM, Husbands BD, Kamerling SG, Simpson H, Kurzman ID, McDonnell A. Phase I Study to Determine the Maximal Tolerated Dose and Dose-Limiting Toxicities of Orally Administered Idarubicin in Dogs with Lymphoma. J Vet Intern Med. 2012;26: 608–613. doi:10.1111/j.1939-1676.2012.00896.x

247. Lachâtre F, Marquet P, Ragot S, Gaulier JM, Cardot P, Dupuy JL. Simultaneous determination of four anthracyclines and three metabolites in human serum by liquid chromatography–

electrospray mass spectrometry. J Chromatogr B Biomed Sci App. 2000;738: 281–291. doi:10.1016/S0378-4347(99)00529-0

248. Sottani C, Tranfo G, Bettinelli M, Faranda P, Spagnoli M, Minoia C. Trace determination of anthracyclines in urine: a new high-performance liquid chromatography/tandem mass spectrometry method for assessing exposure of hospital personnel. Rapid Commun Mass Spectrom. 2004;18: 2426–2436. doi:10.1002/rcm.1642

RINGRAZIAMENTI

Giunti a questo punto non posso che ringraziare il professor Berti e il dottor Toffoli per avermi dato la possibilità di consolidare e approfondire la mia preparazione in questo ambito a me caro e che auspico di poterlo continuare a studiare anche nel prossimo futuro.

In particolare, voglio ringraziare il professor Berti per la costante disponibilità e presenza, seppur a distanza.

Mentre il dottor Toffoli lo voglio ringraziare per avermi dato la possibilità di svolgere anche il mio periodo di dottorato presso la struttura operativa complessa di farmacologia sperimentale clinica da lui diretta.

Il raggiungimento di questo importante traguardo è stato possibile non solo al grazie all'impegno e alla dedizione personale, ma soprattutto grazie al supporto e alla collaborazione di tutti voi.

In *primis*, devo ringraziare il mitico gruppo di Fasi 1, che non è stato solo il gruppo di colleghi, ma con molti di loro si è instaurato un rapporto di vera e propria amicizia. A tal proposito non posso fare a meno di non citare le ragazze che sono riuscite a convincermi a svegliarsi alle 6.00 pur di riuscire ad andare a nuotare tutte insieme, oppure la mia guida alpina, e non solo, che mi e ci ha portate alla scoperta delle montagne venete.

Queste ragazze sono le "veterane" del gruppo, ma questo così come il tempo dove il presente non è uguale né al passato né al futuro, non posso non ringraziare alcuni ex e alcuni nuovi membri.

La prima ad abbandonare il gruppo è stata la cara Luciana, che non perde occasione di venirci a trovare, in modo da non farci sentire mai la sua mancanza.

In seguito, il nostro gruppo allargato è stato nuovamente decurtato di due fantastiche persone: Eva e Elena, che mi hanno lasciato un enorme bagaglio non solo professionale, ma anche umano.

Infine, anche Mauro e Valentina hanno deciso di abbandonarci, ma nonostante questo sono sempre pronti ad un confronto, un suggerimento, una cena.

Il gruppo si è arricchito anche di Giovanni, Marco ed Ariana, la quale sta facendo il mio stesso percorso, alla quale faccio un sincero in bocca al lupo.

Recentemente è arrivata Nicole che tutti i giorni passa sempre a salutare e se capisce che non è giornata mi invita ad andare nella stanza "borsisti" e tirarmi su con una delle leccornie della loro infinita scorta. Il suo supporto non si esaurisce in questi piccoli gesti, infatti è sempre pronta ad aiutarmi nei momenti di crisi. Come dimenticare quella volta delle eppendorf.

L'FSC è un gruppo abbastanza numeroso, al quale rivolgo uno speciale ringraziamento per essermi stata accanto non solo durante il periodo di tesi di laurea magistrale, ma soprattutto durante questo ultimo triennio di dottorato.

Infine, un ringraziamento speciale va alla mitica Anto, sempre pronta a risolvere qualsiasi questione amministrativa, ma anche a dare una parola di incoraggiamento nei diversi momenti di sconforto che ci sono stati lungo questo percorso e a gioire durante i momenti di gloria.

Non me ne voglia nessuno, ma il gruppo di fasi 1 non sarebbe lo stesso senza le sue “veterane”: Bianca, Sara e Michela che, durante questi oltre quattro anni di lavoro assieme, sono sempre state presenti, collaborative e disponibili a aiutare, ma soprattutto a spiegarmi e a farmi crescere sia professionalmente sia umanamente.
La vita non è fatta solo di lavoro per questo un ringraziamento va fatto anche a Martina, Matteo, Fabio, Alice, Marina, Cristina, Alice e Luca, amici storici, sempre presenti. Così come lo sono state le amiche universitarie, Agata, Martina, Silvia e Genny che nonostante i miei periodi di assenza e di lontananza geografica.
Dulcis in fundo, voglio ringraziare di cuore la mia famiglia, senza la quale non sarei sicuramente arrivata dove sono arrivata. In particolare, la nonna per essermi stata sempre vicina e cercare sempre di capire quello che sto facendo.
La mamma per avermi sempre sopportato, soprattutto durante questo ultimo periodo, e per avermi preparato ogni mattina la tanto da lei amata “scatoletta” per pranzo; mentre il papà per avermi sempre supportato e aver “parato” alcuni colpi con la mamma.
Infine, ringrazio mia sorella per avermi sempre supportato e ascoltato soprattutto mentre preparavo le varie presentazioni per *lab meeting, summer school,* presentazioni di vario genere, nonostante lei non capisca nulla di tutto ciò.